Synthesis of Various Classes of Chiral Polymers and their Application in Enantioselective Separation

by

Shrikant Babanrao Nikam

10CC15A26027

A thesis submitted to the
Academy of Scientific & Innovative Research
for the award of the degree of
DOCTOR OF PHILOSOPHY
in
SCIENCE

Under the supervision of

Dr. Asha S. K.

CSIR- National Chemical Laboratory, Pune

Academy of Scientific and Innovative Research
AcSIR Headquarters, CSIR-HRDC campus
Sector 19, Kamla Nehru Nagar,
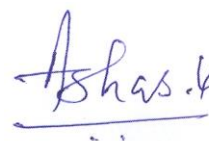Ghaziabad, U.P. – 201 002, India
December-2021

Certificate

This is to certify that the work incorporated in this Ph.D. thesis entitled, _"Synthesis of Various Classes of Chiral Polymers and their Application in Enantioselective Separation",_ submitted by _Mr. Shrikant Babanrao Nikam_ to the Academy of Scientific and Innovative Research (AcSIR), in partial fulfillment of the requirements for the award of the Degree of _Doctor of Philosophy in Science_, embodies original research work carried-out by the student. We, further certify that this work has not been submitted to any other University or Institution in part or full for the award of any degree or diploma. Research material(s) obtained from other source(s) and used in this research work has/have been duly acknowledged in the thesis. Image(s), illustration(s), figure(s), table(s) _etc_., used in the thesis from other source(s), have also been duly cited and acknowledged.

Mr. Shrikant Babanrao Nikam

Research Student

Date:30/12/2021

Dr. Asha S. K.

Research Supervisor

Date: 30/12/2021

STATEMENTS OF ACADEMIC INTEGRITY

I Mr. Shrikant Babanrao Nikam, a Ph.D. student of the Academy of Scientific and Innovative Research (AcSIR) with Registration No. 10CC15A26027 hereby undertake that, the thesis entitled "Synthesis of Various Classes of Chiral Polymers and their Application in Enantioselective Separation" has been prepared by me and that the document reports original work carried out by me and is free of any plagiarism in compliance with the UGC Regulations on *"Promotion of Academic Integrity and Prevention of Plagiarism in Higher Educational Institutions (2018)"* and the CSIR Guidelines for *"Ethics in Research and in Governance (2020)"*.
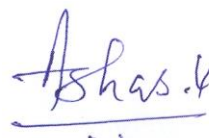
Signature of the Student

Date   :30/12/2021

Place : Pune

It is hereby certified that the work done by the student, under my/our supervision, is plagiarism-free in accordance with the UGC Regulations on *"Promotion of Academic Integrity and Prevention of Plagiarism in Higher Educational Institutions (2018)"* and the CSIR Guidelines for *"Ethics in Research and in Governance (2020)"*.

Signature of the Supervisor

Name : Dr. Asha S. K.

Date   : 30/12/2021

Place : Pune

Dedicated to
My Beloved Parents

Shri. Babanrao R. Nikam
Smt. Alka B. Nikam

<u>ACKNOWLEDGEMENT</u>

I thank almighty with all my heart for giving me the strength to keep going. By the grace of God, I would be able to complete the work that was initiated years ago. Although Ph.D. is awarded to the individual, in reality, it's the hidden effort of so many people who contributed to the cause.

I feel honored to express my deepest gratitude to my research supervisor, Dr. Asha S. K. I feel incredibly privileged and fortunate for her scientific inputs and for helping me in sorts to complete the degree. Scrutinized scientific discussions and her encouraging words always push me beyond my limits to deliver my best in research. Ph.D. comes with lots of odds and few even moments. There were moments in the Ph.D. when I felt like my dreams were shattered like pieces of glass that broke me entirely from inside, but she made me learn to fight against the odds. She built confidence in me during the ups and downs of my research and personal life. Her constant support and encouragement throughout this tenure made me believe in myself. I will always be grateful to her for being ready to help approach with an evergreen smile which made this journey unforgettable. Madam, my family and I will always be thankful to you forever. I want to extend my sincere gratitude to Prof. M. Jayakannan (IISER, Pune) for introducing me to the basics of polymers science. His fantastic teaching skills help me to grow my interest in understanding polymer chemistry during his coursework classes. I feel blessed to learn scientific ethics and training from him during a discussion that sometimes goes on for hours. Other than research, his out of the box effort and scrutiny helps me to learn several soft skills. Sir is like coconut, hard from outside but and soft and kind-hearted from inside. His welcoming nature makes his home a place where I found a solution for many scientific or personal problems. I will always be thankful to sir for his motivation and encouragement and for making every facility in IISER available to me over a single phone call.

I owe special thanks to my DAC members Dr. Ashish V. Orpe, Dr. Kadhiravan Shanmuganathan, for their timely discussion and valuable suggestions during my DAC sessions. I want to especially thank Dr. K. Krishnamoorthy for his advice and guidance, which helps me to complete my first project successfully. Dr. K. Krishnamoorthy took special efforts and personally demonstrated the preparation of chiral membranes and helped in setting up diffusion experiments during paper revision.

Acknowledgement

Acknowledgement

Deepak, Nitin, Dr. Ram, Prashant, Prem, Dr. Ambarish, Indrajeet, Avinash, Dr. Swechcha, Dyaneshwar Anirban, Mahendra (Pawar and Wagh), Pratiksh, and Bharat for their endless support and motivation.

"A father's goodness is higher than the mountain. A mother's goodness deeper than the sea." I could   Mere words could never express my feelings towards to my beloved parents Shri. Babanrao R. Nikam (father) And Mrs. Alka B. Nikam (mother). Their unconditional love and sacrifices are a huge source of inspiration and courage for me. Their enormous support in every decision I took allowed my kite to fly in an open sky. I also would like to express a profound sense of gratitude towards my brother Shri. Sandip B. Nikam and sister-in-law Mrs. Sandhya S. Nikam for their support. My nieces Devyani and Kalyani are a source of joy. Their pure smile dissolves all the sorrows in life.

I would like to express my gratitude towards all teachers from my school (J. N. V. Washim). The school plays a massive role in shaping my career. I don't believe I would have achieved even half if I had not got a chance to study in J. N. V. I especially want to thank my guru Dr. K. N. Puri (Assistant Prof. Shri Shivaji College, Akola), for constantly encouraging me to choose Chemistry for my post-graduation instead of MBA and supporting in up and down.

Last but not least, I am thankful to unknown reviewers of the thesis for investing their precious time and knowledge in reviewing the work.

-Shrikant B. Nikam

ABBREVIATIONS AND SYMBOLS

Mn	Number average molecular weight
Mw	Weight average molecular weight
Đ$_M$	Polydispersity index
PDI	Polydispersity index
Xn	Degree of polymerization
DCM	Dichloromethane
RT	Room temperature
h	Hour
g	Gram
mg	Milligram
μL	Microlitre
mL	Millilitre
μm	micrometre
nM	nanomolar
nm	Nanometre
mol	Mole
mmol	Millimole
ppm	Parts per million
EA	Ethyl acetate
DMSO	Dimethyl sulfoxide
THF	Tetrahydrofuran
DMAP	N, N-Dimethyl aminopyridine
DCC	Dicyclohexylcarbodiimide

Et$_3$N	Triethylamine
TBAB	Tetrabutylammonium bromide
KBr	Potassium bromide
FT-IR	Fourier transform Infra-Red
NMR	Nuclear magnetic resonance
DLS	Dynamic light scattering
GPC	Gel permeation chromatography
SEC	Size exclusion chromatography
SEM	Scanning electron microscope
FE-SEM	Field emission-scanning electron microscope
TLC	Thin-layer chromatography
CD	Circular dichroism
HPLC	High-performance liquid chromatography
AIBN	Azobisisobutyronitrile
St	Styrene
PS	Polystyrene
LED	Light emitting diode
OLED	Organic light-emitting diode
OFET	Organic field-effect transistors
pH	Power of hydrogen
λ	wavelength
λem	Emission wavelength
λmax	Maximum intensity wavelength
UV	Ultraviolet
UV-Vis	Ultraviolet-visible

Abbreviations and Symbols

COF	Covalent organic framework
MOF	Metal-organic framework
DHAP	Direct heteroarylation polymerization
H-bonding	Hydrogen bonding
AAO	Anodic aluminium oxide
ee	Enantiomeric excess
% ee	% Enantiomeric excess
Asp	Aspartic acid
Trp	Tryptophan
Glu	Glutamic acid
Leu	Leucine
Fl	Fluorene
PF	Polyfluorene
Pd	Palladium
Boc	Tert-butoxycarbonyl
DI water	Deionized water

SYNOPSIS

1 Introduction

Chirality is an integral part of the living world. The specific chirality in the biomolecules like DNA, proteins, amino acids, and sugars governs the chemistry of life. These molecules make the physiological processes highly stereospecific. The absolute chirality of biomolecules discriminates among enantiomers of the drugs regarding their pharmacokinetics and pharmacodynamics activities. Even our taste buds can differentiate between the enantiomers.[1] The requirement of enantiopure starting compounds in pharmaceutical, food, fragrance, and agrochemical industries demand considerable attention from the scientific community to develop efficient, cost-effective chiral selectors and separation methods for enantioselective separation. Here, we discuss the development of various polymeric chiral selectors and simple filtration methods, which are efficient, cost-effective, and do not require high-end chromatographic instruments for carrying out enantioselective separation of a racemic mixture.

2 Statement of problem

Asymmetric synthesis is the most common method to obtain enantiopure compounds. Asymmetric synthesis needs enantiopure starting materials and expensive chiral catalysts. Little change in the reaction conditions like temperature, solvent, or pH can skew the yield of enantiomers.[2] The other method is an enantioselective separation, where compounds are racemic forms followed by separation using different chromatographic techniques.[3] The chromatographic methods use costly and high-end instruments that need skilled workforce to operate these instruments, significantly increasing the final product cost. There is a need to develop an alternative affordable solution like simple filtration methods, where no costly instruments are required. The membrane or particle-based enantioselective separation can effectively be used to make the enantioselective separation cost-effective. The development of polymeric chiral selectors can solve the problems like stability issues. It can improve the separation efficiency by forming secondary structures by intra-chain and interchain interactions compared to small molecules-based chiral selectors. We have optimized synthetic procedures from conventional Suzuki polymerization to greener direct

Heteroarylation polymerization (DHAP) for getting more and cleaner polymer without any organometallic impurities.

Similarly, we have developed different classes of polymers like polyfluorene, polythiophene-fluorene copolymers, and cost-effective polymers based on commodity polystyrene. We used the RAFT polymerization method to synthesize polystyrene, followed by post polymer modifications with acid chlorides of Phthaloyl protected L-leucine. The protected L-leucine induces chirality in achiral polystyrene. Overall we developed a greener and cost-effective way of synthesizing different classes of chiral polymers, which were then used to carry out enantioselective separation of an aqueous racemic mixture of native amino acids in 24 hours without using any chromatographic instrumental setup.

3 Objectives of the thesis

The objectives of the thesis are given below

- Synthesis and characterization of chiral polymers (polyfluorenes, modified polystyrene, and fluorene-thiophene copolymers)
- Fabrication and characterization of chiral polymer-coated anodic aluminium oxide (AAO) membranes
- Carrying out enantioselective separation of racemic mixtures of amino acids using polymer-coated porous AAO membranes
- To study the effect of pore size of polymer coated membranes on enantioselective separation efficiency
- To check the kinetics of separation and achieving maximum separation using extra AAO membranes
- Determining the amount of polymers used for carrying out enantioselective separation of a racemic mixture
- To study the effect of different chiral handles on the selectivity and separation efficiency
- To study and understand the mechanism of discrimination of enantiomers by chiral selectors using 3-point interaction models
- Synthesis and characterization of chiral polystyrene by post polymer modification approach using Friedel-Crafts acylation with an acid chloride of Phthaloyl protected L-leucine

- The fabrication and characterization of chiral polymeric microspheres and using them for carrying out enantioselective separation of native amino acid racemic mixtures
- Synthesis and characterization of chiral ∏-conjugated polymers by clean and green DHAP approach
- To study the structure-property relationship using ^{1}H NMR spectroscopy and photophysical characterizations like absorbance and emission study

Significant outcomes from the individual thesis chapters

Chapter 2 **Enantioselective Separation Using Chiral Amino Acid Functionalized Polyfluorene Coated on Mesoporous Anodic Aluminium Oxide Membranes**

Simple, efficient, and cost-effective filtration methods can be of great importance in enantioselective separation. This chapter discusses the synthesis and characterization of protected D/L-aspartic acid-containing polyfluorenes. Chiral AAO membranes were fabricated by coating these polymers on (200 nm) porous AAO membranes.
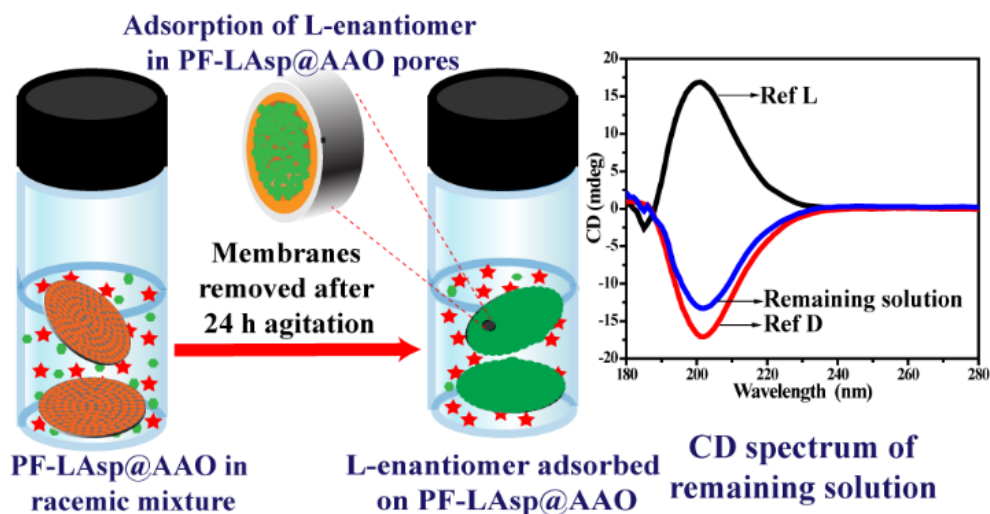
These polymer-coated chiral membranes were characterized and used to carry out enantioselective separation of aqueous racemic mixtures of 9 different amino acids. The highest separation could be achieved for native D/L-glutamic acid (~95 % ee), while the amino acids like alanine, leucine, lysine, and aspartic acid showed % ee > 80. The kinetics of separation was studied, and it was observed that both the D and L membranes showed almost similar kinetics, and most of the separation happened in the first 20 hours. Calculations based on the data revealed that 1 mg of polymer could separate around 3.5 mg

of D/L glutamic acid. The effect of pore size on the separation efficiency was also studied and found that 100 and 200 nm pore sized membrane achieved almost similar separation, ~93 and ~95 % respectively, but the separation efficiency drastically reduced to 28 % for 20 nm pore sized membranes, as the pore was clogged by film formation on the membrane surface. From this observation, it could be concluded that separation happened inside the pores and not on the membrane surface. These observations and findings could provide an efficient and cost-effective alternative for enantioselective separation.

Chapter 3 **Effect of Chiral Handles on Selectivity and Separation Efficiency**

This chapter studied the effect of different chiral handles on selectivity and separation efficiency. Polyfluorene appended with protected L-glutamic acid and L-tryptophan synthesized by Suzuki polymerization of corresponding monomers with 1, 4-benzenediboronic ester was used for the studies. Chiral AAO membranes of 200 nm pore size were coated with these polymers. These polymer-coated membranes were further used to efficiently separate the aqueous racemic mixture of 10 different amino acids.

PF-LGlu   PF-LTrp
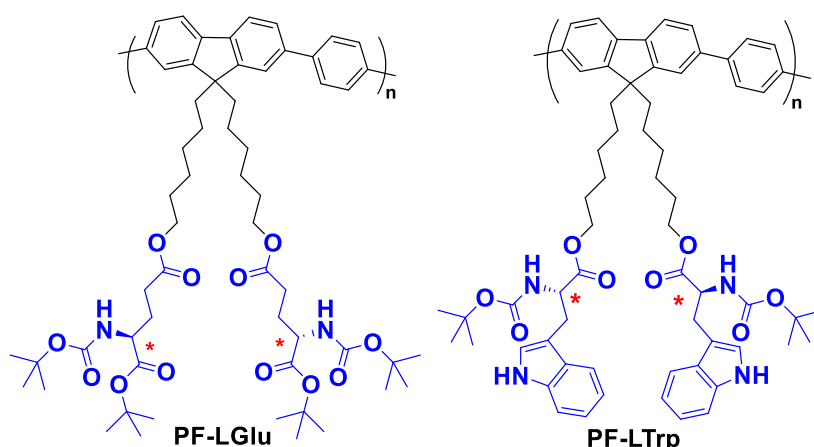
The membranes exhibited selectivity towards different amino acids depending on the chirality of the coated polymer. The tryptophan-containing polymer (PF-LTrp@AAO) demonstrated maximum separation for the tryptophan (~91 % ee) followed by phenylalanine (87 % ee), while the glutamic acid-containing polymer (PF-LGlu@AAO) achieved maximum separation for glutamic acid (~92 % ee) followed by lysine (~84 % ee). The PF-LGlu@AAO could separate glutamic and other aliphatic amino acids, while PF-LTrp@AAO could separate tryptophan and another aromatic amino acid with higher efficiency. These studies indicated the probable existence of selective interactions in these

polymers. The separation mechanism could be understood using the "3-point interaction model", which explains the formation of different binding energy transition state complexes between the chiral sector and enantiomers. It is anticipated that these interactions could be π-π interactions in the case of aromatic pendant containing polymer (PF-LTrp@AAO) or hydrogen bonding in the aliphatic pendant containing polymer (PF-LGlu@AAO).

Chapter 4 Enantioselective Separation of Amino Acids Using Chiral Polystyrene Microspheres synthesized by Post Polymer Modification Approach
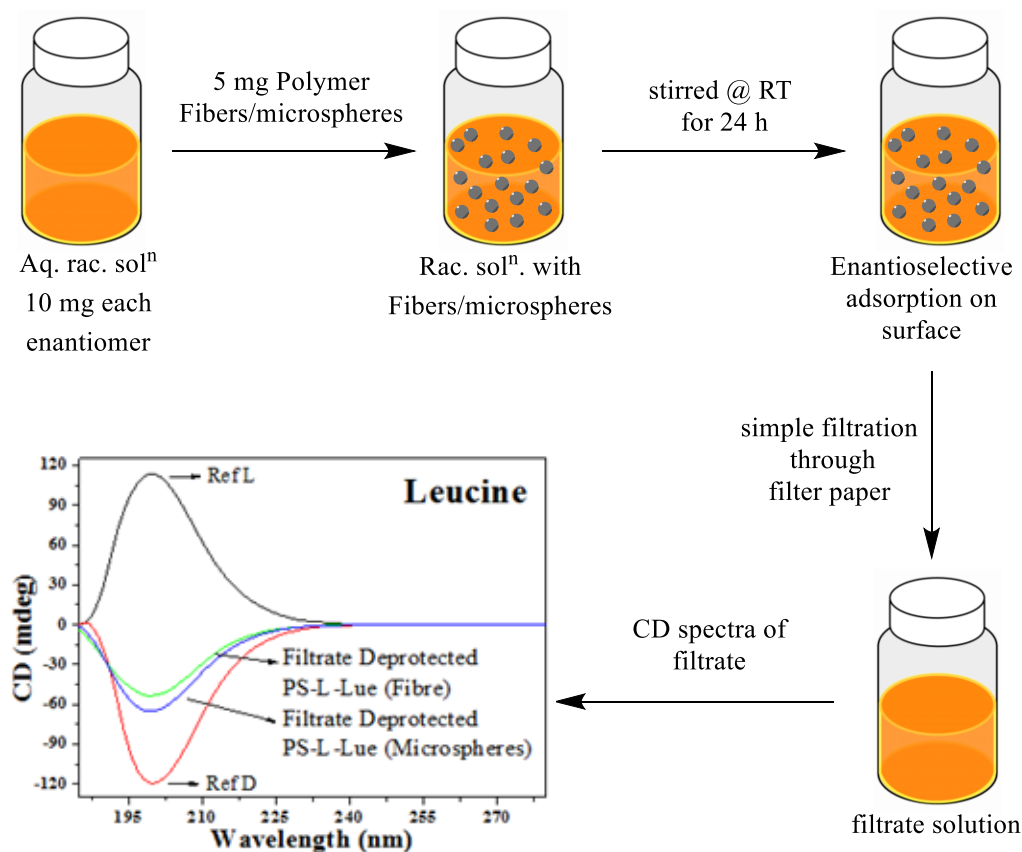
Chapter 4 discusses the synthesis and characterization of chiral polystyrenes by post polymer modification. Friedel-Craft acylation was carried out on polystyrene using acid chloride of Phthaloyl protected L-leucine. This was followed by deprotection of the Phthaloyl group resulting in deprotected PS-L-Leu. The protected and deprotected PS-L-Leu powder was made into spherical microspheres by solvent emulsion using 4 % aqueous tween 80 surfactants. These chiral polymer powder /microspheres were used to carry out enantioselective separation of aqueous amino acid racemic mixtures. The protected PS-L-Leu powder/microspheres could achieve the separation of leucine and alanine. The

separation efficiency of microspheres was observed to be almost double compared to that of as-is-precipitated polymer powder for both alanine (16.52/**35.24** % ee) and leucine (19.45/**42.06** % ee). An increase in the separation efficiency in microspheres compared to polymer powder is anticipated to arise from the increased surface area in the former.

Chapter 5 **Synthesis of Chiral ∏-Conjugated Polymers by DHAP Route**

This chapter focuses on synthesizing chiral ∏-conjugated polymers by the clean and green Direct Hetero Arylation Polymerization (DHAP) approach compared to conventional methods like Suzuki and Stille polymerization. Traditional methods produce a stoichiometric amount of hazardous organometallic by-products, which reduces the atom economy of these reactions. Additionally, conventional methods need pre-functionalization of the monomers with organometallic functionality. This additional step in monomer synthesis makes these methods non-economical. On the other hand, DHAP is a greener approach. It does not produce such hazardous byproducts resulting in increased atom economy. These reactions do not need pre-functionalized monomers, making these reactions economical compared to conventional methods. Regioregular polythiophenes, as well as chiral fluorene-thiophene copolymers, were successfully synthesized by DHAP route. The structure-property relationship was studied to understand the defects formed in the polymers using ^{1}H NMR spectroscopy and photophysical characterization of these polymers.
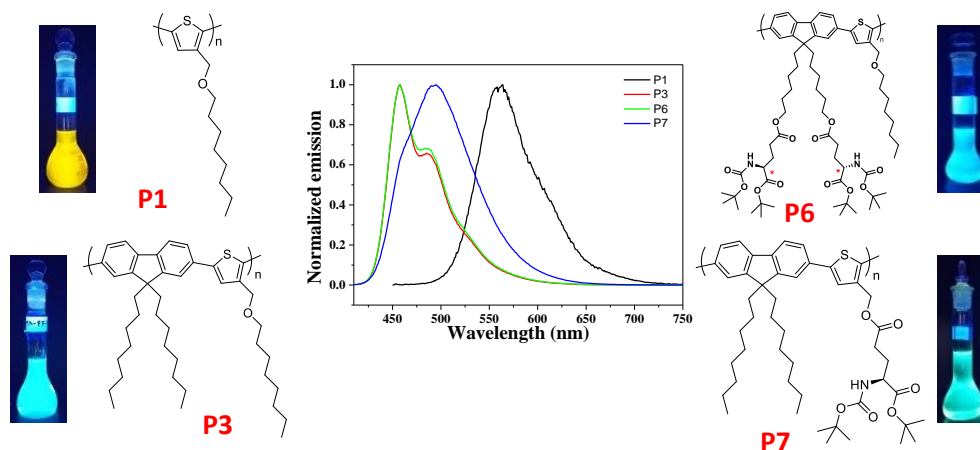
Summary

In this thesis, we focused on developing polymeric chiral selectors for carrying out simple filtration-based enantioselective separation. Various classes of chiral polymers were synthesized by different polymerization approaches. In **chapter 2,** chiral polyfluorene

bearing protected D/L-aspartic acid as pendants were synthesized. Chiral AAO membranes were fabricated by coating these polymers on the commercially available porous AAO membranes. These membranes were then used to carry out enantioselective separation of an aqueous racemic mixture of 9 different amino acids. The highest separation was achieved in the case of D/L-glutamic acid (~95 % ee). In **chapter 3,** the effects of different chiral handles on selectivity and separation efficiency were studied. Chiral AAO membranes coated with chiral polymers having different chiral pendants (PF-LTrp@AAO and PF-LGlu@AAO) were used to carry out enantioselective separation of various amino acids. These studies indicated the probable existence of selective interactions with analytes in these polymers. In **chapter 4,** chiral polystyrene microspheres were developed by a post polymer modification approach. These microspheres showed enhanced (almost double) separation efficiency as compared to polymeric powder. In **chapters 2** and **3,** chiral ∏-conjugated polyfluorenes were synthesized by conventional Suzuki polymerization, where pre-functionalization of monomers is required and produced stoichiometric amounts of hazardous byproducts. In chapter 5, chiral ∏-conjugated fluorene-thiophene copolymers were synthesized by DHAP route, a relatively economical and green method. In DHAP, monomers need no pre-functionalization and do not produce hazardous byproducts. The structure-property relationship was studied between these polymers to understand the defects using ^{1}H NMR and UV-visible spectroscopy.

References

(1)   Mane, S. Racemic Drug Resolution: A Comprehensive Guide. *Anal. Methods* **2016**, *8* (42), 7567–7586.

(2)   Bhadra, S.; Yamamoto, H. Substrate Directed Asymmetric Reactions. *Chem. Rev.* **2018**, *118* (7), 3391–3446.

(3)   Ward, T. J.; Ward, K. D. Chiral Separations: Fundamental Review 2010. *Anal. Chem.* **2010**, *82* (12), 4712–4722.

List of publications

1. T. Senthilkumar, N. Parekh, **<u>Shrikant B Nikam</u>**, Asha S. K. Orientation effect induced selective chelation of Fe^{2+} to a glutamic acid appended conjugated polymer for sensing and live-cell imaging. *J. Mater. Chem. B,* **2016**, *4*, 299-308.

2. **<u>Shrikant B Nikam,</u>** Asha S.K. Enantioselective Separation Using Chiral Amino Acid Functionalized Polyfluorene Coated on Mesoporous Anodic Aluminum Oxide Membranes. *Anal. Chem.* **2020**, *92*, 10, 6850–6857.

3. B. P. Mali, S. R. Dash, **<u>Shrikant B. Nikam</u>**, A. Puthuvakkal, K. Vanka, K. Manoj and R. G. Gonnade. Five concomitant polymorphs of a green fluorescent protein chromophore (GFPc) analogue: understanding variations in photoluminescence with p-stacking interactions. *Acta Cryst. B* **2020**, *76*, 1-15.

4. **<u>Shrikant B. Nikam,</u>** Asha S. K. Enantioselective separation of amino acids using chiral polystyrene microspheres synthesized by post polymer modification approach *ACS Polymer Au*

5. **<u>Shrikant B. Nikam,</u>** Asha S. K. Synthesis of Chiral ∏-Conjugated Polymers by DHAP Route *(Manuscript under preparation)*

<u>Patents</u>

1. **<u>Shrikant B. Nikam</u>**, Asha S. K. A Process for Enantioselective Separation of Amino Acids Using Chiral Polystyrene *(Provisional application number 202111058074)*

Table of Content

CHAPTER 2
Enantioselective Separation Using Chiral Amino Acid Functionalized Polyfluorene Coated on Mesoporous Anodic Aluminium Oxide Membranes

CHAPTER 3
Effect of Chiral Handles on Selectivity and Separation Efficiency

CHAPTER 4
Enantioselective Separation of Amino Acids Using Chiral Polystyrene Microspheres Synthesized by Post Polymer Modification Approach

CHAPTER 5
Synthesis of Chiral ∏-Conjugated Polymers by DHAP Route

CHAPTER 6
Conclusion and Future Perspectives

CHAPTER 1

General Introduction and Literature

Outline of introduction

1.1 History and background

Louis Pasteur introduced the concept of chirality, in 1848 just eight months after completing his Ph.D., while studying the structural theory of organic molecules. While examining sodium ammonium paratartrate crystals, he identified two distinct types of crystals present in a 1:1 ratio. It was discovered that the two crystal types were non-superimposable mirror reflections. With a pair of tweezers, he manually separated the two forms into two piles and observed that one form's solution rotated polarised light clockwise, while the other form's solution rotated the light anticlockwise, and an equal mix of the two did not rotate the light at all.[1] It was the first successful attempt to understand chirality. In the conclusion of these experiments, pasture rightly stated. "*Asymmetry establishes perhaps the only well-marked line of demarcation that can at present be drawn between the chemistry of dead matter and the chemistry of living matter.*"[2,3] In 1874, two scientists, J. A. Le Bel and Dr. J. H. Van't Hoff, separately proposed that the four groups surrounding carbon atoms organized themselves in a tetrahedral pattern. The traditional thinkers harshly criticized them both for their unconventional thinking. The work of Dr. Van't Hoff was dismissed as "childish fantasy" and was further chastised for having "no taste for accurate chemical investigation." Van't Hoff's tireless efforts in the investigation yielded a plethora of evidence supporting their idea, and in 1901 Van't Hoff was the first recipient of the Noble Prize for chemistry. Van't Hoff proposed the asymmetric carbon atom with correct tetrahedral symmetry, whereas Le Bel proposed a square pyramid. The work done by van't Hoff and Le Bel laid the foundation for stereochemistry.[4]

Introduction to asymmetry or chirality can be best started with the most typical example of the human body. Although the human body looks symmetric, it is a different story inside. Most vital organs such as the heart, stomach, spleen, and pancreas lie toward the left while the gallbladder and most of the liver are on the right side.[5] Even the pair of lungs shows dissimilarity where the left one has only two lobes while the right one has three. Although the two sides of the brain look symmetrical, they function differently.[6] One theory suggests that this asymmetry comes right from the embryo.[7] Though the brand new embryo looks highly symmetrical on both left and right sides, the tiny hairs like cilia present on the nodes whirl around rapidly all in the same direction; this synchronous rotation pulls fluid from the right side to the left, causing the right and left sides to be chemically different, resulting in

the embryo developing asymmetry within 3 hours.[8] However, despite lacking the embryonic cilia, some animals like pigs still have asymmetric internal organs. Could all cells be asymmetric? If we look inside more thoroughly, the cell organelles are placed in an entirely asymmetric fashion.[9] The basic building blocks of the cell, like nucleic acids (DNA and RNA),[10] amino acids,[11,12] proteins,[13,14] and sugars,[15] are inherently asymmetric.[16] The proteins and nucleic acid have complex asymmetric shapes. These asymmetric proteins govern how the cells migrate, the way embryonic cilia whirls resulting in asymmetry. All these biomolecules have a property called chirality, in which the biomolecules and their mirror image are not identical. Although our right and left hands look the same, it is impossible to wear the right-hand gloves on the left and vice versa. These asymmetries at the molecular level result in asymmetry in cells, embryos, organs, and organisms.[17]
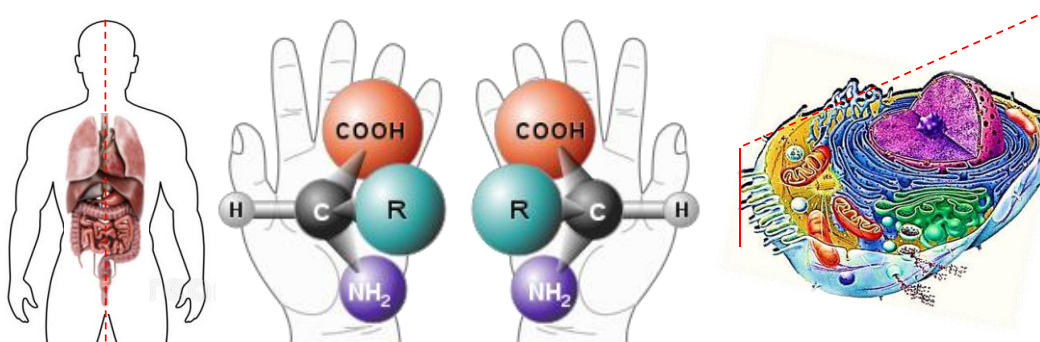
Figure 1.1 Asymmetry in the nature

1.2 Concept of chirality

Anything that cannot dissect into two equal halves is asymmetric. The asymmetry at a molecular level is called chirality. The word chiral is derived from the Greek word (cheir), which means hand. Based on molecular symmetry, the molecule that does not possess an improper axis of rotation (Sn) like a plane of symmetry or center of symmetry is called a chiral molecule. The molecule or ion is called chiral if it cannot superimpose on its mirror image even after any probable combination of rotation or translation. Enantiomers are the pair of molecules or ions with the same molecular formula and atomic connectivity but differ only in 3-dimensional spatial arrangements of atoms or groups. Enantiomers have the same physical and chemical properties but differ when reacting with other chiral molecules or in a chiral environment. Enantiomers show equal and opposite optical rotation when plane polarized light passes through its solution.[18] The enantiomer, which rotates plane polarized light in a clockwise direction, is called dextrorotatory and denoted by symbol d or (+) sign

and isomer which rotates plane polarized light in an anticlockwise direction as levorotatory and denoted by symbol *l* or (-) sign.[18]
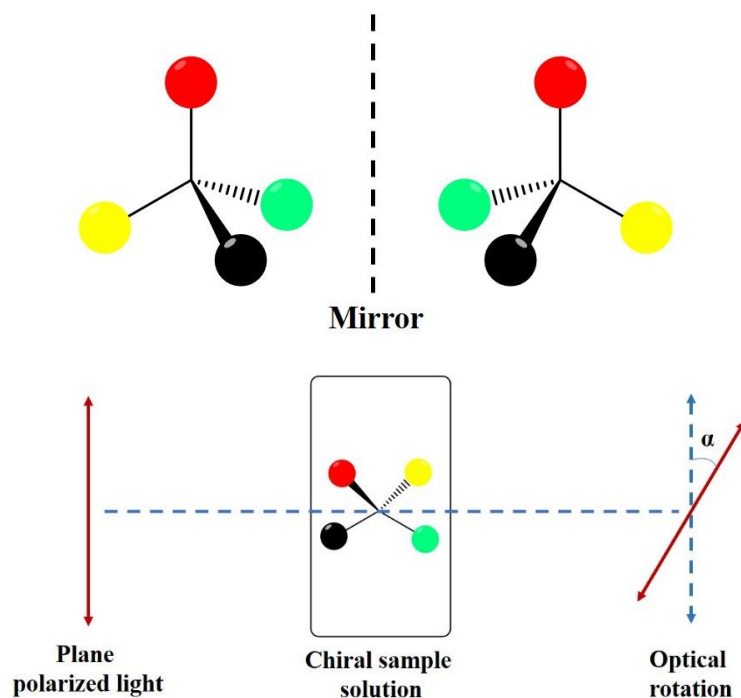
Figure 1.2 Schematic representation of enantiomer mirror images and optical rotation

1.3 Background and motivation

The biomolecules that govern life's chemistry like nucleic acid (DNA and RNA), carbohydrate, amino acids, and proteins are chiral. These biomolecules are present in nature exclusively in single forms, like DNA form right-handed helix exclusively, all the natural amino acids are present in its L-from, while the sugars are present in their D-form.[19] Even the complex structures of proteins are highly asymmetric.[20] This exclusive stereochemistry in biomolecules makes the biochemical process highly stereospecific. The activities in the physiological system and resulting physiological effects towards metabolic processes are highly stereospecific.[21–23] Even our taste buds can differentiate between the enantiomers. The particular taste of lemon is because of (S)-(-)-Limonene, while (R)-(+)-Limonene is responsible for the particular taste of oranges, similarly (S)-(+)-Carvone is responsible for the taste of cumin seeds while (R)-(-)-Carvone tastes likes mint leaves.[24] Approximately 80% of the drug molecules marketed today have a minimum one chiral center in their structures. The enantiomers of these drug molecules differ dramatically in terms of their therapeutic effectiveness, pharmacodynamic and pharmacokinetic behavior, as the chiral biomolecules react with these enantiomers entirely differently.[25–27]

1.4 Need of enantiopure compounds

The production of chemical compounds in enantiopure forms is of great interest in drug, agrochemical, food, and fragrance industries. Despite having the same chemical structures, enantiomers of drugs significantly differ in their therapeutic efficacy and pharmacokinetics, resulting in diversified pharmacological actions and pharmacodynamics.[28–30] A typical example is the thalidomide drug. Thalidomide was used widely in its racemic form during the 1960s to treat nausea and morning sickness during pregnancy. Later, women using this drug gave birth to babies with teratogenic effects. After further investigation, it was found that only the R-isomer of thalidomide is a safe sedative among R and S, while the S-form, unfortunately, causes severe congenital disabilities and deformities.[31] There are many examples where only one enantiomer of a drug is highly potent while other enantiomers are inactive or produce adverse toxic effects and cause serious side effects. Selective and most common are listed below in Table 1.1.

Chiral drugs	Biological effects of enantiomers
Thalidomide	(R)-thalidomide helpful to treat pregnancy nausea, while (S)-thalidomide proved to produce a teratogenic effect in developing fetuses, causing fetal deformities such as underdeveloped limbs.
Penicillamine	(S)-penicillamine is an antirheumatic drug used to treat rheumatoid arthritis and Wilson disease. It helps to reduce pain, tenderness, and swelling in joints. (R)-penicillamine shows extreme toxicity as it inhibits the action of pyridoxine (vitamin B_6).
Ethambutol	(S, S)-ethambutol is used in the treatment of tuberculosis. (R, R)-ethambutol causes swelling in the optic nerve, leading to temporary vision loss or permanent blindness.
Ibuprofen	(S)-ibuprofen has anti-inflammatory, antipyretic, and analgesic properties, while (R)-ibuprofen is inactive.
Citalopram	(S)-citalopram is antidepressant and used to treat depression, while (R)-citalopram is inactive.

Table 1.1 List of some common examples of drugs where enantiomers differ in their activity

US food and drug administration demand detailed documentation about each enantiomer's pharmacological and pharmacokinetic behavior separately and in combination to ensure the

safety and potency of drugs. It permits only one enantiomer to enter the market if the individual enantiomer or its combination shows differences in its activity.[32]

The enantiomers of flavoring agents differ in terms of their activities, or specific composition of enantiomers is essential to produce the authentic flavor, like γ-decalactone [(R)-(+) 89.4% : (S)-(-) 10.6%], and γ-octalactone [(R)-(+) 50.2% : (S)-(-) 49.8%] gives the genuine raspberry flavor. Similarly, the (6'S)-α-carotene is mainly responsible for carrot's particular taste and color while (6'R)-α-carotene is present in negligible amounts.[33,34] Karl-Heinz Engel studied the relative assessment of the sensory properties of β-mercaptoalkanones and β-mercaptoalkanols and found enantiomers of these compounds differed in terms of their flavoring properties. The odor threshold and odor properties of each stereoisomer of β-mercaptoalkanones and -alkanols were studied to understand the fundamental role of the substituent R4 in the tropical olfactophore model. 4-Mercapto-2-alkanones and 4-mercapto-2-alkanols containing methyl substituent R4 showed a tropical, fruity flavor. The (S) enantiomer 4-mercapto-2-alkanones has a higher odor threshold than (R) enantiomer. (R, R) the enantiomer of 4-mercapto-2-alkanols has a lesser odor threshold compared to its other enantiomers. In the case of 2-mercapto-4-alkanones, the (R) and (S) enantiomer has similar odor threshold but depending upon the chain length, they differ in their flavor, while 2-mercapto-4-alkanols with (S, R) configuration show a higher odor threshold compared to (S, S), and odor type even depend upon the chiral length of the substituent at R4.[35]

4-mercapto-2-alkanones

Odor thresholds: (R) < (S)
Odor properties:
(R): Fruity
(S) Sulfury

2-mercapto-4-alkanones

Odor thresholds: (R) ~ (S)
Odor properties:
C6-C8 Pungent, vegetable
C9-C10 Mashroom earthy

4-mercapto-2-alkanols

Odor thresholds: (R,R) lowest
Odor properties:
C6-C7 Fruity, Sulfury
C8-C10 Plastic pungent

2-mercapto-4-alkanols

Odor thresholds: (S,S) ~ (S,R)
Odor properties:
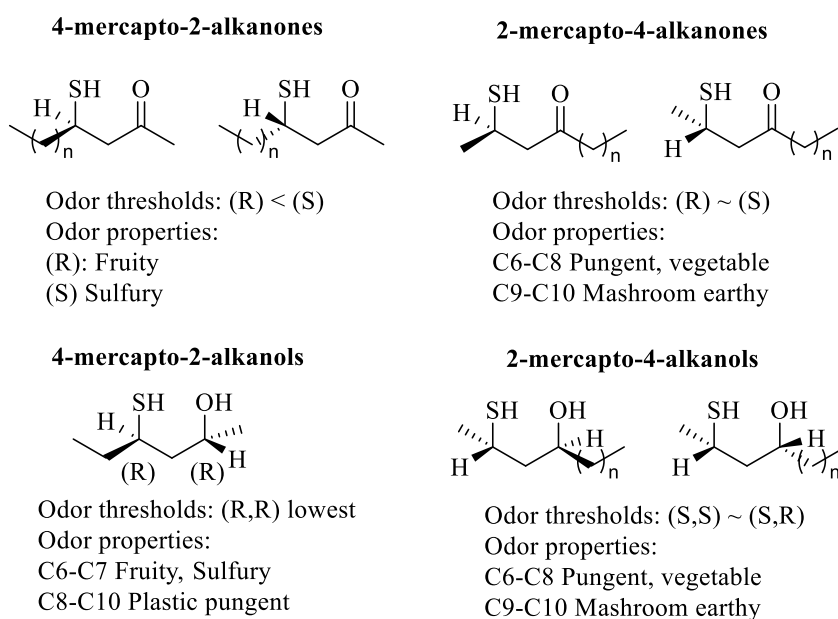C6-C8 Pungent, vegetable
C9-C10 Mashroom earthy

Figure 1.3 Comparative assessment of the sensory properties of β-mercaptoalkanones and β-mercaptoalkanols.[36]

Similarly, the agrochemical industry, which is worth 208.6 billion USD, with the potential to grow to up to 246.1 billion USD by 2025, is always on the lookout for compounds with the best efficacy, lowest field application rates, increased selectivity, acceptable toxicological and environmental safety, improved user-friendliness, and economic viability.[37] The agrochemical industry's ambitious goal can be achieved by using molecules having asymmetric centers.[38] Currently, 30% of the total marketed agrochemicals have a minimum one chiral center in their structures.[39] Unintended economic and environmental problems may arise with increasing chiral products due to unnecessary chiral components in the molecules. Among the 44 new launch products between the year 2007-2018 43 % have at least one chiral center in their structure, and (47 %) among them were launched as a racemic mixture.

These differences in the activities of enantiomers of chiral molecules have developed a quest among the scientific community and industries to synthesize chemical compounds with absolute enantiopurity using robust, scalable, and efficient strategies.

1.5 Approaches to obtain enantiopure compounds

The approaches to obtain chemical compounds in their enantiopure form are categorized into "chiral approach" and "racemic approach." The chiral approach is related to developing asymmetric synthesis methods to produce only one enantiomer. In contrast, the racemic approach mainly synthesized all the enantiomers followed by subsequent enantioselective separation of active enantiomers from the racemic mixture.[40] Though the chiral approach is the most adapted method for producing enantiopure compounds; it is associated with some shortcomings. Some common disadvantages associated with asymmetric synthesis are the use of transition metal complexes with chiral ligands that are highly expensive, environmentally hazardous, difficult to store at ambient environmental conditions, and highly unstable.[41–43]

One has to be very cautious while setting such sensitive asymmetric reactions. Little change in reaction conditions like the purity of starting material, nature of ligands, the temperature of the reaction, solvents, pH, or even the protecting groups can alter the configuration of the product or can severely skew the isolated yield, particularly enantiopure compound. There is a need to shift the focus toward using a racemic approach in this scenario. Reaction sequences in the racemic approach are cost-effective. They do not require expensive chiral ligand containing catalysts, enantiopure starting materials, and a slight alteration of reaction conditions does not impact yield very adversely.

1.6 Different methods to achieve enantioselective separation

In the chiral approach, different methods are used to separate enantiomers from their racemic mixture. Some of the most common methods are listed below with a brief discussion.

i)   **Enantioselective crystallization**

ii)   **Chiral chromatographic methods**

iii)   **Converting enantiomers into diastereomers**

iv)   **Membrane-based filtration methods**

v)   **Chiral Extractions**

vi)   **Enantioselective Distillation and Foam Flotation**

vii)   **Enantioselective filtration methods**

The introduction of chirality to the world came with the understanding that enantiomers are mirror images that are non-superimposable on one another even after all possible rotations. Thus, enantioselective or preferential crystallization is the method of choice for bringing about enantioselective separation. Generally, enantiomer crystallizes preferentially compared to others in the presence of an external enantiopure seeding agent. Sometimes both the enantiomer crystalizes, but in different shapes and sizes as conglomerates, which are mechanical mixtures, that can be separated easily. The other commonly adopted method for separating enantiomers is converting them into diastereomers by reacting with other enantiopure compounds that can be detached easily, followed by their separation. As diastereomers are not mirror images of one another, they differ in their chemical and physical properties like boiling, melting, freezing, and other physical properties and can be easily separated. These methods have common limitations like they need an enantiopure sacrificial agent. Additionally, preferential crystallization is associated with the drawback, like it needs a high level of procedure optimization, and the pure crystals can often get contaminated after a particular time as other enantiomers start nucleating.

The chiral chromatographic techniques are one of the most explored areas to obtain enantiopure compounds commercially. There are different chiral chromatographic techniques such as capillary electrophoresis (CE), Supercritical Fluid Chromatography (SFC),[44] Gas Chromatography (GC), High-Performance Liquid Chromatography (HPLC),[45] Simulated Moving Bed Chromatography (SMBC) that are successfully used for commercial purposes at large or moderately large scale. In addition to these methods, Thin Layer Chromatography (TLC) can be used at a preparative level.[46] Though chiral chromatographic

methods have been most successful, they are still associated with drawbacks like it requires costly high-end instrumentation and a skilled workforce to handle these instruments, which will add to the final product cost.[47]

The membrane-based enantioselective separation methods are relatively new but getting considerable attention from the scientific community as they can be used for continuous operation. Different membranes like chiral polymeric membranes, MOF, COF, and polymer-coated membranes are used for carrying out enantioselective separation.[48] Charles R. Martin, *et al.* demonstrated for the first time the use of porous anodic aluminium oxide (AAO) membranes (400 nm pore size) coated with D-amino acid oxidase apoenzyme (apo-D-AAO) for enantioselective transport of D-phenylalanine over L-phenylalanine.[49] Jun Yong Chan *et al.* reported enantioselective separation of phenylethanol racemic mixture using chiral L-Histidine containing zeolite (L-His-ZIF-8) membranes where porous AAO membranes (20 nm pore size) were used as a carrier for enantioselective diffusion. The membranes exhibited a higher affinity towards S-phenylethanol, which quickly accumulated in the chiral channel, while R-phenylethanol preferentially passed through the membrane. A maximum ee of 76 % was achieved initially, which decreased with the separation time extension.[50]
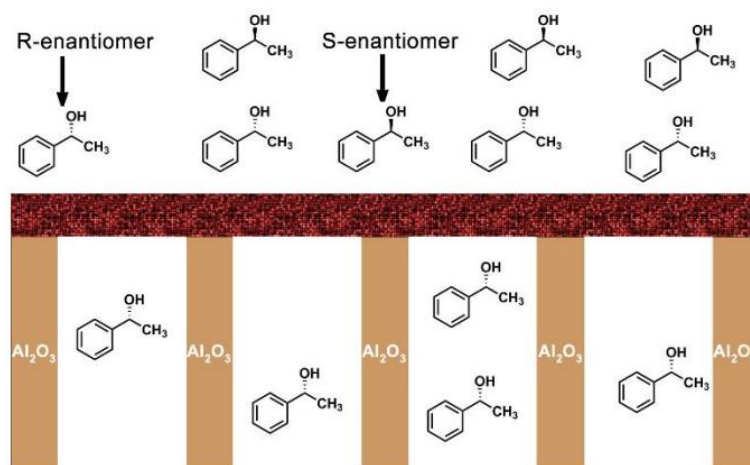
Figure 1.4 Schematic representation of a homochiral L-His-ZIF-8-membrane on 20 nm porous AAO for enantioselective separation of 1-phenylethanol racemic mixture[50]

The AAO membranes with different pore diameters are available commercially and have great potential to serve as a template for coating chiral organic selectors. It additionally provides the porous morphology needed for enantioseparation. Due to mechanical and technical constraints, membrane-based technologies are sometimes only applicable on a preparative scale. Low flow rate, chiral selector saturation, and decrease in enantioselectivity

over time are all common issues with the approach. Limitations might be overcome in the near future.

The methods like foam floatation and distillation are well adapted at the industrial level for the separation. These methods can be converted from non-selective to enantioselective using chiral selectors in the medium. Gerd Kaupp first separated a racemic mixture of 2, 2-dihydroxy-1, 1-binaphthyl by forming a diastereomeric inclusion complex with N-benzylcinchonidium chloride. One diastereomeric inclusion complex (+) separated enantiomer by crystallization in benzene. These separated enantiopure (+) and (-) 2, 2-dihydroxy-1, 1-binaphthyl were further used as chiral selectors where it formed inclusion complex with enantiomers of several compounds which differed in their boiling points and could be separated easily by distillation.[51] There are very few reports available where the chiral foam floatation method was used to separate the enantiomers from the racemic mixture. In 1994 Daniel W. Armstrong used chiral selectors including L-hydroxyproline, β-cyclodextrin derivatives like permethylated -cyclodextrin, vancomycin, and digitonin to distinguish racemic amino acid derivatives and medicines like warfarin. Using permethyl-β-cyclodextrins as a foaming agent, the racemic combination of N-tert-butoxycarbonyl-D-phenylalanine separated with the highest 76 % ee in a 40 cm column.[52] The price and quantity of enantiopure chiral selector required in the process do not make this process industrially feasible.

The liquid-liquid solvent extraction process is another approach that is already used on an industrial scale as it does not require any sophisticated instrument. This process has great potential to be used for chiral separation if chiral selectors are used in the medium. The enantiomers are separated based on the principle of difference in the affinity towards chiral selectors in the medium. This method needs chiral selectors with the highest affinity as water is one medium that can get solvated quickly and hamper the separation efficiency. An additional step is needed to separate the chiral selector from the enantiomer. Haofei Huang *et al.* reported continuous solvent extraction methods involving racemization and deracemization in the acid of unprotected amino acids in the presence of a chiral selector.[53] Boelo Schuur reported crown ether, binol, TRISPHAT salts, Deoxyguanosine derivatives, Alkyl tartrate with β-cyclodextrin, and Palladium BINAP complexes as chiral selectors in an enantioselective separation of different racemic mixtures.[54]

The method like enantioselective adsorption followed by simple filtration is of great economic interest as it does not require high-end chromatographic instruments and a skilled workforce, which subsequently reduces the final product cost. In this method, the chiral

selector is suspended in the racemic mixture, followed by enantioselective adsorption of one enantiomer on the selector's chiral surface, leaving behind others in the solution that can be separated by simple filtration.

T. Senthilkumar *et al.* reported protected L-glutamic acid appended chiral polyfluorene, mimicking the α-helical porous morphology. This α-helical porous polymer was used to carry out enantioselective separation of organic acids, amino alcohol, sugars, and amino acids by simple filtration method.[55] Ahmadabad F. K. reported the enantioseparation of α-methylbenzylamine, alanine, valine, tartaric acid, and phenylalanine racemic mixture following a simple filtration method using phosphoramide-methacrylate monomers, hydroxy functionalized monomer, and crosslinker containing polymer hydrogel packed in a teabag.[56]

1.7 Different types of chiral selectors

All enantioselective separation methods described above need material to distinguish between the enantiomers. Different chiral selectors were successfully employed to achieve enantioselective separation of the racemic mixture at the academia and commercial level. For any molecule to act as an ideal chiral selector, it should have some common properties like absolute chirality, good enantiomer recognition ability, delayed or no saturation over time, reusability of material, and low manufacturing cost. Some of the commonly used chiral selectors reported in the literature are briefly described below.

a) **Cyclodextrins**
b) **Polysaccharides**
c) **Micelles**
d) **Proteins**
e) **Macrocyclic glycopeptides**
f) **Crown ethers**
g) **Metal-organic framework (MOF), covalent organic framework (COF)**
h) **High miller indices metal surfaces**
i) **Polymers**

Cyclodextrin and its derivatives are the most commonly used chiral selectors, as it has multiple sites where it can be easily modified to modulate its desired enantioselective separation performance. Cyclodextrins are available with different ring sizes (α, β, and γ)

and can be made into neutral cationic or anionic by specific functionalization with specific groups. These easy modifications in CDs make it a versatile chiral selector. Jie Zhou reviewed the cationic cyclodextrins as a chiral selector to conduct enantioselective separation of different racemic mixtures.[57]
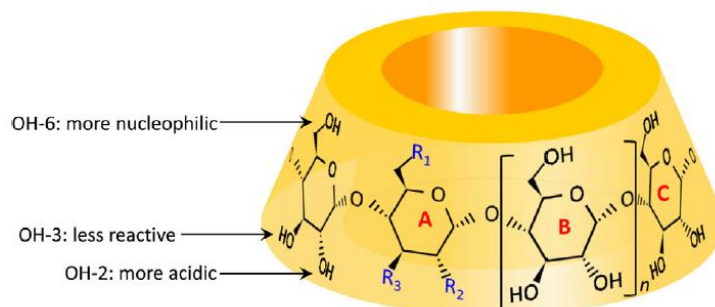
Figure 1.5 Cartoon representations of cyclodextrins along with sites of modification[58]

Polysaccharides with multiple functionalities and chiral centers make them versatile chiral selectors to conduct the enantioselective separation of different analytes.
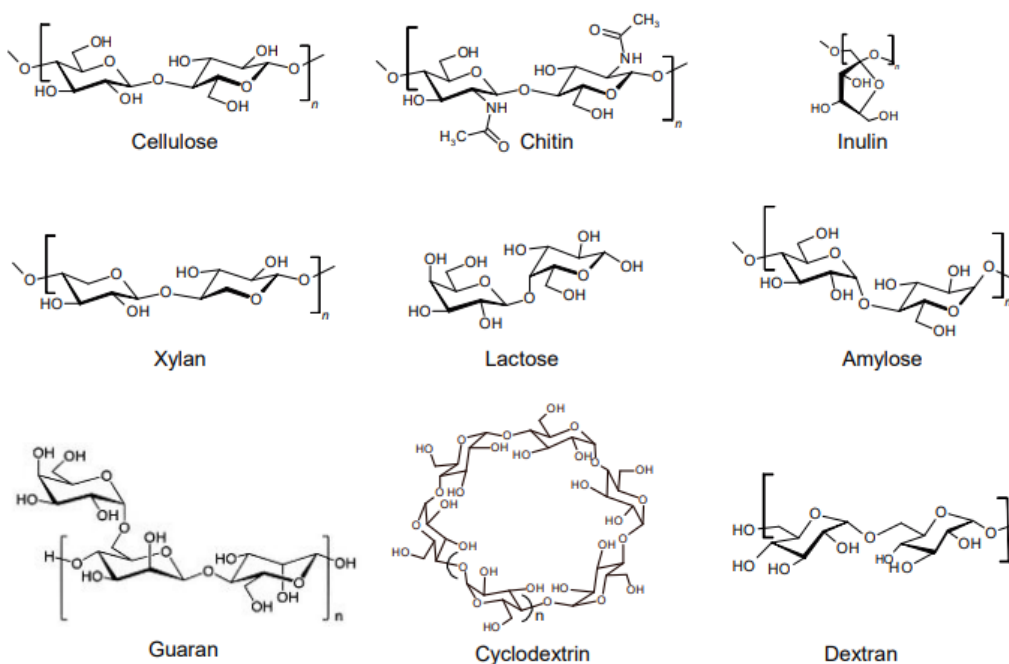
Figure 1.6 Different polysaccharides used as chiral selectors[59]

Additionally, polysaccharides can form asymmetric 3D structures with multiple enantioselective separation sites. Pioneering work on amylose and cellulose-based chiral materials was done by Y Okamoto *et al.*[45,60–62] Eric R. Francotte *et al.* studied different polysaccharides as chiral selectors.[59] The chiral monomeric and polymeric surfactant can

discriminate between the pair of enantiomers. The use of micelles has created a new field, micellar electrokinetic chromatography (MEKC) and capillary electrophoresis (CE), to separate neutral molecules.[63] Jian Wang *et al.* separated 1, 1-bi-2-naphthol, and laudanosine racemic mixture using chiral micelle polymer, poly(sodium N-undecylenyl-L-valinate). These micelles were added to the buffer solution to achieve chiral separations.[64] Proteins, which have various functionalities and intrinsic chirality from their naturally occurring L-amino acid content, can be employed as an excellent chiral selector for enantioselective separation of racemic mixtures. Alfonso Aguilar-Gallardo *et al.* reported separation of p- and m-Imazamethabenz-methyl Enantiomers using protein as a chiral selector by Direct Chiral HPLC.[65] Macrocyclic glycopeptides are naturally occurring chiral selectors produced by the microorganism. István Ilisz reported macrocyclic glycopeptide and cyclofructan-based chiral stationary phases for the enantioselective separation of phenylisoserine derivatives through HPLC.[66] Chirality induced into crown ethers by reacting with an enantiopure chiral compound can distinguish between enantiomers.[67,68] Reinhard Kuhn *et al.* used 18-crown-6-tetracarboxylic acid crown ether to separate a racemic mixture of different amine-containing compounds.[69] The mechanical stability of crown ether can be further improved by binding it to different inorganic stationary phases.[70,71]

Chiral Metal-organic framework (MOF) and covalent organic framework (COF) can act as excellent chiral selectors for enantioselective separation applications as it provides high specific surface area, porous morphology, and excellent stability. Yongwu Peng *et al.* used manganese-containing chiral MOF to separate benzylamine and its derivatives in reverse phase HPLC.[72] Hong Jiang reported Zirconium containing MOF with excellent stability as stationary phase in RP-HPLC for separating 16 different racemates.[73] Though COF are recently developed materials (2005), it attracts considerable attraction from the scientific community due to its utility to perform different applications.[74] In recent reports, Siqi Zhuo *et al.* synthesized carboxyl-functionalized COF (TpBD-3COOH) first and then integrated a chiral molecule, heptakis (6-amino-6-deoxy)-β-CD, to induce chirality. The simple filtration method used this chiral COF further as a chiral selector to separate the different amino acid racemic mixtures.[75] However, MOF and COF have limitations like non-uniform crystal growth, which generate defects and easy saturation of selectors.

Very few reports are available for using high Miller index metal surfaces as chiral selectors for enantioselective adsorption of enantiomers. Copper (Cu) metal surfaces are commonly

utilized as chiral selectors for the enantioselective separation of various amino acids in the literature.[73,76,77]
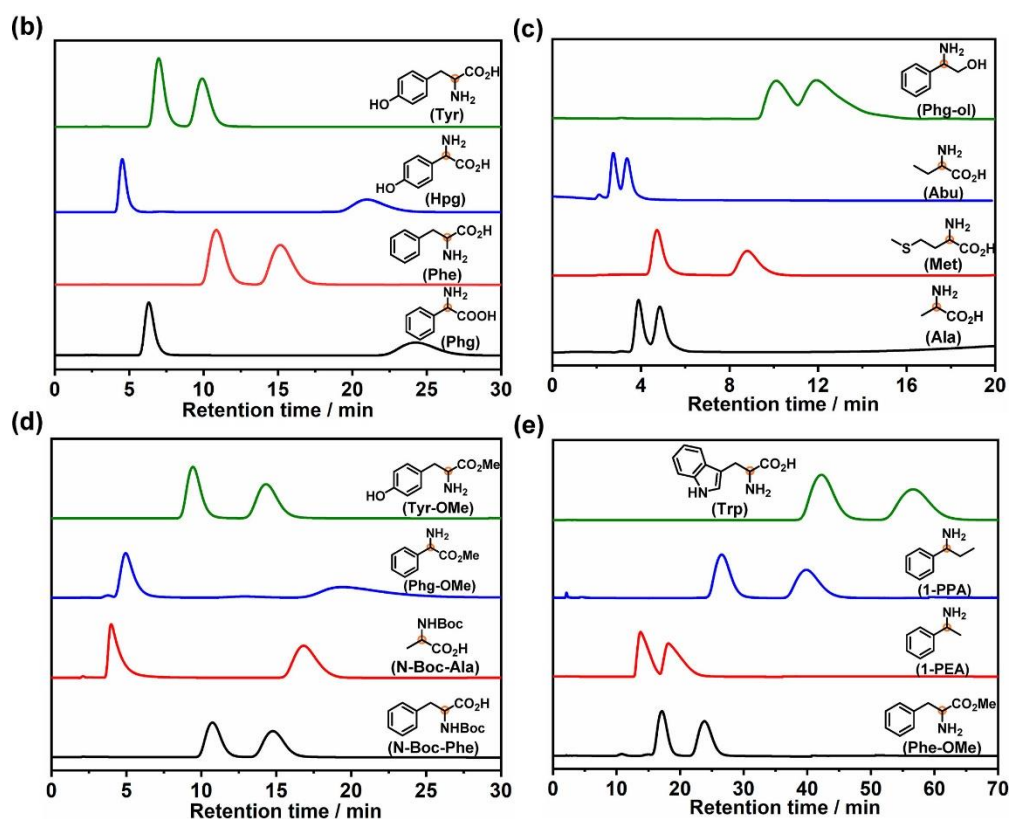
Figure 1.7 Zr based MOF used for the enantioselective separation of 16 different analytes in RP-HPLC[73]

Chiral polymers are a distinct class of material used as a chiral selector to separate a racemic mixture. The functional polymers provide multiple sites to undergo different interactions like hydrogen bonding, ionic interaction, steric interactions, or Van der Waals forces of attraction with the analytes.[78] Polymers show easy processability and can be fabricated in different porous morphology needed for the application. Additionally, polymers have moderate to excellent mechanical stability. The mechanical stability of polymer can be further improved by using inorganic materials to form a high-strength composite.[79–81] The polymers are classified into three classes (natural, synthetic, and semisynthetic) depending upon their origin. The naturally occurring polymers like cyclodextrins, polysaccharides, protein, and glycopeptides described above have intrinsic chirality and are used as chiral selectors. In the case of synthetic polymers, chirality can be induced by different methods like using chiral catalyst or environment during polymerization of achiral monomers, memory-based chiral induction, or directly polymerizing the chiral monomers. In chiral monomers, chiral centers can be a part of polymer backbone or pendant groups. Another

way to introduce chirality in polymers is by molecular imprinting with specific enantiomers. Detailed description with examples for each class is given below.

1.8 Chiral polymers

1.8.1 Polymerization of achiral monomers

Even achiral monomers that do not contain chiral centers anywhere in their structures can polymerize into chiral polymers with specific chirality or helicity and be used as chiral selectors. In these cases, specific chirality or helicity can be induced using a chiral catalyst, chiral molecular imprinting, or memory-based chirality induction strategy.

1.8.2 Chiral catalyst

The achiral monomers can polymerize into the chiral polymer with specific helicity by using a catalyst with chiral ligands. For the first time, Yoshio Okamoto reported the synthesis of one-handed helical polymethacrylate, PTrMA, with approximately 100 % isotacticity utilizing an achiral bulky monomer, the complex of n-butyllithium (n-BuLi) with chiral ligands.[82]

Toshiki Aoki et al. used a chiral catalytic system, [Rh(nbd)Cl]^2 (nbd: norbornadiene), and (R)/(S)-phenylethylamine as cocatalyst to synthesize a helical polymer from an achiral phenylacetylene monomer having two hydroxy groups.
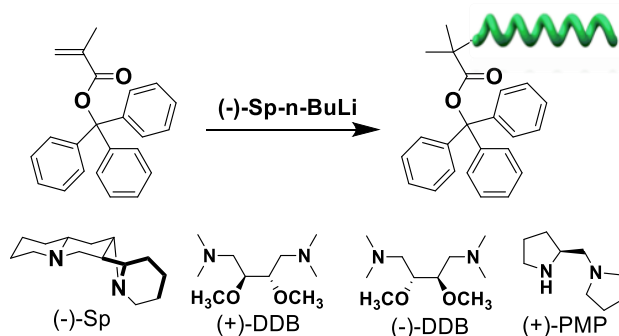
Figure 1.8 Representative example of chiral polymer synthesis from achiral monomer using chiral ligand containing catalyst.[82]

1.8.3 Memory-based polymers

When polymerized in the presence of external chiral molecules or extracted with specific solvents, achiral monomers induce specific helicity in the polymer structure. These external chiral molecules used during polymerization or solvents to extract

polymers induced external supramolecular chiral memory in resultant polymers. Even after removing these external chiral entities, the formed polymer retained chiral memory. These polymers with specific handedness and chirality were successfully employed to achieve racemic mixtures' enantioselective separation. Yin Zhao *et al.* first obtained chiral polyfluorene with preferred chiral memory using (R)- (+)-limonene and (S)-(−)-limonene which underwent sol-gel transition at -20 °C, which induced supramolecular chirality.[84]
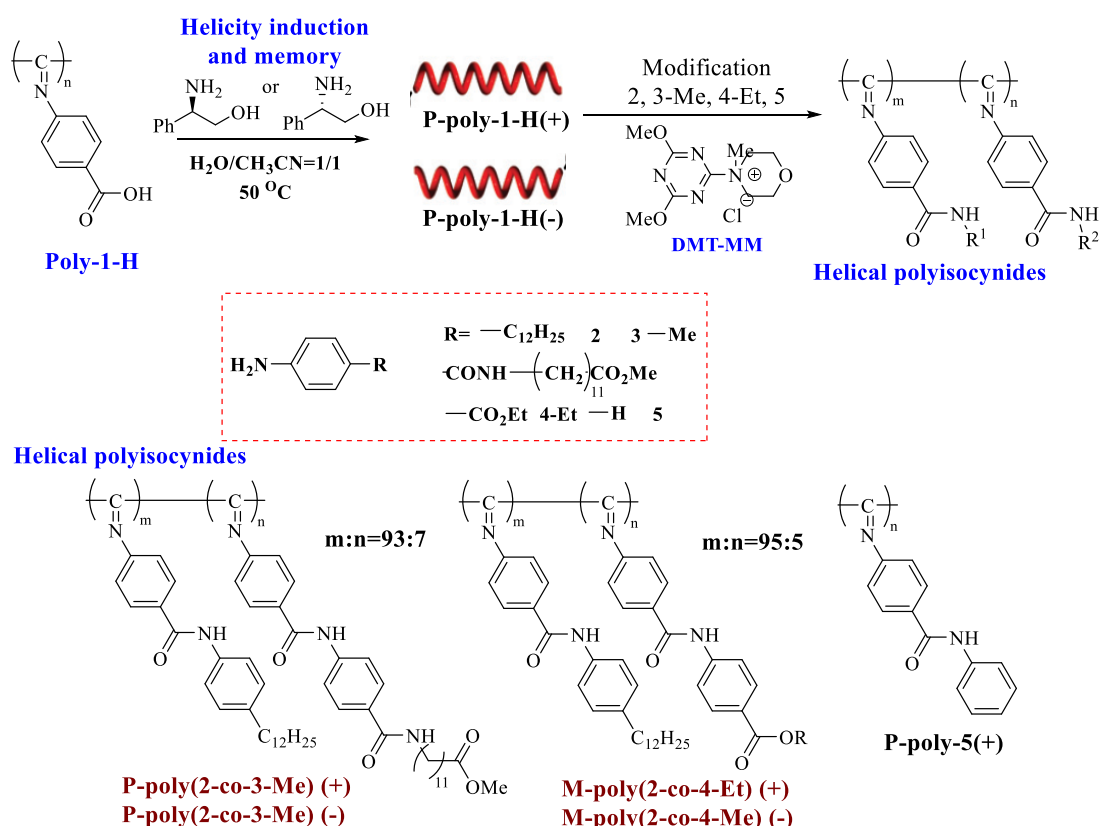
Figure 1.9 A schematic illustration of one-handed helicity induction using (S)- and (R)-phenylglycinol and further modification of the side groups[85]

Toshitaka Miyabe et al. in 2011 reported a noncovalent "helicity induction and memory technique" using (S)- and (R)-phenylglycinol to synthesize some optically active poly(phenyl isocyanide)s with achiral benzanilide pendant groups. The polymers with molecular helicity memory were immobilized on 3-aminopropyl-silanized silica gel by covalent linkage and used as chiral stationary phase in HPLC. Enantioselective separation of various racemates, including cyclic ether, amine, ketones, and metal acetylacetonate

complexes, was achieved using the columns.[85] Recently, Chuanqiang Zhou *et al.* published the synthesis of complex asymmetric nanostructure by oxidative polymerization of aniline into polyaniline (PANI) in a complete achiral environment (HCl/isopropyl alcohol/water solvent). The oligoaniline nanoribbon developed in the early stage had a specific right or left-handed twist depending upon the solvent composition. These nanoribbons acted as a sacrificial template for the growth of PANI on the surface. The oligomers then removed by solvent washing gave PANI having hollow nano twist morphology. The nano twists were used for the enantioselective separation of amino acid racemates.[86]
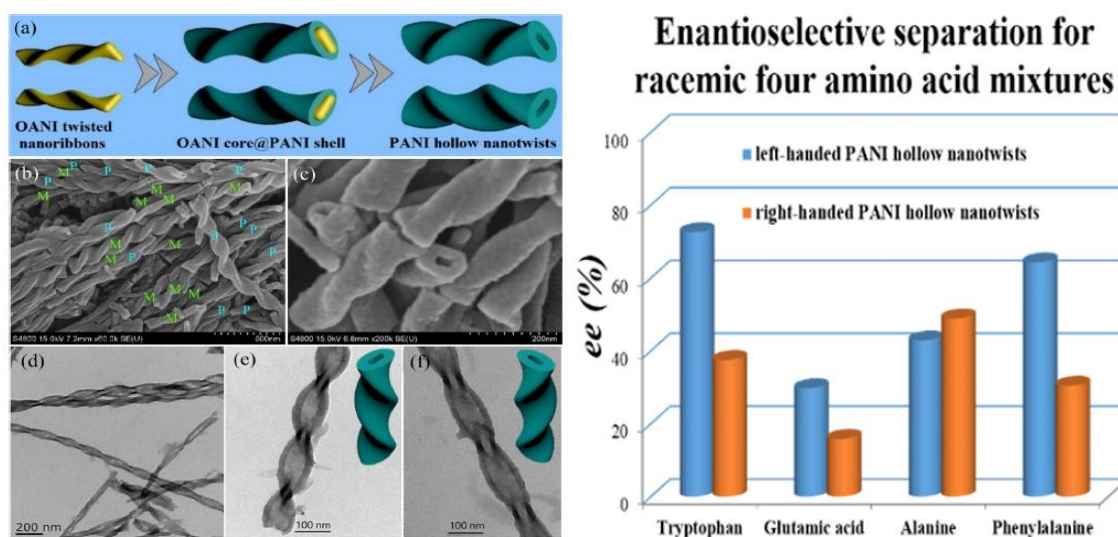
Figure 1.10 SEM micrographs of PANI hollow nano twist and its application in enantioselective separation of different amino acids[86]

1.8.4 Molecularly imprinted polymers

After molecular imprinting with enantiopure chiral molecules, the achiral polymer can also be used as a chiral selector. Covalent or noncovalent techniques are used to make molecularly imprinted polymers (MIPs), depending on the chemical composition of the template molecule and interactive functional groups. After removing templated molecules, the generated MIPs with a highly stereospecific void can enantiospecifically adsorb one enantiomer from the racemic mixture.[87]
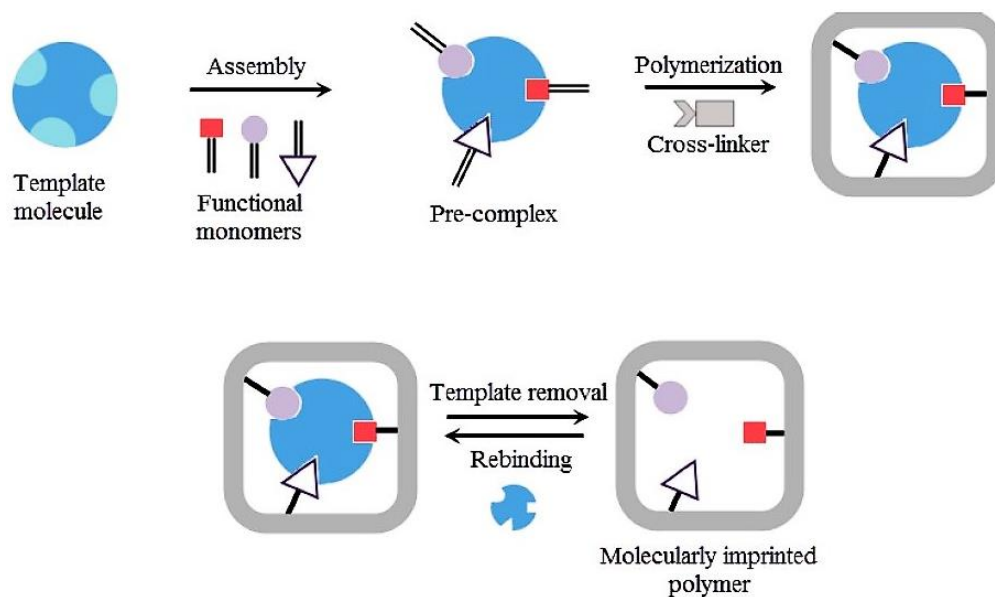
Figure 1.11 Schematic representation of molecularly imprinted polymer preparation[88]

These types of MIP with stereospecific voids have great potential to function as a chiral selector. Yidan Wang *et al.* synthesized magnetic surface molecularly imprinted polymers (MIPs) on γ-methacryl oxypropyl trimethoxy silane (MPS)-modified Fe3O4@SiO2 particle surface by utilizing chiral dehydroabietylamine (DHA) as a functional monomer and R-mandelic acid as a template molecule (DHAMIPs). These chiral MIPs were then utilized to perform chiral resolution of mandelic acid racemic mixture via enantioselective adsorption, where 53.7 % ee was achieved for the separation.[89]

The achiral polymers used in enantioselective separation have severe limitations, like low separation efficiency, the need for an expensive chiral catalyst, and enantiopure chiral molecules during polymerization. The induced chirality is highly sensitive to the solvent, pH, and temperature. Secondary structures formed are not stable as they result from weak interaction, and the alteration of the secondary structure can lead to the loss of the polymer's ability to carry out the enantioselective separation. Though the MIPs show better stability, they can separate only a particular molecule, and MIPs get saturated with time.

1.8.5 Polymerization of chiral monomers

The polymers with an inbuilt chiral center in their monomer structure are developed to overcome issues with achiral polymers. Chiral centers give intrinsic chirality and secondary helical structures to the polymers. The inbuilt chirality and secondary helical

structure help to achieve better enantioselective separation. The secondary structure of the polymer is not affected much by changing conditions as it forms through the interaction of multiple functional groups present in the polymeric structure compared to achiral polymers. Chiral polymers are further divided into two classes based on the position of the chiral center in the polymer structure, polymer with chiral backbone and polymer with chiral pendant groups.

1.8.6 Polymers with chiral backbone

The presence of a chiral center in the polymer backbone makes the polymer chiral by introducing helicity in the polymer backbone, resulting in a complex asymmetric 3D structure. A chiral center in the polymer backbone induces high mechanical stability to complex architecture as it is unaffected by solvent or other external factors. Jang Hoon Kim *et al.* reported the synthesis of stable sodium alginate (SA) membranes prepared using glutaraldehyde as a crosslinker. The polymer has different swelling indices. The membranes are used for optical resolution of amino acids, like tryptophan and tyrosine in a high-pressure membrane cell.[90] Paik *et al.* reported a synthesis of various block copolymers of PEG with protected polyglutamate or polyaspartate having a chiral center in the polymer backbone, which is further used to achieve chiral separation of a different amino acid racemic mixture.[91–93] The polymers having a chiral center in the backbone have some drawbacks, like a chiral center in the backbone is not accessible for the analyte, thus showing low separation efficiency values.
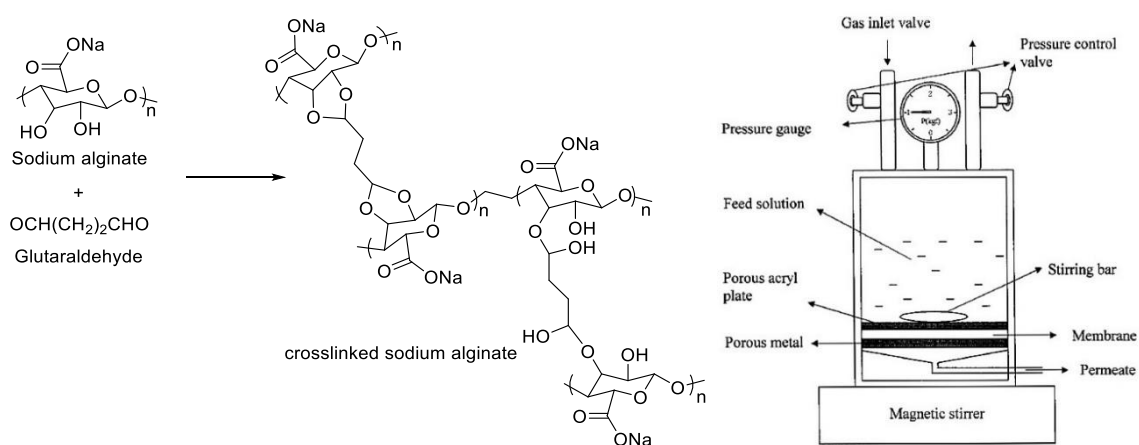
Figure 1.12 Schematics for the synthesis of SA enantioselective membranes and high-pressure membrane cell[90]

1.8.7 Polymers with chiral pendants

The chiral polymers with flexible chiral alkyl groups are of great interest as it provides easy accessibility of chiral center for the enantioselective separation. Additionally, post polymer modification can add multiple chiral centers to the polymer structure, further improving the interaction between analyte and polymer. Reports are available where chiral pendant containing polymers were successfully employed to carry out enantioselective separation of different analytes like drugs, amino acids, sugars, amino alcohols, esters, acids, and different commercially valuable compounds like agrochemical products or food products. In 2015 Senthilkumar *et al.* reported the synthesis of chiral polyfluorene having protected L-glutamic acid as pendent. The chiral polyfluorene formed an α-helical porous morphology that separated racemic mixtures of different analytes like amino acids, sugars, amino alcohols and acids with excellent % ee.[55] Ahmad F. K. reported phosphoramide-methacrylate monomers, hydroxy functionalized monomer and crosslinker containing polymer where phosphoramide-methacrylate monomer was a part of the pendant group. This polymer-based hydrogel was packed in a teabag and used for enantioselective separation of α-methylbenzylamine, alanine, valine, tartaric acid and phenylalanine racemic mixture by simple filtration.[56]

Figure 1.13 Representative examples of enantioselective separation by enantioselective filtration method by using a) chiral polyfluorene[55] b) phosphoramide-methacrylate containing polymer hydrogel[56]

In a recent report, Yanli Zhou synthesized two phenylacetylene derivatives containing different L-proline dipeptide sequences. Then, these dipeptides polymerized successfully, employing Rh(nbd)BPh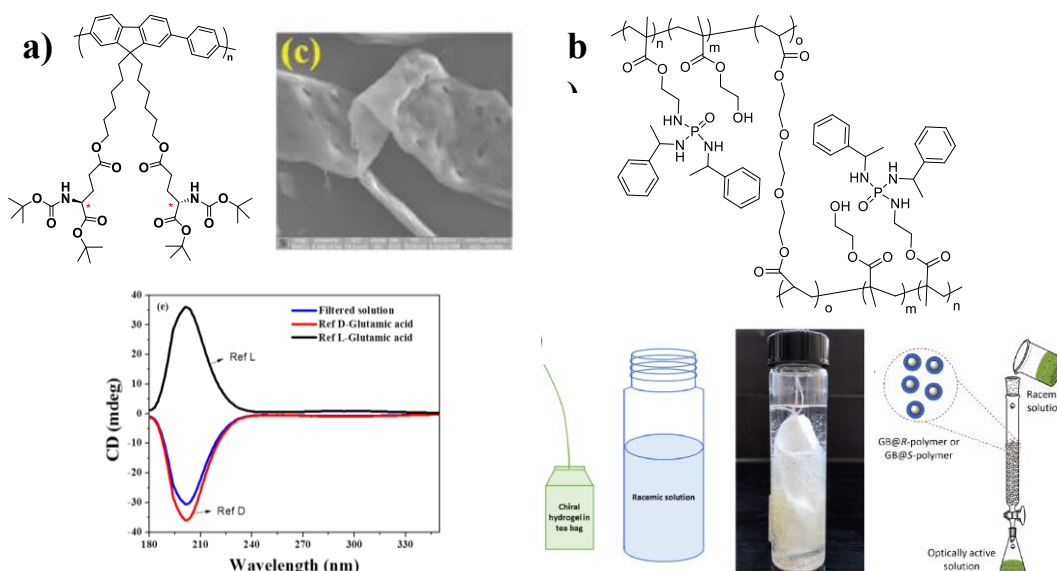$_4$ as a catalyst. The solvents and chiral pendants produce a one-handed helical structure in the polymers. The polymers were further checked for enantioselective separation application as chiral stationary phase for HPLC.[94] In another report in the same year, the same group reported the synthesis of phenylacetylene derivatives having two chiral centers.

The Rh(nbd)BPh$_4$ catalyst was then used to polymerize these monomers. The synthesized polymer showed specific chirality where two chiral centers and solvent influenced the handedness. The polymer bearing two chiral centers with an S–R configuration showed high order steric sense than others with an S–S configuration. The polymer bearing two chiral centers showed better chiral recognition abilities than earlier reported polymer with one chiral center in a pendant.[95]

1.9 Comparison between different chiral polymers

Among all types of polymeric chiral selectors discussed above, the polymer with the chiral pendant groups is of great interest as it has intrinsic chirality and easy accessibility of chiral centers present in the flexible pendants. The chiral polymers synthesized from the polymerization of achiral monomers produce asymmetric polymer architecture with specific helicity, which is sensitive toward change in conditions like pH, temperature, or solvent as it is formed by the weak interactions or specific arrangement of achiral monomers. In the case of an imprinted polymer, the formed void is so stereospecific that only a particular enantiomer fits into it and cannot be used to separate another compound. Additionally, MIP can be saturated easily. The chiral polymer with a chiral center in the polymeric backbone shows good stability of the formed asymmetric structure. However, a chiral center in the core part of the structure makes it inaccessible to analyte enantiomers, hindering its enantioselective separation efficiency. Polymers with flexible alkyl groups as a pendant can solve both the problems, where chiral center in the pendant can induce chirality in polymeric backbone at the same time flexibility of alkyl chain makes it easily accessible for analytes.

1.10 Limitations and scopes in polymeric chiral selectors

The standard limitation of using a polymer as a chiral selector is maintaining the balance between mechanical stability and accessibility of the chiral center. The accessibility of the chiral center can be addressed by using a chiral polymer with flexible alkyl handles. The

mechanical stability of polymers can be enhanced by coating on rigid organic or inorganic substrates. The reports are available where chiral polymers were coated or chemically immobilized on a different substrate, which can be used as a stable chiral stationary phase in the HPCL or perform the separation operation for a more extended period.[96] Paik *et al*. reported the synthesis of different block-co-polymers using PEG as macroinitiators to grow second blocks of different amino acids like D/L-aspartic acid, D/L-glutamic acid, and D/L - phenylalanine. These chiral block copolymers were templated on different substrates like mesoporous polypyrrole (PPy) or mesoporous silica (MS) particles.[91–93]

Porous morphology is highly recommended in polymer architecture to improve its separation efficiency. In the case of nonporous polymers, porosity can be incorporated by coating or immobilizing on the mesoporous or microporous organic or inorganic templates.[97] Additionally, techniques like breath figure methods can also help to achieve porous morphology.[98] Materials with a high surface area are desirable for improving the enantioselective separation efficiency as enantioselective adsorption is a surface phenomenon. The surface area can be improved by synthesizing polymers with intrinsic porous morphology, which have inbuilt high specific surface area.[55] The surface area can also be improved by coating polymer on a porous template or making polymeric microspheres or nanospheres.[49]

1.11 Mechanism of enantioselective separation

The identical behavior of the enantiomers in their chemical and physical properties in an achiral environment makes molecular recognition highly difficult. These difficulties make the enantioselective separation highly challenging and an important field of research. The difficulties in molecular recognition can be resolved by using chiral selectors to distinguish between enantiomers. Additionally, the structure and size of the chiral selectors play a vital role in choosing the correct chiral selector. The chiral selector should be of similar size and structure as the analyte for effective separation efficiency. The exact mechanism for the enantioselective separation is still not realized completely. The reason for this is the complex structures of the chiral selectors. Very little is known about the exact structure of the derivatized macromolecules and polymers. Sometimes computational molecular modeling can be helpful but cannot precisely understand the exact behavior as a solvent system can affect the interactions drastically.[99] The critical step in chiral recognition is forming a transient diastereomeric complex of different Gibbs free energy between the chiral selector

and enantiomers.[100] The chiral selectors with absolute chirality form long-lived transient state diastereomeric complexes with enantiomers that differ in their thermodynamic stability, solvation in the liquid mobile phase, or binding energy with the solid support. The difference in the thermodynamic stability, solvation, and binding can be well explained by the "three-point interaction model" suggested by the biologist Easson and Stedman in 1933.[101] The model was introduced to understand the stereochemical differences in pharmacological activity. The model suggested that the chiral recognition depended upon the degree of interactions between the enantiomers and the chiral selector. One enantiomer (eutomer) reacts with all three points simultaneously, while the other enantiomer (distomer), which differs in terms of the spatial arrangement of atoms around the chiral centre, can interact through a maximum of two points.[102]

Enantiomer (I)   **Enantiomer (II)**
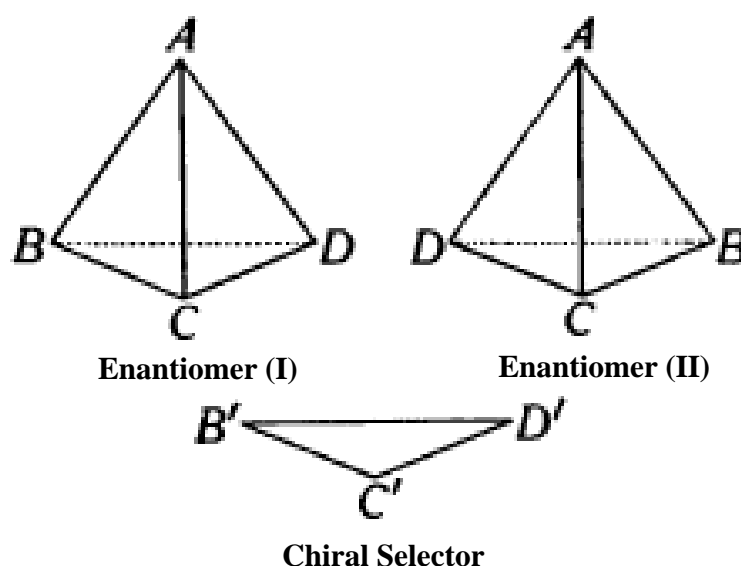
Chiral Selector

Figure 1.14 Three-point interaction model representation[101]

In Figure 1.14, two enantiomers (I) and (II) form long lived transient state complex of different energy with chiral selector (given below in figure 1.14). It can be seen from Figure 1.14 that the chiral selector can interact through all three points B' C,' and D' with corresponding three points (B, C, and D) on the enantiomer (I), but can react through only one point (C') with enantiomer (II). The interaction can be of both types, repulsive or attractive, and depends highly upon the structure, functional groups, bulkiness, and charges around the chiral center of selectors and analytes. Though the three-point interaction model has been widely accepted, recently Tristan D. Booth *et al.* argued that the biomolecules like enzymes interact using spatial environment or cavity and not through particular points.[103]

Andrew D. Mesecar *et al.* separately challenged the three-point interaction model by taking the example of D- and L-isocitrate.

When the D/L-isocitrate racemate was introduced to isocitrate dehydrogenase, the L-isocitrate bonded exclusively to the protein crystals in the absence of Mg^+, whereas the D-isomer binds in the presence of Mg^+. The crystal structure of isocitrates revealed that three of the four groups on the following carbon atom attach to the same three residues, not the fourth. As a result, it may be concluded that in the active site of proteins, not three but four sites are required to distinguish between the two enantiomers.[23] The three-point interaction model cannot explain this as it does not consider the direction of the approach. Thus, the "four location model" was introduced to explain such cases where the direction of approach was taken into consideration.
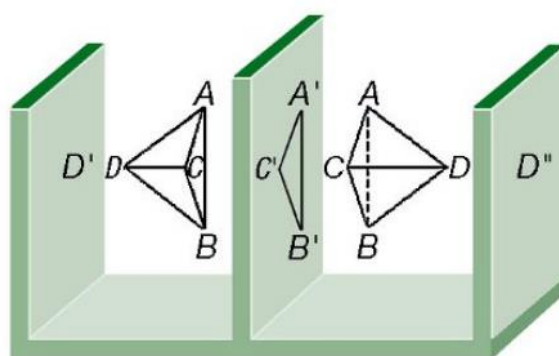
Figure 1.15 Four location model where the direction of analyte binding involves the fourth point in chiral recognition[23]

Though some models explain the specific cases considering special conditions and interaction, the three-point interaction model is the most common and widely accepted. The enantiomers and chiral selectors interact through different forces like electrostatic interactions, dipole-dipole interactions, hydrogen bonding, steric interactions, Van der Waals forces. The details about the different types of interactions, their strength, direction, and ranges are given in the table[102]

Type of interaction	Strength	direction	range
Coulomb or electric	Very strong	Attractive or repulsive	Medium
Hydrogen bond	Very strong	Attractive	Long
Steric hindrance Very	Very strong	Repulsive	short
π-π	Strong	Attractive (donor or acceptor) or repulsive	Medium
Ion–dipole	Strong	Attractive	Short
Dipole–dipole	Intermediate	Attractive	Short
Dipole-induced dipole	Weak	Attractive	Very short
London dispersion or Van der Waals	Very weak	Attractive	Very short

Table 1.2 Different types of interactions and their characteristics[102]

The separation mechanisms and the type of interaction depend highly on the nature and type of chiral selectors. Depending upon origin, the chiral selectors are divided into three categories: synthetic, semisynthetic and natural chiral selectors. The details about the type of chiral selector, its mechanisms, and the primary interaction involved in binding to analytes are given in Table 1.3.

Selector	Mechanism	Primary interaction
Synthetic selectors		
Ligand exchange	Diastereoisomeric Selector-metal-ion-analyte complex	Coulomb or ion-dipole
π-Complex	Transient three-point selector-analyte association	π- π
MIPs	Key-and-lock association	Selective shape interaction with the imprint
Chiral crown ethers	Inclusion complexation	Ion–dipole
Polymers	Diastereoisomeric selector–analyte complex	Hydrogen bond
Natural selectors		
Proteins	Multiple binding sites	Variable
Polysaccharides	Insertion into helical structures	Hydrogen bond, dipolar, or steric
CDs	Inclusion complexation	Hydrogen bond
Macrocyclic glycopeptides	Multiple binding sites	Variable
Cinchona alkaloids	Ion pairing	Coulomb

Table 1.3 Table lists the different chiral selectors, their mechanism, and type of interaction it undergoes with enantiomers[102]

Additionally, the enantioselective recognition ability of the chiral selector depends strongly upon the composition, temperature, and pH of the mobile phase. Thus, separation media or mobile phase optimization should be accomplished to achieve maximum separation efficiency.

1.12 Polymers and methods- our choice

1.12.1 polyfluorene

Polyfluorenes are π-conjugated conducting polymers which have a planar biphenyl unit coupled through an sp3 hybridized carbon atom at the ninth position in the backbone. The aromatic backbone of polyfluorene enables a natural tendency to absorb and emit light. Because of the π-π* transition with a single peak maximum, the polyfluorenes absorb at around 387 nm. Polyfluorenes emits a bright blue colour in the 400-450 nm range due to three well-defined vibrionic transitions corresponding to the 0-0, 0-1, and 0-2 intrachain singlet transitions. The most powerful peak is the 0-0 fundamental transition. Polyfluorenes show an excellent quantum yield of >50 % in solution and solid-state. The two hydrogens on the ninth carbon atom are substituted with different functional groups, bringing processability that is essential in developing polymer for specific applications. Polyfluorenes find potential application in organic light-emitting diodes (OLED), organic field-effect transistor (OFET), solar cells, chemo, and biosensors. The polyfluorene shows intrinsic helicity and can be made chiral using a flexible chiral alkyl chain as a pendant on the carbon atom at the ninth position. Polyfluorene chemical structure is shown in Figure 1.16
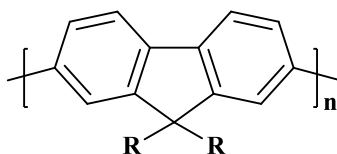
Figure 1.16 Representation of the chemical structure of polyfluorene.

1.12.1a Synthesis of polyfluorenes:

The polyfluorene undergoes aggregation due to strong π-π interactions. Thus, the dialkylated fluorene monomers are used for polymerization. The formed poly(dialkylfluorene)s (PDAFs) show good solubility, making it easily processible. The functionalization of dialkylfluorene monomers provided a solid foundation for the synthesis of several PDAF derivatives for varied applications depending on the nature of pendants. The standard methods practiced to synthesize PDAFs are described below. PDAFs can be synthesized by oxidative coupling of fluorene monomer using iron(III) chloride. Using this methodology,

Yoshino et al. synthesized Poly(9,9-dihexyl-2,7-fluorene) with low molecular weight (5000).

Figure 1.17 Synthesis of poly(dialkylfluorene) by oxidative coupling.

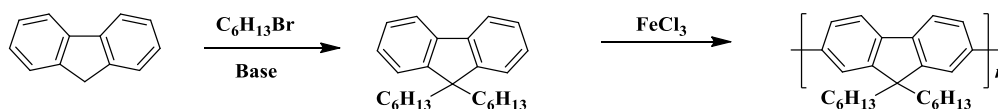This synthetic method is avoided as it produces a polymer with a low degree of polymerization and oxidative addition can happen at other positions than second and seventh, which generates defects in the polymer structure and drastically reduces its fluorescence efficiency. Suzuki polymerization is adapted to polymerize 2,7-dibromofluorene monomers (figure 1.18).
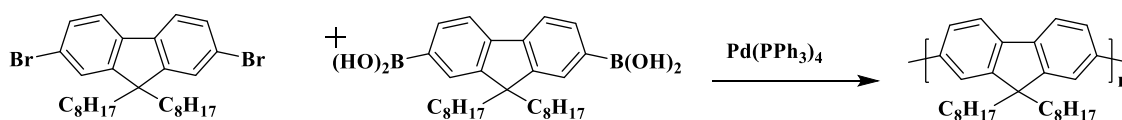

Figure 1.18 Synthesis of Polydialkylfluorene through Suzuki polycondensation.

In less than 24 hours reaction, poly(9,9-dioctylfluorene) with an Mn >100,000 g/mol was produced. Copolymers of polyfluorenes with 1,4-phenylboronic acid/ester or thiophene monomers are also synthesized by the same methods or by Heck, Sonogarshira, and Stille coupling polymerization. Polyfluorenes have also been synthesized utilizing Yamamoto or Kumada coupling with a Ni(0) catalyst. Recently adapted relatively green method like direct hetero arylation (DHAP) is also used to synthesize fluorene copolymers.

1.12.2 Fluorene-thiophene copolymers synthesis by DHAP

Fluorene-thiophene copolymers are a class of π-conjugated conducting polymers. These polymers find their applications in optoelectronics, photovoltaics, and organic solar cells. Well-known coupling reactions like Suzuki[104,105] Stille,[106] Grignard Metathesis[107] are conventionally used to synthesize these copolymers. All these methods need pre-functionalization of monomers as an additional step, and these coupling reactions produced a stoichiometric amount of hazardous organometallic by-products. Additionally, these metallic impurities in the polymers hamper their performance and are not recommended for biological applications. The recently adopted unconventional direct heteroarylation

polymerization (DHAP) method solves these problems. The method does not require pre-functionalization of monomer (as it is a reaction between the activated aromatic hydrogen and aryl halide), making it economically favorable. Additionally, by-products of reactions are comparatively less hazardous, making it a green process than traditional processes.[108]
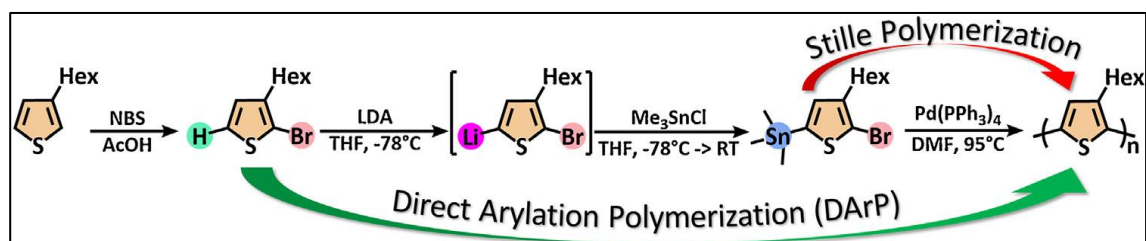

Figure 1.19 Schematic representation of comparison between Stille and DHAP[108]

1.12.3 Effect of appendages on polyfluorenes:

Appending different groups to polyfluorenes is important for deciding their uses since it modifies the characteristics of the polyfluorenes. The pendants used are alkyl chains, aromatic pendants, polar pendants and chiral pendants.

Alkyl chains such as hexyl, octyl, decyl, and dodecyl improve the solubility and processability of polyfluorene. Additionally, these alkyl pendants also determine the morphology. The polar pendants are an exciting pendant class as they enhance the properties and applicability in OLED, OFET, chemo, and biosensors. The polar pendant groups are divided into polar ionic and neutral polar pendants. The polar ionic pendants like cationic, anionic, and zwitterionic pendants containing polyfluorenes are called conjugated polyelectrolytes. The ions in the pendent groups make the polymer water-soluble, which is used in biological applications. These charges help the polymer to interact strongly with analytes through ionic interactions. The neutral pendants such as sugars and ethylene glycol improve water solubility and specificity in recognizing targeted analytes.

Another important class of pendants is a chiral pendant. The chiral pendant can induce chirality to the polymer backbone by conferring three-dimensional structures with specific helical morphology. Chiral pendants such as chiral alkyl chains, chiral binaphthol units and amino acids induce asymmetry in the polymer structure. Chiral polyfluorenes pack efficiently, resulting in a high level of crystallinity which enables efficient charge transfer, thus finding applications in electronic devices. Other areas of application of chiral polymers are in photonics, as a chiral catalyst, in enantioselective sensing and separation. Senthilkumar *et al.* reported the synthesis of protected L-glutamic acid-containing polyfluorene as a chiral selector for the heterogeneous enantioselective separation of

different racemic mixtures. Further deprotection gave water-soluble polyfluorene which was used for the Fe^{2+} ion sensing with very high selectivity and sensitivity and live-cell imaging.[55,109]
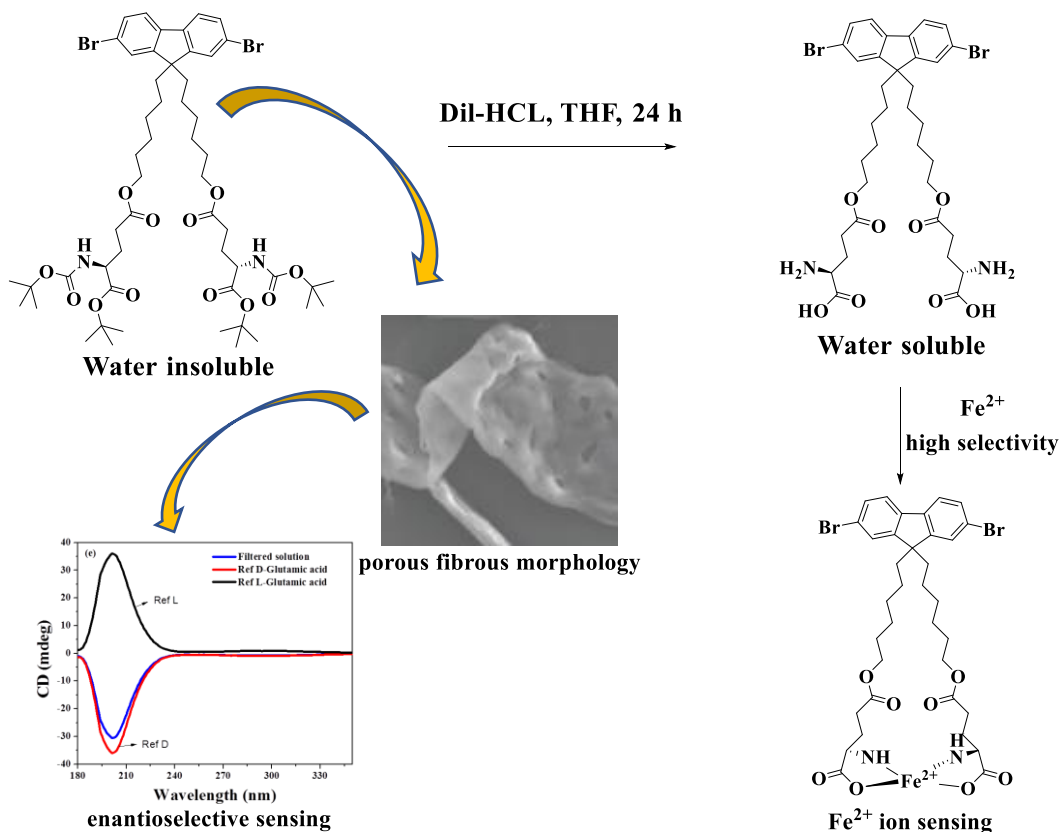
Figure 1.20 Polyfluorenes with chiral pendant groups and their application in enantioselective separation and Fe2+ ion sensing and live-cell imaging[55,109]

1.12.4 Polystyrene

Polystyrene is one of the highest commercially valued polymers, with 7% of total polymer consumption worldwide. The properties like optical clarity, rigidness, brittleness, moderately strong behaviors, lack of crystallinity and good thermal and electrical insulation properties make it a material of choice for commodity application. Its solubility in a halogenated or aromatic solvent at room temperature eases its processability.

1.12.4a Polystyrene synthesis

Polystyrene is synthesized by polymerizing petroleum-based styrene monomers by chain growth polymerization, where monomer gets added to the end of the growing polymer chain. The polymer molecular weight increases with an increase in time. The four most common

types of polymerization are free radical, anionic, cationic and coordination. Radical polymerization is of great commercial interest due to ease of reaction. In radical polymerization, radical initiators like AIBN are used, which initiate the chain propagation by reacting with a double bond of styrene monomer.
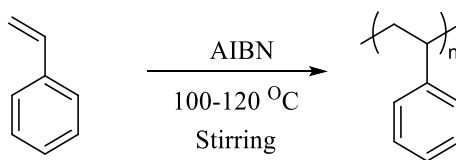

Figure 1.21 Schematic representation of polystyrene synthesis by radical polymerization

The chain growth polymerization has the advantage that polymer can be synthesized with and without using solvent (bulk polymerization). However, getting control over the molecular weight and polydispersity (PDI) is challenging. Controlled radical polymerization (CRP) or living radical polymerization was developed to avoid these problems. The first "controlled" living polymerization was reported by Krzysztof Matyjaszewski, where halogenated compounds were added to the polymerization and called atom transfer radical polymerization (ATRP).[110] In 1993, Georges published his first paper on the synthesis of the bulk radical polymerization of styrene in the presence of nitroxy compound where TEMPO was used as a radical stabilizer. The process is called nitroxy mediated polymerization (NMP), where reasonable control over the molecular weight and PDI was achieved.[111] After the first report in 1998 by Rizzardo *et al.* on reversible addition-fragmentation chain transfer (RAFT), the polymerization method became versatile where control over molecular weight and PDI was achieved.[112] In RAFT polymerization, a thiocarbonylthio group maintained the balance between dormant and active growing chain species, which helped to achieve control over molecular weight and PDI. The mechanism of the RAFT polymerization is given below in Figure 1.22. The method is of great interest that between 2013-2016, almost 900 research articles were published every year. The method is so versatile that it can be helpful for the different monomers and their derivatives containing different functional groups.[113]
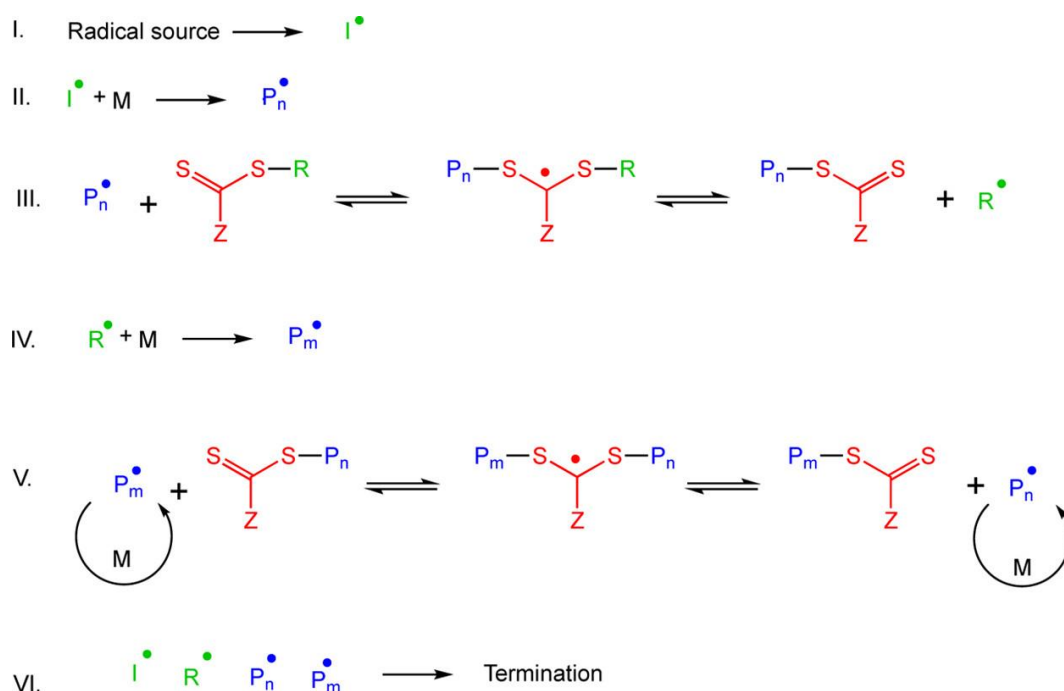
Figure 1.22 Proposed Mechanism of Reversible Addition−Fragmentation Chain Transfer Polymerization[113]

1.12.4b Post polymer modification on polystyrene

Living polymerization like RAFT provides an additional advantage. It allows another block to grow on the existing polymer where properties of the existing polymers can be modulated according to need and by maintaining the length of each block, different polymer morphology can be obtained.[114,115] Additionally, aromatic polystyrene rings are also available where post polymer modification can be done with electrophilic substitutions like sulfonation, chlorosulfonation, nitration, Friedel Crafts acylation, and alkylation. Ngadiwiyana *et al.* reported sulfonation of polystyrene by reacting with sulfuric acid and sulfonating agents, which improved the conductivity of formed polyelectrolyte.[116] Anselmo del Prado reported the chlorosulfonation of polystyrene, which generated the modified polystyrene with improved transparency; these chlorosulfonated polystyrenes were then used in ELISA assay.[117] Mukul Biswas *et al.* synthesized modified carboxylic acid-containing polystyrene by reacting polystyrene with phthalic anhydrides and its derivative by Friedel Craft acylation.[118] A similar report for acylation of polystyrene using anhydride is reported.[119] Polystyrene can also undergo acylation or alkylation using acid chloride or alkyl halide of organic compounds.[120]

1.12.5 Overview of appendages, post polymer modification, and applications in the thesis

This thesis develops polymeric chiral selectors to carry out enantioselective separation of an aqueous racemic mixture of different amino acids. We used polyfluorene containing four chiral pendents like protected L-aspartic acid, D-aspartic acid, L-glutamic acid, and L-tryptophan as chiral selectors. In other cases, post polymer modification on polystyrene was done using N-phthaloyl protected L-leucine acid chloride.

1.12.5a Appendages explored in the thesis

a) Appendage I: L-Aspartic acid

L-aspartic acid is one of the building block constituents of protein structure. It is a non-essential amino acid, which means it can be produced by the body. Under physiological conditions, it is negatively charged due to carboxylate ion in the alkyl chain. Aspartate is a precursor for other amino acids like methionine, threonine, isoleucine, and lysine. It is a urea cycle metabolite that contributes to gluconeogenesis. Figure 1.23 shows the structure of L-aspartic acid
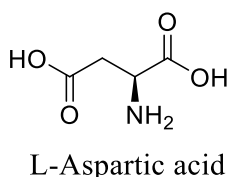
L-Aspartic acid

Figure 1.23 Chemical structure of L-aspartic acid

b) Appendage II: D-Aspartic acid

D- aspartic acid is a negatively charged non-proteogenic amino acid due to carboxylate ions in the alkyl chain. D-aspartic acid is used to boost testosterone levels. It primarily works by boosting the levels of follicle-stimulating hormone and luteinizing hormone, which stimulates the testes' Leydig cells to generate more testosterone. The chemical structure of D-aspartic acid is given in Figure 1.24
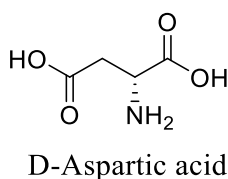
D-Aspartic acid

Figure 1.24 Chemical structure of D-aspartic acid

c) Appendage III: L-Glutamic acid

L-glutamic acid is a proteogenic amino acid. It is negatively charged (glutamate) due to the carboxylate ion in the alkyl chain. Monosodium glutamate is generally added to chinese food as a flavor enhancer. Glutamic acid is mainly involved in cellular metabolic processes. It acts as a neurotransmitter in the nervous system. Glutamate is also a precursor for the inhibitory amino acid gamma-aminobutyric acid (GABA). The structure of L-glutamic acid is given in Figure 1.25
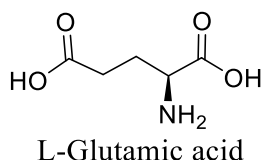
L-Glutamic acid

Figure 1.25 Chemical structure of L-glutamic acid.

d) Appendage IV: L-Tryptophan

L-Tryptophan is an essential amino acid. It is a constituent of protein structure. The presence of an indole ring makes it aromatic amino acid with intrinsic fluorescent properties. It is a neutral amino acid in physiological pH. It is an essential amino acid, and the body cannot synthesize it. Tryptophan is a precursor to serotonin, melatonin, and vitamin B3. In several European nations, L-tryptophan is prescribed to treat severe depression. The structure of L-tryptophan is given in Figure 1.26.
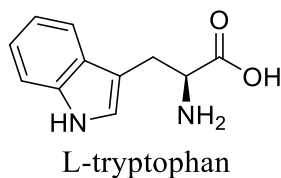
L-tryptophan

Figure 1.26 Chemical structure of L-tryptophan.

e) Appendage V: L-Leucine

L-Leucine is an essential proteogenic amino acid. The side chain contains an isobutyl group. It is a non-polar aliphatic amino acid present in the zwitterion form. In humans, leucine and a minor leucine metabolite, β-hydroxy β-methylbutyric acid, have a pharmacological effect and increase protein production. The chemical structure of leucine is given in Figure 1.27
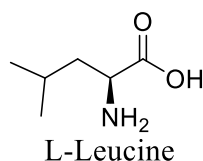
L-Leucine

Figure 1.27 Chemical structure of L-leucine.

1.12.6 Membranes and microspheres

The mechanical properties, surface area, porosity and 3D confinement of the polymer structures are essential in the enantioselective separation applications. Paik *et al.* reported the use of mesoporous silica and polypyrrole as templates for coating polymer, which provide mechanical stability and high surface area for separation. The membrane can also provide the porous architecture required for separation and confine the 3D structure.[50] The surface area of polymers can also be improved by preparing macro or nanospheres.

1.12.7 Enantioselective filtration methods

Enantioselective adsorption on the polymer surface followed by simple filtration can be a cost-effective and straightforward alternative to costly equipment and skilled labor requiring chromatographic methods.[55,56] We have developed a competitive assay for the enantioselective separation of analytes in their native form by simple filtration-based protocol, which is reported in this thesis. The polymer-coated membranes (commercially available nanoporous AAO membranes) or microspheres can be directly suspended in the aqueous racemic mixture of native analytes followed by enantioselective adsorption of one of the enantiomers. The method will not require high-end chromatographic instruments or a skilled workforce, making the method cost-effective and easy to operate.

1.13 Aim of the thesis

The above thorough literature survey about the need for enantioselective separation, different methods and materials available for the separation and separation mechanism showcased the importance of developing robust, simple, cost-effective and scalable enantioselective separation methodology and understanding the mechanism. This thesis aims to develop polymer-based chiral selectors and a cost-effective and straightforward enantioselective separation protocol.

Although different polymeric chiral selectors are currently available, which are associated with complicated synthesis or need several chiral monomers and crosslinkers in a fixed proportion, or sometimes separation takes longer. Additionally, there is a need to develop an enantioselective separation method that is simple, cost-effective, and does not require high-end chromatographic instruments. In this thesis, we report the design of polymers like polyfluorene with a chiral pendant like protected D/L-Aspartic acid, protected L-glutamic acid, protected L-tryptophan and cost-effective commodity polymers like chiral polystyrene

synthesized by post polymer modifications and simple filtration based enantioselective separation methodology using these chiral polymers. The enhanced mechanical stability, porosity and high available surface area can be incorporated into the polymer by coating it on commercially available porous Anodic aluminium oxide membranes (AAO) or by preparing polymeric microspheres in case of chiral polystyrene. The thesis also reports the synthesis of fluorene-thiophene chiral π-conjugated polymers using a relatively green approach of direct heteroarylation polymerization (DHAP).

The key features of synthesized polymeric chiral selectors and developed methods are highlighted below.

1) The protected D/L-aspartic, L-glutamic acid, L-tryptophan acid-containing polyfluorenes with moderately high molecular weight and low PDI are synthesized using the simple Suzuki polymerization method.

2) The chiral polyfluorene-coated porous AAO membranes are used in simple filtration-based enantioselective separation of native amino acids without any high-end chromatographic instrument.

3) Exceptionally high % ee could be achieved with these chiral membranes compared to the available literature.

4) Polystyrene with desired molecular weight and low PDI was synthesized by RAFT polymerization followed by efficient post polymer modification with chiral protected L-leucine by Friedel Crafts acylation.

5) The polystyrene microspheres were prepared and used for simple filtration-based enantioselective separation of amino acids.

6) The chiral π-conjugated fluorene-thiophene copolymer was synthesized by a green and cost-effective direct heteroarylation (DHAP) approach and studied for their structure-property relationship.

The thesis mainly emphasized the following mentioned aspects

a) Development of the polymeric chiral selectors for enantioselective separation applications.

b) Development of simple, efficient, and cost-effective enantioselective separation assay.

c) Using commodity polymer for carrying out enantioselective separation of amino acids by simple filtration method.

d) Improving the polymer surface area and porosity by using inorganic porous AAO membranes or preparing polymer microspheres.

e) Achieving a high degree of enantioselective separation of analytes in their native form without chemical modification.

f) Understanding the mechanism of separation and types of interactions between polymeric chiral selectors and analytes.

g) Synthesizing chiral π-conjugated polymers by simple, cost-effective, and green method.

The aim of the thesis and comparison between commercially available chiral selectors summarized in the literature demonstrated the need for synthesized polymeric chiral selectors and developed simple enantioselective separation methods.

The overall outcome of polymeric chiral material synthesized and developed enantioselective separation methods in the present Ph.D. is summarized in chapter 6 with its future perspective.

1.14 REFERENCES

(1)   Gal, J. Pasteur and the Art of Chirality. *Nat. Chem.* **2017**, *9* (7), 604–605.

(2)   Gal, J. Molecular Chirality in Chemistry and Biology: Historical Milestones. *Helv. Chim. Acta* **2013**, *96* (9), 1617–1657.

(3)   Avnir, D. Critical Review of Chirality Indicators of Extraterrestrial Life. *New Astron. Rev.* **2021**, *92* (July 2020), 101596.

(4)   Grossman, R. B. Van't Hoff, Le Bel, and the Development of Stereochemistry: A Reassessment. *J. Chem. Educ.* **1989**, *66* (1), 30–33.

(5)   Glavin, D. P.; Burton, A. S.; Elsila, J. E.; Aponte, J. C.; Aponte, J. C.; Dworkin, J. P. The Search for Chiral Asymmetry as a Potential Biosignature in Our Solar System. *Chem. Rev.* **2020**, *120* (11), 4660–4689.

(6)   Raya, A.; Belmonte, J. C. I. Left-Right Asymmetry in Humans. *Encycl. Life Sci.* **2006**, 1–5.

(7)   Von Kraft, A. Symmetry and Asymmetry in the Development of Inner Organs in Parabiotic Twins of Amphibians (Urodela). *Laterality* **1999**, *4* (3), 209–255.

(8)   Nigel, A.; Brown, A. The Embryo â€™ S One-Sided Genes. *Curr. Biiology* **1995**, *5* (12).

(9)   Chen, Y.; Ma, W. The Origin of Biological Homochirality along with the Origin of Life. *PLoS Comput. Biol.* **2020**, *16* (1).

(10)   Watson, J. D.; Crick, F. H. C. Molecular Structure of Nucleic Acids: A Structure for Deoxyribose Nucleic Acid. *Nature* **1953**, *171* (4356), 737–738.

(11)   Akram, M.; Asif, H. M.; Uzair, M.; Akhtar, N.; Madni, A.; Ali Shah, S. M.; Hasan, Z. U.; Ullah, A. Amino Acids: A Review Article. *J. Med. Plants Res.* **2011**, *5* (17), 3997–4000.

(12)   Meierhenrich, U. J. Amino Acids and the Asymmetry of Life. *Eur. Rev.* **2013**, *21* (2), 190–199.

(13)   Janin, J.; Bahadur, R. P.; Chakrabarti, P. Protein-Protein Interaction and Quaternary Structure. *Q. Rev. Biophys.* **2008**, *41* (2), 133–180.

(14)   Niemann, C.; Pauling, B. L.; Niemann, C. Linus Pauling The Structure of Proteins and. **1939**, *2162* (8), 1860–1867.

(15)   Shallenberger, R. S.; Wienen, W. J. Carbohydrate Stereochemistry. *J. Chem. Educ.* **1989**, *66* (1), 67.

(16)   Blackmond, D. G. The Origin of Biological Homochirality. *Cold Spring Harb. Perspect. Biol.* **2019**, *11* (3).

(17)   Inaki, M.; Liu, J.; Matsuno, K. Cell Chirality: Its Origin and Roles in Left-Right Asymmetric Development. *Philos. Trans. R. Soc. B Biol. Sci.* **2016**, *371* (1710).

(18)   Burke, D.; Henderson, D. J. Chirality: A Blueprint for the Future. *Br. J. Anaesth.*

2002, *88* (4), 563–576.

(19) Sojo, V. On the Biogenic Origins of Homochirality. *Orig. Life Evol. Biosph.* **2015**, *45* (1–2), 219–224.

(20) Mason, S. F. Origins of Biomolecular Handedness. *Nat. Chem.* **1984**, *311*, 276–279.

(21) Sun, T.; Han, D.; Rhemann, K.; Chi, L.; Fuchs, H. Stereospecific Interaction between Immune Cells and Chiral Surfaces. *J. Am. Chem. Soc.* **2007**, *129* (6), 1496–1497.

(22) Umair, M.; Jabbar, S.; Sultana, T.; Ayub, Z.; Abdelgader, S. A.; Xiaoyu, Z.; Chong, Z.; Fengxia, L.; Xiaomei, B.; Zhaoxin, L. Chirality of the Biomolecules Enhanced Its Stereospecific Action of Dihydromyricetin Enantiomers. *Food Sci. Nutr.* **2020**, *8* (9), 4843–4856.

(23) Mesecar, A. D.; Koshland, D. E. A New Model for Protein Stereospecificity. *Nature* **2000**, *403* (6770), 614–615.

(24) Goodacre, R. The Blind Men and the Elephant: Challenges in the Analysis of Complex Natural Mixtures. *Faraday Discuss.* **2019**, *218*, 524–539.

(25) Liu, Y.; Gu, X. PHARMACOLOGY OF CHIRAL DRUGS. **2011**, 323–345.

(26) Calcaterra, A.; D'Acquarica, I. The Market of Chiral Drugs: Chiral Switches versus de Novo Enantiomerically Pure Compounds. *Journal of Pharmaceutical and Biomedical Analysis*. Elsevier B.V. January 5, 2018, pp 323–340.

(27) Lees, P.; Hunter, R. P. Pharmacokinetics and Pharmacodynamics of Stereoisomeric Drugs with Particular Reference to Bioequivalence Determination. **2012**, *35*, 17–30.

(28) Dong, H.; Guo, X.; Li, Z. *PHARMACOKINETICS OF CHIRAL DRUGS*; 2011.

(29) Lees, P.; Hunter, R. P.; Reeves, P. T.; Toutain, P. L. Pharmacokinetics and Pharmacodynamics of Stereoisomeric Drugs with Particular Reference to Bioequivalence Determination. *Journal of Veterinary Pharmacology and Therapeutics*. April 2012, pp 17–29.

(30) Higuchi, A.; Tamai, M.; Ko, Y. A.; Tagawa, Y. I.; Wu, Y. H.; Freeman, B. D.; Bing, J. T.; Chang, Y.; Ling, Q. D. Polymeric Membranes for Chiral Separation of Pharmaceuticals and Chemicals. *Polym. Rev.* **2010**, *50* (2), 113–143.

(31) Tokunaga, E.; Yamamoto, T.; Ito, E.; Shibata, N. Understanding the Thalidomide Chirality in Biological Processes by the Self-Disproportionation of Enantiomers. *Sci. Rep.* **2018**, *8* (1).

(32) Mane, S. Racemic Drug Resolution: A Comprehensive Guide. *Anal. Methods* **2016**, *8* (42), 7567–7586.

(33) Zawirska-Wojtasiak, R. *CHIRALITY AND THE NATURE OF FOOD AUTHENTICITY OF AROMA*; 2006; Vol. 5.

(34) Zawirska-wojtasiak, R. Chirality And The Nature Of Food Authenticity Of Aroma. *Acta Sci. Pol. Technol. Aliment.* **2006**, *5* (1), 21–36.

(35) Engel, K. H. Chirality: An Important Phenomenon Regarding Biosynthesis,

Perception, and Authenticity of Flavor Compounds. *Journal of Agricultural and Food Chemistry*. American Chemical Society September 23, 2020, pp 10265–10274.

(36)   Engel, K. H. Chirality: An Important Phenomenon Regarding Biosynthesis, Perception, and Authenticity of Flavor Compounds. *J. Agric. Food Chem.* **2020**, *68* (38), 10265–10274.

(37)   Lamberth, C.; Jeanmart, S.; Luksch, T.; Plant, A. Current Challenges and Trends in the Discovery of Agrochemicals. *Science (80-.).* **2013**, *341* (6147), 742–746.

(38)   Sekhon, B. S. Chiral Pesticides. *Journal of Pesticide Science*. 2009, pp 1–12.

(39)   Jeschke, P. Current Status of Chirality in Agrochemicals. *Pest Management Science*. John Wiley and Sons Ltd November 1, 2018, pp 2389–2404.

(40)   Gogoi, A.; Mazumder, N.; Konwer, S.; Ranawat, H.; Chen, N. T.; Zhuo, G. Y. Enantiomeric Recognition and Separation by Chiral Nanoparticles. *Molecules*. MDPI AG 2019.

(41)   Steinreiber, J.; Schürmann, M.; Wolberg, M.; Van Assema, F.; Reisinger, C.; Fesko, K.; Mink, D.; Griengl, H. Overcoming Thermodynamic and Kinetic Limitations of Aldolase-Catalyzed Reactions by Applying Multienzymatic Dynamic Kinetic Asymmetric Transformations. *Angew. Chemie - Int. Ed.* **2007**, *46* (10), 1624–1626.

(42)   Bhadra, S.; Yamamoto, H. Substrate Directed Asymmetric Reactions. *Chem. Rev.* **2018**, *118* (7), 3391–3446.

(43)   O'Brien, P. Sharpless Asymmetric Aminohydroxylation: Scope, Limitations, and Use in Synthesis. *Angew. Chemie - Int. Ed.* **1999**, *38* (3), 326–329.

(44)   Felletti, S.; Ismail, O. H.; De Luca, C.; Costa, V.; Gasparrini, F.; Pasti, L.; Marchetti, N.; Cavazzini, A.; Catani, M. Recent Achievements and Future Challenges in Supercritical Fluid Chromatography for the Enantioselective Separation of Chiral Pharmaceuticals. *Chromatographia*. Friedr. Vieweg und Sohn Verlags GmbH January 17, 2019, pp 65–75.

(45)   Li, J. Q.; Ikai, T.; Okamoto, Y. Preparation and HPLC Application of Chiral Stationary Phase from 4-Tert-Butylphenylcarbamates of Cellulose and Amylose Immobilized onto Silica Gel. *J. Sep. Sci.* **2009**, *32* (17), 2885–2891.

(46)   Ward, T. J.; Ward, K. D. Chiral Separations: A Review of Current Topics and Trends. *Anal. Chem.* **2012**, *84* (2), 626–635.

(47)   Wan, H.; Blomberg, L. G. *Chiral Separation of Amino Acids and Peptides by Capillary Electrophoresis*; 2000; Vol. 875.

(48)   Han, H.; Liu, W.; Xiao, Y.; Ma, X.; Wang, Y. Advances of Enantioselective Solid Membranes. *New J. Chem.* **2021**.

(49)   Lakshmi, B. B.; Martin, C. R. Enantioseparation Using Apoenzymes Immobilized in a Porous Polymeric Membrane. *Nature* **1997**, *388* (6644), 758–760.

(50)   Chan, J. Y.; Zhang, H.; Nolvachai, Y.; Hu, Y.; Zhu, H.; Forsyth, M.; Gu, Q.; Hoke, D. E.; Zhang, X.; Marriot, P. J.; Wang, H. Incorporation of Homochirality into a

Zeolitic Imidazolate Framework Membrane for Efficient Chiral Separation. *Angew. Chemie* **2018**, *130* (52), 17376–17380.

(51)   Kaupp, G. Resolution of Racemates by Distillation with Inclusion Compounds. *Org. Synth. Highlights III* **2008**, No. 7, 84–88.

(52)   Armstrong, D. W.; Zhou, E. Y.; Chen, S.; Le, K.; Tang, Y. Foam Flotation Enrichment of Enantiomers. *Anal. Chem.* **1994**, *66* (23), 4278–4282.

(53)   Huang, H.; Jin, Y.; Shirbhate, M. E.; Kang, D.; Choi, M.; Chen, Q.; Kim, Y.; Kim, S. J.; Byun, I. S.; Wang, M.; Bouffard, J.; Kim, S. K.; Kim, K. M. Enantioselective Extraction of Unprotected Amino Acids Coupled with Racemization. *Nat. Commun.* **2021**, *12* (1), 1–7.

(54)   Schuur, B.; Verkuijl, B. J. V.; Minnaard, A. J.; De Vries, J. G.; Heeres, H. J.; Feringa, B. L. Chiral Separation by Enantioselective Liquid-Liquid Extraction. *Org. Biomol. Chem.* **2011**, *9* (1), 36–51.

(55)   Senthilkumar, T.; Asha, S. K. An Easy "Filter-and-Separate" Method for Enantioselective Separation and Chiral Sensing of Substrates Using a Biomimetic Homochiral Polymer. *Chem. Commun.* **2015**, *51* (43), 8931–8934.

(56)   Ahmadabad, F. K.; Pourayoubi, M.; Bakhshi, H. Chiral Phosphoric Triamide-Based Polymers for Enantioseparation. *J. Appl. Polym. Sci.* **2019**, *136* (41), 1–10.

(57)   Zhou, J.; Tang, J.; Tang, W. Recent Development of Cationic Cyclodextrins for Chiral Separation. *TrAC - Trends Anal. Chem.* **2015**, *65*, 22–29.

(58)   Fejős, I.; Kalydi, E.; Malanga, M.; Benkovics, G.; Béni, S. Single Isomer Cyclodextrins as Chiral Selectors in Capillary Electrophoresis. *J. Chromatogr. A* **2020**, *1627*, 461375.

(59)   Francotte, E. R. Polysaccharide Derivatives as Unique Chiral Selectors for Enantioselective Chromatography. *Chimia (Aarau).* **2017**, *71* (7–8), 430–450.

(60)   Yamamoto, C.; Inagaki, S.; Okamoto, Y. Enantioseparation Using Alkoxyphenylcarbamates of Cellulose and Amylose as Chiral Stationary Phase for High-Performance Liquid Chromatography. *J. Sep. Sci.* **2006**, *29* (6), 915–923.

(61)   Yamamoto, C.; Hayashi, T.; Okamoto, Y.; Ohkubo, S.; Kato, T. Direct Resolution of C76 Enantiomers by HPLC Using an Amylose-Based Chiral Stationary Phase. *Chem. Commun.* **2001**, *3* (10), 925–926.

(62)   Ikai, T.; Muraki, R.; Yamamoto, C.; Kamigaito, M.; Okamoto, Y. Cellulose Derivative-Based Beads as Chiral Stationary Phase for HPLC. *Chem. Lett.* **2004**, *33* (9), 1188–1189.

(63)   Shamsi, S. A.; Warner, I. M. Monomeric and Polymeric Chiral Surfactants as Pseudo-Stationary Phases for Chiral Separations. *Electrophoresis* **1997**, *18* (6), 853–872.

(64)   Wang, J.; Warner, I. M. Chiral Separations Using Micellar Electrokinetic Capillary Chromatography and a Polymerized Chiral Micelle. *Anal. Chem.* **1994**, *66* (21), 3773–3776.

(65) Zurita-Pérez, J.; Santos-Delgado, M. J.; Crespo-Corral, E.; Polo-Díez, L. M.; Aguilar-Gallardo, A. Separation of Para-Andmeta-Imazamethabenz-Methyl Enantiomers by Direct Chiral HPLC Using a Protein Chiral Selector. *Chromatographia* **2012**, *75* (15–16), 847–855.

(66) Ilisz, I.; Grecsó, N.; Forró, E.; Fülöp, F.; Armstrong, D. W.; Péter, A. High-Performance Liquid Chromatographic Separation of Paclitaxel Intermediate Phenylisoserine Derivatives on Macrocyclic Glycopeptide and Cyclofructan-Based Chiral Stationary Phases. *J. Pharm. Biomed. Anal.* **2015**, *114*, 312–320.

(67) Yoon, J. C.; Hee, J. C.; Myung, H. H. Synthesis of New Chiral Crown Ethers Incorporating Two Different Chiral Units And "matched/mismatched" effect of the Two Chiral Units on the Chiral Recognition. *Bull. Korean Chem. Soc.* **2007**, *28* (12), 2531–2534.

(68) Berkecz, R.; Németi, G.; Péter, A.; Ilisz, I. Liquid Chromatographic Enantioseparations Utilizing Chiral Stationary Phases Based on Crown Ethers and Cyclofructans. *Molecules* **2021**, *26* (15).

(69) Kuhn, R.; Erni, F.; Bereuter, T.; Håusler, J.; Bereuter, T.; Håusler, J. Chiral Recognition and Enantiomeric Resolution Based on HostGuest Complexation with Crown Ethers in Capillary Zone Electrophoresis. *Anal. Chem.* **1992**, *64* (22), 2815–2820.

(70) Paik, M. J.; Kang, J. S.; Huang, B. S.; Carey, J. R.; Lee, W. Development and Application of Chiral Crown Ethers as Selectors for Chiral Separation in High-Performance Liquid Chromatography and Nuclear Magnetic Resonance Spectroscopy. *J. Chromatogr. A* **2013**, *1274*, 1–5.

(71) Adhikari, S.; Lee, W. Chiral Separation Using Chiral Crown Ethers as Chiral Selectors in Chirotechnology. *J. Pharm. Investig.* **2018**, *48* (3), 225–231.

(72) Peng, Y.; Gong, T.; Zhang, K.; Lin, X.; Liu, Y.; Jiang, J.; Cui, Y. Engineering Chiral Porous Metal-Organic Frameworks for Enantioselective Adsorption and Separation. *Nat. Commun.* **2014**, *5*.

(73) Jiang, H.; Yang, K.; Zhao, X.; Zhang, W.; Liu, Y.; Jiang, J.; Cui, Y. Highly Stable Zr(IV)-Based Metal-Organic Frameworks for Chiral Separation in Reversed-Phase Liquid Chromatography. *J. Am. Chem. Soc.* **2021**, *143* (1), 390–398.

(74) Zhuo, S.; Zhang, X.; Luo, H.; Wang, X.; Ji, Y. The Application of Covalent Organic Frameworks for Chiral Chemistry. *Macromol. Rapid Commun.* **2020**, *41* (20), 1–22.

(75) Zhuo, S.; Wang, X.; Li, L.; Yang, S.; Ji, Y. Chiral Carboxyl-Functionalized Covalent Organic Framework for Enantioselective Adsorption of Amino Acids. *ACS Appl. Mater. Interfaces* **2021**, *13* (26), 31059–31065.

(76) Gellman, A. J. An Account of Chiral Metal Surfaces and Their Enantiospecific Chemistry. *Accounts Mater. Res.* **2021**, *2* (11), 1024–1032.

(77) Song, H. S.; Han, J. W. Tuning the Surface Chemistry of Chiral Cu(531)S for Enhanced Enantiospecific Adsorption of Amino Acids. *J. Phys. Chem. C* **2015**, *119* (27), 15195–15203.

(78)   Okamoto, Y. Chiral Polymers. *Prog. Polym. Sci.* **2000**, *25* (2), 159–162.

(79)   Ingole, P. G.; Bajaj, H. C.; Srivastava, D. N.; Rebary, B.; Singh, K. Preparation of Thin Film Polymer Composite Membranes for Optical Resolution of Racemic Mixture of α-Amino Acids. *Sep. Sci. Technol.* **2013**, *48* (12), 1777–1787.

(80)   Cepak, V. M.; Martin, C. R. Preparation of Polymeric Micro- and Nanostructures Using a Template-Based Deposition Method. *Chem. Mater.* **1999**, *11* (5), 1363–1367.

(81)   Tsioupi, D. A.; Stefan-van Staden, R. I.; Kapnissi-Christodoulou, C. P. Chiral Selectors in CE: Recent Developments and Applications. *Electrophoresis* **2013**, *34* (1), 178–204.

(82)   Okamoto, Y.; Suzuki, K.; Ohta, K.; Hatada, K.; Yuki, H. Optically Active Poly(triphenylmethyl Methacrylate) with One-Handed Helical Conformation. *J. Am. Chem. Soc.* **1979**, *101* (16), 4763–4765.

(83)   Aoki, T.; Kaneko, T.; Maruyama, N.; Sumi, A.; Takahashi, M.; Sato, T.; Teraguchi, M. Helix-Sense-Selective Polymerization of Phenylacetylene Having Two Hydroxy Groups Using a Chiral Catalytic System. *J. Am. Chem. Soc.* **2003**, *125* (21), 6346–6347.

(84)   Zhao, Y.; Abdul Rahim, N. A.; Xia, Y.; Fujiki, M.; Song, B.; Zhang, Z.; Zhang, W.; Zhu, X. Supramolecular Chirality in Achiral Polyfluorene: Chiral Gelation, Memory of Chirality, and Chiral Sensing Property. *Macromolecules* **2016**, *49* (9), 3214–3221.

(85)   Miyabe, T.; Iida, H.; Ohnishi, A.; Yashima, E. Enantioseparation on Poly(phenyl Isocyanide)s with Macromolecular Helicity Memory as Chiral Stationary Phases for HPLC. *Chem. Sci.* **2012**, *3* (3), 863–867.

(86)   Zhou, C.; Ren, Y.; Han, J.; Xu, Q.; Guo, R. Chiral Polyaniline Hollow Nanotwists toward Efficient Enantioselective Separation of Amino Acids. *ACS Nano* **2019**, *13* (3), 3534–3544.

(87)   Hou, L. T.; Chen, J. J.; Fu, H. J.; Fu, X. L. Chiral Recognition of L-Carnitine Using Surface Molecularly Imprinted Microspheres via RAFT Polymerization. In *Advanced Materials Research*; 2014; Vol. 884–885, pp 33–36.

(88)   Saylan, Y.; Akgönüllü, S.; Yavuz, H.; Ünal, S.; Denizli, A. Molecularly Imprinted Polymer Based Sensors for Medical Applications. *Sensors (Switzerland)* **2019**, *19* (6).

(89)   Wang, Y.; Chen, Y.; Li, C.; Zhu, Y.; Ge, L.; Yang, K. Magnetic Molecularly Imprinted Polymers Based on Dehydroabietylamine as Chiral Monomers for the Enantioseparation of RS-Mandelic Acid. *ACS Omega* **2021**, *6* (23), 14977–14984.

(90)   Kim, J. H.; Jegal, J.; Kim, J. H.; Lee, K. H.; Lee, Y. Enantioselective Permeation of α-Amino Acid Optical Isomers through Crosslinked Sodium Alginate Membranes. *J. Appl. Polym. Sci.* **2003**, *89* (11), 3046–3051.

(91)   Paik, P.; Gedanken, A.; Mastai, Y. Chiral-Mesoporous-Polypyrrole Nanoparticles : Its Chiral Recognition Abilities and Use in Enantioselective Separation †. **2010**, 4085–4093.

(92)   Paik, P.; Gedanken, A.; Mastai, Y. Enantioselective Separation Using Chiral

Mesoporous Spherical Silica Prepared by Templating of Chiral Block Copolymers. *ACS Appl. Mater. Interfaces* **2009**, *1* (8), 1834–1842.

(93) Paik, P.; Gedanken, A.; Mastai, Y. Chiral Separation Abilities: Aspartic Acid Block Copolymer-Imprinted Mesoporous Silica. *Microporous Mesoporous Mater.* **2010**, *129* (1–2), 82–89.

(94) Zhou, Y.; Zhang, C.; Zhou, Z.; Zhu, R.; Liu, L.; Bai, J.; Dong, H.; Satoh, T.; Okamoto, Y. Influence of Different Sequences of L-Proline Dipeptide Derivatives in the Pendants on the Helix of Poly(phenylacetylene)s and Their Enantioseparation Properties. *Polym. Chem.* **2019**, *10* (35), 4810–4817.

(95) Zhou, Y.; Zhang, C.; Ma, R.; Liu, L.; Dong, H.; Satoh, T.; Okamoto, Y. Synthesis of Helical Poly(phenylacetylene) Derivatives Bearing Diastereomeric Pendants for Enantioseparation by HPLC. *New J. Chem.* **2019**, *43* (8), 3439–3446.

(96) Chen, C.; Zhao, B.; Deng, J. Optically Active Porous Microspheres Consisting of Helical Substituted Polyacetylene Prepared by Precipitation Polymerization without Porogen and the Application in Enantioselective Crystallization. *ACS Macro Lett.* **2015**, *4* (4), 348–352.

(97) Prosuntsova, D. S.; Plodukhin, A. Y.; Ananieva, I. A.; Beloglazkina, E. K.; Nesterenko, P. N. New Composite Stationary Phase for Chiral High-Performance Liquid Chromatography. *J. Porous Mater.* **2021**, *28* (2), 407–414.

(98) Zhang, A.; Bai, H.; Li, L. Breath Figure: A Nature-Inspired Preparation Method for Ordered Porous Films. *Chem. Rev.* **2015**, *115* (18), 9801–9868.

(99) Yamamoto, C.; Okamoto, Y. Optically Active Polymers for Chiral Separation. *Bull. Chem. Soc. Jpn.* **2004**, *77* (2), 227–257.

(100) Scriba, G. K. E. Chiral Recognition in Separation Science – an Update. *J. Chromatogr. A* **2016**, *1467*, 56–78.

(101) Easson, L. H.; Stedman, E. Studies on the Relationship between Chemical Constitution and Physiological Action. *Biochem. J.* **1933**, *27* (4), 1257–1266.

(102) Berthod, A. Chiral Recognition Mechanisms. *Anal. Chem.* **2006**, *78* (7), 2093–2099.

(103) Booth, T. D.; Wahnon, D.; Wainer, I. W. Is Chiral Recognition a Three-Point Process? *Chirality* **1997**, *9* (2), 96–98.

(104) Tokita, Y.; Katoh, M.; Kosaka, K.; Ohta, Y.; Yokozawa, T. Precision Synthesis of Fluorene-Thiophene Alternating Copolymer by Means of Suzuki-Miyaura Catalyst-Transfer Condensation Polymerization: Importance of the Position of Alkyl Substituent on Thiophene of Biaryl Monomer to Suppress Disproportionation. *Polym. Chem.* **2021**.

(105) Liu, B.; Yu, W. L.; Lai, Y. H.; Huang, W. Synthesis, Characterization, and Structure-Property Relationship of Novel Fluorene-Thiophene-Based Conjugated Copolymers. *Macromolecules* **2000**, *33* (24), 8945–8952.

(106) Carsten, B.; He, F.; Son, H. J.; Xu, T.; Yu, L. Stille Polycondensation for Synthesis of Functional Materials. *Chem. Rev.* **2011**, *111* (3), 1493–1528.

(107) Hardeman, T.; Koeckelberghs, G. The Synthesis of Poly(thiophene-Co-Fluorene) Gradient Copolymers. *Macromolecules* **2015**, *48* (19), 6987–6993.

(108) Gobalasingham, N. S.; Thompson, B. C. Direct Arylation Polymerization: A Guide to Optimal Conditions for Effective Conjugated Polymers. *Prog. Polym. Sci.* **2018**, *83*, 135–201.

(109) Senthilkumar, T.; Parekh, N.; Nikam, S. B.; Asha, S. K. Orientation Effect Induced Selective Chelation of Fe2+ to a Glutamic Acid Appended Conjugated Polymer for Sensing and Live Cell Imaging. *J. Mater. Chem. B* **2015**, *4* (2), 299–308.

(110) Wang, J.-S.; Matyjaszewski, K. Controlled/"living" radical Polymerization. Atom Transfer Radical Polymerization in the Presence of Transition-Metal Complexes. *J. Am. Chem. Soc.* **1995**, *117* (20), 5614–5615.

(111) Georges, M. K.; Veregin, R. P. N.; Kazmaier, P. M.; Hamer, G. K. Narrow Molecular Weight Resins by a Free-Radical Polymerization Process. *Macromolecules* **1993**, *26* (11), 2987–2988.

(112) Moad, G.; Rizzardo, E. A 20th Anniversary Perspective on the Life of RAFT (RAFT Coming of Age). *Polym. Int.* **2020**, *69* (8), 658–661.

(113) Perrier, S. 50th Anniversary Perspective: RAFT Polymerization - A User Guide. *Macromolecules* **2017**, *50* (19), 7433–7447.

(114) Nieswandt, K.; Georgopanos, P.; Abetz, C.; Filiz, V.; Abetz, V. Synthesis of poly(3-Vinylpyridine)-Block-Polystyrene Diblock Copolymers via Surfactant-Free RAFT Emulsion Polymerization. *Materials (Basel).* **2019**, *12* (19), 3–6.

(115) Roy, M.; Rajamohanan, P. R.; Ravindranathan, S.; Asha, S. K. Self-Assembly of Bispentadecylphenol Substituted Perylenediimide with PS- B-P4VP for Structure-Property Insight into the Core of Core-Shell Micelles. *ACS Appl. Polym. Mater.* **2020**, *2* (2), 805–816.

(116) Ngadiwiyana; Ismiyarto; Gunawan; Purbowatiningrum, R. S.; Prasetya, N. B. A.; Kusworo, T. D.; Susanto, H. Sulfonated Polystyrene and Its Characterization as a Material of Electrolyte Polymer. *J. Phys. Conf. Ser.* **2018**, *1025* (1).

(117) Del Prado, A.; Briz, N.; Navarro, R.; Pérez, M.; Gallardo, A.; Reinecke, H. Chlorosulfonation of Polystyrene Substrates for Bioanalytical Assays: Distribution of Activated Groups at the Surface. *Analyst* **2012**, *137* (23), 5666–5671.

(118) Biswas, M.; Chatterjee, S. Chemical Modification of Polystyrene. I. Electrophilic Substitution of Polystyrene with Aromatic Anhydrides. *J. Appl. Polym. Sci.* **1982**, *27* (10), 3851–3857.

(119) Coustet, M. E.; Cortizo, M. S. Functionalization of Styrenic Polymer through Acylation and Grafting under Microwave Energy. *Polym. J.* **2011**, *43* (3), 265–271.

(120) Mallakpour, S. E. A New Method for Producing Optically Active Polybutadiene. *Polym. Int.* **1998**, *47* (2), 193–197.

CHAPTER 2

Enantioselective Separation Using Chiral Amino Acid Functionalized Polyfluorene Coated on Mesoporous Anodic Aluminium Oxide Membranes

2.1 INTRODUCTION

Chirality is omnipresent in nature; the handedness of biomolecules like DNA,[1] protein,[2] enzymes, sugars,[3] and amino acids have a significant influence on the life on Earth.[4,5] The active sites of biomolecules bind exclusively to only one enantiomer of chiral substrates. This handedness of biomolecules often contributes to the exceptional specificity and selectivity toward metabolic processes and therapeutic efficacy.[6] In this context, it is important to realize that more than 50% of the drugs currently in pharmaceutical use have at least one chiral center in their structure.[7] The enantiomers of many chiral drugs differ significantly in their pharmacokinetic parameters resulting in diversified pharmacological actions and pharmacodynamics despite having the same chemical structure.[8–10] The requirement for the safe and effective therapeutic use of the drug has resulted in a scientific quest for the development of robust, scalable, and efficient strategies for the synthesis of drugs in their enantiopure form.[11] This quest has given a tremendous boost in the progress of asymmetric synthesis, which is the most common approach for the synthesis of a single enantiomer.[12–15] Although this is the currently favored approach for accessing enantiopure molecules, it has several disadvantages, including its requirement for expensive and environmentally hazardous transition metal catalyst with chiral ligands and highly enantiopure starting material.[16–21] The regioselectivity observed with some of these asymmetric reactions are such that small changes in the nature of the ligand, solvent, or even that of the protecting groups can severely skew the isolated yields of the enantiomerically pure compound.[16] Resolution of a racemic mixture in enantiomerically pure form is another approach that has attracted great attention in the recent decades. Generally, this is achieved with the help of various chromatographic techniques which usually need a skilled operator for handling the high end instrumentation.[22,23] These resolution techniques need chiral selectors, which should discriminate between pairs of enantiomers. The most commonly used chiral selectors are polysaccharides, cyclodextrins, proteins, crown ethers, micelles, and macrocyclic glycopeptides.[24,25] Apart from these, chiral polymers are a distinct class of material used as a chiral selector for carrying out enantioselective separation of racemic mixtures.[26–31] In most published reports, chiral polymers are coated on solid mesoporous materials, making the surface chiral in nature.[32–35] Mesoporous material not only acts as a solid support but also gives additional stability to the chiral polymers and provides high surface area for enantioselective separation.[36,37] Among chiral polymers, polyfluorenes were synthesized and studied extensively by Meskers *et al.* in terms of its chiroptical properties,

supramolecular chirality, liquid crystalline, and biomimetic properties.[38–42] Very few reports are available where chiral polyfluorene was used for carrying out an enantioselective separation of the racemic mixture.[43,44] Senthilkumar *et al.* reported the synthesis of L-glutamic acid (protected) appended chiral polyfluorene and its application for the heterogeneous enantioselective separation of a wide range of racemic mixtures of amino acids, sugars, amino alcohol, hydroxy acid, ascorbic acid, etc. from their aqueous solution.[45] A helical porous morphology enabled the enantioselective uptake of the L-form of the enantiomer from their racemic mixture in water, leaving the water enriched with the D-enantiomer.

The current chapter focuses on the enantioselective separation of racemic mixtures using mesoporous anodic aluminium oxide (AAO) membranes coated with chiral polyfluorene. Two optically active chiral polyfluorenes, PF-LAsp and PF-DAsp, bearing protected L- and D-aspartic acid as pendant groups, respectively, were synthesized and coated on AAO membranes. The 2D (dimensional) confinement of chiral polymer within the cylindrical channels of the AAO membrane was expected to increase the available chiral surface area, resulting in enhanced enantioselective chiral separation.[46–48] An unprecedented ee of ~95% could be achieved for the separation of glutamic acid from its aqueous racemic mixture. This is the first report of the application of polyfluorene-coated chiral AAO membranes for enantioselective separation of an aqueous racemic mixture of amino acids in their native form. The current work also explores the enantioselective uptake, kinetics of separation, and effect of pore size of AAO membrane on separation efficiency.

2.2 EXPERIMENTAL SECTION

2.2.1 Materials

2,7-Dibromofluorene and 6-bromo-1-hexanol were purchased from TCI Chemicals. 4-Dimethylaminopyridine (DMAP), dicyclohexylcarbodiimide (DCC), and tetrabutylammonium bromide (TBAB) were purchased from Spectrochem Pvt. Ltd. (India). Pd(PPh$_3$)$_4$, benzene-1, 4-diboronic acid, IR grade potassium bromide (KBr), and CDCl$_3$ were purchased from Sigma-Aldrich. N-Boc-L-aspartic acid-1-tert butyl ester, N-Boc-D-aspartic acid-1-tert butyl ester, (Boc = tert-butoxycarbonyl) were purchased from Alfa Aesar Chemical Ltd. NaOH, Na$_2$SO$_4$, Na$_2$CO$_3$, K$_2$CO$_3$, and solvents like toluene, tetrahydrofuran (THF), methanol, and dichloromethane (DCM) were purchased from Merck Chemicals.

Ethyl acetate and pet ether were purchased locally. Solvents were dried by standard drying procedures. HPLC grade THF was purchased from Merck Chemicals. Anodic aluminium oxide membrane with nominal pore diameters of 200, 100, and 20 nm respectively, diameter 13 mm, mass 10−20 mg, 50 μm nominal thickness, porosity of 0.12−0.15, pore density 5×10^8 (±20%), 2×10^9 (±20%), and 5.8×10^{10} (±20%) cm^{-2}, respectively, air permeability at 20 °C in the range of 10^{-8} to 10^{-4} cm/s/Pa and water permeability at 20 °C in the range of 10^{-10} to 10^{-6} cm/s/Pa were purchased from SPI supplies USA (the characterization details are as provided by the supplier).

2.2.2 Measurements

All of the materials (small molecules, monomers, and polymers) were structurally characterized by recording ^{1}H and ^{13}C NMR spectra with Bruker-AVENS 200 and 400 MHz spectrometers. Chemical shifts were measured in parts per million (ppm) at 25°C in CDCl$_3$ using a trace amount of tetramethylsilane (TMS) as an internal reference. FT-IR spectra were recorded using BRUKER alpha-E Fourier transform (FT-IR) for monomers and polymers' structural and functional group characterization. MALDI-TOF analysis of monomers were performed using Voyager-De-STRMALDI-TOF (Applied Biosystems, Framingham, MA, USA) equipped with 337 nm pulsed nitrogen laser. The 2 μM monomer solution was mixed well with the 2, 5-dihydroxybenzoic acid (DHB) matrix in THF before being spotted on a 96-well stainless steel MALDI plate using the dried droplet method. Gel Permeation Chromatography (GPC) with a ViscotekVE 1122 solvent delivery system and a ViscotekVE 3580 RI detector was used to determine the molecular weight of the polymers. The instrument was calibrated with polystyrene standards, and analysis was performed at a 1 ml/min flow rate with tetrahydrofuran (THF) as a mobile phase. The morphological characterizations of chiral AAO were performed using FE-SEM with an FEI Nova Nano SEM 450. Bare AAO and polymer-coated chiral AAO were mounted directly on the top of grooved edge aluminium SEM specimen stub with the help of carbon tape. Before conducting morphological studies, the membranes were coated with a 5 nm thick gold film by a sputtering method. The polymers' absorbance spectra were recorded using a Perkin Elmer lambda-35 UV/Vis spectrometer with deuterium and tungsten source lamps that cover a wavelength range of 190-1100 nm. Solution state Circular Dichroism (CD) measurements were performed using a JASCO-815 CD spectrometer equipped with a Jasco PTC-424 S-5 S/15 Peltier system. 2 mm path-length quartz cuvettes were used for a sample volume of

400 µl in Milli-Q water at 25 °C. Three scans were averaged for each sample with a 100 nm/min scanning rate.

2.2.3 Methods

A) Preparation of Chiral Mesoporous Aluminium Oxide Membranes

Chiral AAO membranes were prepared by a simple vacuum filtration method. 5 mg of polymer was dissolved in 1 ml of THF to prepare a polymer solution. 2-3 drops of the polymer solution were drop-casted on AAO membranes kept on Buchner funnel equipped with a vacuum pump for applying suction. The applied suction helped the polymer solution enter inside the pores of AAO membranes and form a thin coating on the inner walls of the pores. Excess polymer solution on the surface was removed by wiping the surface with THF solvent. The polymer-coated AAO membranes were kept in the vacuum oven at 60 °C for complete solvent evaporation.

B) Sample Preparation for CD Measurement

Polymer-coated chiral AAO membrane was crushed into a fine powder and to this HPLC grade THF was added and this was sonicated multiple times with fresh solvent until the polymer was completely extracted from the crushed membrane. Complete extraction of polymer from AAO was confirmed by the disappearance of polymer fluorescence (as observed under a hand-held UV lamp). The THF was evaporated to a fixed volume of 1 ml. Out of this, 500 µl solution was used to record the solution state CD spectrum. The remaining 500 µl was dried completely and the obtained dry polymer was ground into a fine powder with 50 mg of IR grade KBr, made into transparent pellet to measure solid-state CD spectra. For quantitative estimation of the coated polymer, two chiral AAO membranes were used. The extracted polymer was diluted to 100 ml in a volumetric flask with HPLC grade THF and absorption spectrum was recorded.

C) Enantioselective Recognition Method

Two PF-DAsp coated chiral AAO membranes were suspended in a solution of D-glutamic acid (1 mg of D-glutamic acid dissolved in 3 ml Milli-Q water) and it was agitated on a mechanical shaker for 24 hours at RT (22-30 °C). The membranes were removed from the aqueous mixture after 24 h. A series of similar experiments were set up and stopped after different time intervals like 6, 12, and 18 hours by removing AAO membranes from the

solution.CD spectra of the resultant solutions were measured after completion of the enantioselective recognition experiment and plotted along with the CD spectra of pure D-glutamic acid (1 mg/3 ml) in water (0 h).

D) Determination of Pore Diameter

Two half U-tubes were connected with the help of screw tight clamps pasting the AAO membrane in the junction. The feed side of the U-tube was filled with 50 ml 2×10^{-4} M naphthalene solution and the reservoir side with an equal amount of DI water. UV Visible absorption spectroscopy was used to monitor the amount of naphthalene molecules transferred from the feed to the reservoir.

Figure 2.1 Naphthalene transport study through membranes using U-tube setup

The average pore diameter of polymer-coated AAO membrane (200 nm) (PF-LAsp@AAO) was determined from the naphthalene diffusion through the membrane using Fick's law of diffusion.

$$J = \frac{DC_f \pi r^2 n}{l} \dots\dots\dots\dots\dots\dots \text{(1)}$$

Where J = flux, D = diffusion coefficient, C_f = feed concentration, r = radius of pore, n = pore density, l = membrane thickness. The equation for bare 200 nm AAO membrane and polymer-coated AAO membrane is given as equations 2 and 3, respectively.

$$J_{200} = \frac{DC_f \pi r_{200}^2 n}{l} \dots\dots\dots\dots\dots \text{(2)}$$

$$J_{poly} = \frac{DC_f \pi r_{poly}^2 n}{l} \dots\dots\dots\dots (3)$$

J_{200} and J_{poly} is flux $r_{200,}$ and r_{poly} is the radius of bare 200 nm pore sized AAO membrane (AAO 200 nm) and polymer-coated AAO membranes (Poly.AAO), respectively. The relative average pore radius was calculated assuming that polymer modification altered only the pore size. The relative average pore radius of polymer-coated AAO membrane is calculated as

$$\frac{J_{200}}{J_{poly}} = \frac{r_{200}^2}{r_{poly}^2} \dots\dots\dots\dots\dots (4)$$

E) Sample Preparation for Recording FT-IR

Polymer solutions were prepared by dissolving 1 gm of polymer (PF-LAsp and PF-DAsp) separately in 1 ml of HPLC grade THF. Similarly, 3 mg each of L-glutamic acid and D-glutamic were dissolved separately in 1 ml of methanol (partially dissolved). The FT-IR spectra of these samples were recorded separately in ATR mode in the solid-state. Hydrogen bonding interaction between chiral selector and analyte was probed by recording FT-IR spectra of their mixture. Equal quantities of polymer and amino acid solution were mixed, and this solution was allowed to stand for 30 minutes. This polymer-amino acid mixed solution was drop casted and allowed to dry completely, and FT-IR spectra of the dry samples were recorded.

2.2.4 Synthesis and characterizations

The synthesis of the D and L-aspartic acid appended polyfluorene PF-DAsp and PF-LAsp was completed as shown below in Scheme 2.1. The detailed synthesis and characterization of small molecules and monomers can be found below in section 1 of synthesis and characterizations. The detailed synthesis of protected D/L -aspartic acid-containing chiral polyfluorene by Suzuki polymerization can be found in section 2 of the synthesis and characterization. The molecular weights (*Mn and Mw*) and polydispersity index of polymers (*ĐM*) were determined by GPC using THF as the solvent (Figure 2.18). The number and weight-average molecular weight (Mn and Mw), polydispersity index (ĐM) and degree of polymerization (Xn) for both the polymers PF-LAsp and PF-DAsp are shown in Table 2.1.

PF-LAsp had an Mn of 25000 (∼51 repeating units), while PF-DAsp had an Mn of 21400 (∼43 repeating units).
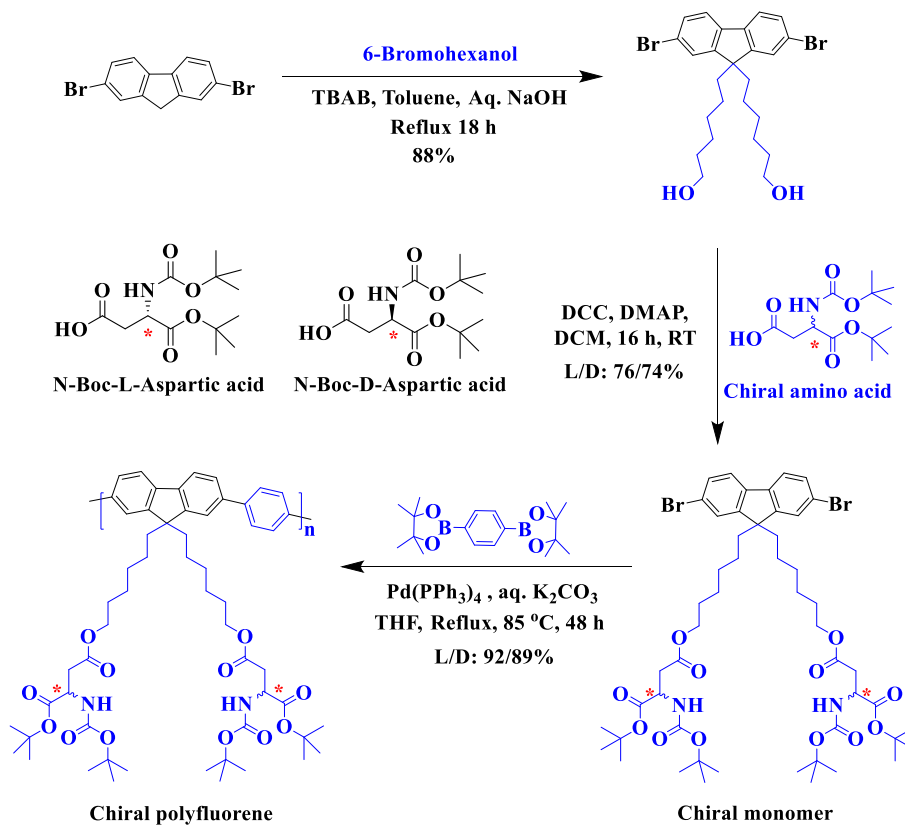
Scheme 2.1 Schematics for the Synthesis of Chiral Polyfluorenes PF-LAsp (5a) and PF-DAsp (5b) having N-Boc-L-Aspartic Acid (a) and N-Boc-D-Aspartic Acid (b) as Pendent groups, respectively

1) Synthesis of small molecules and monomers
a) Synthesis of 2, 7-dibromo-9, 9-di-n-hexanolfluorene

2, 7-dibromofluorene (5 g, 15.43 mmol), 6-bromo-1-hexanol (6.1 ml, 46.29 mmol) and tetrabutylammonium bromide (2.5 g, 7.71 mmol) were dissolved in toluene (100 ml) in a 250 ml two necked round bottom flask equipped with a magnetic stirring bar. 50 ml of 50 weight % of aqueous NaOH solution was added to this reaction mixture. A reflux condenser was attached to the round bottom flask to reflux resultant reaction mixture at 120 °C in an inert atmosphere for 18 hours. After that, the reaction mixture was left to cool to ambient temperature. The reaction mixture was transferred to water (150 ml), and extracted with ethyl acetate. The organic layer was extracted with water several times till the solution turned yellow. Ethyl acetate layer was dried by passing through anhydrous sodium sulphate. The crude product was obtained by evaporating ethyl acetate under reduced pressure.

Obtained crude product was purified by column chromatography with petroleum ether: ethyl acetate (50:50). Yield = 88 %. ^{1}H NMR spectrum (400 MHz, CDCl$_3$) δ 7.45-7.56 (m, 6H), δ 3.26-3.33 (t, 4H), δ 1.98 (m, 4H), δ 1.64-1.67 (m, 4H), δ 1.09-1.20 (m, 8H), 0.59-0.63 (m, 4H).
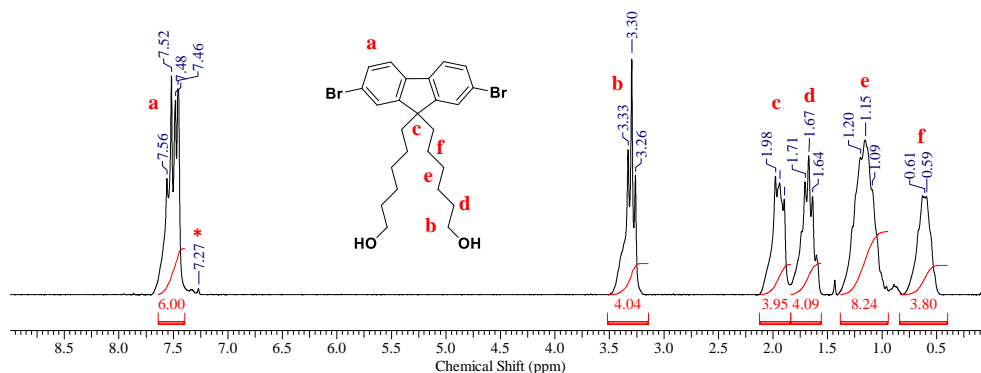
Figure 2.2 ^{1}H NMR spectrum of 2, 7-dibromo-9, 9-di-n-hexanolfluoren (CDCl$_3$)

b) Synthesis of Boc protected-L-aspartic acid-containing monomer

In an inert environment, 4-(dimethylamino) pyridine (DMAP) (1.1 g, 8.39 mmol) and N-Boc-L-aspartic acid-1-tert-butyl ester (2.5 g, 8.39 mmol) were introduced to a two-necked round bottom flask with a magnetic stirring bar. A syringe was used to add dry DCM to the reaction mixture. The reaction mixture was cooled to 0 °C with continuous stirring. N, N'-Dicyclohexylcarbodiimide (DCC) (1.5 g, 9.54 mmol) was added to reaction mixture after 5 minutes and the reaction mixture was stirred for 1 hour at the same temperature followed by addition of 2, 7-dibromo-9, 9-di-n-hexanolfluorene (2 g, 3.81 mmol) to the reaction mixture at 0 °C. The reaction mixture was gradually brought to room temperature and stirred at that temperature for 16 hours. The reaction mixture was diluted by adding DCM. The organic layer washed twice with 0.02 M NaOH, followed by saturated NaHCO$_3$ and brine separately. The organic layer was finally extracted with water and evaporated under reduced pressure. The product was purified by column chromatography using pet ether: ethyl acetate (70:30). Yield 76 %. ^{1}H NMR spectrum (400 MHz, CDCl$_3$) δ 7.43- 7.54 (m, 6H), δ 5.41-5.43 (d, 2H), δ 4.42 (d 2H), δ 3.96 (t, 4H), δ 3.26-3.33 (q, 2H), δ 2.92 (m, S-9 2H), δ 2.73 (m, 2H), δ 1.92 (m, 4H), δ 1.63 (m, 4H),δ 1.42-1.45 (s, 40), δ1.10 (m, 8H), 0.57 (m, 4H). ^{13}C NMR spectrum (100 MHz, CDCl$_3$) δ 170.84, 169.85, 155.27, 152.07, 138.94, 130.19, 125.94, 121.11, 80.02, 79.60, 64.71, 55.43, 50.38, 39.97, 29.56, 28.35, 28.30, 28.19, 27.74, 25.41, 23.40. MALDI-TOF analysis; Calculated mass-1066.96; observed-1105.28 [M+K]$^+$; FT-IR

stretching frequency (υ) in cm^{-1}; 3337, 2980, 2930, 2856, 1705, 1490, 1449, 1368, 1250, 1151 and 1043.
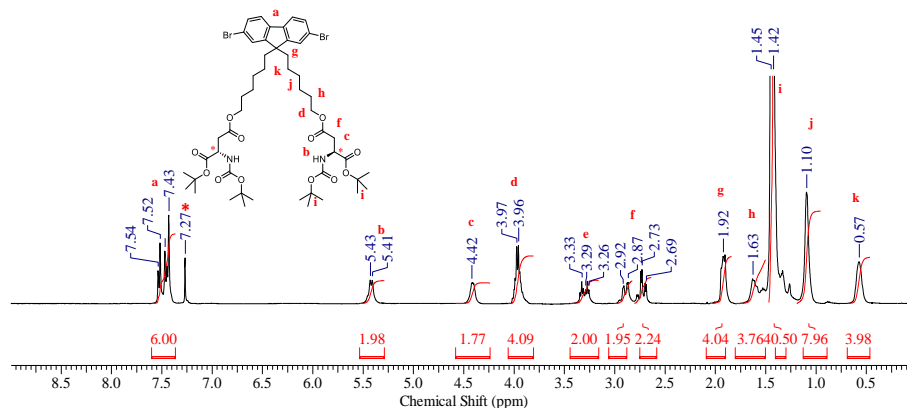
Figure 2.3 ^{1}H NMR spectrum of Boc protected-L-aspartic acid containing monomer (CDCl$_3$)
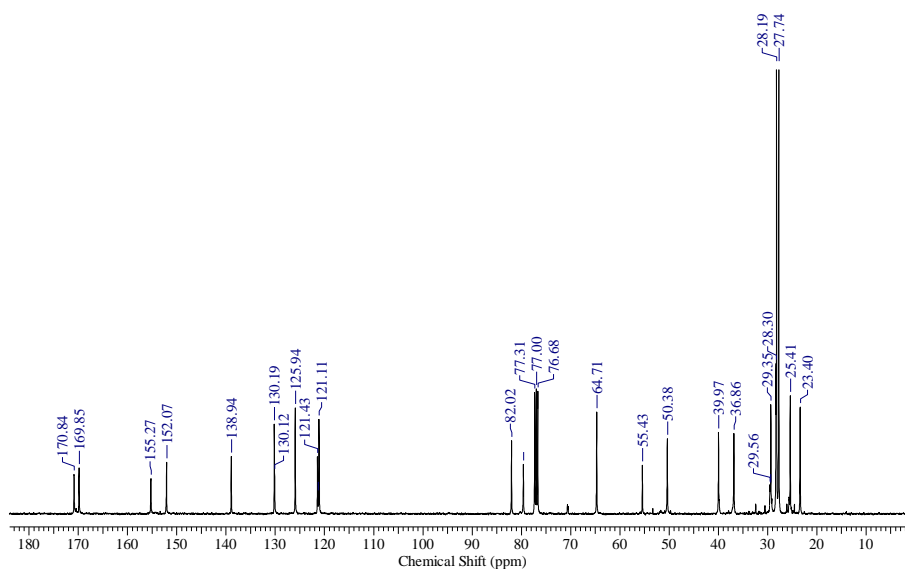

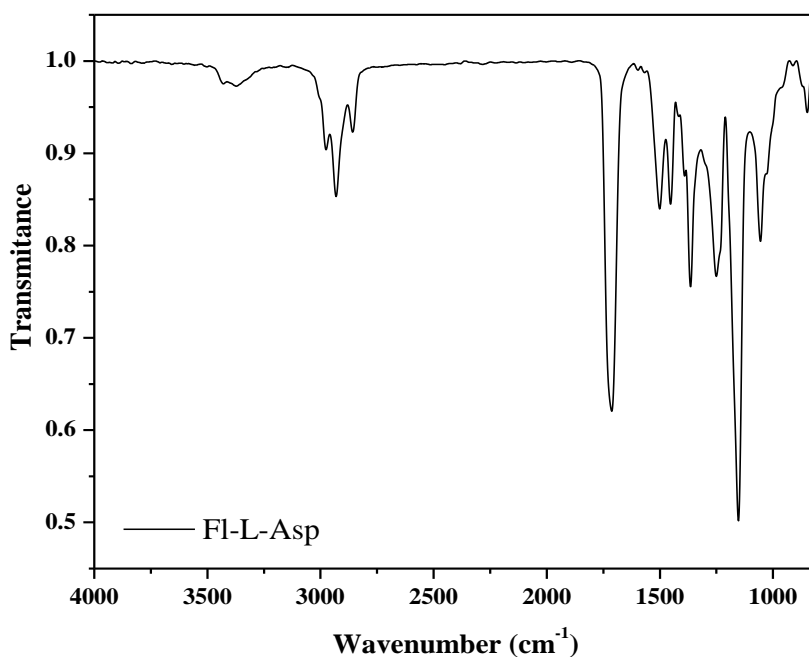**Figure 2.4** ^{13}C NMR spectrum of Boc protected-L-aspartic acid containing monomer (CDCl$_3$)

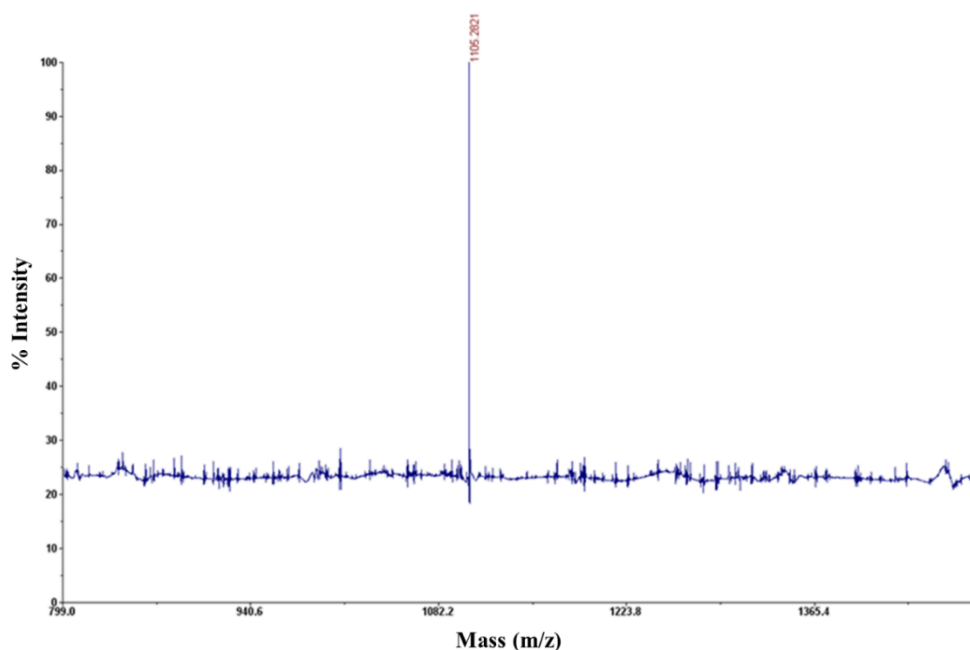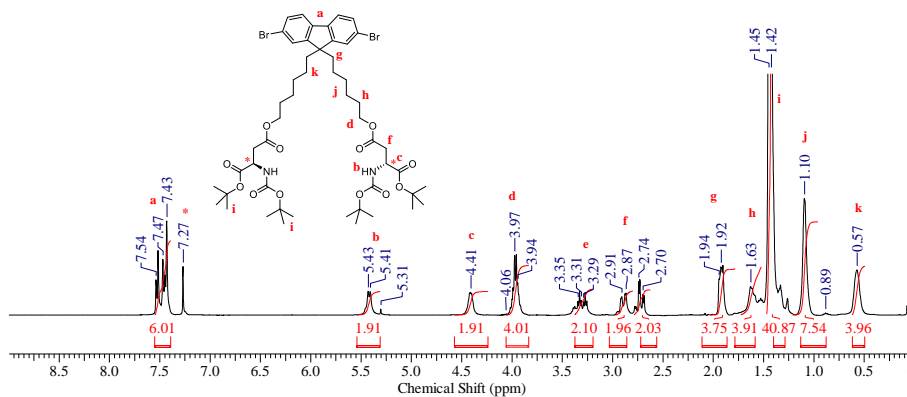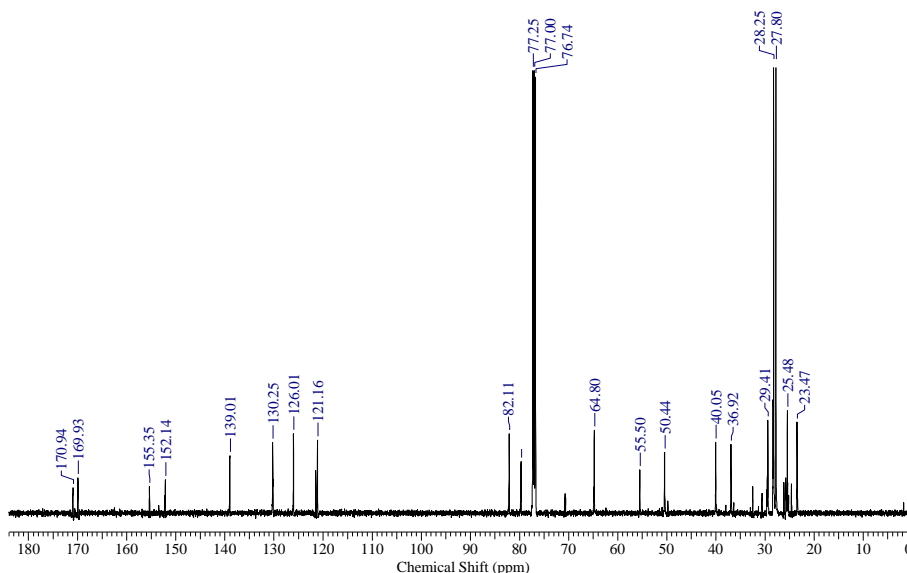**Figure 2.5** FT-IR spectrum of Boc protected-L-aspartic acid-containing monomer

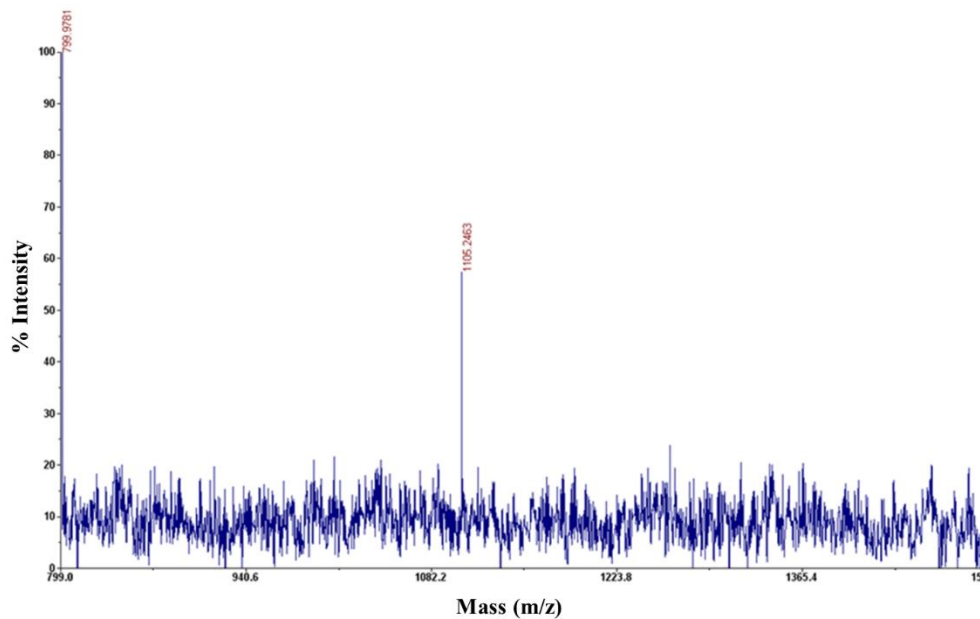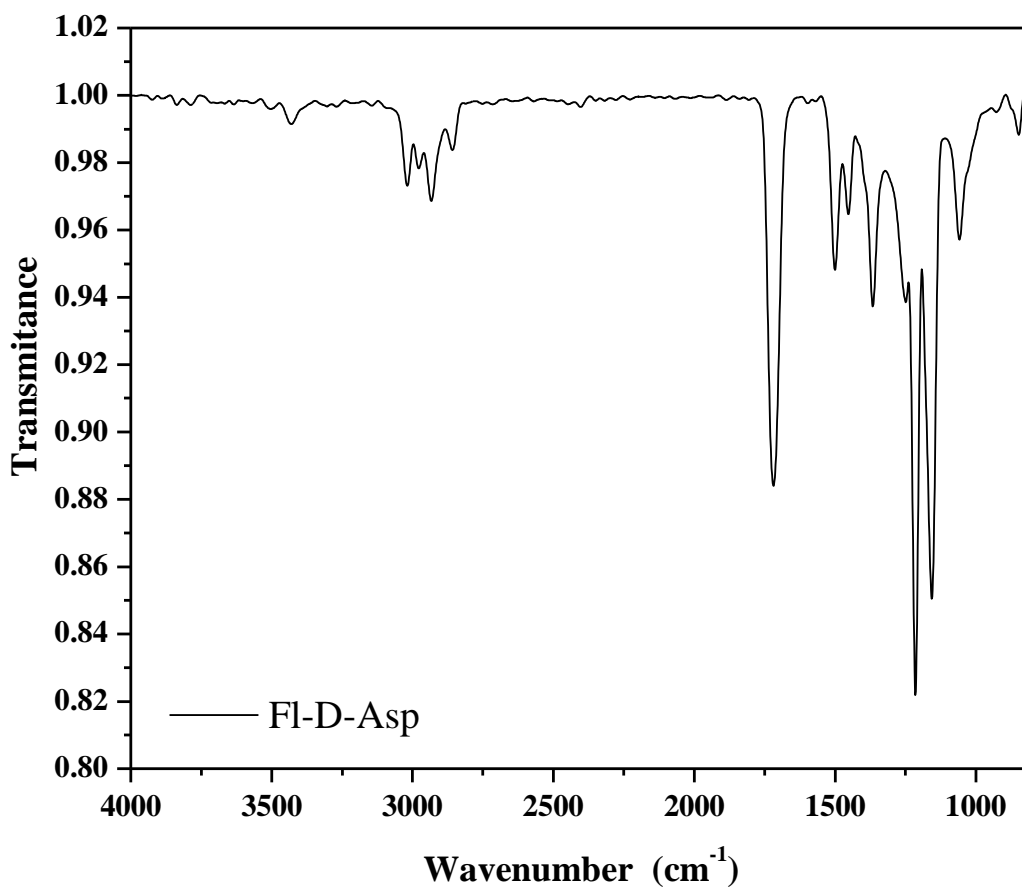**Figure 2.6** MALDI-TOF spectrum of Boc protected-L-aspartic acid containing monomer

c) Synthesis of Boc protected-D-aspartic acid containing monomer

Boc protected-D-aspartic acid containing fluorene monomer was synthesized by DCC, DMAP coupling of N-Boc-D-aspartic acid-1-tert-butyl ester with 2, 7-dibromo-9, 9-di-n-hexanolfluorene following similar reaction condition mentioned above for the synthesis of Boc protected-L-aspartic acid containing monomer. The product was purified by column chromatography using pet ether: ethyl acetate (70:30). Yield 74 %. ^{1}H NMR spectrum (400

MHz, CDCl$_3$) δ 7.43-7.52 (m, 6H), δ 5.41-5.43 (d, 2H), δ 4.42 (d 2H), δ 3.97 (t, 4H), δ 3.27-3.33 (q, 2H), δ 2.88-2.91 (m, 2H), δ 2.74 (m, 2H), δ 1.90-1.94 (m, 4H), δ 1.63 (m, 4H), δ 1.42-1.45 (s, 40), δ1.10 (m, 8H), 0.57 (m, 4H). ^{13}C NMR spectrum (100 MHz, CDCl$_3$) δ 170.84, 169.85, 155.27, 152.07, 138.94, 130.19, 125.94, 121.11, 80.02, 79.60, 64.71, 55.43, 50.38, 39.97, 29.56, 28.35, 28.30, 28.19, 27.74, 25.41, 23.40. MALDI-TOF analysis; Calculated mass-1066.96; observed-1105.24 [M+K]$^+$; FT-IR stretching frequency (υ) in cm^{-1}; 3435, 3021, 2987, 2930, 2864, 1712, 1495, 1466, 1367, 1207, 1159 and 1053.

Figure 2.7 ^{1}H NMR spectrum of Boc protected-D-aspartic acid containing monomer (CDCl$_3$)

Figure 2.8 ^{13}C NMR spectrum of Boc protected-D-aspartic acid containing monomer (CDCl$_3$)

Figure 2.9 MALDI-TOF spectrum of Boc protected-D-aspartic acid-containing monomer

Figure 2.10 FT-IR spectrum of Boc protected-D-aspartic acid-containing monomer

d) Synthesis of 1, 4-benzenediboronic acid bis(pinacol) ester

1,4-Benzenediboronic acid (2.00 g, 12.07 mmol) and Pinacol (3 g, 24.20 mmol) were added in two necked round bottom flask equipped with a magnetic stirring bar and Dean-Stark apparatus. Dry DCM (100 ml) was added in an inert atmosphere using a syringe. The resultant solution was refluxed for 12 hours in an inert atmosphere. The solvent accumulated in the Dean-Stark apparatus was periodically removed and the reaction mixture was replaced with new dry DCM. The organic layer was dried over anhydrous Na_2SO_4 after the reaction was completed and the solvent was removed in a vacuum to yield an off-white solid. Obtained crude product was recrystallized from n-hexane/CHCl$_3$ to obtain the white crystalline pure product. Yield 80 %. ^{1}H NMR spectrum (400 MHz, CDCl3) δ 7.81 (s 4H), δ1.36 (s, 24H). ^{13}C NMR spectrum (100 MHz, CDCl$_3$) δ 133.88, 83.84, 24.86. FT-IR stretching frequency (υ) in cm^{-1}; 2975, 2928, 1595, 1510, 1335, 1207, 1159 and 1053.
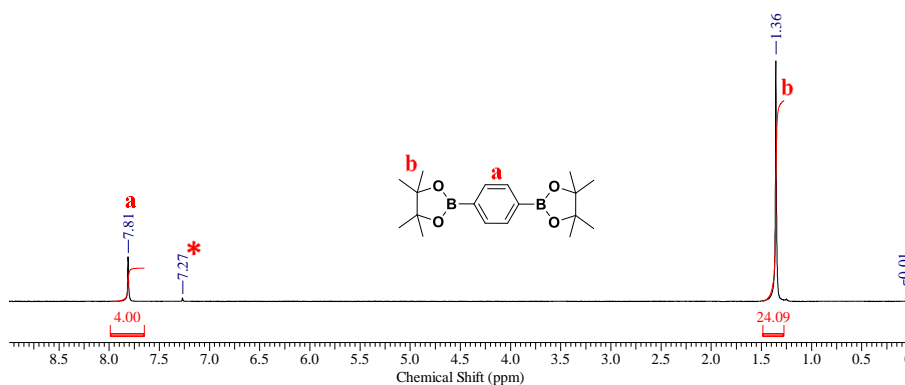
Figure 2.11 ^{1}H NMR spectrum of 1, 4-benzenediboronic acid bis(pinacol)ester (CDCl$_3$)

2) Synthesis of Boc Protected L and D Aspartic Acid Appended Polyfluorenes

e) Synthesis of Boc protected-L-aspartic acid-containing polymer (PF-LAsp)

1, 4-benzene diboronic acid bis(pinacol)ester (346 mg, 0.94 mmol) and Boc protected-L-aspartic acid-containing monomer (1 g, 0.94 mmol) were taken in Schlenk tube equipped with a magnetic stirring bar and a reflux condenser. The reaction setup was connected to Schlenk line for maintaining inert atmosphere. Dry THF (8 ml) was added to the reaction mixture using cannula and the reaction mixture was subjected to a sequence of three consecutive freeze-pump-thaw cycles. Pd(PPh$_3$)$_4$ (37 mg, 3 mole percent) was added to this reaction mixture and stirred for 1 hour at room temperature. After 5 minutes of nitrogen purging, an aqueous K_2CO_3 solution (900 mg, 5.64 mmol in 2 ml water) was added to the

reaction mixture, which was then refluxed at 85 °C for 48 hours. Once the reaction was complete, solvent was concentrated to roughly 1 ml under reduced pressure and the polymer was precipitated from THF solution in methanol, water and acetone separately. This repeated precipitation was carried out to remove catalyst, oligomers and salt from the polymer. Yield 92 % ^{1}H NMR spectrum (400 MHz, CDCl**3**) δ 7.82 (m, 6H), δ 7.65-7.69 (m, 4H), δ 5.42-5.44 (d, 2H), δ 4.40 (d 2H), δ 3.96 (t, 4H), δ 3.28-3.32 (q, 2H), δ 2.86-2.89 (m, 2H), δ 2.70 (m, 2H), δ 2.10 (m, 4H), δ 1.64 (m, 4H), δ 1.41-1.45 (s, 40), δ1.15 (m, 8H), 0.78 (m, 4H). ^{13}C NMR spectrum (100 MHz, CDCl3) δ 170.99, 169.95, 155.37, 151.50, 134.94, 127.55, 126.07, 121.23, 120.18, 82.12, 79.08, 70.88, 64.87 55.22, 50.45, 40.54, 36.93, 29.66, 28.27, 27.81, 25.64, 23.85. FT-IR stretching frequency (υ) in cm^{-1}; 3302, 2923, 2843, 1720, 1597, 1448, 1351, 1240, 1140, 1025 and 815.
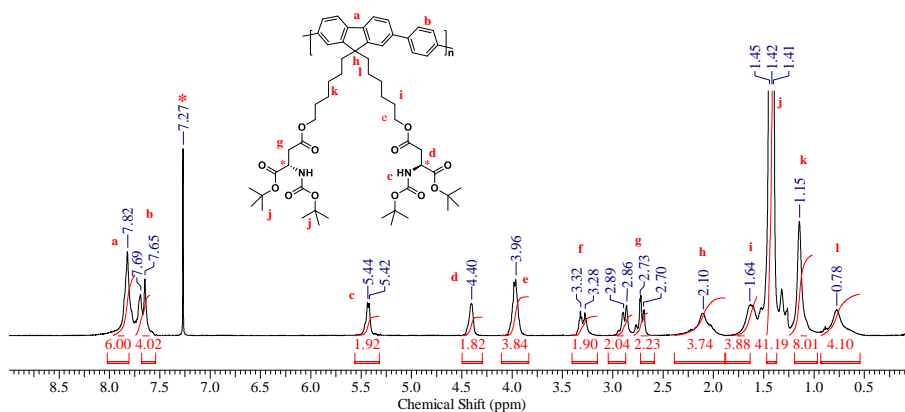
Figure 2.12 ^{1}H NMR spectrum of PF-LAsp polymer (CDCl$_3$)
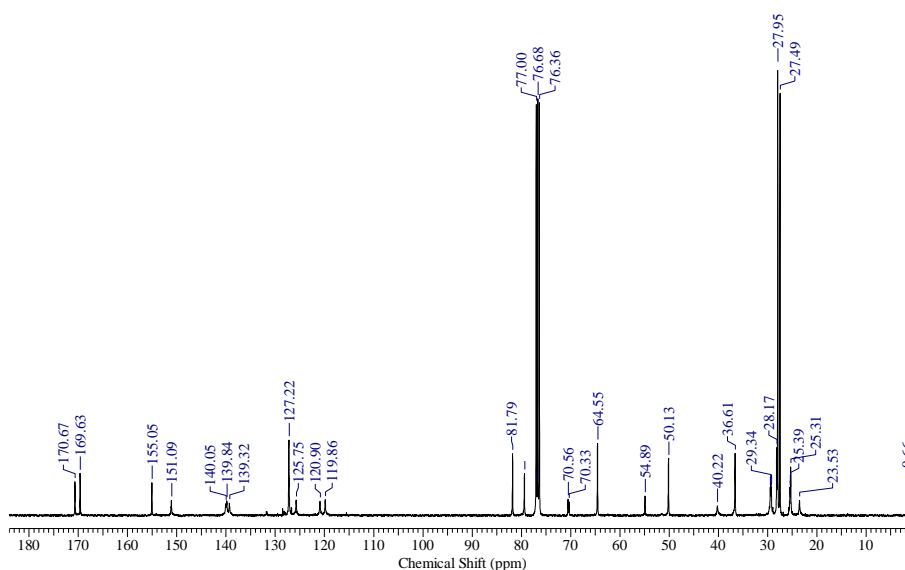
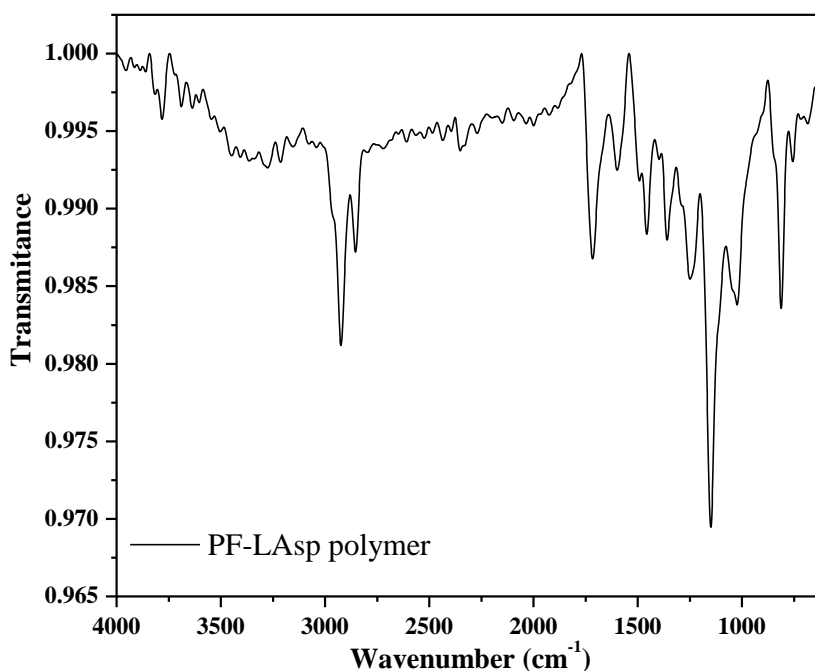**Figure 2.13** ^{13}C NMR spectrum of PF-LAsp polymer (CDCl$_3$)

Figure 2.14 FT-IR spectrum of PF-DAsp polymer

f) Synthesis of Boc protected-D-aspartic acid containing polymer (PF-DAsp)

Boc protected-D-Aspartic Acid containing polymer (PF-DAsp) was synthesized by Suzuki polymerization of Boc protected-D-aspartic acid containing monomer and 1, 4-benzene diboronic acid bis(pinacol)ester under identical reaction conditions as mentioned above for the synthesis of Boc protected-L-Aspartic Acid containing polymer (PF-LAsp). Polymer was purified by repeated precipitation from methanol, water and acetone separately. Yield 89 %; ^{1}H NMR spectrum (400 MHz, CDCl$_3$) δ 7.82 (m, 6H), δ 7.65-7.71 (m, 4H), δ 5.41-5.45 (d, 2H), δ 4.42 (d 2H), δ 3.97 (t, 4H), δ 3.27-3.34 (q, 2H), δ 2.90 (m, 2H), δ 2.65-2.75 (m, 2H), δ 2.04 (m, 4H), δ 1.73 (m, 4H), δ 1.41-1.44 (s, 40), δ 1.14 (m, 8H), 0.77 (m, 4H). ^{13}C NMR spectrum (100 MHz, CDCl$_3$) δ 170.67, 169.63, 155.05, 151.09, 140.05, 139.84, 139.82, 127.22, 125.75, 120.90, 119.86, 81.79, 70.56, 64.55 54.89, 50.13, 40.22, 36.61, 29.24, 27.49, 27.95, 25.31, 25.39, 23.53. FT-IR stretching frequency (υ) in cm^{-1}; 3426, 2924, 2854, 1711, 1598, 1456, 1351, 1245, 1140, 1025 and 806.
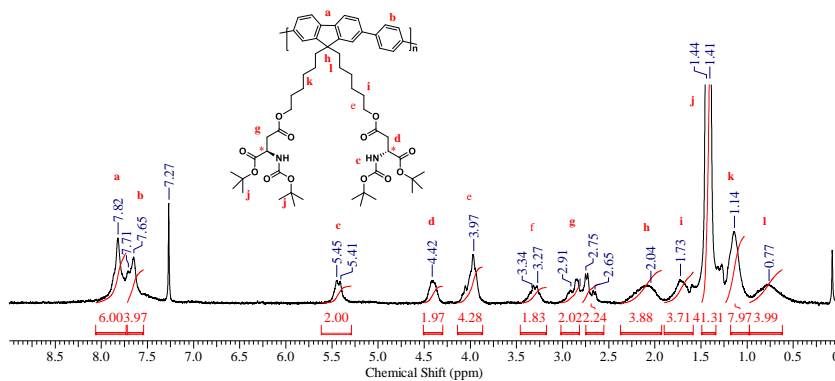
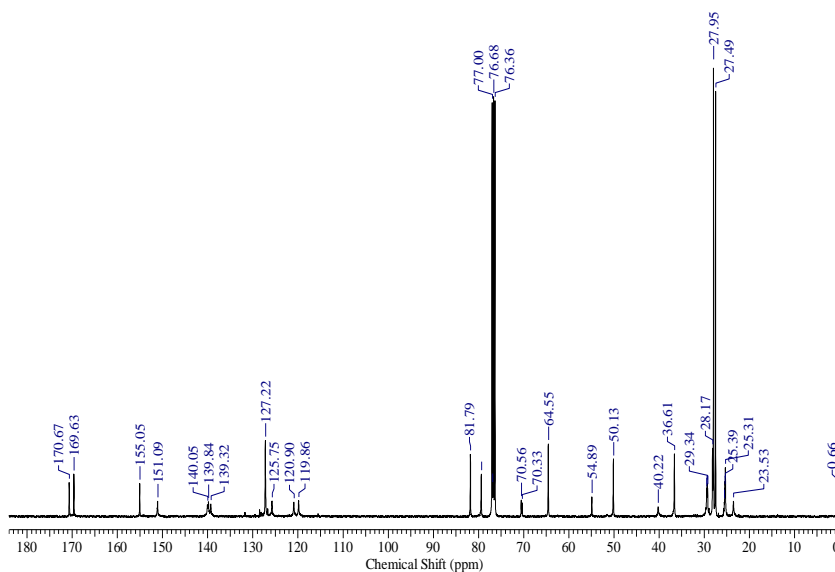**Figure 2.15** ^{1}H NMR spectrum of PF-DAsp polymer (CDCl$_3$)

Figure 2.16 ^{13}C NMR spectrum of PF-DAsp polymer (CDCl$_3$)
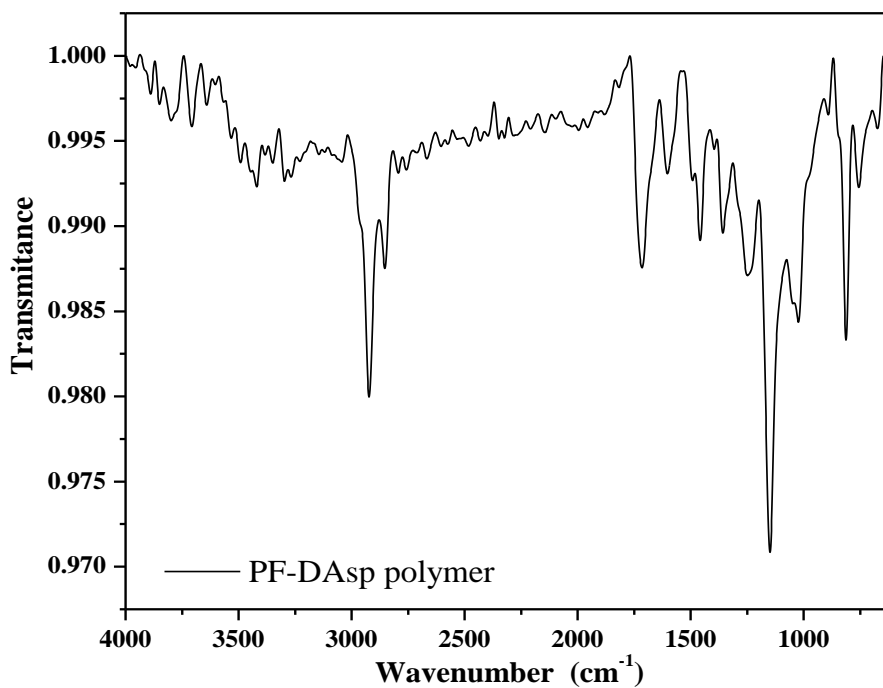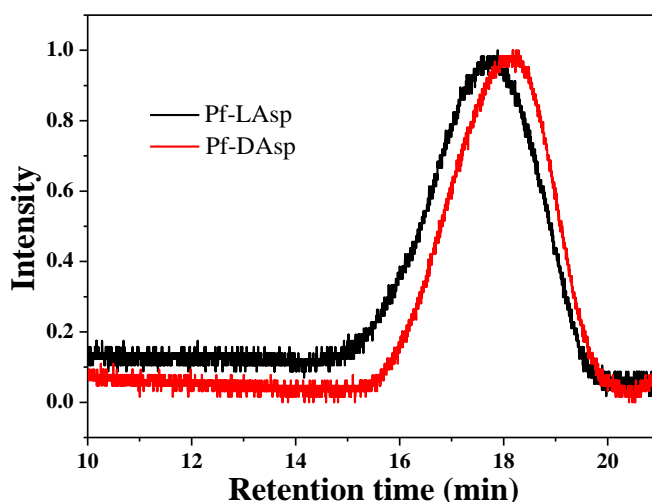

Figure 2.17 FT-IR spectrum of PF-DAsp polymer

Figure 2.18 GPC chromatogram of Boc protected chiral polymers (PF-L/DAsp)

Polymers	Mn[a] (g/mol)	Mw[b] (g/mol)	Đ$_M$[c]	Xn[d]
PF-LAsp	25000	51400	2.1	51
PF-DAsp	21400	46800	2.2	43

Table 2.1 Molecular Weight Parameters of Boc protected chiral Polymers (PF-L/DAsp)

[a]Mn and [b]Mw are number average and weight average molecular weights respectively.

[c]Đ$_M$ is dispersity of the polymers. [d]Xn is the number of repeating units.

2.3 RESULT AND DISCUSSION

Figure 2.18 shows the FE-SEM micrographs of the bare (a) and polymer coated chiral (b) AAO membranes.
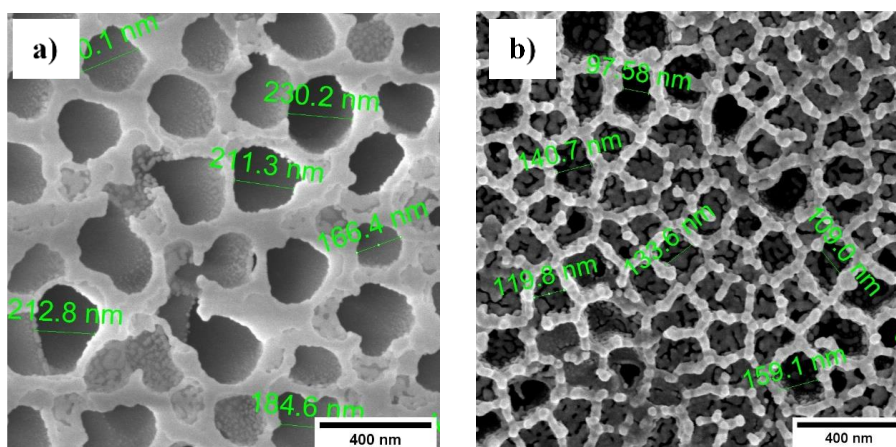

Figure 2.18 FE-SEM micrographs of (a) bare AAO (200 nm) membrane and (b) polymer-coated AAO membrane

The pore size dimensions computed using ImageJ software shows a reduction of average pore size from ~200 nm for the bare AAO membrane to 100−160 nm for the polymer-coated membrane. Although the SEM images provide clear visual evidence for a decrease in pore diameter, it is only qualitative information. Solute diffusion studies through the membrane were carried out to obtain a more quantitative estimate of the reduction in pore dimensions upon polymer modification of the AAO membrane.[49–51]
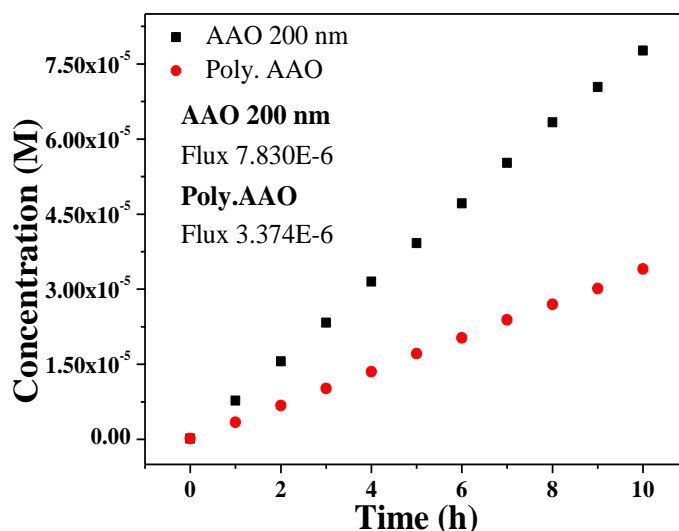

Figure 2.19 Determination of pore diameter by study by Fick's law of diffusion

Using Fick's law of diffusion, the relative average pore diameter was obtained as 131 nm (calculation details are given in experimental section D and Figure 2.19). This value is in concurrence with the observed pore size reduction upon polymer modification in the FE-SEM image. The FE-SEM micrographs also show the polymer organized around the walls of the pores (Figure 2.18b).

The chiral nature of the coated polymer was analyzed by extracting the polymer from the AAO membrane and subjecting to CD analysis. The finely crushed and powdered AAO membrane was extracted with HPLC grade THF multiple times until the polymer was removed entirely. Complete extraction of the polymer was confirmed by the disappearance of the polymer fluorescence from the washing solvent under a hand-held UV lamp.
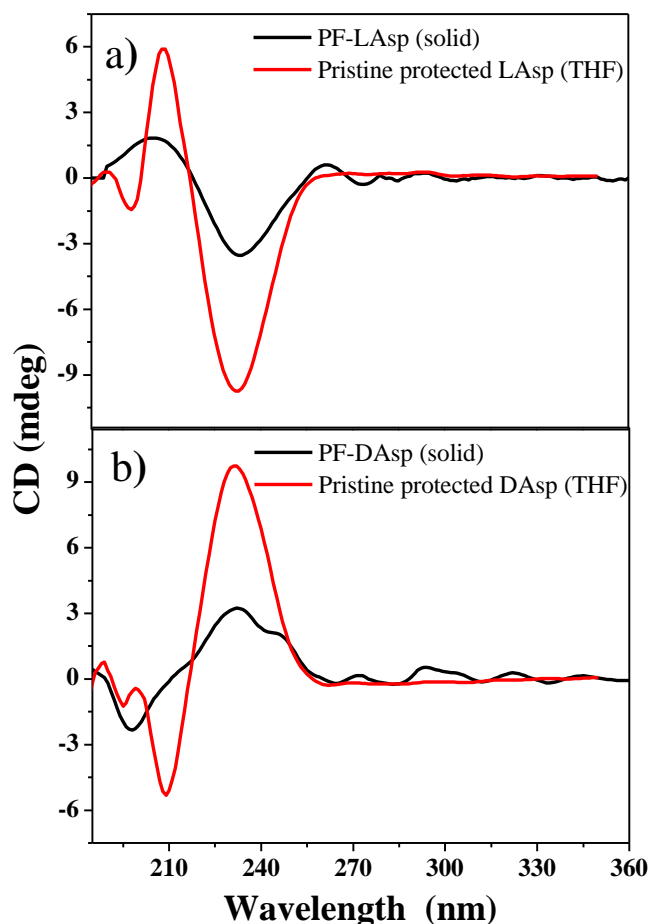
Figure 2.20 CD spectra of (a) PF-LAsp extracted from the AAO membrane in solid-state (KBr) along with protected L-aspartic acid (THF) (b) PF-DAsp extracted from AAO membrane in solid-state (KBr) along with protected D-aspartic acid (THF).

Figure 2.20 compares the CD spectra of the polymers recorded in the solid-state with that of the respective pristine protected D/L aspartic acid. Pristine protected L-aspartic acid shows a peak maxima at 208 nm and minima at 232 nm, while a mirror image CD spectra is observed in the case of pristine protected D-aspartic acid with minima at 208 nm and maxima at 232 nm. The CD spectra of both chiral polymers resemble that of the corresponding protected aspartic acid enantiomer, indicating the appendage's ability to induce chirality in the polymers. Quantitative estimation of the amount of polymer coated on the AAO membrane was carried out using the absorption coefficient value (54.95×10^3 L mol^{-1}cm^{-1} in THF) of the polymer calculated using the Beer−Lambert equation (Figure 2.21).
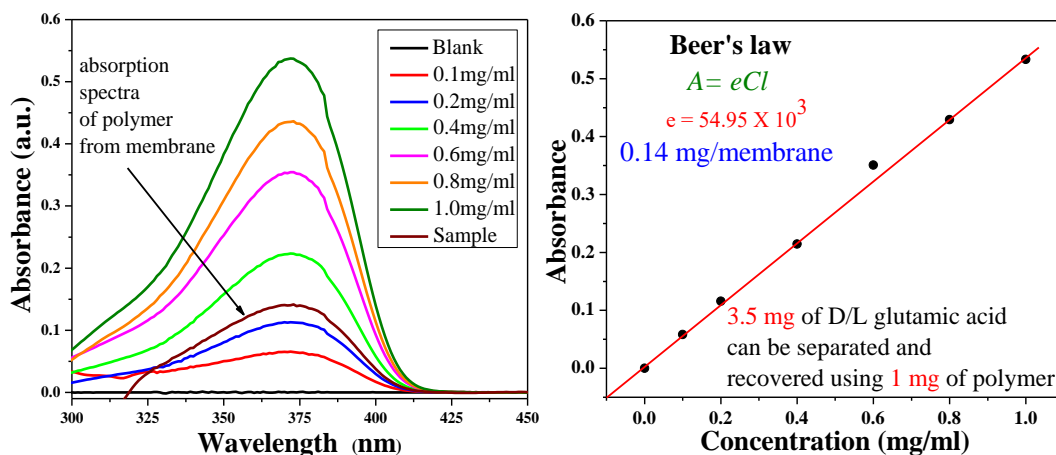
Figure 2.21 Estimation of the amount of polymer coated on the AAO membrane

The polymer was extracted completely from two chiral AAO membranes, dissolved in HPLC grade THF and used as the unknown sample for the estimation. An average amount of 0.14 mg of polymer is found to be coated on a single AAO membrane.

2.3.1 Enantioselective Recognition, Separation, and Kinetics

Evidence for the chiral nature of the pore channels was sought from enantioselective recognition experiments conducted to study the ability of the AAO membranes to discriminate between pairs of enantiomers (Figure 2.22a). Figure 2.22b bottom shows the reduction in the intensity of the CD spectra over time for a solution of native D-glutamic acid into which two PF-DAsp coated AAO membranes (PF-DAsp@AAO) were suspended, indicating its adsorption into the pore channel of the AAO membrane. The top plot in Figure 2.22b corresponds to a similar experiment conducted in a native L glutamic acid solution, which remains intact without any reduction in intensity despite prolonged exposure time.
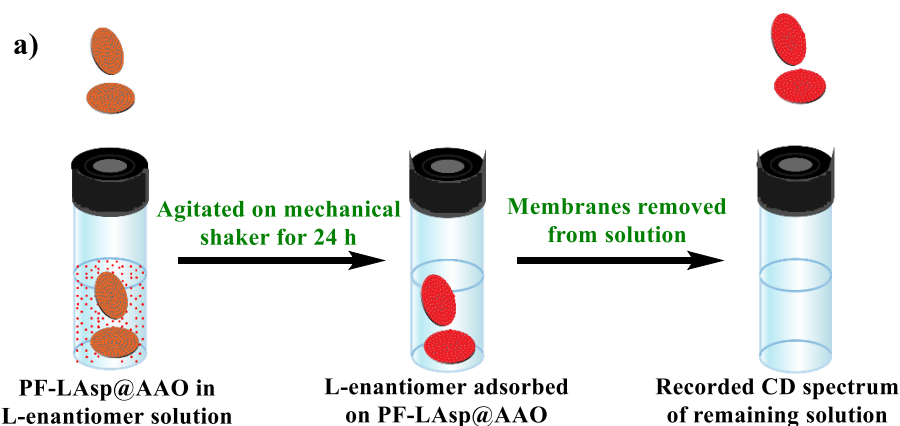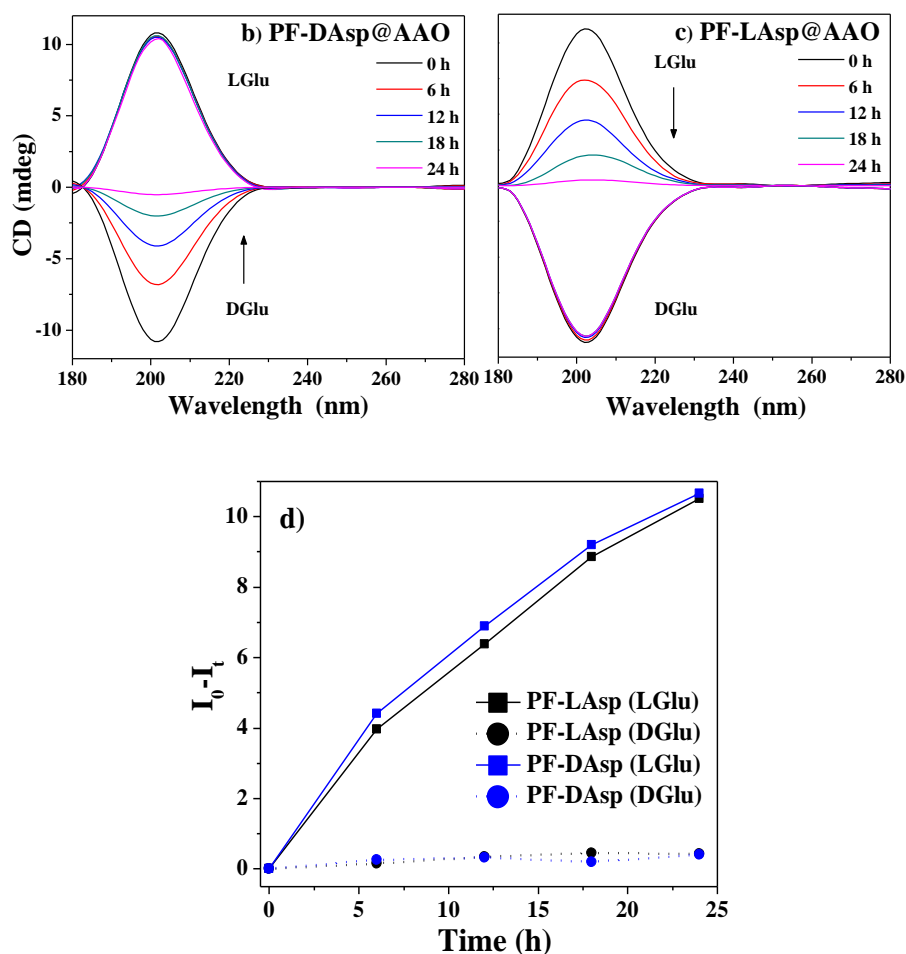
Figure 2.22 a) Schematic representation of experimental setup b) CD spectra to show enantioselective recognition of D-glutamic acid by PF-DAsp@AAO and (c) CD spectra to show enantioselective recognition of L-glutamic acid by PF-LAsp@AAO. d) Combined plot showing enantioselective sensing of D and L-glutamic acid by PF-DAsp and PF-LAsp coated chiral AAO membranes, respectively.

The same is true for PF-LAsp@AAO, which selectively adsorbs L-glutamic acid from the solution resulting in a reduction in the intensity of the CD spectra only when immersed in a solution of L-glutamic acid (Figure 2.22c, top plot). Figure 2.22d is a combined plot of the difference in peak intensity ($I_0 - I_t$) at λ_{max} 202 nm as a function of time, where I_t and I_0 are peak intensity of CD signal at time t and at time t = 0 h, respectively. The combined plot summarizes the observations from these experiments confirming that polymer-coated chiral AAO membranes have the ability to discriminate between pairs of enantiomers. PF-LAsp@AAO adsorbs only L-glutamic acid, whereas PF-DAsp@AAO membrane adsorbs only D-glutamic acid; the adsorption of enantiomers with opposite chirality is negligible.

After establishing the selective recognition ability of the AAO membranes toward the different enantiomers, the ability to bring about an enantioselective separation of racemic mixtures was tested. For this, the polymer-coated AAO membranes were suspended in a solution of an equimolar racemic mixture of 1 mg each of D and L native amino acid (D and L-glutamic acid as a representative analyte) dissolved in 3 ml of Milli-Q water as shown schematically in Figure 2.23.
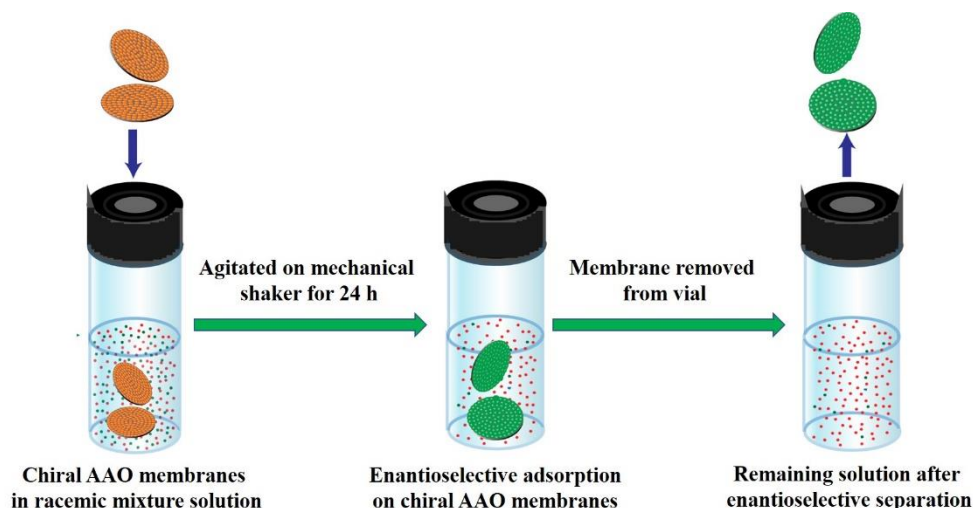

Figure 2.23 Schematic representation showing enantioselective separation of a racemic mixture using chiral AAO.

The racemic mixture treated with PF-LAsp@AAO started showing a peak for D-glutamic acid (Figure 2.24, bottom plot (dotted lines)) while the racemic mixture treated with PF-DAsp@AAO started showing a peak for L-glutamic acid (top plot). The peak intensity increases with the increase in time. It is also seen that both the polymer-coated chiral AAO membranes exhibit almost similar kinetics for separation of the racemic mixture, and most of the enantioselective separation is accomplished within the first 20 h (Figure 2.24 inset plot) thereafter, the change in the CD spectrum is marginal.
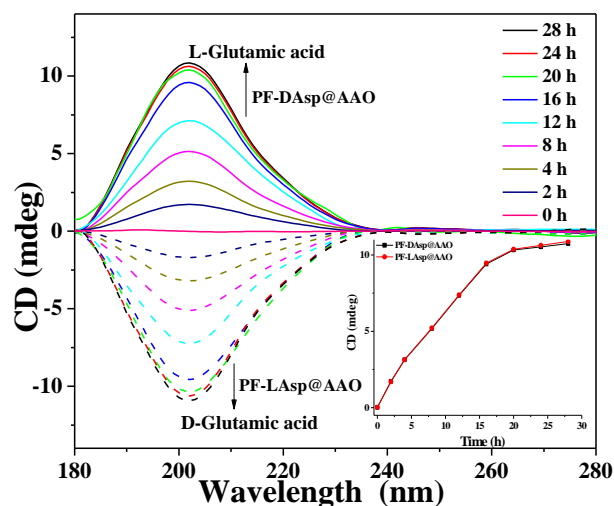
Figure 2.24 CD spectra for enantioselective separation of racemic mixture of glutamic acid using PF-DAsp@AAO and PF-LAsp@AAO membranes. (Inset) Kinetics of enantioselective separation of racemic mixture.

This demonstrates that 24 h is sufficient for enantioselective separation to occur. Similar enantioselective separations were carried out for racemic mixtures of various other native amino acids like alanine, aspartic acid, leucine, lysine, serine, phenylalanine, proline, and valine in Mili-Q water for 24 h. The chemical structures of native D and L amino acids screened in the present study are given in Figure 2.25 and the CD spectra plotted are given in Figure 2.26
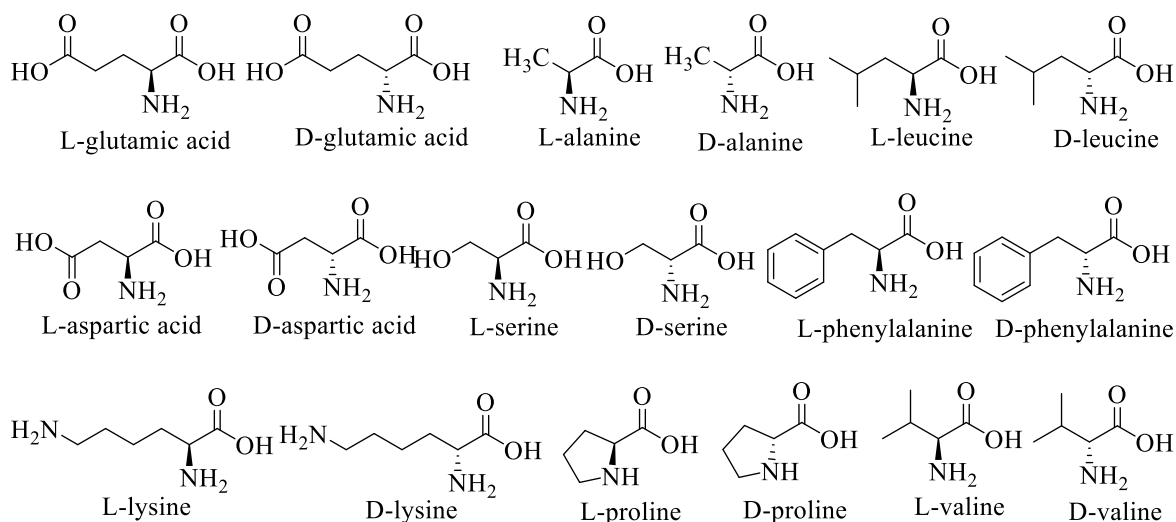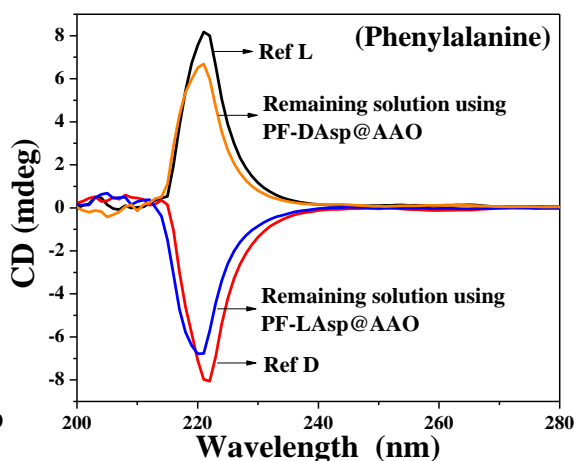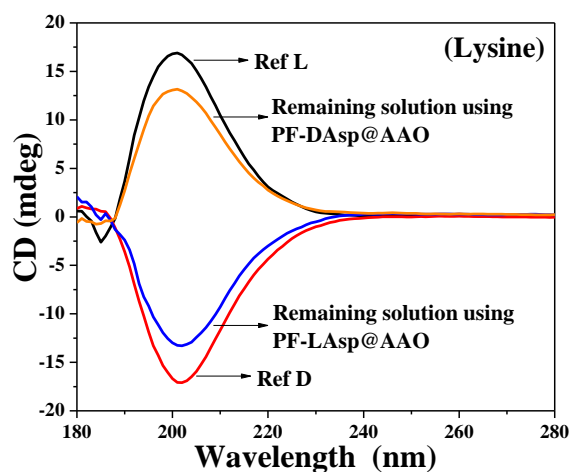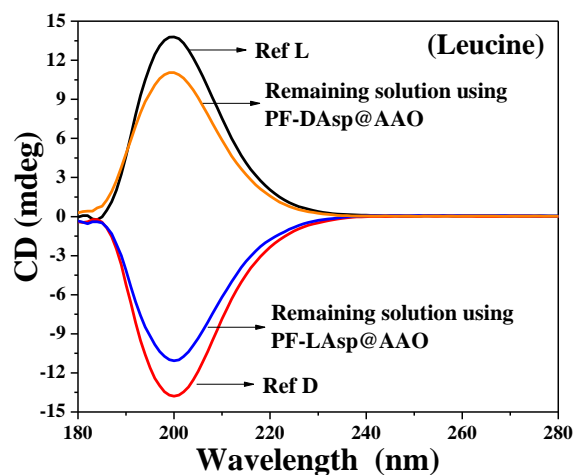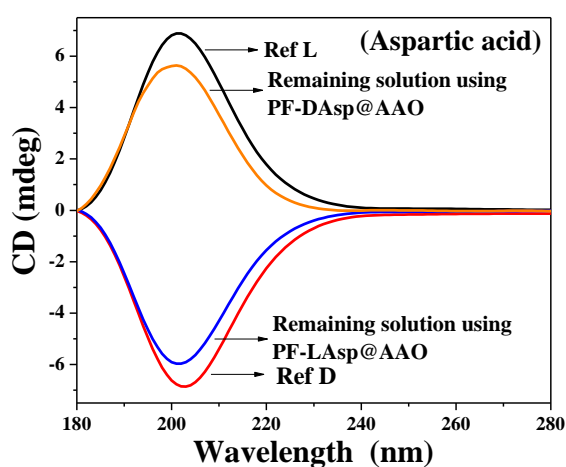

Figure 2.25 Structure of analytes screened for enantioselective separation
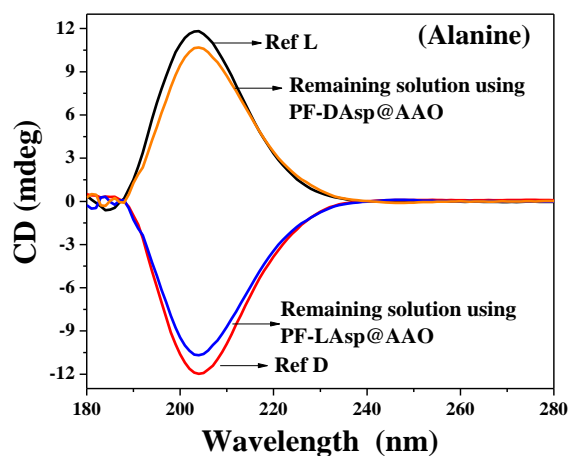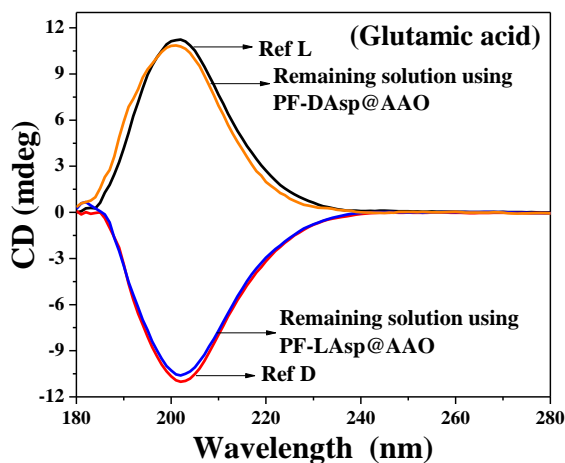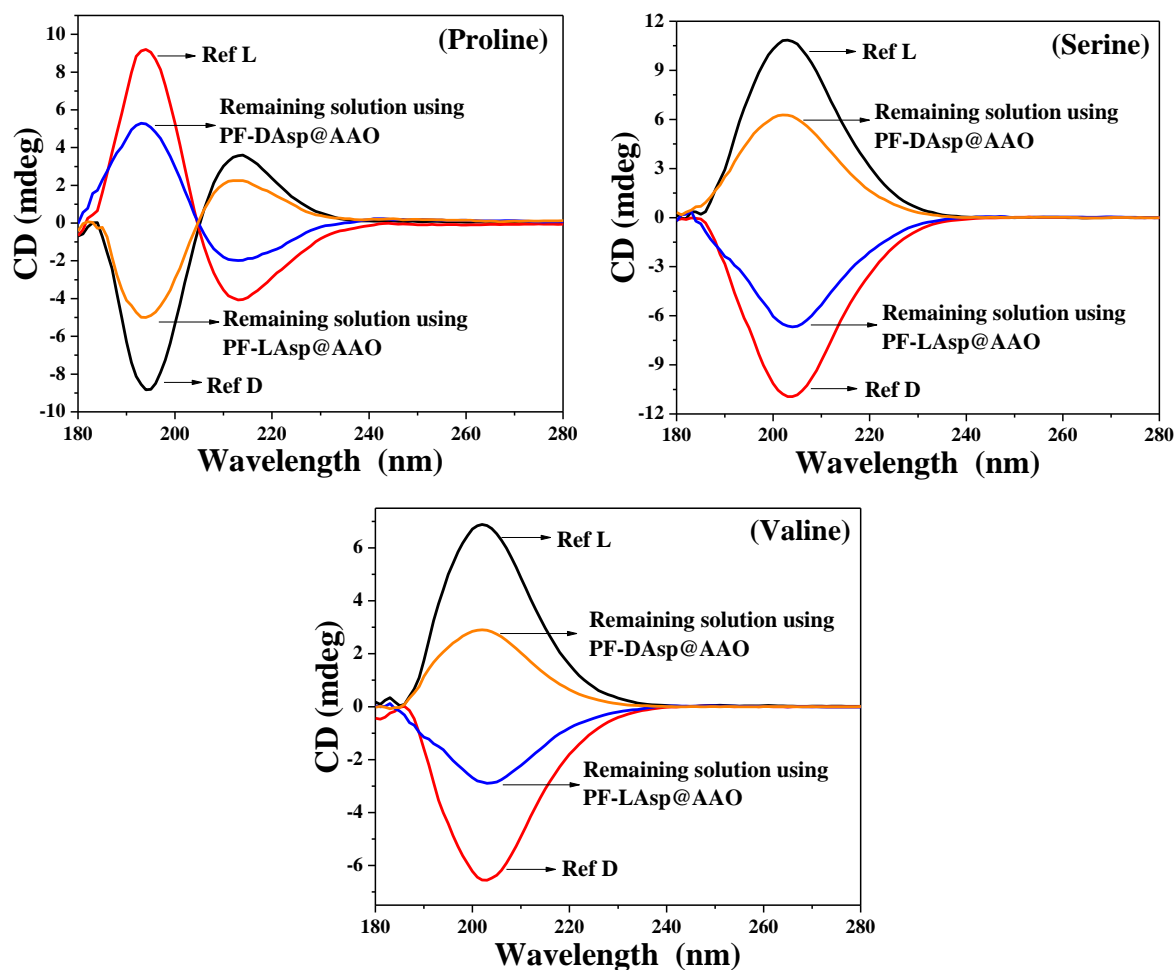
Figure 2.26 CD spectra of remaining solution after enantioselective separation plotted against the pure enantiomer

The % ee was calculated from the ratio of areas under the curve of CD spectra for the solution remaining after 24 h to that of the pure enantiomer. Table 2.2 summarizes the % ee separation obtained from CD data for the various native amino acids used as analytes.

Racemic mixture (native amino acids)	% Enantiomeric excess (ee)[a]	
	PF-LAsp@AAO	PF-DAsp@AAO
Glutamic acid	95.2	94.7
Alanine	88.3	91.3
Leucine	80.6	82.9
Lysine	80.8	83.3
Aspartic acid	80.2	79.0
Phenylalanine	72.0	71.5
Proline	66.1	66.9
Serine	63.0	60.7
Valine	46.4	47.7

Table 2.2 % Enantiomeric Excess (ee) Values Obtained from CD Data.

[a]% Enantiomeric excess (ee) obtained by taking ratio of area under the CD curve.

Both the D and L aspartic acid appended polymer coated AAO membranes exhibits similar separation capabilities. From the table it is seen that the maximum ee of ~95% is observed when glutamic acid is the analyte.

The % ee can be improved by adding two fresh polymer coated AAO membranes to the racemic mixture at the end of 24 h. Figure 2.27 shows that although prolonging the time of incubation of two polymer coated AAO membranes with the racemic mixture of aspartic acid does not bring about noticeable improvement in % ee, almost complete enantiomeric separation of racemic mixture is achieved with a total of four PF-D/LAsp polymer coated AAO membranes.
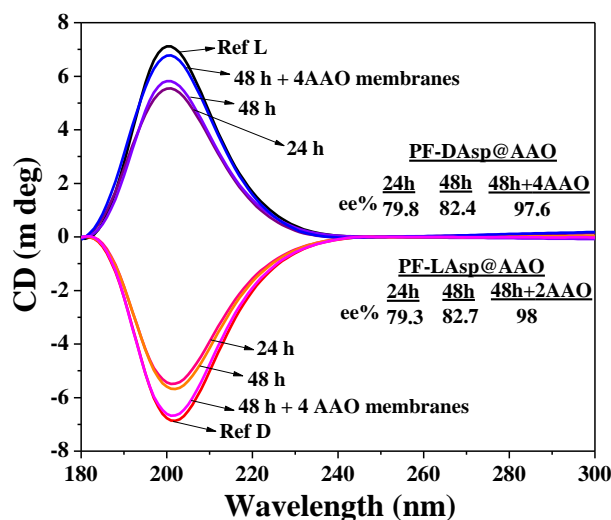
Figure 2.27 CD spectra for enantioselective separation of a native aspartic acid racemic mixture using PF-D/LAsp@AAO membranes incubated for 24 h, 48 h, and 48 h with the addition of two fresh PF-D/LAsp@AAO membranes at the end of 24 h. Inset: Table showing % ee for the different time periods.

An experiment was conducted to recover the adsorbed native amino acid from the AAO membrane and to quantify it. For this, two chiral AAO membranes used in enantioselective separation experiments were crushed and sonicated in a small amount of milli-Q water repeatedly. The polymer and residues of the membrane remain insoluble in the water, which is separated by simple filtration. The water is removed completely by freeze-drying, and the recovered amino acid is solubilized again in 3 mL of fresh milli-Q water. The solution state CD spectra were recorded (Figure 2.28), and its quantification was done by taking the ratio of areas under the curve against that of pure enantiomer (1 mg of pure enantiomer in 3 mL of Milli-Q water). Analyte recovery was carried out for a few representative examples of glutamic acid, aspartic acid, serine, and valine.

Figure 2.28 CD spectra of remaining solution and enantiomer extracted from membranes
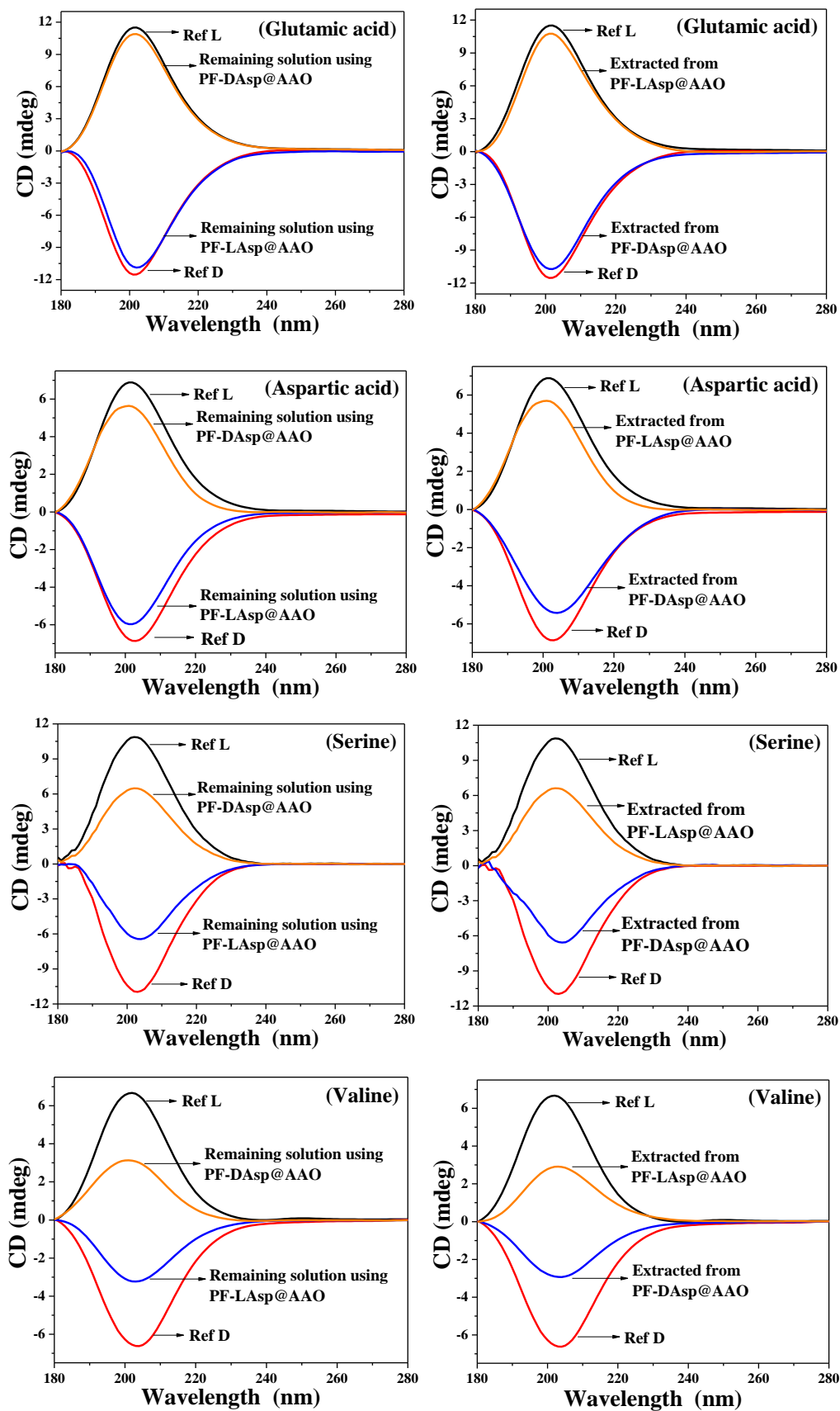
The value obtained from the CD data is comparable with ee % values obtained from the CD signal of the remaining solution (Table 2.3).

Analytes	% enantiomeric excess for remaining water		% enantiomeric excess for extracted analyte	
	PF-LAsp@AAO	PF-DAsp@AAO	PF-LAsp@AAO	PF-DAsp@AAO
Glutamic acid	95.2	94.7	94.7	95.1
Aspartic acid	80.2	79.0	80.0	82.5
Serine	63.0	60.7	60.8	61.0
Valine	46.4	47.7	45.8	47.2

Table 2.3 % Enantiomeric excess values for remaining solution and quantification of enantiomer extracted from AAO membrane after enantioselective separation

As discussed earlier, the PF-D/LAsp coated on the AAO membrane was quantified using the Beer−Lambert equation to average about 0.14 mg/membrane. The amino acid adsorbed on the AAO membranes was also quantified after extracting them from the crushed membranes. Using simple arithmetic, it can be seen that about 3.5 mg of D/L glutamic acid can be separated and recovered using 1 mg of chiral AAO membrane in 24 h. The template approach adopted in this work provides increased surface area for separation and eliminates the requirement of inherent porous fibrous morphology as a prerequisite for the chiral amino acid appended polyfluorene to achieve enantioselective separation of racemic mixtures. The direct dispersion of the chiral polyfluorene in water for 48 h results in a change in the pattern of the CD signal (our previous report)[52], whereas no change in the CD signal pattern is observed when the PF-D/LAsp polymers are coated on the AAO membrane (Figure 2.28).
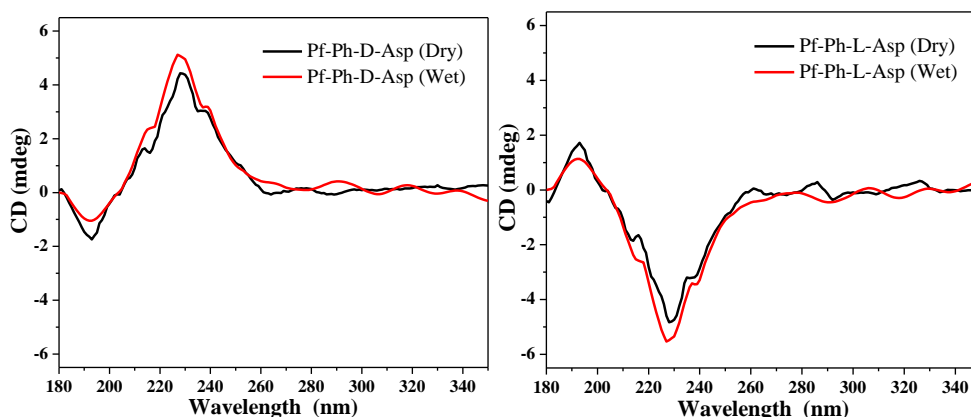
Figure 2.28: CD spectra of polymer extracted from the membrane after 24 hours water treatment

2.3.2 Effect of Pore Size on Enantioselective Separation

The size of the Nanoporous channel could be expected to influence the % ee separation. In order to understand the role of pore size on the efficiency of enantioselective separation and also to analyze whether the separation occurs inside chiral pore or on the membrane surface as well, AAO membranes with different pore sizes (200, 100, and 20 nm) were chosen to coat the D- and L-aspartic acid appended polyfluorene.
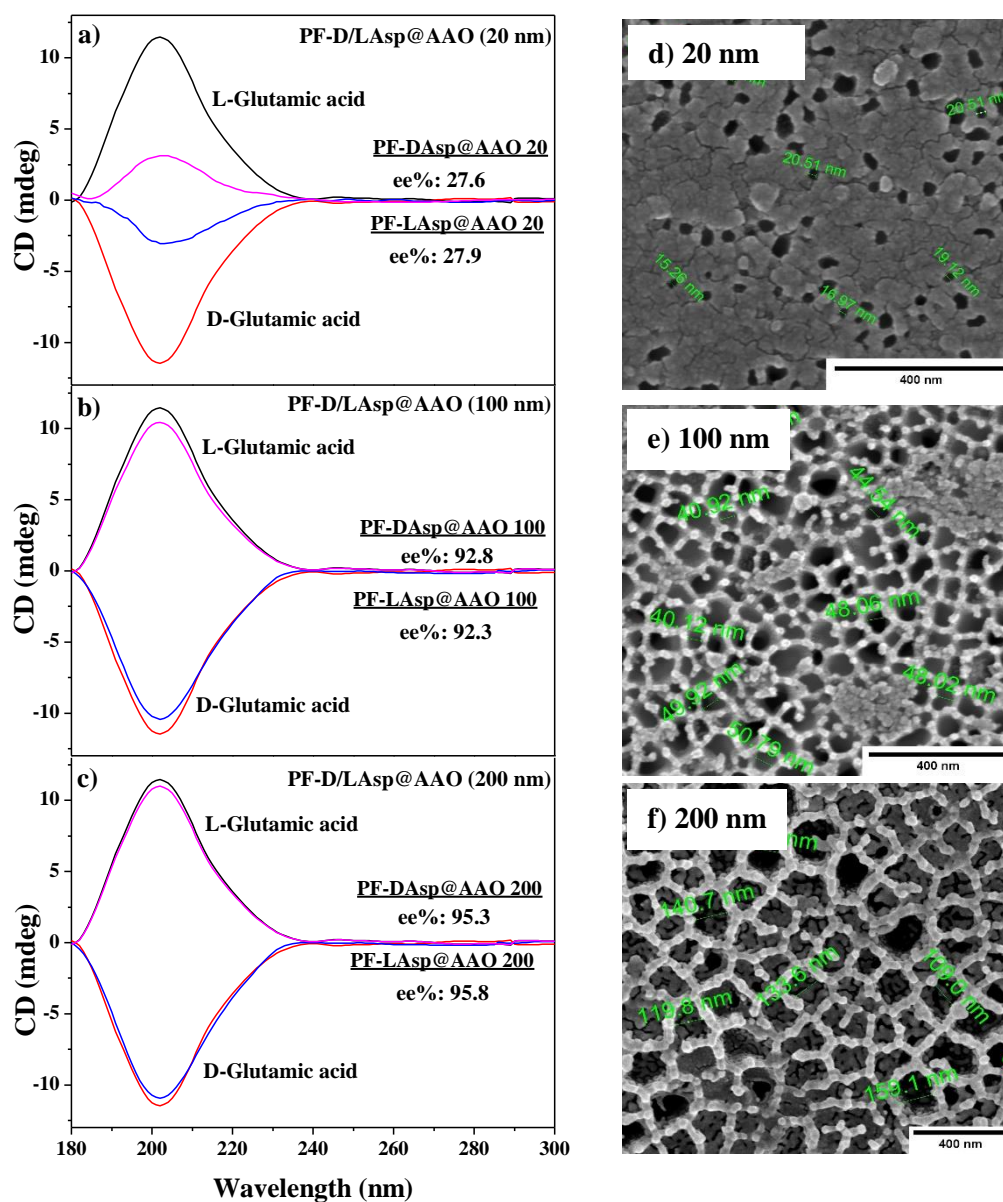
Figure 2.29 (a−c) CD spectra of enantioselective separation of glutamic acid racemic mixture with 20, 100, and 200 nm pore size chiral AAO membranes, respectively. Inset: Table showing % ee. (d−f) FE-SEM micrographs of polymer-coated chiral AAO membranes with different sizes 20 nm, 100 nm, and 200 nm.

These different pore-sized chiral AAO membranes were used to carry out the enantioselective separation of the native glutamic acid racemic mixture as a representative analyte. The CD spectra of the remaining solution after 24 h interaction with the AAO membrane was recorded and plotted against the pure enantiomers (Figure 2.29). From the figure, it is seen that the 100 nm pore size polymer-coated membranes also achieve similar enantiomeric excess (~93%) as that of the 200 nm pore size membranes (~95%), but the separation efficiency is drastically decreased in the case of the 20 nm AAO membranes (~28%). The values of enantiomeric excess are tabulated in the inset in Figure 2.29. The reason for the drastic decrease of separation efficiency in the case of a 20 nm pore-sized membrane can be elaborated with the help of FE-SEM micrographs of the polymer-coated membranes (Figure 2.29d−f). In the case of the 100 and 200 nm pore-sized polymer-coated membrane, the average pore size reduces to 49−72 nm and 100−160 nm, respectively, with a clear opening of the pores (as observed from the pore size dimensions determined using ImageJ software). However, in the case of the 20 nm AAO membrane, the pores are severely clogged with polymer, and the average pore size drastically reduces to 15−17 nm. This experiment clearly conveyed that the separation is severely hampered when the pores are clogged. Thus, one can safely conclude that the process of enantiomer separation occurs inside the chiral pores and not on the surface of the membranes.

2.4 DISCUSSION

An important step in the chiral recognition and enantiomeric separation involving chiral polymeric selectors is the formation of labile diastereoisomeric complexes between the enantiomers and the chiral selector.[53] The ability to discriminate between the enantiomers arises from the different points of interaction of the two enantiomers with the selector. One of the commonly accepted mechanisms for the formation of the labile diastereoisomeric complex is by a 3-way interaction, where only one enantiomer can match exactly the three sites of interaction on the chiral carbon of the selector, while for the other enantiomer, only two sites of interaction would be possible after all possible rotations.[54] These points of interaction, which should be between three different substituents of the chiral analyte and selector, could be either hydrogen bonding, $\pi-\pi$, or even repulsive interactions. Hydrogen bonding is expected to be at the forefront of interactions with amino acid selectors. Indeed, FT-IR experiments indicated the existence of differential interaction of the D and L-protected amino acid appended selector polymer toward D-glutamic acid in its native form

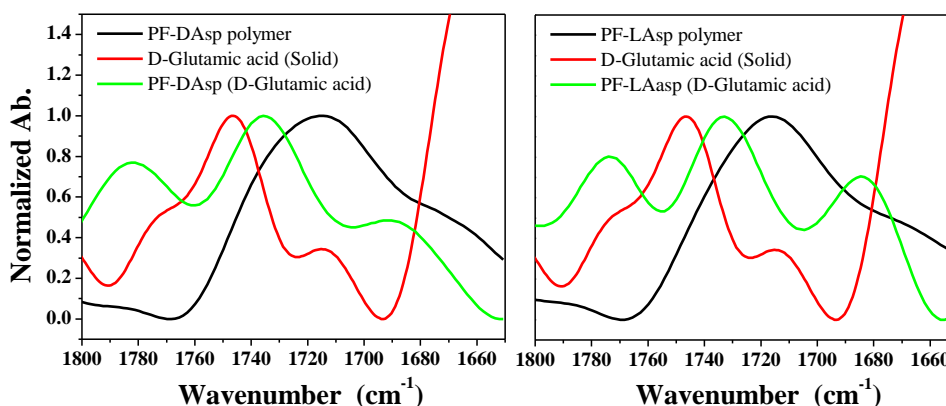as a typical analyte. Details of the FT-IR experiments are provided below in Figure 2.30 and Table 2.4.

Figure 2.30 FT-IR spectra of polymers mixed with enantiomers of glutamic acid

Sample	Non hydrogen bonded peak region (cm^{-1})	Non hydrogen bonded peak area	Hydrogen bonded peak region (cm^{-1})	Hydrogen bonded peak area	Peak area ratio	% Reduction in Hydrogen bonding (Peak area ratio of pristine – Peak area ratio of mixture)/ peak area ratio of pristine x100
D-Glutamic acid	1785-1763	4.67	1763-1724	12.66	2.71	
PF-DAsp + D-Glutamic acid	1800-1760	26.43	1760-1705	40.68	1.53	43
PF-LAsp + D-Glutamic acid	1798-1755	26.64	1755-1705	36.57	1.37	49

Table 2.4 % Reduction in Hydrogen bonding interaction

The existence of such differential interaction supports the matched and mismatched orientation mechanism for enabling chiral recognition and enantiomeric separation.

2.5 CONCLUSIONS

In summary, we have demonstrated a simple filtration method for the enantioselective separation of native amino acids using chiral D/L aspartic acid appended polyfluorene-coated AAO membranes. Although porous AAO membranes have been widely reported for fabrication of polymer nanostructures by the templating approach, this is the first report, as

far as we know, where it has been used for enantioselective separation. The polymer-coated chiral AAO membranes can discriminate between pairs of enantiomers from an aqueous racemic mixture and bring about their separation by selectively adsorbing one enantiomer within the chiral pores leaving the filtrate enriched with the other enantiomer. The adsorbed amino acid can be recovered from the AAO membrane by repeated extraction with milli-Q water. A maximum enantiomeric excess of 95% is achieved when glutamic acid is the analyte, while other amino acids like alanine, leucine, lysine, and aspartic acid are separated with ee % > 80. The ee % can be enhanced for these amino acids also by increasing the number of polymer-coated AAO membranes used for the separation process. By varying the pore size of the AAO membrane, the ee % can be modulated as the pore size controls the degree of confinement of the chiral polyfluorene.

2.6 REFERENCES

(1)   Watson, J. D.; Crick, F. H. C. Molecular Structure of Nucleic Acids: A Structure for Deoxyribose Nucleic Acid. *Nature* **1953**, *171* (4356), 737–738.

(2)   Giuliano, M. W.; Maynard, S. J.; Almeida, A. M.; Guo, L.; Guzei, I. A.; Spencer, L. C.; Gellman, S. H. A γ-Amino Acid That Favors 12/10-Helical Secondary Structure in A/γ-Peptides. *J. Am. Chem. Soc.* **2014**, *136* (42), 15046–15053.

(3)   Shallenberger, R. S.; Wienen, W. J. Carbohydrate Stereochemistry. *J. Chem. Educ.* **1989**, *66* (1), 67–73.

(4)   Wang, Z.; Xu, W.; Liu, L.; Zhu, T. F. A Synthetic Molecular System Capable of Mirror-Image Genetic Replication and Transcription. *Nat. Chem.* **2016**, *8* (7), 698–704.

(5)   Mason, S. F. Origins of Biomolecular Handedness. *Nat. Chem.* **1984**, *311*, 276–279.

(6)   Müller, T. A.; Kohler, H. P. E. Chirality of Pollutants - Effects on Metabolism and Fate. *Appl. Microbiol. Biotechnol.* **2004**, *64* (3), 300–316.

(7)   Mane, S. Racemic Drug Resolution: A Comprehensive Guide. *Anal. Methods* **2016**, *8* (42), 7567–7586.

(8)   Hutt, A. J.; O'Grady, J. Drug Chirality: A Consideration of the Significance of the Stereochemistry of Antimicrobial Agents. *J. Antimicrob. Chemother.* **1996**, *37* (1), 7–32.

(9)   Landoni, M. F.; Soraci, A. L.; Delatour, P.; Lees, P. Enantioselective Behaviour of Drugs Used in Domestic Animals: A Review. *J. Vet. Pharmacol. Ther.* **1997**, *20* (1), 1–16.

(10)   Davies, N. M.; Wei Teng, X. Importance of Chirality in Drug Therapy and Pharmacy Practice: Implications for Psychiatry. *Adv. Pharm.* **2003**, *1* (3), 242–252.

(11)   Diëguez, M.; Pàmies, O.; Claver, C. Ligands Derived from Carbohydrates for Asymmetric Catalysis. *Chem. Rev.* **2004**, *104* (6), 3189–3215.

(12)   Farina, V.; Reeves, J. T.; Senanayake, C. H.; Song, J. J. Asymmetric Synthesis of Active Pharmaceutical Ingredients. *Chem. Rev.* **2006**, *106* (7), 2734–2793.

(13)   Bhadra, S.; Yamamoto, H. Substrate Directed Asymmetric Reactions. *Chem. Rev.* **2018**, *118* (7), 3391–3446.

(14)   Enders, D.; Hüttl, M. R. M.; Raabe, G.; Bats, J. W. Asymmetric Synthesis of Polyfunctionalized Mono-, Bi-, and Tricyclic Carbon Frameworks via Organocatalytic Domino Reactions. *Adv. Synth. Catal.* **2008**, *350* (2), 267–279.

(15) Wang, X.; Ma, Z.; Lu, J.; Tan, X.; Chen, C. Asymmetric Synthesis of Ageliferin. *J. Am. Chem. Soc.* **2011**, *133* (39), 15350–15353.

(16) O'Brien, P. Sharpless Asymmetric Aminohydroxylation: Scope, Limitations, and Use in Synthesis. *Angew. Chemie - Int. Ed.* **1999**, *38* (3), 326–329.

(17) Verendel, J. J.; Pàmies, O.; Diéguez, M.; Andersson, P. G. Asymmetric Hydrogenation of Olefins Using Chiral Crabtree-Type Catalysts: Scope and Limitations. *Chem. Rev.* **2014**, *114* (4), 2130–2169.

(18) Steinreiber, J.; Schürmann, M.; Wolberg, M.; Van Assema, F.; Reisinger, C.; Fesko, K.; Mink, D.; Griengl, H. Overcoming Thermodynamic and Kinetic Limitations of Aldolase-Catalyzed Reactions by Applying Multienzymatic Dynamic Kinetic Asymmetric Transformations. *Angew. Chemie - Int. Ed.* **2007**, *46* (10), 1624–1626.

(19) Seebach, D.; Sting, A. R.; Hoffmann, M. REVIEWS Abandonment of a Synthetic Principle. *Angew. Chem. Int. Ed. Engl.* **1996**, *35*, 2708–2748.

(20) Huang, K.; Breitbach, Z. S.; Armstrong, D. W. Enantiomeric Impurities in Chiral Synthons, Catalysts, and Auxiliaries: Part 3. *Tetrahedron: Asymmetry* **2006**, *17* (19), 2821–2832.

(21) Zhang, L.; Fu, N.; Luo, S. Pushing the Limits of Aminocatalysis: Enantioselective Transformations of α-Branched β-Ketocarbonyls and Vinyl Ketones by Chiral Primary Amines. *Acc. Chem. Res.* **2015**, *48* (4), 986–997.

(22) Gübitz, G.; Schmid, M. G. Chiral Separation by Chromatographic and Electromigration Techniques. A Review. *Biopharm. Drug Dispos.* **2001**, *22* (7–8), 291–336.

(23) Ward, T. J.; Ward, K. D. Chiral Separations: Fundamental Review 2010. *Anal. Chem.* **2010**, *82* (12), 4712–4722.

(24) Scriba, G. K. E. Chiral Recognition in Separation Science – an Update. *J. Chromatogr. A* **2016**, *1467*, 56–78.

(25) Scriba, G. K. E. Chiral Recognition in Separation Sciences. Part II: Macrocyclic Glycopeptide, Donor-Acceptor, Ion-Exchange, Ligand-Exchange and Micellar Selectors. *TrAC - Trends Anal. Chem.* **2019**, *119*, 115628.

(26) Prasad, B. B.; Tiwari, M. P.; Madhuri, R.; Sharma, P. S. Enantioselective Separation and Electrochemical Sensing of D- and L-Tryptophan at Ultratrace Level Using Molecularly Imprinted Micro-Solid Phase Extraction Fiber Coupled with Complementary Molecularly Imprinted Polymer-Fiber Sensor. *J. Chromatogr. B*

Anal. Technol. Biomed. Life Sci. **2011**, *879* (5–6), 364–370.

(27) Xiao, Y.; Wang, H.; Zhang, H.; Jiang, Z.; Wang, Y.; Li, H.; Zhu, Y.; Wu, Z. Grafting Polymerization of Single-Handed Helical Poly (Phenyl Isocyanide) S on Graphene Oxide and Their Application in Enantioselective Separation. **2017**, 2092–2103.

(28) Zhu, F.; Du, Y.; Chen, J.; Chen, B.; Zhu, Y.; Zhai, X.; Xu, S.; Zhou, W. Enantioselective Separation of Basic Drugs by CE with Polygalacturonic Acid as a Novel Chiral Selector. *Chromatographia* **2009**, *69* (11–12), 1315–1320.

(29) Okamoto, Y. Chiral Polymers. *Prog. Polym. Sci.* **2000**, *25* (2), 159–162.

(30) Zhu, B.; Yao, Y.; Deng, M.; Jiang, Z.; Li, Q. Enantioselective Separation of Twelve Pairs of Enantiomers on Polysaccharide-Based Chiral Stationary Phases and Thermodynamic Analysis of Separation Mechanism. *Electrophoresis* **2018**, *39* (19), 2398–2405.

(31) Zhou, C.; Ren, Y.; Han, J.; Xu, Q.; Guo, R. Chiral Polyaniline Hollow Nanotwists toward Efficient Enantioselective Separation of Amino Acids. *ACS Nano* **2019**, *13* (3), 3534–3544.

(32) Paik, P.; Gedanken, A.; Mastai, Y. Enantioselective Separation Using Chiral Mesoporous Spherical Silica Prepared by Templating of Chiral Block Copolymers. *ACS Appl. Mater. Interfaces* **2009**, *1* (8), 1834–1842.

(33) Armstrong, D. W.; Jin, H. L. Enrichment of Enantiomers and Other Isomers with Aqueous Liquid Membranes Containing Cyclodextrin Carriers. *Anal. Chem.* **1987**, *59* (18), 2237–2241.

(34) Xie, R.; Chu, L. Y.; Deng, J. G. Membranes and Membrane Processes for Chiral Resolution. *Chem. Soc. Rev.* **2008**, *37* (6), 1243–1263.

(35) Kong, J.; Mu, Y.; Xiong, Y.; Zheng, M.; Wang, Y. Fabrication of Both TiO2 Nanostructures and Cysteine-Modified AAO Membranes and Their Application in Chiral Selective Transport of Proteins. *J. Electron. Mater.* **2019**, *48* (2), 964–971.

(36) Ha, J. J.; Hyun, M. H. Enantioselective Separation of α-Amino Acids on (S)-Leucinol-Based Ligand Exchange Chiral Stationary Phases. *Bull. Korean Chem. Soc.* **2016**, *37* (8), 1385–1388.

(37) Kaity, S.; Ghosh, A. Carboxymethylation of Locust Bean Gum: Application in Interpenetrating Polymer Network Microspheres for Controlled Drug Delivery. *Ind. Eng. Chem. Res.* **2013**, *52* (30), 10033–10045.

(38) Lakhwani, G.; Meskers, S. C. J.; Janssen, R. A. J. Circular Differential Scattering of

Light in Films of Chiral Polyfluorene. *J. Phys. Chem. B* **2007**, *111* (19), 5124–5131.

(39) Lakhwani, G.; Meskers, S. C. J. Insights from Chiral Polyfluorene on the Unification of Molecular Exciton and Cholesteric Liquid Crystal Theories for Chiroptical Phenomena. *J. Phys. Chem. A* **2012**, *116* (4), 1121–1128.

(40) Savoini, M.; Wu, X.; Celebrano, M.; Ziegler, J.; Biagioni, P.; Meskers, S. C. J.; Duò, L.; Hecht, B.; Finazzi, M. Circular Dichroism Probed by Two-Photon Fluorescence Microscopy in Enantiopure Chiral Polyfluorene Thin Films. *J. Am. Chem. Soc.* **2012**, *134* (13), 5832–5835.

(41) Lakhwani, G.; Janssen, R. A. J.; Meskers, S. C. J. Anisotropic Dielectric Tensor for Chiral Polyfluorene at Optical Frequencies. *J. Phys. Chem. B* **2009**, *113* (43), 14165–14171.

(42) Savoini, M.; Biagioni, P.; Meskers, S. C. J.; Duò, L.; Hecht, B.; Finazzi, M. Spontaneous Formation of Left- and Right-Handed Cholesterically Ordered Domains in an Enantiopure Chiral Polyfluorene Film. *J. Phys. Chem. Lett.* **2011**, *2* (12), 1359–1362.

(43) Ozawa, H.; Fujigaya, T.; Niidome, Y.; Hotta, N.; Fujiki, M.; Nakashima, N. Rational Concept to Recognize/extract Single-Walled Carbon Nanotubes with a Specific Chirality. *J. Am. Chem. Soc.* **2011**, *133* (8), 2651–2657.

(44) Akazaki, K.; Toshimitsu, F.; Ozawa, H.; Fujigaya, T.; Nakashima, N. Recognition and One-Pot Extraction of Right- and Left-Handed Semiconducting Single-Walled Carbon Nanotube Enantiomers Using Fluorene-Binaphthol Chiral Copolymers. *J. Am. Chem. Soc.* **2012**, *134* (30), 12700–12707.

(45) Senthilkumar, T.; Asha, S. K. An Easy "Filter-and-Separate" Method for Enantioselective Separation and Chiral Sensing of Substrates Using a Biomimetic Homochiral Polymer. *Chem. Commun.* **2015**, *51* (43), 8931–8934.

(46) Chi, M. H.; Su, C. H.; Cheng, M. H.; Chung, P. Y.; Peng, C. H.; Chen, J. T. Shaping the Light: The Key Factors Affecting the Photophysical Properties of Fluorescent Polymer Nanostructures. *Macromol. Rapid Commun.* **2016**, *37* (24), 2037–2044.

(47) Cepak, V. M.; Martin, C. R. Preparation of Polymeric Micro- and Nanostructures Using a Template-Based Deposition Method. *Chem. Mater.* **1999**, *11* (5), 1363–1367.

(48) Xue, J.; Xu, Y.; Jin, Z. Interfacial Interaction in Anodic Aluminum Oxide Templates Modifies Morphology, Surface Area, and Crystallization of Polyamide-6 Nanofibers. *Langmuir* **2016**, *32* (9), 2259–2266.

(49)   Das, C.; Krishnamoorthy, K. Disassembly of Micelles in Nanoscopic Space to Prepare Concentric Nanotubes with Variable Hydrophobic Interiors. *Chem. Commun.* **2014**, *50* (44), 5905–5908.

(50)   Das, C.; Jain, B.; Krishnamoorthy, K. Phenols from Green Tea as a Dual Functional Coating to Prepare Devices for Energy Storage and Molecular Separation. *Chem. Commun.* **2015**, *51* (58), 11662–11664.

(51)   Clark Wooten, M. K.; Koganti, V. R.; Zhou, S.; Rankin, S. E.; Knutson, B. L. Synthesis and Nanofiltration Membrane Performance of Oriented Mesoporous Silica Thin Films on Macroporous Supports. *ACS Appl. Mater. Interfaces* **2016**, *8* (33), 21806–21815.

(52)   Senthilkumar, T.; Asha, S. K. An Easy "Filter-and-Separate" Method for Enantioselective Separation and Chiral Sensing of Substrates Using a Biomimetic Homochiral Polymer. *Chem. Commun.* **2015**, *51* (43), 8931–8934.

(53)   Berthod, A. *Chiral Recognition in Separation Methods: Mechanisms and Applications*; Springer Berlin Heidelberg, 2010.

(54)   Easson, L. H.; Stedman, E. Studies on the Relationship between Chemical Constitution and Physiological Action. *Biochem. J.* **1933**, *27* (4), 1257–1266.

CHAPTER 3

Effect of Chiral Handles on Selectivity and Separation Efficiency

3.1 INTRODUCTION

Natural processes have chiral recognition ability, where the physiological processes are highly stereospecific.[1–5] Natures ability to distinguish between enantiomers of chiral compound generated tremendous scientific quest for synthesizing chemical compounds like drugs,[6] herbicides,[7] pesticides,[8] flavoring agents in their enantiopure form.[9] Different methods like enantioselective crystallization,[10] converting enantiomers into diastereomers,[11] chiral chromatography,[12] and membrane-based filtration[13] are used to separate enantiomers from their racemic mixtures.[14] These enantioselective separation methods used chiral selectors, distinguishing between enantiomers and separating from their racemic mixtures.[15] It is tough to develop a universal chiral selector that can separate all enantiomers, as very little is known about the separation mechanism.[16] Different mechanisms and interactions are involved in the chiral recognition processes due to the structural differences of chiral selectors and analytes. The interaction between the chiral selectors and enantiomers like ionic interactions, ion-dipole or dipole-dipole interactions, H-bonding, van der Waals interactions, and π–π interactions vary depending upon their chemical structure, pH, and nature of mobile phase.[17]

Membrane-based enantioselective filtration of enantiomer attracted considerable attention of the scientific community as it is energy efficient, simple, and able to operate continuously at the industrial level.[18–20] Metal-organic framework (MOF),[21] Covalent organic frameworks (COF),[22] zeolites,[23] and chiral polymer membranes are used in literature for carrying out enantioselective separation of different analytes.[24,25] In chapter 2 of the thesis, we have developed chiral anodic aluminium oxide (AAO) membranes by coating protected D/L-aspartic acid-containing chiral polyfluorene, which was used to separate enantiomers of different amino acids. The protected aspartic acid-containing polymer-coated membranes showed the highest (95 %) ee for separation of glutamic acid and minimum separation for valine racemic mixture (46 % ee). The reason behind these differences in % ee lies in the chemical structure, size, changes, and type of interactions between analytes and chiral selectors.

This chapter demonstrates the synthesis of two chiral polyfluorenes (PF-LTrp and PF-LGlu) containing different chiral handles like N-Boc-L-glutamic acid-1-tert butyl ester and N-Boc-L-tryptophan. These chiral pendent-containing polymers were coated separately on the commercially available 200 nm pore size AAO membranes. These polymer-coated chiral

AAO membranes were utilized for the enantioselective separation of an aqueous racemic mixture of different amino acids. The PF-LTrp coated membrane (PF-LTrp@AAO) separated tryptophan racemic mixture with the highest % ee (91.3 % ee), while the PF-LGlu coated AAO membrane (PF-LGlu@AAO) separated glutamic acid racemic mixture with the highest % ee (91.9%).

3.2 EXPERIMENTAL SECTION

3.2.1 Materials

2,7-Dibromofluorene and 6-bromo-1-hexanol were purchased from TCI Chemicals. 4-Dimethylaminopyridine (DMAP), dicyclohexylcarbodiimide (DCC), and tetrabutylammonium bromide (TBAB) were purchased from Spectrochem Pvt. Ltd. (India). Pd(PPh$_3$)$_4$, benzene-1, 4-diboronic acid, IR grade potassium bromide (KBr), and CDCl$_3$ were purchased from Sigma-Aldrich. N-Boc-L-aspartic acid-1-tert butyl ester, N-Boc-D-aspartic acid-1-tert butyl ester, (Boc = tert-butoxycarbonyl) were purchased from Alfa Aesar Chemical Ltd. NaOH, Na$_2$SO$_4$, Na$_2$CO$_3$, K$_2$CO$_3$, and solvents like toluene, tetrahydrofuran (THF), methanol, and dichloromethane (DCM) were purchased from Merck Chemicals. Ethyl acetate and pet ether were purchased locally. Solvents were dried using standard drying procedures. HPLC grade THF was purchased from Merck Chemicals. Anodic aluminium oxide membranes with nominal pore diameters of 200 nm, mass 10−20 mg, 50 μm nominal thickness, the porosity of 0.12−0.15, pore density 5×10^8 (±20%), cm^{-2}, air permeability at 20 °C in the range of 10^{-8} to 10^{-4} cm/s/Pa and water permeability at 20 °C in the range of 10^{-10} to 10^{-6} cm/s/Pa were purchased from SPI supplies USA (the characterization details are as provided by the supplier).

2.2.2 Measurements

Structural characterizations of all the samples (small molecules, monomers, and polymers) were done by recording ^{1}H and ^{13}C NMR spectrum using Bruker-AVENS 200 and 400 MHz spectrometers. Chemical shifts were reported in ppm at 25 °C using CDCl$_3$ as solvent containing trace quantity of tetramethylsilane (TMS) as an internal standard. FT-IR spectra were recorded using BRUKER alpha-E Fourier transform (FT-IR) for monomers and polymers' structural and functional group characterization. The molecular weights of the polymer were determined by Gel Permeation Chromatography (GPC), equipped with a ViscotekVE 1122 solvent delivery system and ViscotekVE 3580 RI detector. The

instrument was calibrated with polystyrene standards, and analysis was carried out at a 1 ml/min flow rate with tetrahydrofuran (THF) as a mobile phase. The morphological characterizations of chiral AAO were performed using FE-SEM with an FEI Nova Nano SEM 450. Bare AAO and polymer-coated chiral AAO were mounted directly on the top of grooved edge aluminium SEM specimen stub with the help of carbon tape. Before conducting morphological studies, the membranes were coated with a 5 nm thick gold film by a sputtering method. Solution state Circular Dichroism (CD) measurements were done using a JASCO-815 CD spectrometer equipped with a Jasco PTC-424 S-5 S/15 Peltier system. 2 mm path-length quartz cuvettes were used for a sample volume of 400 µl in Milli-Q water at 25 °C Three scans were averaged for each sample with a 100 nm/min scanning rate.

3.2.3 Methods

A) Preparation of Chiral Mesoporous Aluminium Oxide Membranes

Chiral AAO membranes were prepared by a simple vacuum filtration method. Polymer solutions were prepared by separately dissolving 5 mg of polymers in 1 ml of THF. The polymer solutions were used to coat 200 nm pore size AAO membranes. The detailed protocol for the preparation of chiral mesoporous AAO membranes was adapted from chapter 2 (experimental section, 2.2.3 Methods)

B) Sample Preparation for CD Measurement

Polymer-coated chiral AAO membranes were crushed into a fine powder, and HPLC grade THF was added to this to extract coated polymers from the AAO membrane pores. The crushed membranes were sonicated multiple times by adding fresh THF until the polymers were wholly extracted from the crushed membrane. The detailed sample preparation protocol was adapted from chapter 2 (experimental section, 2.2.3 Methods)

C) Enantioselective Separation Method

Two PF-LTrp or PF-LGlu coated chiral AAO membranes were suspended in an aqueous amino acid racemic mixture solution, prepared by dissolving an equal quantity of D and L enantiomers of amino acids in DI water (1 mg of D and L amino acid in 3 ml Milli-Q water). Aqueous amino acid racemic mixtures with suspended chiral membranes were agitated on a mechanical shaker for 24 hours at room temperature. After 24 hours, the membranes were

removed from the aqueous mixture measured after completing the enantioselective separation experiment. CD spectra of the resultant solutions (filtrate) were measured and plotted along with the CD spectra of corresponding pure D and L enantiomers of amino acids (1 mg/3 ml) in water. The ratio of area under the curve of filtrate solution and corresponding D enantiomer solution was utilized to quantify enantioselective separation (% ee).

3.2.4 Synthesis and characterization
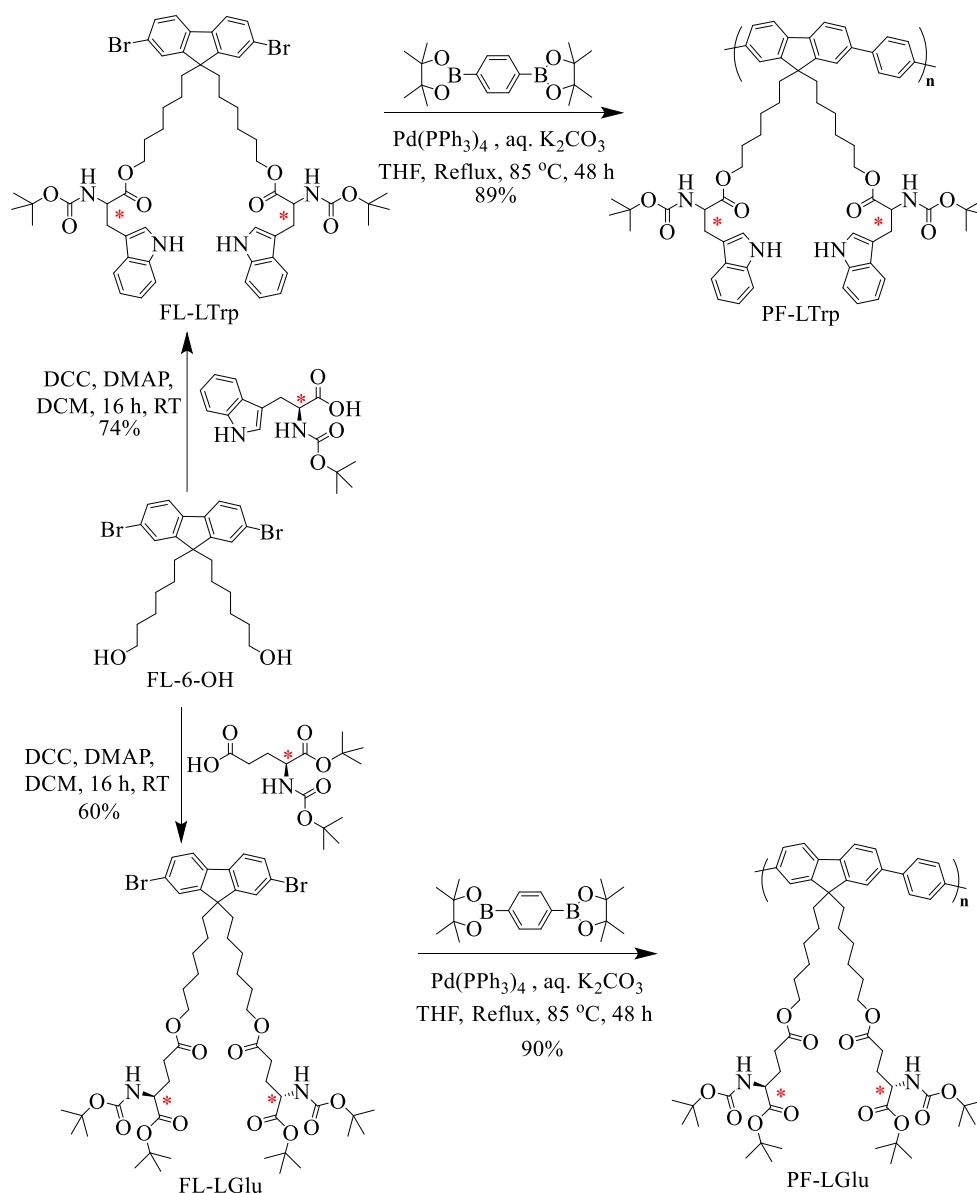
Scheme 3.1 Schematics for the Synthesis of Chiral Polyfluorenes PF-LTrp and PF-LGlu Having N-Boc-L-Tryptophan and N-Boc-L-Glutamic Acid as Pendent groups, respectively

a) Synthesis of Boc protected L-tryptophan
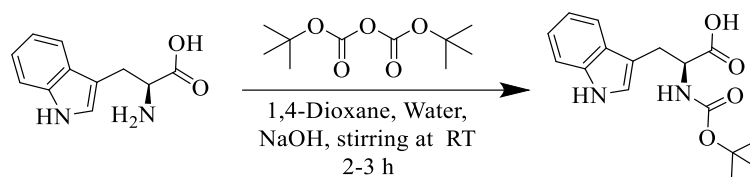
L-tryptophan (5 gm, 24.48 mmols) was dissolved in 1N, 50 ml NaOH solution in two necked round bottom flask kept in an ice bath. Di-tert-butyl dicarbonate (Boc anhydride) (8.1 gm, 36.71 mmols) was dissolved in 50 ml dioxane. The Boc anhydride solution was added dropwise to the L-tryptophan solution at 0 °C. The reaction mixture was continuously stirred for 2-3 hours at room temperature (25-30 °C). After completing the reaction, Dioxane was removed from the reaction mixture under reduced pressure on a rotary evaporator. The reaction mixture was washed with diethyl ether to remove excess Boc anhydride. The aqueous layer was separated and acidified with KHSO$_4$ solution and adjusted to the pH between 2-3 using litmus paper. The whole reaction setup was kept in a cold bath with constant stirring. This solution was washed three times with ethyl acetate, and the organic layer was collected, passing through Na$_2$SO$_4$ and concentrated using a rotary evaporator. Yield 90% ^{1}H NMR spectrum (400 MHz, CDCl$_3$) δ 8.10 (s, 1H), δ 7.63,7.60 (d, 1H), δ 7.35 (d, 1H), δ 7.22,-7.13 (m, 2H), δ 7.01 (s, 1H), δ 5.08 (s 1H), δ 4.72-4.65 (s, 1H) δ 1.44, 1.31 (s, 9H), ^{13}C NMR spectrum (100 MHz, CDCl$_3$) δ 176.34, 155.64, 136.08, 127.72, 123.02, 122.19, 119.69, 118.76, 111.20, 109.91, 80.28, 54.20, 28.31, 28.00, 27.51, FT-IR stretching frequency (υ) in cm-1; 3340, 3060, 2928, 2860, 1722, 1641, 1401, 1233, 1155 and 1040.
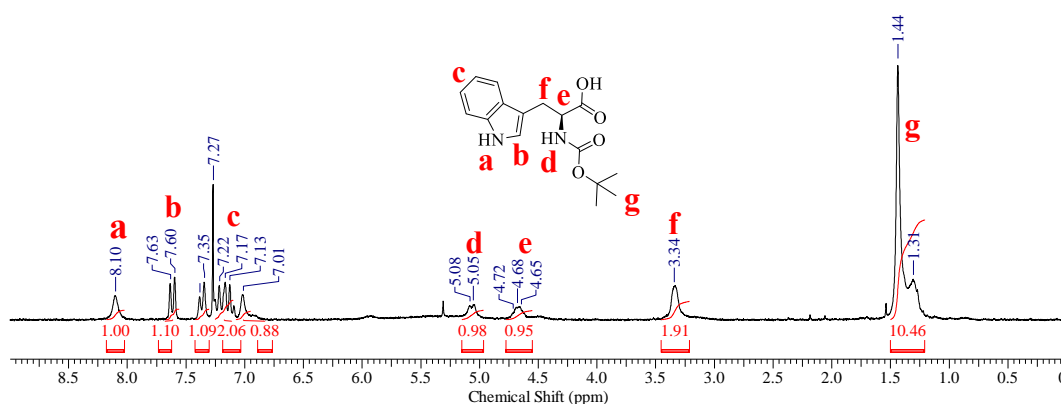

Figure 3.1 ^{1}H NMR spectrum of Boc protected L-tryptophan (CDCl$_3$)
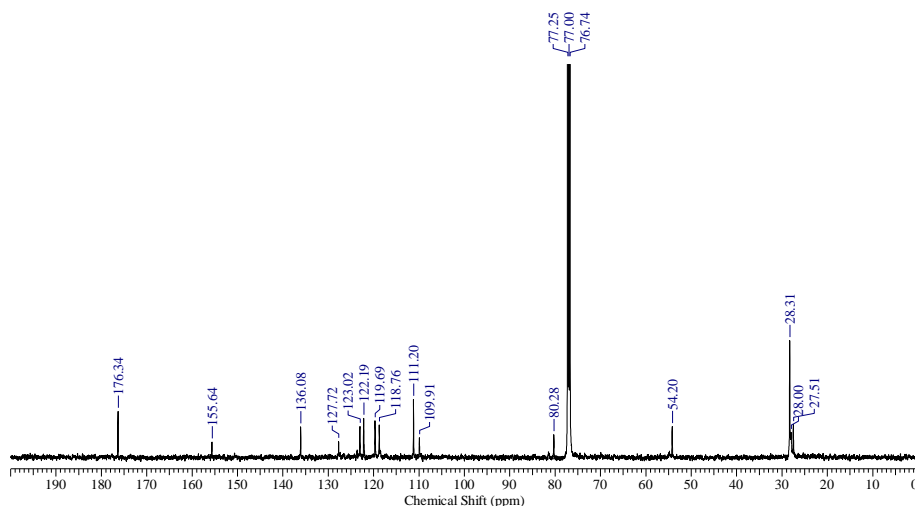
Figure 3.2 ^{13}C NMR spectrum of Boc protected L-tryptophan (CDCl$_3$)
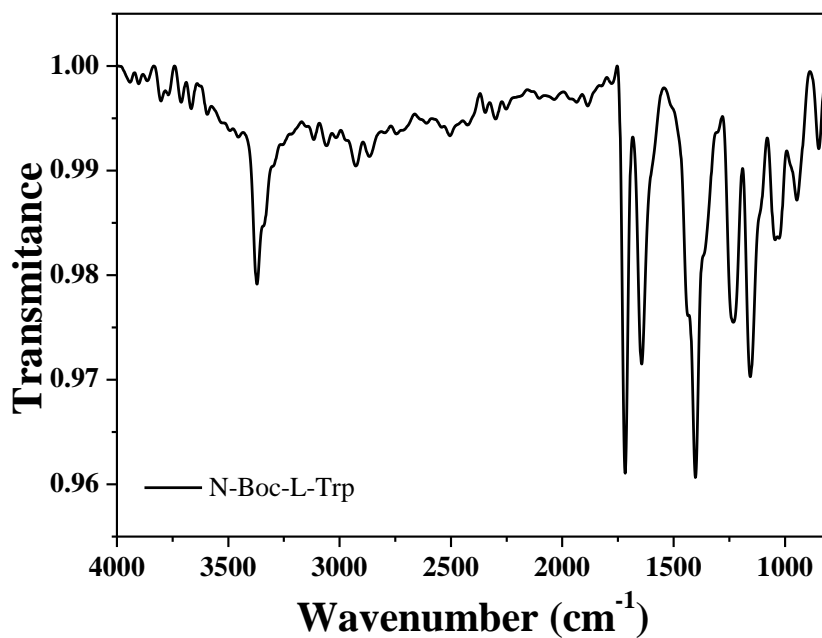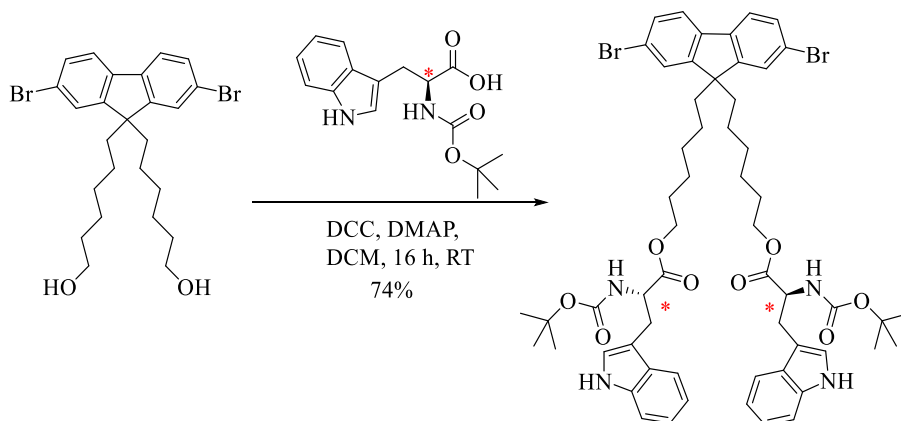

Figure 3.3 FT-IR spectrum of Boc protected L-tryptophan

b) Synthesis of protected L-tryptophan containing fluorene monomer

4-(dimethylamino)pyridine (DMAP) (1.5 gm, 11.91 mmol) and N-Boc-L-tryptophan (3.7 gm, 11.91 mmol) were added in two necked round bottom flask equipped with a magnetic stirring bar in inert atmosphere. Dry DCM was added to the reaction mixture through a syringe. The reaction mixture was cooled to 0 °C with continuous stirring. After 5 minutes, N, N'-Dicyclohexylcarbodiimide (DCC) (1.9 gm, 11.91 mmol) was added, and the reaction mixture was stirred for 1 hour at the same temperature. 2, 7-dibromo-9, 9-di-n-hexanolfluorene (2.5 gm, 4.76 mmol) was added to reaction mixture at 0 °C. The reaction mixture was warmed slowly to room temperature and stirred for 16 hours at the same temperature. The reaction mixture was diluted with DCM, and the organic layer was extracted twice with 0.02 M NaOH, followed by saturated $NaHCO_3$ and brine separately. The organic layer was finally extracted with water. The solvent was evaporated under reduced pressure. The product was purified by column chromatography using pet ether: ethyl acetate (70:30). Yield 84 %. ^{1}H NMR spectrum (400 MHz, CDCl3) δ 7.99 (s, 2H), δ 7.59-7.51 (m, 10H), δ 7.24-7.07 (m, 4H), δ 6.96 (s, 2H), δ 5.08, 5.04 (d, 2H), δ 4.61, 4.57 (d, 2H), δ 3.95-3.89 (t, 4H), δ 3.26 (s, 4H), δ 1.90, 1.85 (m, 4H), δ 1.42 (b, 30), δ 0.96 (b, 8H), 0.53 (b, 4H). ^{13}C NMR spectrum (100 MHz, CDCl3) δ 172.88, 171.35, 155.37, 151.50, 150.68, 130.80, 128.86, 127.59, 122.82, 113.67, 110.25, 82.08, 64.69, 53.43, 30.30, 28.57, 28.31, 27.98, 25.70, FT-IR stretching frequency (υ) in cm^{-1}; 3366, 3274, 2937, 2856, 1719, 1590, 1461, 1262, 1155 and 1102.
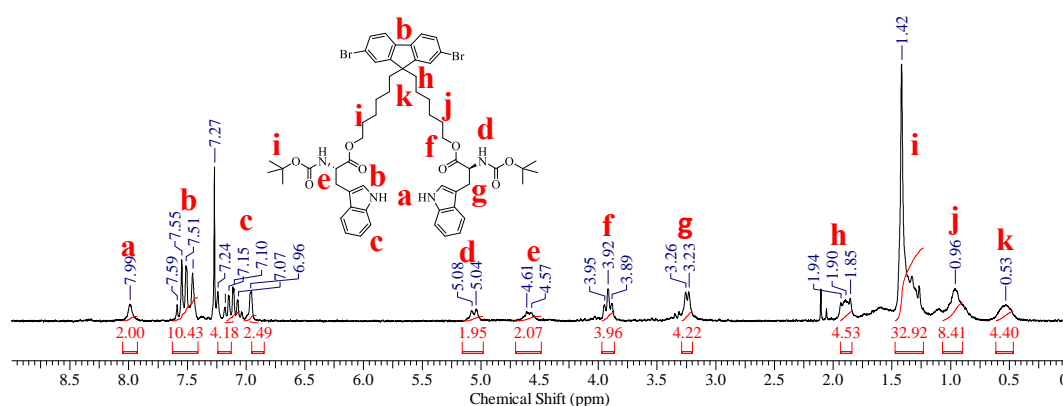

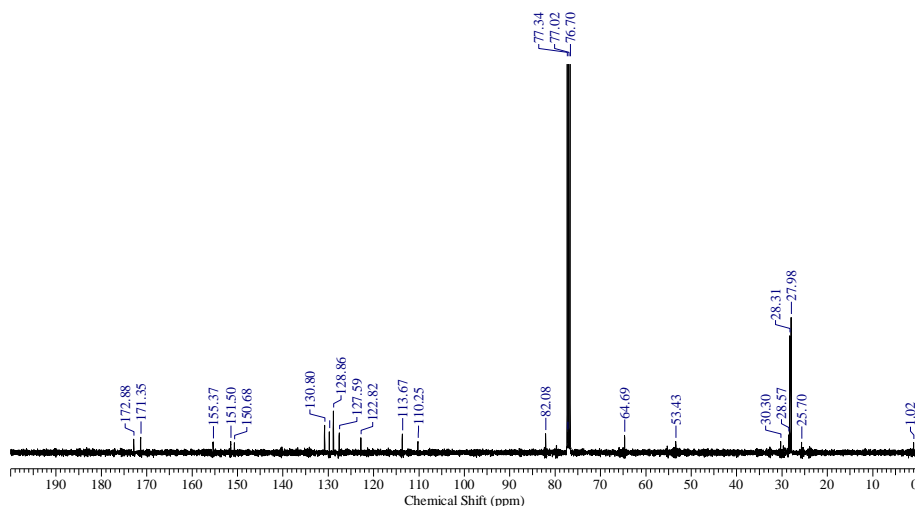**Figure 3.4** ^{1}H NMR spectrum of protected L-tryptophan containing fluorene monomer (CDCl3)

Figure 3.5 ^{13}C NMR spectrum of protected L-tryptophan containing fluorene monomer (CDCl$_3$)
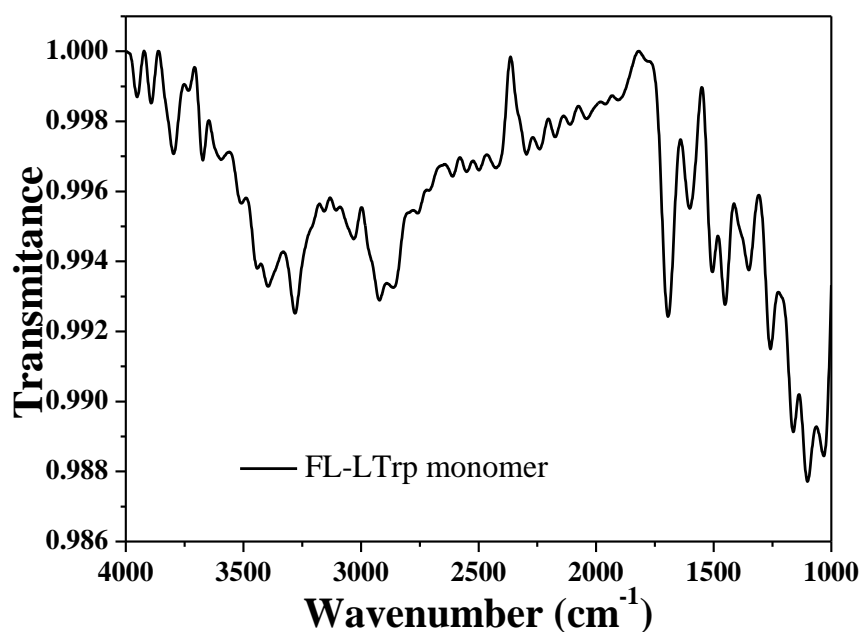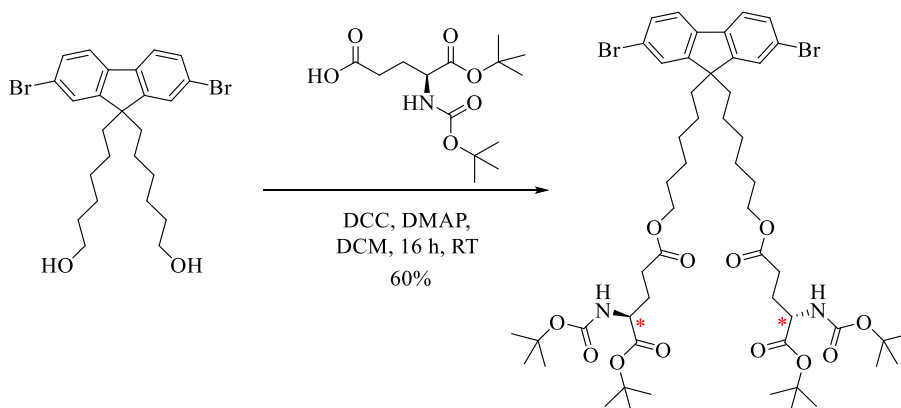

Figure 3.6 FT-IR spectrum of protected L-tryptophan containing fluorene monomer

c) Synthesis of protected L-glutamic acid-containing fluorene monomer

4-(dimethylamino)pyridine (DMAP) (1.3 gm, 10.48 mmol) and N-Boc-L-glutamic acid -1-tert butyl ester (3.2 gm, 10.48 mmol) were added in two necked round bottom flask equipped with a magnetic stirring bar in inert atmosphere. Dry DCM was added to the reaction mixture through a syringe. The reaction mixture was cooled to 0 °C with continuous stirring. After 5 minutes, N, N'-Dicyclohexylcarbodiimide (DCC) (1.82 gm, 11.75 mmol) was added, and the reaction mixture was stirred for 1 hour at the same temperature. 2, 7-dibromo-9, 9-di-n-hexanolfluorene (2.2 gm, 4.195 mmol) was added to reaction mixture at 0 °C. The reaction mixture was warmed slowly to room temperature and stirred for 16 hours at the same temperature. The reaction mixture was diluted with DCM, and the organic layer was extracted twice with 0.02 M NaOH, then saturated $NaHCO_3$ and brine separately. The organic layer was finally extracted with water. The solvent was evaporated under reduced pressure. The product was purified by column chromatography using pet ether: ethyl acetate (70:30). Yield 84 %. ^{1}H NMR spectrum (400 MHz, $CDCl_3$) δ 7.51-7.40 (m, 6H), δ 5.10-5.08 (d, 2H), δ 4.14 (b, 2H), δ 3.93 (t, 4H), δ 2.34-2.27 (m, 4H), δ 2.09-1.85 (dd, 4H), δ 1.43 (m, 40H), δ1.06 (b, 8H), 0.54 (b, 4H). ^{13}C NMR spectrum (100 MHz, $CDCl_3$) δ 171, 169.99, 155.42, 152.30, 139.07, 130.31, 126.08, 121.55, 121.22, 82.18, 70.81, 55.56, 50.51, 40.11, 29.48, 28.43, 28.31, 27.86, 25.54, 23.53. FT-IR stretching frequency (υ) in cm^{-1}; 3747, 3680, 3554, 3028, 2926, 1745, 1365, 1215, 1091, and 1038.
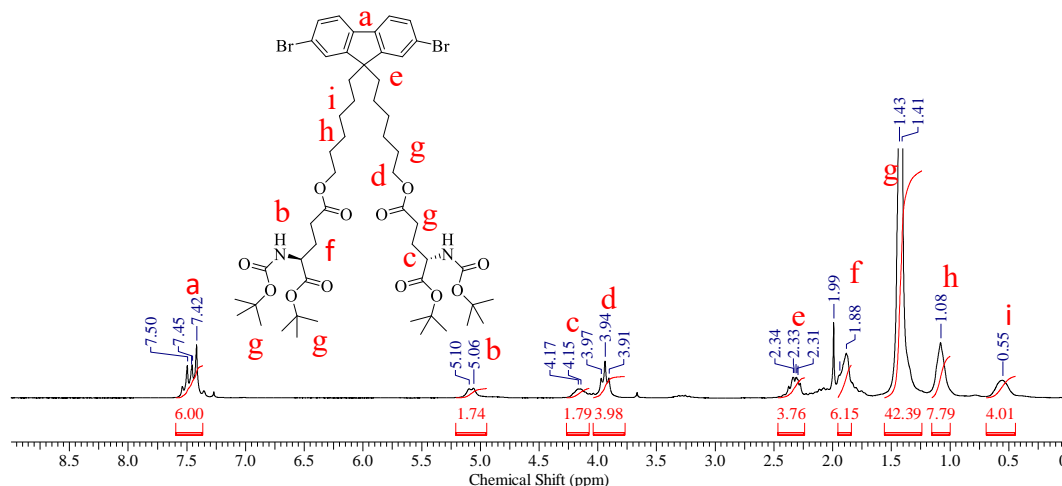

Figure 3.7 ^{1}H NMR spectrum of protected L-glutamic acid-containing fluorene monomer ($CDCl_3$)
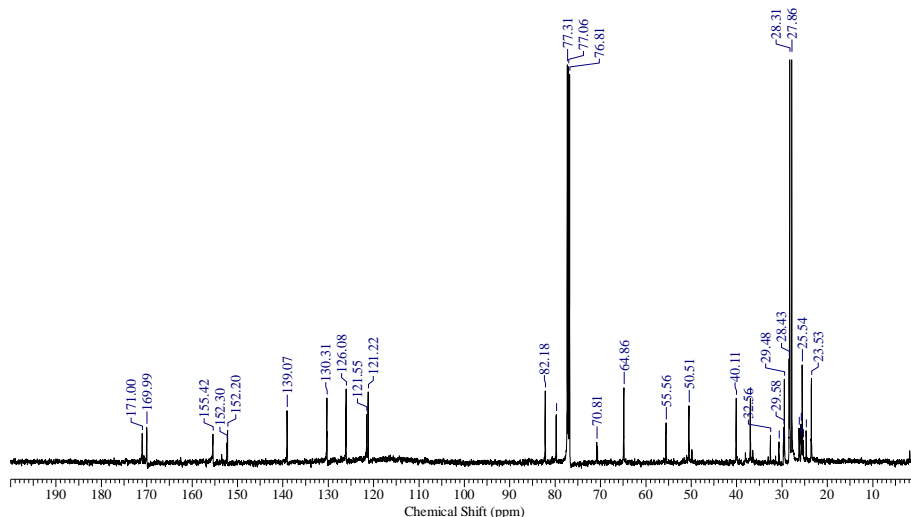
Figure 3.8 ^{13}C NMR spectrum of protected L-glutamic acid-containing fluorene monomer (CDCl$_3$)
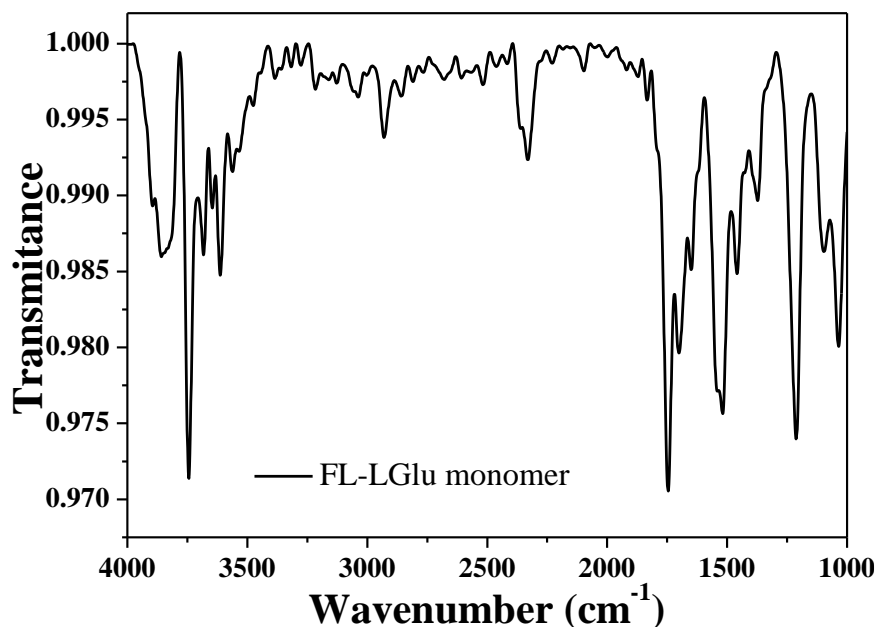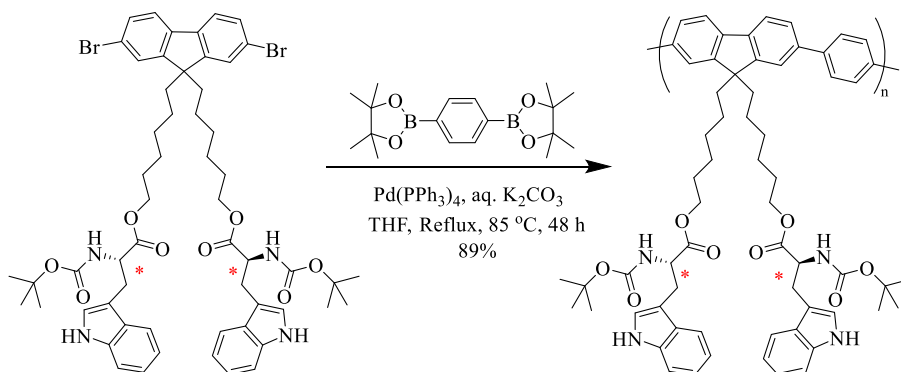

Figure 3.9 FT-IR spectrum of protected L-glutamic acid-containing fluorene monomer

d) Synthesis of Boc Protected-L-tryptophan containing polyfluorene

Boc protected-L-tryptophan containing fluorene monomer (500 mg, 0.46 mmol) and 1, 4-benzene diboronic acid bis(pinacol)ester (151 mg, 0.46 mmol) were taken in Schlenk tube equipped with a magnetic stirring bar and a reflux condenser connected to Schlenk line for continuous nitrogen flow. Dry THF (5 ml) was added to the reaction mixture through a cannula, and the reaction mixture was subjected to a sequence of three freeze-pump-thaw cycles. Pd(PPh3)4 (16 mg, 3 mole %) was added to this reaction mixture and stirred at room temperature for 1 hour. An aqueous solution of K_2CO_3 (380 mg, 2.74 mmol in 1 ml water) was added to the reaction mixture after 5 min of nitrogen purging, and the reaction mixture was refluxed at 85 °C for 48 hours. After completion of the reaction, the solvent was concentrated to approximately 1 ml under reduced pressure. The polymer was precipitated from THF solution into methanol, water, and acetone separately. This repeated precipitation was carried out to remove catalyst, oligomers, and salt from the polymer. Yield 92 % ^{1}H NMR spectrum (400 MHz, CDCl**3**) δ8.10 (b, 2H). δ 7.88-7.83 (b, 4H), δ 7.74-7.86 (b, 4H), δ 7.16-7.03 (b, 5H), δ 6.85 (b, 2H), δ 5.08, 5.06 (d, 2H), δ 4.56 (b 2H), δ 3.89 (b, 4H), δ 3.20 (b, 4H), δ 2.70 (m, 2H), δ 2.06 (b, 4H), δ 1.62 (b, 16H), δ 1.40 (b, 20), δ1.05, 0.93 (d, 8H), 0.70 (b, 4H). ^{13}C NMR spectrum (100 MHz, CDCl3) δ 172.37, 155.20, 152.35, 139.09, 130.37, 126.16, 122.60, 121.59, 121.29, 119.57, 118.85, 111.08, 82.12, 65.34, 55.62, 40.09, 36.93, 29.44, 28.35, 25.41, 23.55. FT-IR stretching frequency (υ) in cm^{-1}; 3371, 3270, 3065, 2926, 2851, 1698, 1505, 1456, 1257, 1161, 1102, and 1027.
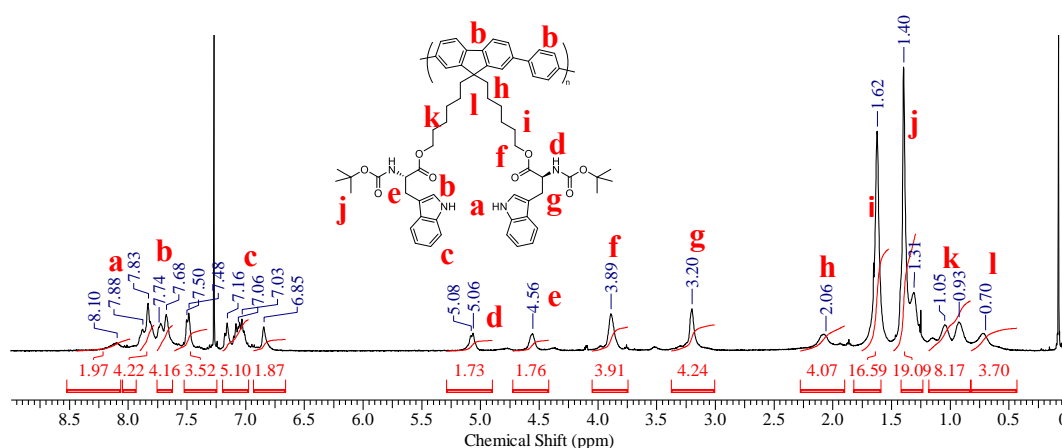

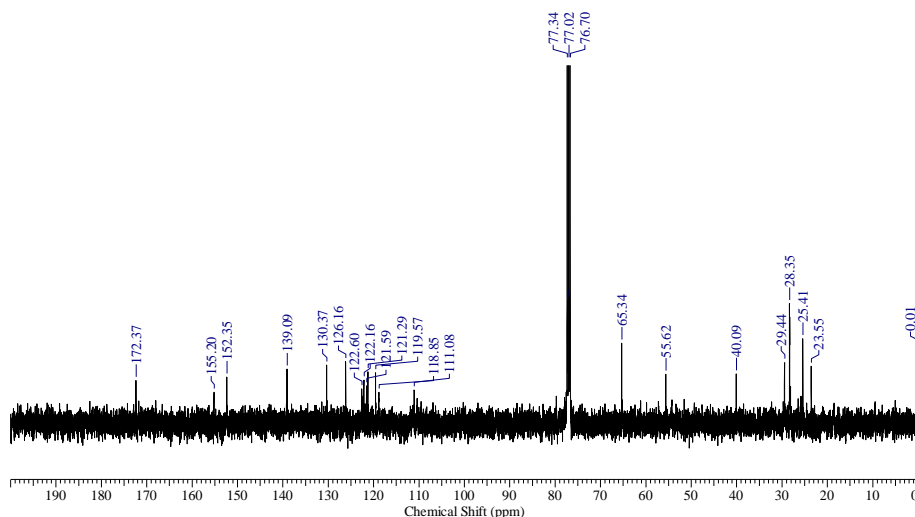**Figure 3.10** ^{1}H NMR spectrum of Boc Protected-L-tryptophan containing polyfluorene (CDCl3)

Figure 3.11 ¹³C NMR spectrum of Boc Protected-L-tryptophan containing polyfluorene (CDCl₃)
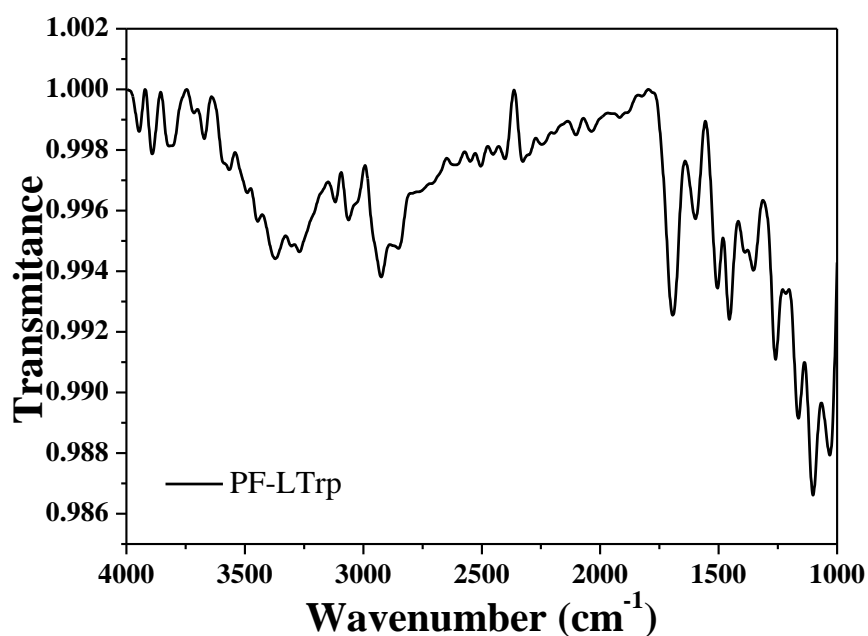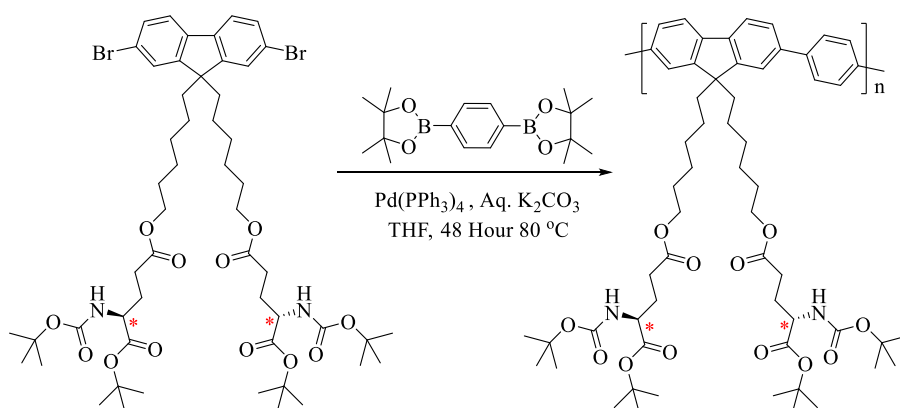

Figure 3.12 FT-IR spectrum of Boc Protected-L-tryptophan containing polyfluorene

e) Synthesis of Boc Protected-L-glutamic acid-containing polyfluorene

Boc protected-L-glutamic acid-containing fluorene monomer (918 mg, 0.84 mmol) and 1, 4-benzene diboronic acid bis(pinacol)ester (277 mg, 0.84 mmol) were taken in Schlenk tube equipped with a magnetic stirring bar and a reflux condenser connected to Schlenk line for continuous nitrogen flow. Dry THF (8 ml) was added to the reaction mixture through a cannula, and the reaction mixture was subjected to a sequence of three freeze-pump-thaw cycles. Pd(PPh3)4 (30 mg, 3 mole %) was added to this reaction mixture and stirred at room temperature for 1 hour. An aqueous solution of K_2CO_3 (695 mg, 5.03 mmol in 1 ml water) was added to the reaction mixture after 5 min of nitrogen purging, and the reaction mixture was refluxed at 85 °C for 48 hours. After completion of the reaction, the solvent was concentrated to approximately 1 ml under reduced pressure. The polymer was precipitated from THF solution into methanol, water, and acetone separately. This repeated precipitation was carried out to remove catalyst, oligomers, and salt from the polymer. Yield 93 % ^{1}H NMR spectrum (400 MHz, CDCl3) δ 7.82 (m, 6H), δ 7.66-7.71 (m, 4H), δ 5.08-5.12 (d, 2H), δ 4.18-4.20 (d 2H), δ 3.93-3.99 (t, 4H), δ 3.51-3.54 (q, 2H), δ 2.31-2.34 (m, 4H), δ 2.08-2.11 (m, 4H), δ 1.85-1.90 (m, 4H), δ 1.42-1.43 (s, 44), δ 1.15 (m, 8H), 0.78 (m, 4H). ^{13}C NMR spectrum (100 MHz, CDCl3) δ 172.91, 171.37, 155.38, 151.48, 140.44, 127.59, 121.30, 120.20, 82.09, 79.70, 64.7053.41, 40.55, 32.56, 30.30, 27.97, 25.70, 23.83. FT-IR stretching frequency (υ) in cm^{-1}; 3366, 3280, 3065, 3017, 2926, 2872, 1714, 1601, 1504, 1451, 1354, 1252, 1145, and 1032.
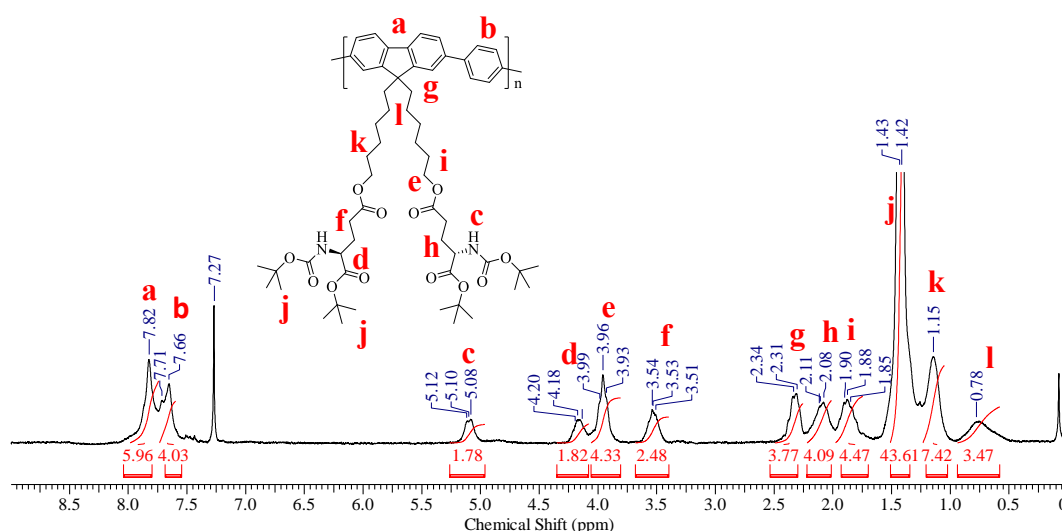
Figure 3.13 ^{1}H NMR spectrum of Boc protected-L-glutamic acid-containing polymer (CDCl3)
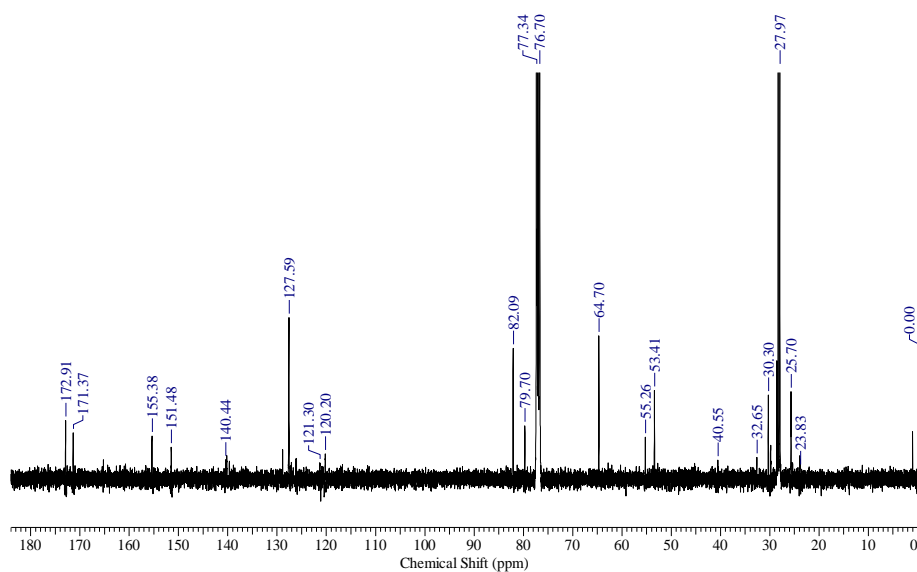
Figure 3.14 ^{13}C NMR spectrum of Boc protected-L-glutamic acid-containing polymer (CDCl$_3$)
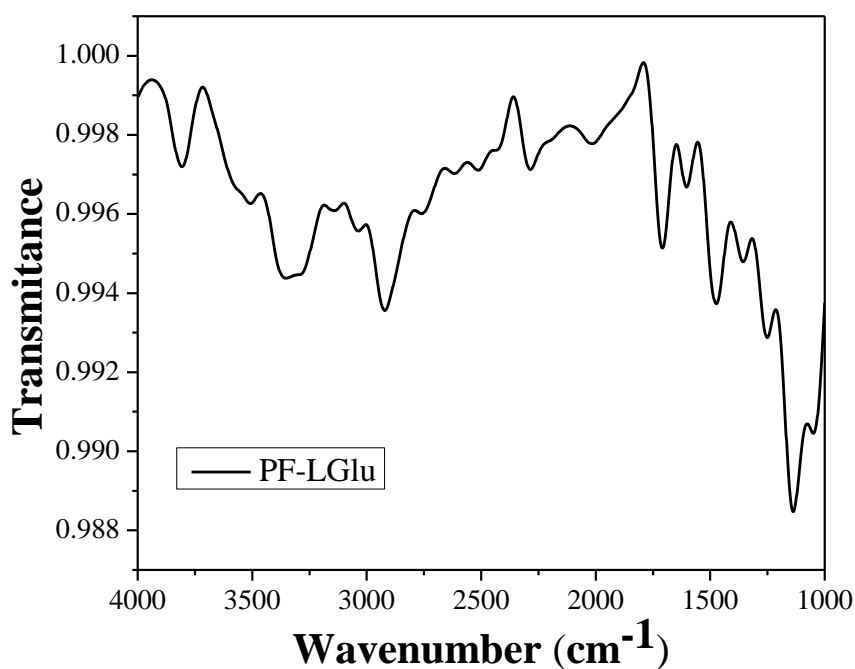
Figure 3.15 FTIR spectrum of Boc protected-L-glutamic acid-containing polymer

3.3 RESULT AND DISCUSSION

The detailed synthesis and structural characterization of monomers and polymers is given in the experimental section and Figure 3.1-3.15. The molecular weights (*Mn, Mw*), polydispersity index (*Đ$_M$*), and degree of polymerization (*Xn*) of synthesized polyfluorenes

(PF-LTrp and PF-LGlu) was determined by recording GPC chromatogram on size exclusion chromatography (SEC) using THF as eluant (Figure 3.16).
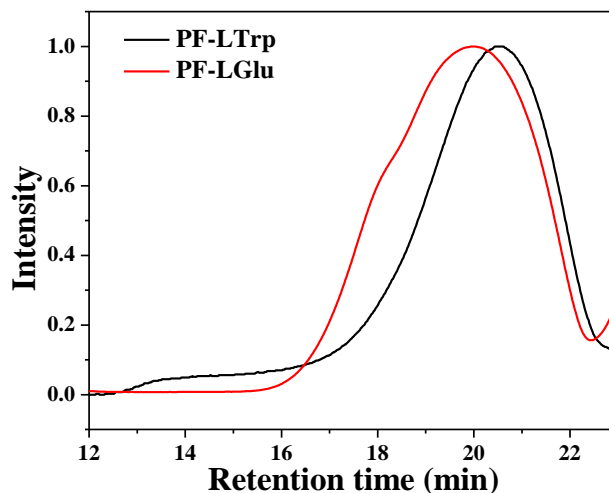
Figure 3.16 GPC chromatogram of synthesized polymers PF-LTrp (black) and PF-LGlu (red) determined using THF as eluant

The PF-LTrp showed number average molecular weight (*Mn*) of 13700 with a polydispersity index (*Đ*$_M$) of 2.4. The (*Mn*) corresponded to the degree of polymerization (*Xn*) 27. Similarly, PF-LGlu showed Mn of 17800 with ĐM of 3.6, corresponding to *Xn* of 35. The molecular weight details of polymers are given in Table 3.1.

Polymer	*Mn*	*Mw*	*Đ*$_M$	*Xn*
PF-LTrp	13700	33300	2.4	27
PF-LGlu	17800	64600	3.6	35

**Table 3.1** Molecular weight details of PF-LTrp and PF-LGlu polymers determined by GPC using THF as eluant

The synthesized polymers were coated on the commercially available 200 nm pore-sized anodic aluminium oxide (AAO) membranes by a vacuum filtration method. The walls of AAO membranes' pores were coated using polymer solution in THF (5 mg/ml). The detailed protocol is given in the experimental section (3.2.3 Methods). The bare AAO membranes showed an open pore with a pore diameter of approximately 200 nm (Figure 3.17 a). Upon polymer coating, a reduction in the pore diameter was observed. The reduced diameters were in the range of 80-170 and 85-180 nm upon coating PF-LTrp and PF-LGlu, respectively

(Figure 3.17 b and c). It could be seen from the micrographs b and c that coated polymer was well distributed around the inner wall of the membrane pores, leaving the pores open.

200 nm AAO Membrane   PF-LTrp@AAO Membrane   PF-LGlu@AAO Membrane
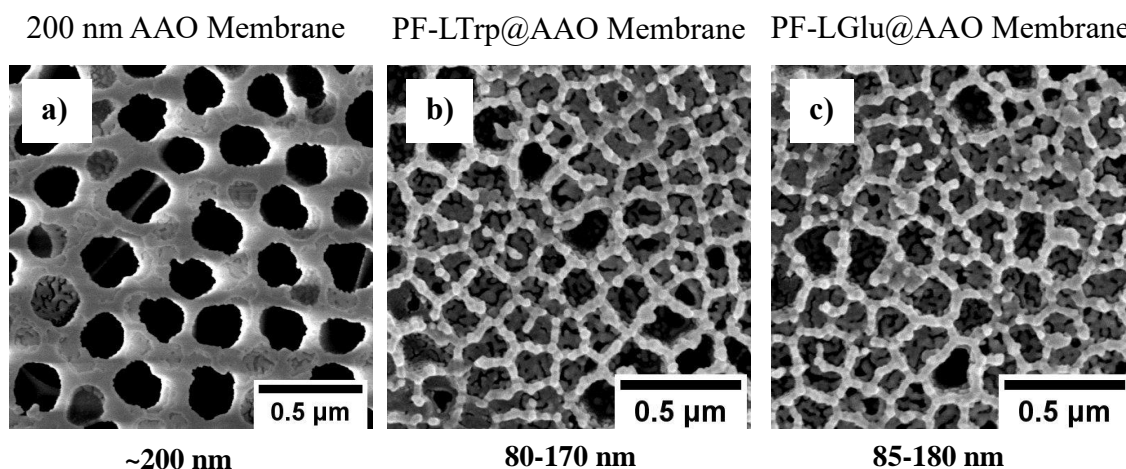

~200 nm   80-170 nm   85-180 nm

Figure 3.17 FE-SEM micrographs of a) bare AAO membrane b) PF-LGlu coated AAO membrane (PF-LGlu@AAO) and c) PF-LTrp coated AAO membrane (PF-LTrp@AAO)

Chiral amino acid appendages (N-Boc-L-glutamic acid-1-tert butyl ester and N-Boc-L-tryptophan) induced chirality in the polyfluorene. The induced chirality in the polymers was determined by recording CD spectra of polymers extracted from membranes. Polymer-coated AAO membranes were crushed into a fine powder, and polymers from membranes were extracted by sonicating multiple times by adding fresh HPLC grade THF (experiment section, 3.2.3 Methods). The complete disappearance of polymeric fluorescence ensured the complete removal of polymers from membranes pores. THF was evaporated entirely on a rotary evaporator, and polymers were redissolved in 1 ml of fresh HPLC grade THF and used to record solution state CD spectra at 25 °C with a scanning speed of 100 nm/min, where three scans were averaged. The solution state CD spectra of protected L-tryptophan containing polyfluorene (PF-LTrp) showed resemblance with the CD spectra of N-Boc-L-tryptophan (N-Boc-LTrp) with peak maxima around 242 nm (Figure 3.18 a), while the CD spectrum of the protected L-glutamic acid-containing polyfluorene with (PF-LGlu) showed peak maximum around 215 nm which resembled the corresponding N-Boc-L-glutamic acid-1-tert butyl ester (N-Boc-LGlu) (Figure 3.18 b). From these CD spectra, it could be concluded that chiral amino acid appendages are able to induce chirality in polymeric structures.
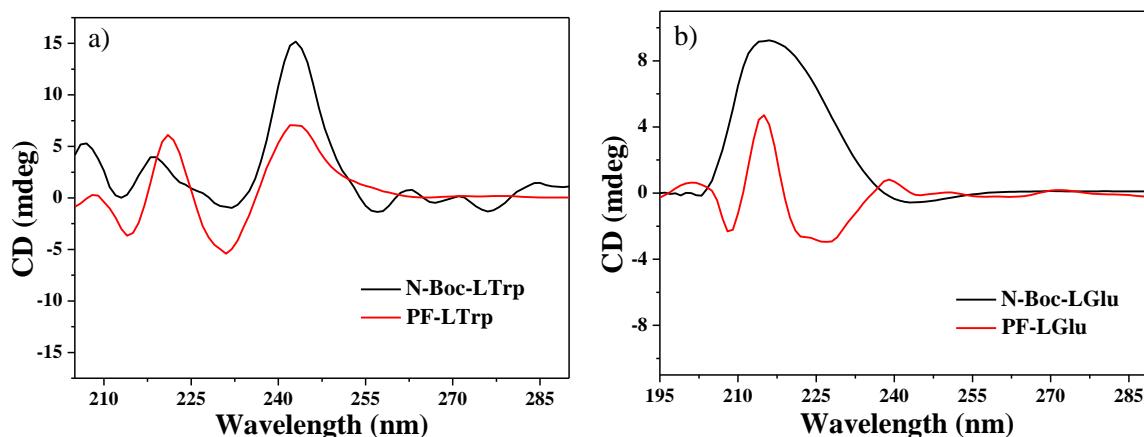
Figure 3.18 CD spectra of a) protected L-tryptophan containing polyfluorene with (PF-LTrp) plotted along with N-Boc-L-tryptophan (N-Boc-LTrp) and b) protected L-glutamic acid-containing polyfluorene with (PF-LGlu) plotted against N-Boc-L-glutamic acid-1-tert butyl ester (N-Boc-LGlu)

Chiral polymer-coated mesoporous AAO membranes were used to conduct enantioselective separation of aqueous racemic mixtures of different amino acids. The aqueous racemic mixtures were prepared by dissolving 1 mg of L and D enantiomers of analytes in 3 ml of DI water. Structures of amino acid analytes used in the study are given in Figure 3.19.
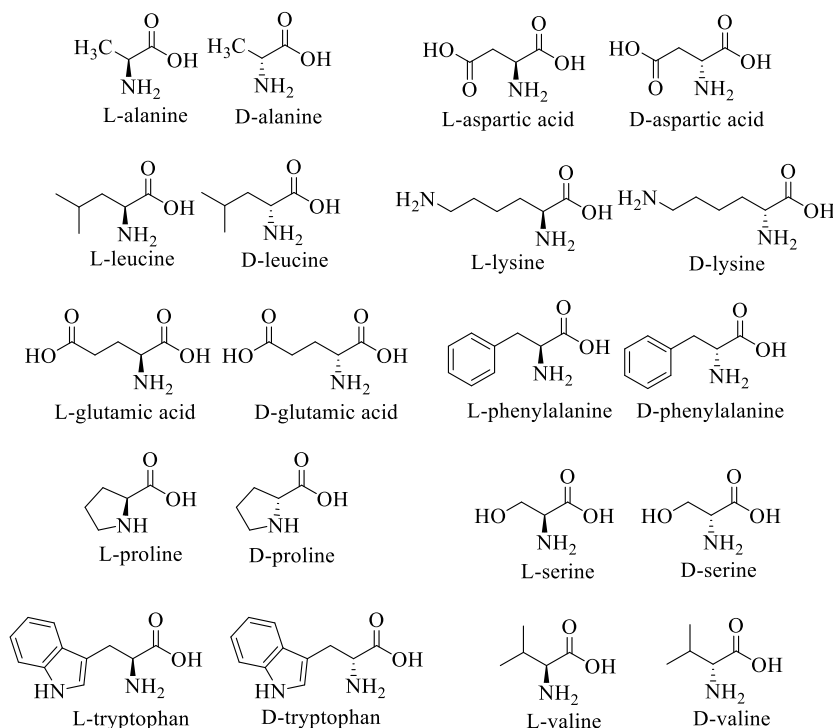
Figure 3.19 Structure of enantiomers of analytes screened for enantioselective separation

Enantioselective experiments were set up by adding two polymer-coated AAO membranes in the racemic mixture solution. Racemic mixture solution with suspended chiral membranes was agitated on a mechanical shaker for 24 hours at room temperature (25-30 °C). After 24 hours, the membranes were removed, and CD spectra of the remaining solution were recorded at 25 °C (Figure 3.20).
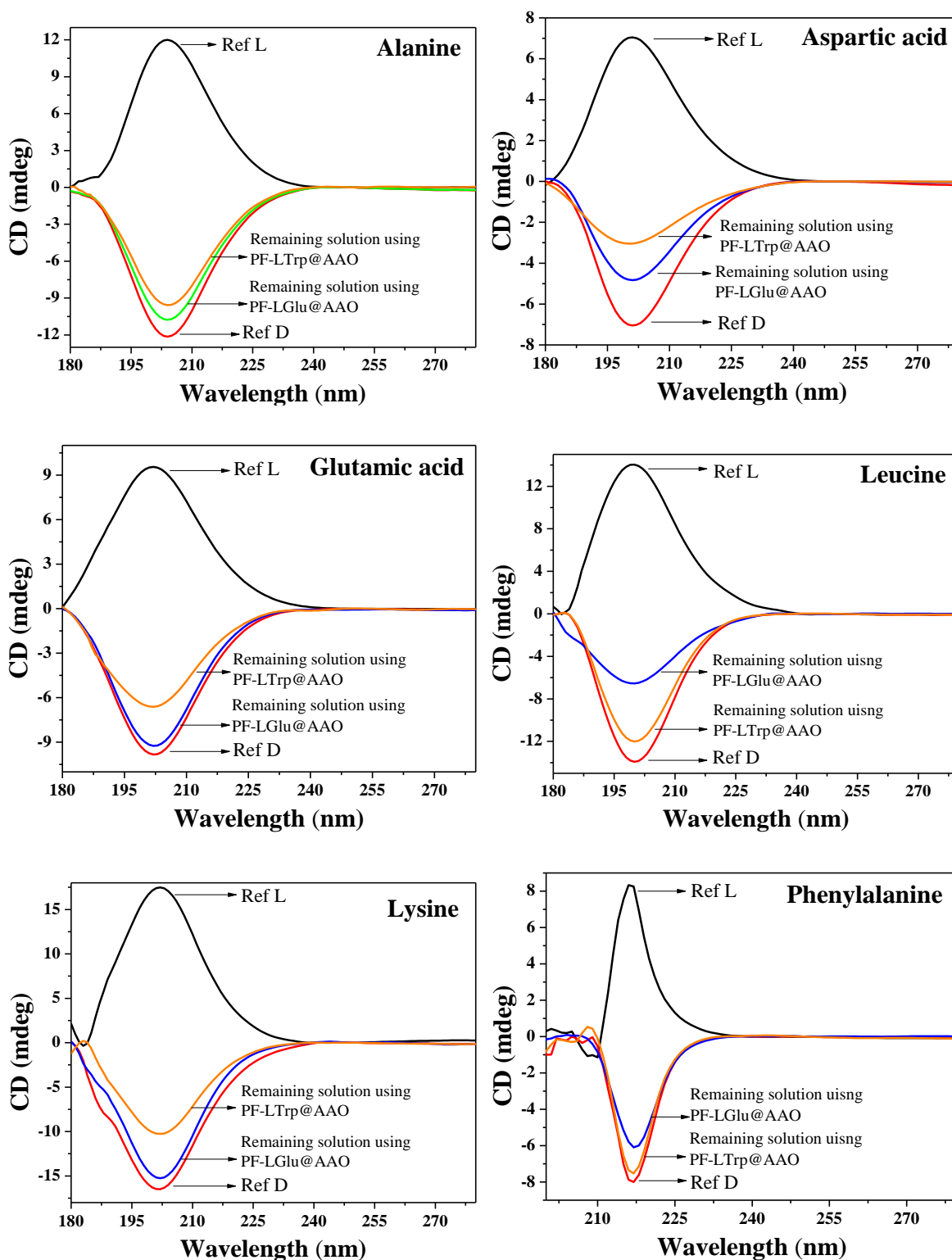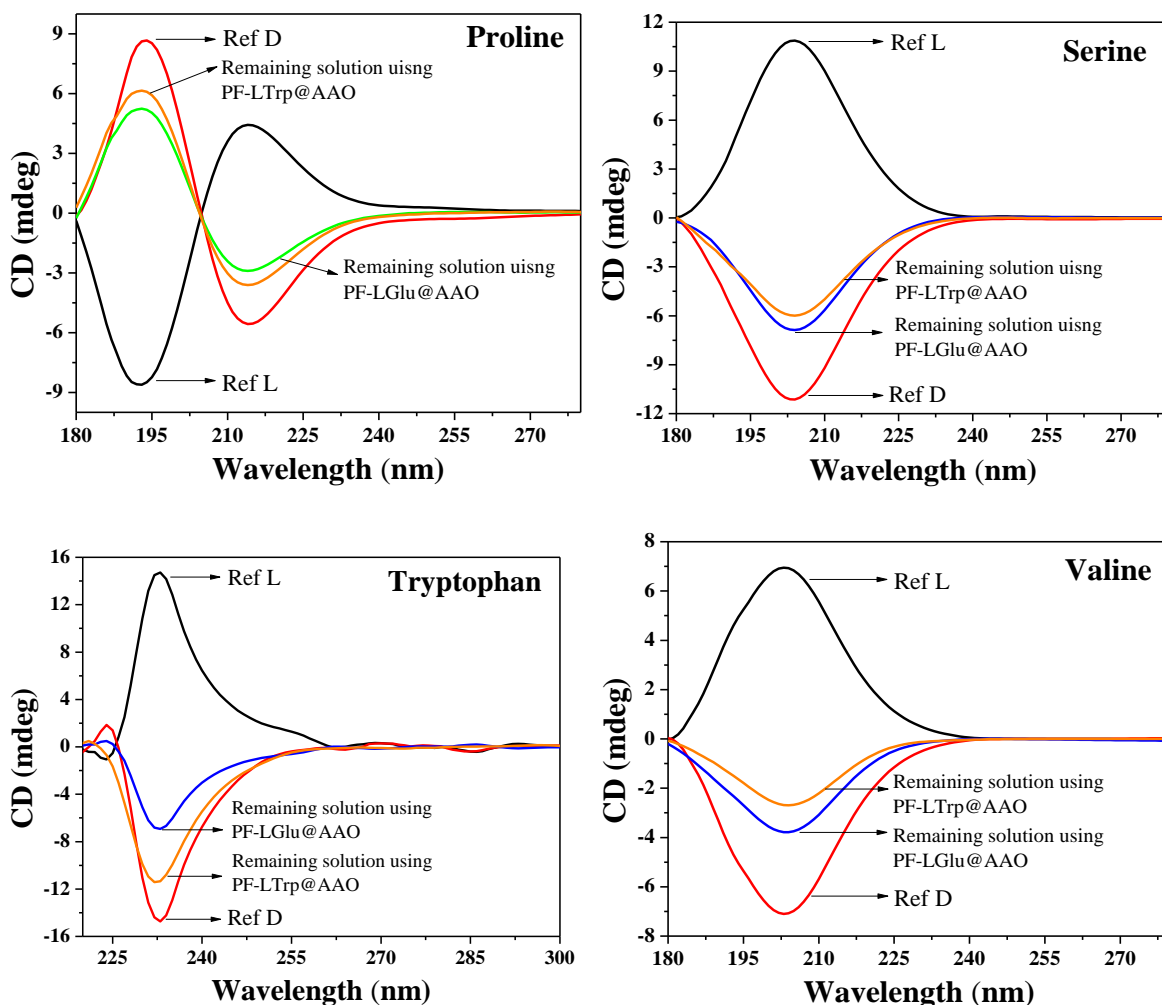
Figure 3.20 CD spectra of remaining solution after enantioselective separation plotted against the pure enantiomer

The CD Spectra of all the analytes showed CD signals corresponding to the D enantiomers. From this, it could be concluded that L-enantiomers of amino acids got selectively adsorbed inside the pores of chiral polymer-coated AAO membranes leaving behind D-enantiomer in the water. CD spectra of the remaining solution were then plotted against the corresponding D and L enantiomer (reference solution). Reference solutions were prepared by dissolving 1 mg of D or L enantiomer in 3 ml of DI water. From CD signals of remaining solution, it could be seen that PF-LGlu@AAO and PF-LTrp@AAO membranes differed in terms of their enantioselective separation ability. Quantitative estimation of enantioselective separation ability of chiral polymer-coated AAO membranes was determined by taking a ratio of area under the curve of remaining solutions and corresponding reference solution (D-enantiomer). The ratio of area under curves, when multiplied by 100, gives % enantiomeric excess (% ee) (Equation 1)[26]

$$\% \; ee = \frac{area \; under \; curve \; (remaining \; sol^n)}{area \; under \; curve \; (reference \; sol^n)} \times 100$$

Equation 1 Equation for calculating % enantiomeric excess of enantioselective separation

The % enantiomeric excess values of enantioselective separation were calculated using equation 1 and given in Table 2

Amino acids	polymers	
	PF-LGlu@AAO	**PF-LTrp@AAO**
Alanine	83.3	78.7
Aspartic acid	70.9	51.1
Glutamic acid	91.9	71.3
Leucine	56.9	86.2
Lysine	84.4	56.8
Phenylalanine	82.6	87.6
Proline	51.7	79.5
Serine	57.5	53.5
Tryptophan	70.5	91.3
Valine	53.2	36.4

Table 2 % enantiomeric excess (% ee) of enantioselective separation using PF-LTrp@AAO and PF-LGlu@AAO membranes was calculated by taking the area under curve of remaining solution and reference solution.

It could be seen from the enantiomeric excess values in Table 2, The PF-LGlu@AAO could separate the glutamic acid racemic mixture with the highest % ee (91.9 %). PF-LGlu@AAO could also separate other amino acids like alanine, lysine, and phenylalanine with % ee more than 80 %. The PF-LTrp@AAO separated the tryptophan racemic mixture with the highest % ee (91.3), while other amino acid racemic mixtures like leucine and phenylalanine could be separated with % ee more than 80. The ability of the chiral selectors to carry out enantioselective separation of analytes depends upon several factors like the type of interactions, the extent of interaction, structural similarity, size, and charges on the analytes.[27] Chiral selectors can undergo different interactions with analytes like Van der Waals, ionic, steric, hydrogen bonding, dipole-dipole, ion-dipole, or π-π interactions.[28] Sometimes multiple forces are also involved that may be either attractive or repulsive. Here it could be seen that glutamic acid-containing polymer-coated membranes (PF-LGlu@AAO) could separate glutamic acid, alanine, lysine, and phenylalanine. Depending

upon the structures of these analytes and groups in the chiral selector, it could be expected that hydrogen bonding interactions were involved in the enantioselective separation process. The aromatic L-tryptophan containing polyfluorene membranes (PF-LTrp@AAO) could separate aromatic amino acids like tryptophan (91.3 % ee) and phenylalanine (87.6 % ee) with the highest % ee. Other amino acids like leucine, proline, and alanine were also separated with considerable % ee. From the results, it could be expected that aromatic analytes underwent π-π interactions with the aromatic chiral selector in addition to hydrogen bonding. In the case of aliphatic amino acids like leucine, proline, and alanine, it could be hydrogen bonding interaction. From these results, it could be concluded safely that the chemical structure of the chiral selector plays an essential role in achieving better enantioselective separation. Enantiomers of any chiral compound can be separated effectively if the structure and interaction are studied carefully.

3.4 CONCLUSION

This chapter demonstrated the synthesis and enantioselective separation application of different chiral handles containing polymer-coated AAO membranes. Protected L-glutamic acid and protected L-tryptophan containing (aromatic) polyfluorene were synthesized and coated on 200 nm pore size AAO membranes. These polymer-coated AAO membranes were used to carry out enantioselective separation of different amino acids. Depending upon the type and extent of interactions, these membranes separated different analytes with different % ee. Aromatic pendant containing polymer-coated AAO membranes (PF-LTrp@AAO) separated aromatic amino acids like tryptophan and phenylalanine with the highest % ee due to π-π interaction. The protected glutamic acid-containing polyfluorenes membranes (PF-LGlu@AAO) separated glutamic acid and other aliphatic amino acids with the highest % ee due to hydrogen bonding interactions.[29] It could be concluded that the chemical structure of the chiral handle plays a crucial role in determining the selectivity and sensitivity of chiral selectors. The tailor-made chiral selectors can achieve enantioselective separation of desired racemic mixtures.

3.5 REFERENCES

(1)   Skolnick, J.; Zhou, H.; Gao, M. On the Possible Origin of Protein Homochirality, Structure, and Biochemical Function. *Proc. Natl. Acad. Sci. U. S. A.* **2019**, *116* (52), 26571–26579.

(2)   Blackmond, D. G. The Origin of Biological Homochirality. *Cold Spring Harb. Perspect. Biol.* **2019**, *11* (3).

(3)   Inaki, M.; Liu, J.; Matsuno, K. Cell Chirality: Its Origin and Roles in Left-Right Asymmetric Development. *Philosophical Transactions of the Royal Society B: Biological Sciences*. Royal Society of London December 19, 2016.

(4)   Blackmond, D. G. The Origin of Biological Homochirality. *Cold Spring Harb. Perspect. Biol.* **2010**, *2* (5), 1–17.

(5)   Zhao, X.; Zang, S. Q.; Chen, X. Stereospecific Interactions between Chiral Inorganic Nanomaterials and Biological Systems. *Chem. Soc. Rev.* **2020**, *49* (8), 2481–2503.

(6)   Calcaterra, A.; D'Acquarica, I. The Market of Chiral Drugs: Chiral Switches versus de Novo Enantiomerically Pure Compounds. *Journal of Pharmaceutical and Biomedical Analysis*. Elsevier B.V. January 5, 2018, pp 323–340.

(7)   Jeschke, P. Current Status of Chirality in Agrochemicals. *Pest Management Science*. John Wiley and Sons Ltd November 1, 2018, pp 2389–2404.

(8)   Sekhon, B. S. Chiral Pesticides. *Journal of Pesticide Science*. 2009, pp 1–12.

(9)   Schäfer, U.; Kiefl, J.; Zhu, W.; Kempf, M.; Eggers, M.; Backes, M.; Geissler, T.; Wittlake, R.; Reichelt, K. V.; Ley, J. P.; Krammer, G. Authenticity Control of Food Flavorings - Merits and Limitations of Chiral Analysis. *ACS Symp. Ser.* **2015**, *1212*, 3–12.

(10)   Medina, D. D.; Goldshtein, J.; Margel, S.; Mastai, Y. Enantioselective Crystallization on Chiral Polymeric Microspheres. *Adv. Funct. Mater.* **2007**, *17* (6), 944–950.

(11)   Harada, M.; Karakawa, S.; Yamada, N.; Miyano, H.; Shimbo, K. Biaryl Axially Chiral Derivatizing Agent for Simultaneous Separation and Sensitive Detection of Proteinogenic Amino Acid Enantiomers Using Liquid Chromatography–tandem Mass Spectrometry. *J. Chromatogr. A* **2019**, *1593*, 91–101.

(12)   Tarafder, A.; Miller, L. Chiral Chromatography Method Screening Strategies: Past, Present and Future. *J. Chromatogr. A* **2021**, *1638*.

(13)   Liu, T.; Li, Z.; Wang, J.; Chen, J.; Guan, M.; Qiu, H. Solid Membranes for Chiral Separation: A Review. *Chemical Engineering Journal*. Elsevier B.V. April 15, 2021.

(14) Scriba, G. K. E. Chiral Recognition in Separation Science – an Update. *J. Chromatogr. A* **2016**, *1467*, 56–78.

(15) Tsioupi, D. A.; Stefan-van Staden, R. I.; Kapnissi-Christodoulou, C. P. Chiral Selectors in CE: Recent Developments and Applications. *Electrophoresis* **2013**, *34* (1), 178–204.

(16) Berthod, A. *Chiral Recognition in Separation Methods: Mechanisms and Applications*; Springer Berlin Heidelberg, 2010.

(17) Berthod, A. Chiral Recognition Mechanisms. *Anal. Chem.* **2006**, *78* (7), 2093–2099.

(18) Yoshikawa, M.; Higuchi, A. *ENANTIOSELECTIVE MEMBRANES*; 2013.

(19) Fernandes, C.; Tiritan, M. E.; Pinto, M. M. M. Chiral Separation in Preparative Scale: A Brief Overview of Membranes as Tools for Enantiomeric Separation. *Symmetry (Basel).* **2017**, *9* (10).

(20) Xie, R.; Chu, L. Y.; Deng, J. G. Membranes and Membrane Processes for Chiral Resolution. *Chem. Soc. Rev.* **2008**, *37* (6), 1243–1263.

(21) Huang, K.; Dong, X.; Ren, R.; Jin, W. Fabrication of Homochiral Metal-Organic Framework Membrane for Enantioseparation of Racemic Diols. *AIChE J.* **2013**, *59* (11), 4364–4372.

(22) Li, Y.; Lin, X.; Qin, S.; Gao, L.; Tang, Y.; Liu, S.; Wang, Y. β-Cyclodextrin-Modified Covalent Organic Framework as Chiral Stationary Phase for the Separation of Amino Acids and β-Blockers by Capillary Electrochromatography. *Chirality* **2020**, *32* (7), 1008–1019.

(23) Chan, J. Y.; Zhang, H.; Nolvachai, Y.; Hu, Y.; Zhu, H.; Forsyth, M.; Gu, Q.; Hoke, D. E.; Zhang, X.; Marriot, P. J.; Wang, H. Incorporation of Homochirality into a Zeolitic Imidazolate Framework Membrane for Efficient Chiral Separation. *Angew. Chemie* **2018**, *130* (52), 17376–17380.

(24) Lakshmi, B. B.; Martin, C. R. Enantioseparation Using Apoenzymes Immobilized in a Porous Polymeric Membrane. *Nature* **1997**, *388* (6644), 758–760.

(25) Higuchi, A.; Tamai, M.; Ko, Y. A.; Tagawa, Y. I.; Wu, Y. H.; Freeman, B. D.; Bing, J. T.; Chang, Y.; Ling, Q. D. Polymeric Membranes for Chiral Separation of Pharmaceuticals and Chemicals. *Polym. Rev.* **2010**, *50* (2), 113–143.

(26) Senthilkumar, T.; Asha, S. K. An Easy "Filter-and-Separate" Method for Enantioselective Separation and Chiral Sensing of Substrates Using a Biomimetic Homochiral Polymer. *Chem. Commun.* **2015**, *51* (43), 8931–8934.

(27) Sadeghi, I.; Kaner, P.; Asatekin, A. Controlling and Expanding the Selectivity of

Filtration Membranes †. *Chem. Mater.* **2018**, *30* (21), 7328–7354.

(28) Berthod, A. Chiral Recognition Mechanisms. *Anal. Chem.* **2006**, *78* (7), 2093–2099.

(29) Nikam, S. B.; Sk, A. Enantioselective Separation Using Chiral Amino Acid Functionalized Polyfluorene Coated on Mesoporous Anodic Aluminum Oxide Membranes. *Anal. Chem.* **2020**, *92* (10), 6850–6857.

CHAPTER 4

Enantioselective Separation of Amino Acids Using Chiral Polystyrene Microspheres synthesized by Post Polymer Modification Approach

4.1 INTRODUCTION

Synthesis of enantiomerically pure molecules is a big industry as it caters to a host of requirements in the pharmaceutical,[1] agrochemicals,[2–4] food additive,[5–7] and fragrance industries.[8,9] Natural sources for enantiopure starting materials are insufficient to meet the continuously growing demand, and thus these compounds have to be synthesized in laboratories.[10] Among the accepted methods of obtaining enantiopure molecules, the widely used 'chiral or asymmetric synthetic approach' requires highly enantiopure starting material, expensive and environmentally hazardous chiral catalysts besides being very sensitive to any changes in the solvent, ligand etc.[11,12] The alternate 'racemic approach' method involves synthesizing chemical compounds in racemic form, followed by their enantioselective separation. Different methods such as chiral chromatography,[13] enantioselective crystallization,[14–16] and enantioselective filtration are used in the racemic approach to separate the synthesized enantiomers.[17] Chiral chromatographic methods are most commonly used but are associated with limitations like the high-end instruments and skilled workforce.[18] Methods like enantioselective crystallization need enantiopure sacrificial compounds. Recently, enantioselective filtration methods using chiral selectors have gained more attention from the scientific community since these methods are simple, straightforward, energy-efficient, and do not require high-end instruments.

Chiral selectors can differentiate between the enantiomers, and they include natural materials like polysaccharides, cyclodextrins, micelles, proteins, macrocyclic glycopeptides, and crown ethers.[19–22] The use of various synthetic polymers as chiral selectors is also increasingly reported.[23–25] Senthilkumar *et al.* reported the application of chiral polyfluorenes for the enantioselective separation of racemic mixtures from various classes of materials like amino acids, amino alcohols, and sugars by a simple filtration method from their aqueous mixtures.[26] Chapter 2 of this thesis presented the extension of this work initiated in our group, where protected D/L-aspartic acid containing chiral polyfluorenes were synthesized and used to fabricate chiral AAO membranes. These polymer coated chiral membranes were then used to carryout enantioselective separation of aqueous racemic mixtures of different amino acids where an improvement was observed in the separation efficiency with highest enantiomeric excess (ee) of ~ 95 %) for native glutamic acid separation.[27] Polymeric microspheres are getting more attention in recent years due to their easy modification and processability, where shape, size, and surface functionality can be easily modified.[28] Chiral polymeric microspheres with particle sizes ranging from 1-200 μm

with high surface area are increasingly reported as stationary phase in chiral chromatography.[29–31] Reports are available using polymeric microspheres or polymer coated on inorganic materials like modified silica or metal nanoparticles as chiral selectors.[32,33] In 2007 Yitzhak Mastai *et al.* synthesized hollow Poly(N-Vinyl-α-L-Phenylalanine microspheres using polystyrene microspheres as a template and used it to carryout enantioselective crystallization of racemic mixture of valine with 25 % ee.[34] Zhang *et.al* reported L-phenylalanine imprinted polymer (MIP) based on monodisperse hybrid silica particles that were utilized as chiral selectors in packed columns for resolution of racemic mixture of phenylalanine.[35] Song et.al reported helical Polyacetylene microspheres modified with multicomponents such as stearyl acrylates, butyl acrylates, and β -cyclodextrin acrylate derivatives which were used to separate racemic mixture of menthol in 6 days.[36] Small changes in the composition was reported to have a significant impact on separation efficiency. Enantioselective separation of racemic mixtures was achieved using magnetic microspheres immobilized with chiral substituents such as human serum albumin (HSA) or β-cyclodextrins.[37,38] There are recent reports on microspheres prepared from amino acid based acrylate polymers, amino acid containing chiral metal organic frame work and chitosan functionalized (P(S-DVB) particles that were used to carryout enantioselective crystallization of racemic mixture of amino acids with 25 % ee, or used as chiral selectors in chiral HPLC for the separation of several racemates with highest separation factor (α) 7.55 for naproxen and benzoin respectively.[28,29,39]

In the current chapter, chiral polystyrene (PS) microspheres were synthesized and used to separate native amino acid racemic mixture from their aqueous solution by enantioselective adsorption followed by a simple filtration method. Chiral PS was synthesized by a post polymer modification approach starting from polystyrene with well-defined molecular weights and molar mass distribution synthesized by RAFT polymerization. The synthesized PS was modified with chiral N-Phthaloyl-L-leucine acid chloride by Friedel–Crafts acylation reaction to give Protected PS-L-Leu. The polymer, upon deprotection, yielded chiral PS with a free amine (Deprotected PS-L-Leu), making the polymer hydrophilic in nature compared to the starting PS or the protected amino acid appended PS. The protected as well as deprotected PS was assembled into microspheres using the surfactant tween 80 (polyoxyethylene sorbitan monooleate) and used for filtration based enantioselective separation of native amino acids from their aqueous racemic mixture. Higher ee % could be achieved with microspheres of deprotected PS with free amine groups. Deprotected PS-L-

Leu microspheres achieved 81.57 % ee for the separation of leucine. According to our knowledge, this is the first report where amino acid modified chiral polystyrene microspheres were synthesized and used to carry out simple filtration-based enantioselective separation of native amino acids from their racemic mixtures. The method is cost-effective as it uses commodity polymer like PS and does not need any high-end chromatographic instruments.

4.2 EXPERIMENTAL SECTION

4.2.1 Materials

Synthetic grade styrene monomer was purchased from Sigma Aldrich and purified by washing with 10% aqueous NaOH solution, water, followed by drying over anhydrous sodium sulfate. It was stirred with calcium hydride and distilled under a vacuum at 40 °C. Synthetic grade AIBN (2, 2′-azobis(2-methylpropionitrile)) was purchased from Aldrich and recrystallized in methanol before being used. The biochemistry grade amino acids like D/L-leucine and D/L-alanine were purchased from Spectrochem Pvt. Ltd. India. RAFT agent was previously synthesized in the lab and used directly without further purification.[40] Phthalic anhydride and hydrazine hydrate were purchased from Sigma Aldrich. Bottle grade THF, methanol, chloroform, 1, 2-dichloroethane, HCL, ethanol, and triethylamine were purchased from Merck Chemicals and used without further purification. Toluene was purchased from Merck Chemicals and predried using $CaCl_2$, CaH_2 and dried by heating over sodium with benzophenone as the indicator. Reagent-grade sodium hydroxide (NaOH), potassium hydroxide (KOH), sodium sulfate (Na_2SO_4), calcium hydride (CaH_2), and HPLC grade THF were purchased from Merck Chemicals. Analytical grade Tween 80 (polyoxyethylene sorbitan monooleate) surfactant was purchased from TCI chemicals. Extra pure anhydrous $AlCl_3$ and synthetic grade $SOCl_2$ were purchased from Loba Chemie Pvt. Ltd India. Analytical grade deuterated $CDCl_3$ was purchased from Sigma Aldrich. 0.45 um Polytetrafluoroethylene (PTFE) and polyvinylidene fluoride (PVDF) filters were purchased from Global Nanotech. Drum grade Ethyl acetate and pet ether were purchased locally and used after distilling through the rotary evaporator.

4.2.2 Measurements

^{1}H NMR spectra were recorded on Bruker Avance 200 and 400 MHz spectrometers in CDCl$_3$. Chemical shifts (δ) are reported in ppm at 25 °C using CDCl$_3$ as solvent containing a trace amount of tetramethylsilane (TMS) as an internal standard. Molecular weights of polymers were measured on ThermoFinnigan make GPC, with RI detector at room temperature. The HPLC grade chloroform was used as eluent with a flow rate maintained at 1 ml/min. The GPC column was standardized using Polystyrene standards with narrow polydispersity. The samples were prepared by dissolving 3 mg polymer in 1.5 ml chloroform and filtered through a 0.45 μm PTFE filter. Infrared spectra were recorded on a Bruker α-T spectrophotometer. Sample pellets were prepared by mixing with 5% w/w in KBr and dried under vacuum before spectra were recorded. The polymeric microspheres were prepared by using a polymeric solution in DCM and 4% tween 80 surfactant solution. The polymer and surfactant solutions were mixed in 1:4 v/v ratio and homogenized using RT Miccra D-9 Digitronic Homogenizer Disperser on Stand, at 16000-21000 rpm for 15 min. The polymeric microsphere suspension was centrifuged on Remi PR-24 research compufuge centrifuge with a 6x15 ml rotor head at 10000 rpm. The average particle size (Z-average), polydispersity index (PDI) of aqueous dispersion of polymeric microspheres were measured using a Zetasizer ZS 90 apparatus from Malvern instruments at a fixed angle of 90° at 25 °C. Zeta potential (ζ) of polymeric microspheres were measured at pH 7 using (0.1 mg/ml) dispersion in 0.1 milli molar KCl. The morphological characterizations of polymeric samples and microspheres were performed using FE-SEM with a FEI Nova Nano SEM 450. The polymer solution in THF (0.2 mg/ml) was drop cast on pre-cleaned silicon wafers. In the case of polymer microspheres, the aqueous dispersion was drop cast on pre-cleaned silicon wafers. The samples were dried overnight under reduced pressure at 45 °C. The sample drop cast silicon wafers were directly mounted on the top of the grooved edge of the aluminium SEM specimen stub with carbon tape. Before conducting morphological studies, the samples were coated with a 5 nm thick gold film by a sputtering method. Water contact angle of polymers were recorded using Drop Shape Analyzer-DSA25- KRUSS GmbH. Solution state Circular Dichroism (CD) measurements were made using a JASCO-815 CD spectrometer equipped with a Jasco PTC-424 S / 15 Peltier system. 10 mm path-length quartz cuvettes were used for a sample volume of 3 ml in Milli-Q water or THF at 25 °C. Three scans were averaged for each sample with a scanning rate of 100 nm/min.

4.2.3 Methods

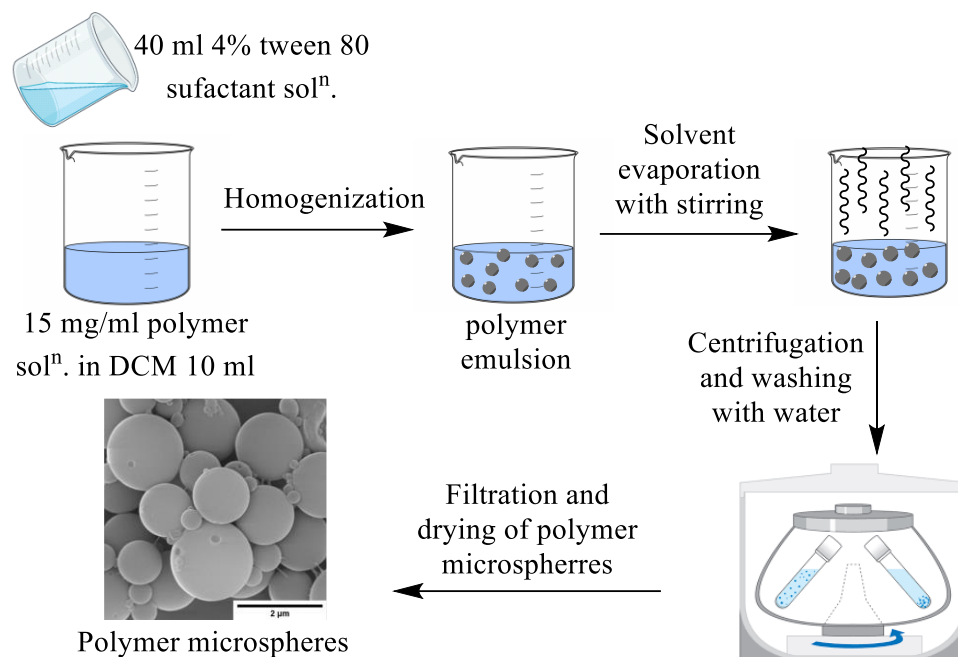#### A) Preparation of polymeric microspheres

Figure 4.1 Schematic representation of polymeric microspheres preparation protocol

150 mg of pristine polystyrene powder was dissolved in 10 ml of HPLC grade DCM. Separately 4% w/v tween 80 (polyoxyethylene sorbitan monooleate) surfactant was prepared by dissolving 2 gram of tween 80 and making up the volume with deionized (DI) water in 50 ml volumetric flask. 40 ml of the surfactant solution was added to the 10 ml of polystyrene solution. The solution was homogenized with the help of a homogenizer at 20000 rpm for 10-15 min until the solution formed a milky white uniform suspension. Homogenization results in the formation of polymeric droplets of uniform size. The shape and size of the polymeric droplet were stabilized by surfactant. Further, the solvent (DCM) was evaporated by subjecting the homogenized polymeric suspension to stirring at 1500 rpm with an overhead stirrer for 3-4 h at 45 °C. Prolonged stirring at 45 °C results in the complete evaporation of DCM from the suspension. The suspension of spherical polymeric particles was then centrifuged at 10000 rpm. As the polymeric particles settled down at the bottom, the supernatant was decanted. The settled polymer particles were washed multiple times (3 times) by adding fresh DI water to ensure the complete removal of the surfactant. Microsphere suspension was then filtered through 0.22 µm pore size PVDF membranes using vacuum filtration assembly. The polymeric particles on the PVDF membrane were then dried overnight in a vacuum oven at 45 °C. The chiral spherical polymeric particles

from the amino acid modified polystyrenes Protected PS-L-Leu and Deprotected PS-L-Leu were prepared by following the same protocol. Figure 4.1 schematically represents the microsphere formation protocol.

B) Dynamic Light Scattering (DLS) and Zeta potential

The 2 Milli molar dispersions of polymeric microspheres (pristine polystyrene, Protected PS-L-Leu and Deprotected PS-L-Leu) were prepared by dispersing 2.1 mg of polymeric particles in 10 ml of DI water. The dispersion was then sonicated on an ultra sonicator for 2 hours. Particle flocculation was avoided by maintaining the bath temperature below 45 °C. The prolonged sonication forms the uniform dispersion of the polymeric microspheres by breaking the particle aggregation. Various dilutions of these polymeric suspensions were subjected to the particle size measurement on the DLS instrument to determine average particle size. The best histograms were obtained at the 0.25 Mili molar concentration (Figure 4.21)

C) Water contact angle measurement for polymer samples

Water contact angle of pristine polystyrene, Protected PS-L-Leu and Deprotected PS-L-Leu were recorded to determine enhancement in the hydrophilicity upon deprotection, which subsequently improves the surface wettability with aqueous racemic mixtures. Polymer solutions (0.1mg/ml) in THF were used to prepare uniform thin films on cover slips with the help of spin coater at a speed of 1000 rpm. 2-3 drops of prepared polymer solution were drop casted and allowed to rotate at same speed for 1min. The polymer coated cover slips were removed, air dried and directly used to determined water contact angle. On the dried membrane surface, water drops of a consistent volume were allowed to fall. A built-in drop shape analysis tool was used to evaluate the digital image from the camera.

4.2.4 Synthesis and characterizations

1) Synthesis of polystyrene by RAFT polymerization (P1)

AIBN 15 mg (0.0907 mmols) and CTA (chain transfer (RAFT) agent) 52 mg (0.1439 mmols) were taken in a Schlenk tube equipped with a magnetic stirring bar. Distilled styrene monomer 4.5 gm (43.206) was added to the reaction mixture with the help of a syringe through a rubber septum. The reaction mixture was then degassed by three freeze pump thaw cycles. The tube was charged with nitrogen gas to maintain the inert atmosphere. The reaction mixture was then heated at 110 °C for 6 hours (until the reaction mixture became so

viscous that the magnetic bead stopped stirring). The Schlenk tube was then cooled in an ice bath which solidified the formed polymer completely, followed by dissolving the polymer in minimum quantity of THF. The polymer was precipitated in excess of MeOH. The precipitation was repeated three times to ensure the complete removal of oligomers that would have formed during polymerization. Yield: 65%. ^{1}H NMR spectrum (400 MHz, CDCl$_3$) δ 7.11, 7.06, (m 3H), δ 6.60-6.48 (M 2H), δ 1.86 (s 1H), δ 1.57-1.45 (s 2H). ^{13}C NMR spectrum (100 MHz, CDCl$_3$) δ 145.29, δ 127.93, δ 127.63, δ 127.40, δ 125.62, δ 125.46, δ 43.76, δ 40.35, FT-IR (CHCl$_3$) stretching frequency (υ) in cm^{-1}: 3065, 3025, 2926, 2845, 1599, 1497, 1445; GPC (CHCl$_3$): Number average molecular weight (*Mn*) 22800 corresponding to the degree of polymerization (*Xn* = 218); NMR (CDCl$_3$): Number average molecular weight (*Mn*) 20800 corresponding to *Xn* = 200
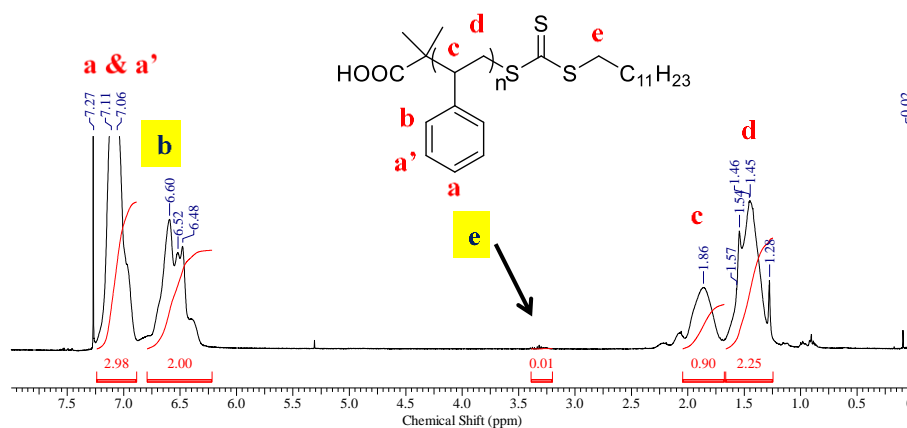

Figure 4.2 ^{1}H NMR spectrum of polystyrene (CDCl$_3$)

Theoretical molecular weight calculations

$$Xn = \frac{[M]}{[I]}P \dots\dots\dots\dots\dots\dots\dots\dots\dots\dots..\dots(1)$$

$$Xn = \frac{[1]}{[0.0033]} 0.65 \dots\dots\dots\dots\dots\dots\dots\dots\dots.\dots\dots.(2)$$

$$Xn = 197 \dots\dots\dots\dots\dots\dots\dots\dots\dots\dots\dots.\dots..\dots(3)$$

$$Mn = 197 * 104.15 \dots\dots\dots\dots\dots\dots\dots..(4)$$

$$Mn = 20500 \dots\dots\dots\dots\dots\dots\dots\dots\dots..(4)$$

The degree of polymerization was calculated by taking the integration ratio of peaks b and e from figure 4.2.

$$Xn = \frac{intigration\ of\ peak\ b}{intigration\ of\ peak\ e}………………… (1)$$

$$Xn = \frac{2}{0.01}……………………………………….. (2)$$

$$Xn = 200……………………………………..….. (3)$$

$$Mn = Xn * \ Reapiting\ unit\ mass..……… (4)$$

$$Mn = 200 * 104.15……………………… (5)$$

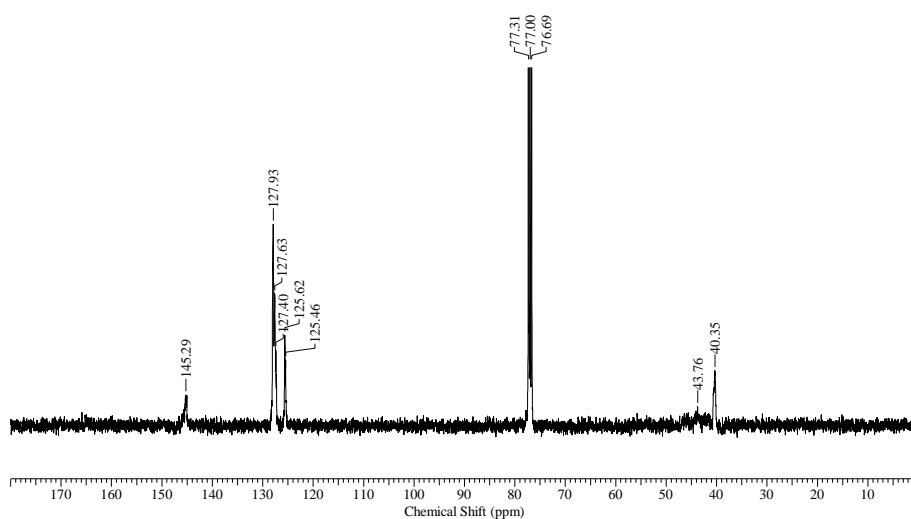$$Mn = 20800\ Daltons……...……………... (6)$$

Figure 4.3 ^{13}C NMR spectrum of polystyrene (CDCl$_3$)
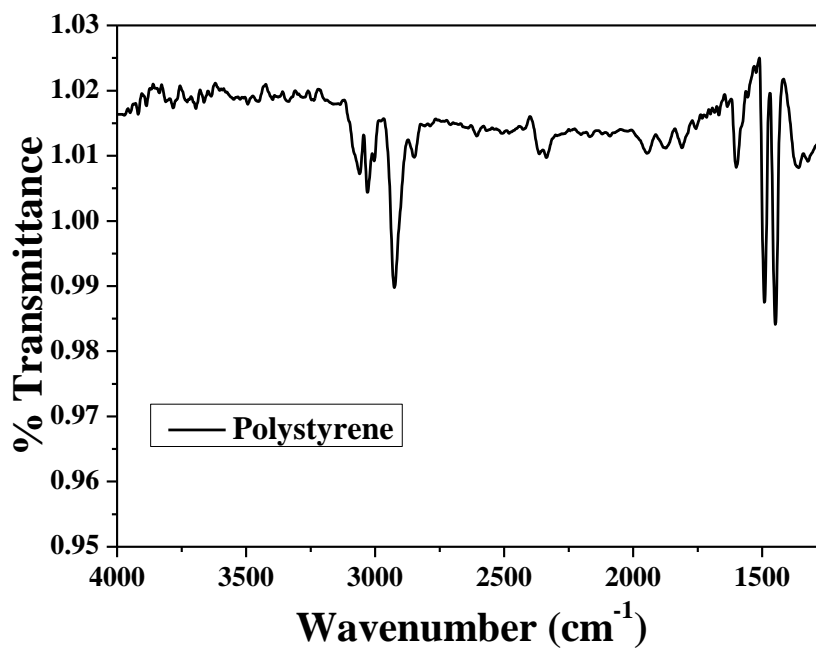
Figure 4.4 FT-IR spectrum of polystyrene

2) Synthesis of small molecules

a) Synthesis of N-Phthaloyl-L-Leucine

L-leucine 2 g (18.3 mmols) was dissolved in 30 ml dry toluene in a 2 neck round bottom flask equipped with magnetic stirring bar under inert atmosphere and connected to a Dean-Stark apparatus. To this solution, triethylamine 2.8 ml (19.8 mmols) was added through a syringe. Phthalic anhydride 2.7 g (15.25 mol) was added to the reaction mixture. The reaction was refluxed at 120 °C with continuous stirring for 6 hours. The solvent collected in the Dean-Stark apparatus was removed, and fresh dry solvent was added to the reaction mixture. For workup, the solvent was evaporated at reduced pressure on a rotary evaporator to obtain the crude product. The product was purified by column chromatography using 30% pet ether, ethyl acetate mixture. Yield 80%. ^{1}H NMR spectrum (200 MHz, CDCl$_3$) δ 7.89-7.85, (m 2H), δ 7.76-7.72, (m 2H), δ 5.04-4.96 (d 1H), δ 2.43-2.32 (d 1H), δ 2.02-1.95 (m 1H). δ 1.54-1.48 (m 1H) δ 0.97-0.91 (s 6H); ^{13}C NMR spectrum (100 MHz, CDCl$_3$) δ 175.42 δ 167.64, δ 134.20, δ 131.73, δ 123.57, δ 50.39, δ 37.00, δ 25.07, δ 23.07, δ 20.96; FTIR stretching frequency (υ) in cm^{-1} (CHCl$_3$) 3040, 2961, 2868, 1771, 1696, 1624, 1388.
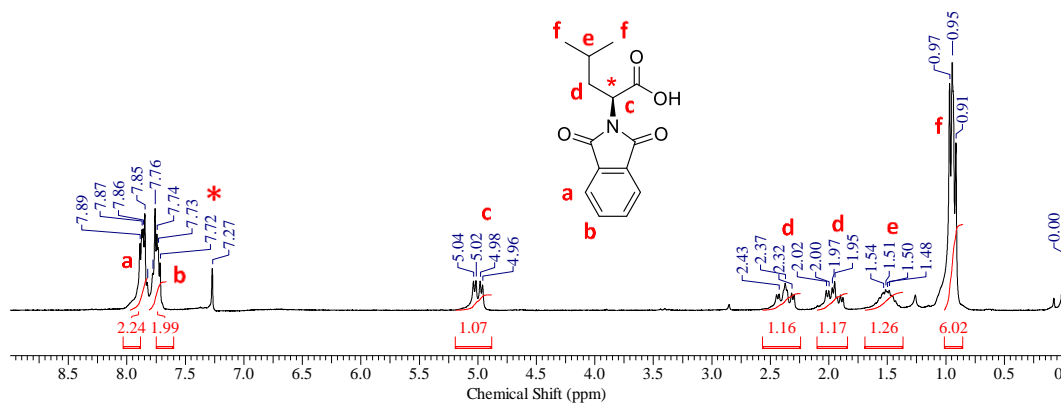

Figure 4.5 ^{1}H NMR spectrum of N-Phthaloyl L-Leucine (CDCl$_3$)
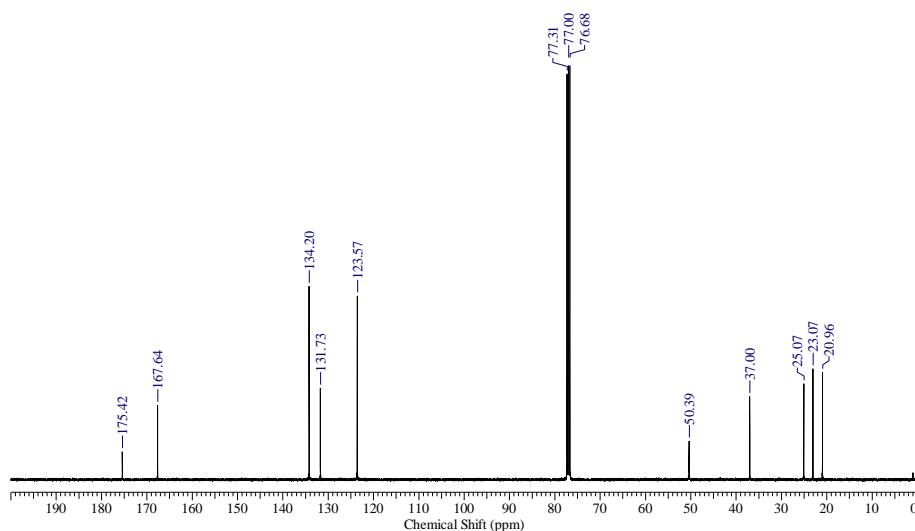
Figure 4.6 ^{13}C NMR spectrum of N-Phthaloyl L-Leucine (CDCl$_3$)
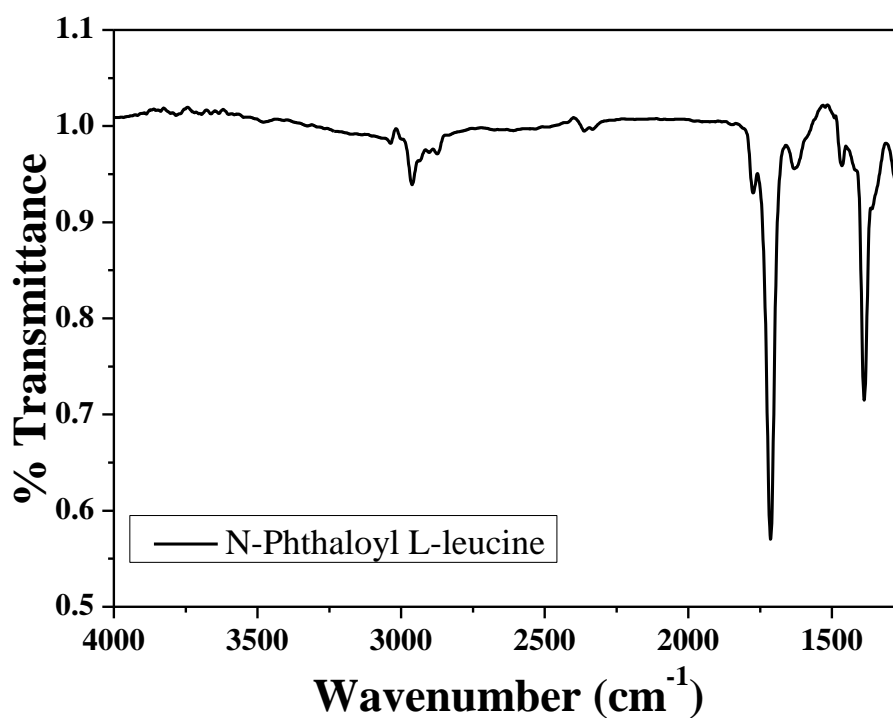

Figure 4.7 FT-IR spectrum of N-Phthaloyl L-Leucine

b) Synthesis of N-Pth-L-Leucine Acid Chloride

N-phthaloyl L-leucine (1.5 g, 5.74 mmols) was dissolved in 15 ml dry DCM in a 100 ml 2 neck round bottom flask. The flask was maintained in an inert atmosphere (N$_2$ gas balloon). The reaction mixture was stirred at 0 °C in an ice bath. SOCl$_2$ (1.3 mL, 17.2 mmols) was added to the reaction mixture and stirred at the same temperature. Once the solution became completely clear the ice bath was removed, and the reaction temperature was raised to room temperature slowly, then refluxed at 50 °C for 2 hours. The solvent and unreacted SOCl$_2$

were removed completely under reduced pressure on rotary evaporator Yield 61%. ^{1}H NMR spectrum (200 MH$_Z$, CDCl$_3$) δ 7.88-7.84, (m 2H), δ 7.75-7.73, (m 2H), δ 5.02, 5.0, 4.96, 4.94 (d 1H), δ 2.33-2.01 (d 1H), δ 1.99-1.94 (m 1H). δ1.50 (m 1H) δ 0.96-0.90 (s 6H); ^{13}C NMR spectrum (100 MH$_Z$, CDCl$_3$) δ 174.52 δ 167.70, δ 134.14, δ 131.77, δ 123.54, δ 50.70, δ 37.18, δ 25.11, δ 23.12, δ 20.98; FTIR stretching frequency (υ) in cm^{-1} (CHCl$_3$) 3035, 2961, 2873, 1776, 1713, 1628, 1388. **Note:** thionyl chloride is toxic in nature and causes irritation of eyes and skin. It hydrolyses upon contact with water and generates toxic and corrosive gasses like sulphur dioxide and hydrogen chloride. The following safety precautions should be taken while using it.

1) Thionyl chloride bottle should be always opened in the fume hood.
2) The use of apron, hand glows, and safety goggle is compulsory.
3) Avoid direct skin or eye contact and avoid direct breathing fume by using mask.
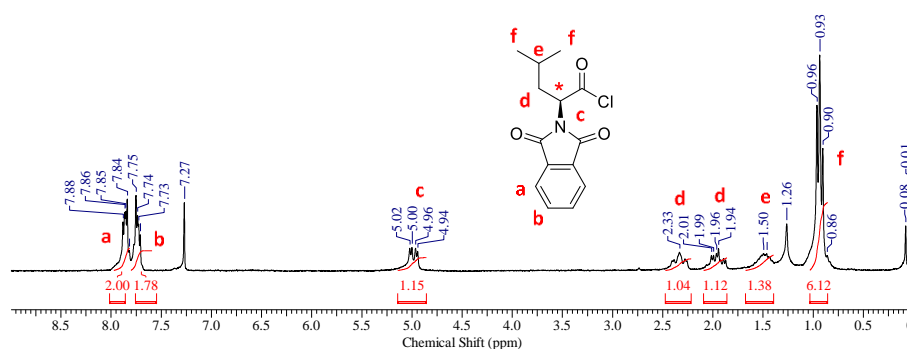4) Close the bottle tightly after use to avoid fume leakage.

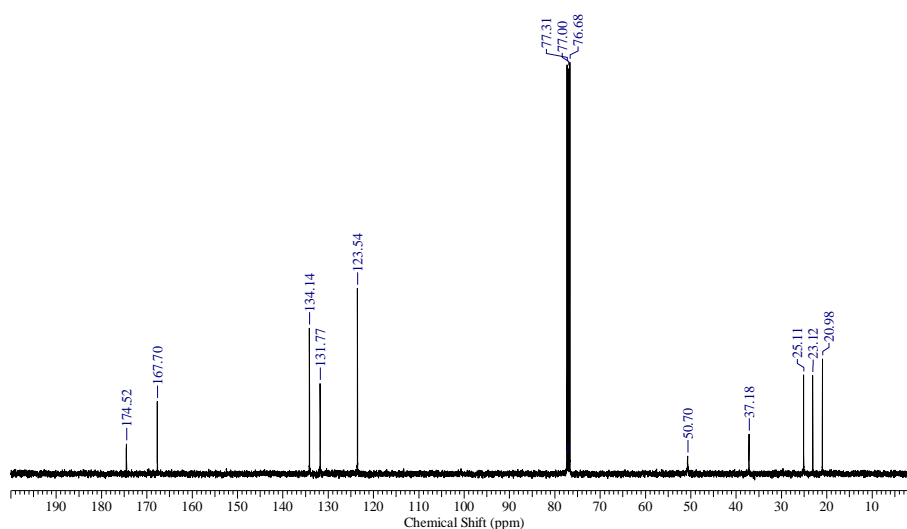**Figure 4.8** ^{1}H NMR spectrum of N-Pth-L-Leucine acid chloride (CDCl$_3$)

Figure 4.9 ^{13}C NMR spectrum of N-Pth-L-Leucine acid chloride (CDCl$_3$)
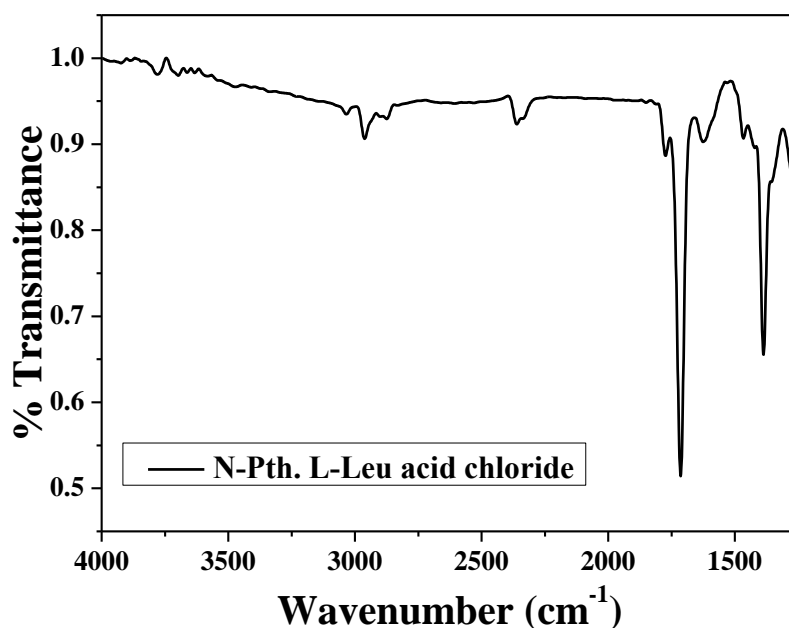
Figure 4.10 FT-IR spectrum of N-Pth-L-Leucine acid chloride

c) Synthesis of Protected PS-L-Leu polymer

N-phthaloyl l-leucine acid chloride (1.6 g, 5.7 mmols) was dissolved in 30 ml 1, 2-Dichloroethane in a 100 ml round bottom flask. The reaction mixture was cooled to 0 °C in ice. The polystyrene (0.6 g, 5.7 mmols) powder was gradually added to the above solution at 0 °C with continuous stirring. After the addition, the reaction mixture was allowed to stir for 30 minutes at the same temperature. AlCl$_3$ (3 g, 22.8 mmols) was added portion-wise to the reaction mixture. The reaction mixture was then allowed to stir at 0 °C for 1 hour. The ice bath was removed, and the temperature of the reaction mixture was raised to room temperature. The reaction mixture was allowed to continue for 2 hours with continuous stirring. The reaction mixture was filtered through Whatman filter paper. The solvent was evaporated at reduced pressure on the rotary evaporator. The product was washed with 10% aqueous hydrochloric acid solution (HCl) followed by 10% aqueous sodium hydroxide solution (NaOH) and distilled water and finally with ethanol to ensure the complete removal of unreacted N-phthaloyl l-leucine acid chloride. The product obtained was dried in an oven at 80 °C for 12 hours. Yield 68%. ^{1}H NMR spectrum (200 MHz, CDCl$_3$) δ 7.83-7.79, (b 2H), δ 7.73-7.71, (m 2H), δ 7.10 (b 3H), δ 6.58 (b 2H) δ 5.02, δ 5.74-5.70 (b 1H), δ 2.48-2.38 (b 1H), δ 2.02 (b 1H), δ1.64 (b 1H), δ 0.97-0.89 (b 6H); ^{13}C NMR spectrum (100 MHz, CDCl$_3$) δ 173.33, δ 167.96, δ 167.68, δ 134.33, δ 134.19, δ 131.75, δ 123.56, δ 123.41, δ 50.32, δ 37.09, δ 25.44, δ 25.08, δ 23.10, δ 20.97; FT-IR stretching frequency (υ) in cm^{-1}: 3005, 2926, 2863, 1709, 1590, 1445. 1382.
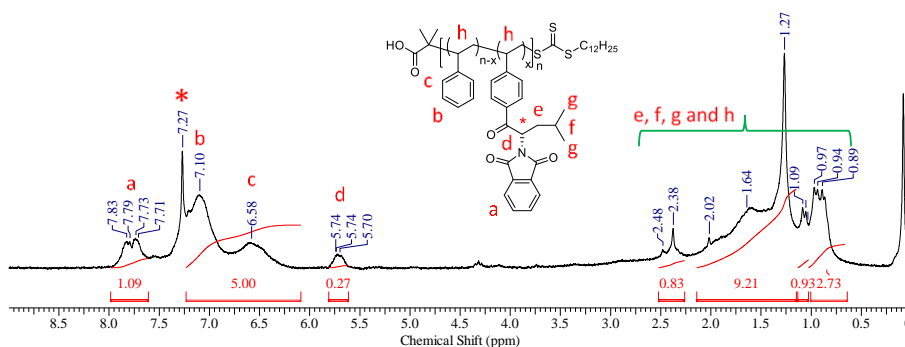
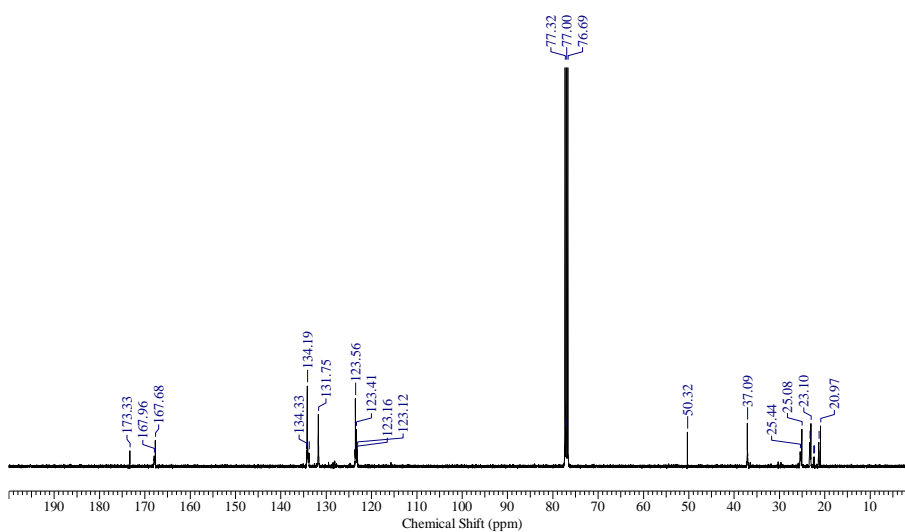**Figure 4.11** ^{1}H NMR spectrum of Protected PS-L-Leu (CDCl$_3$)

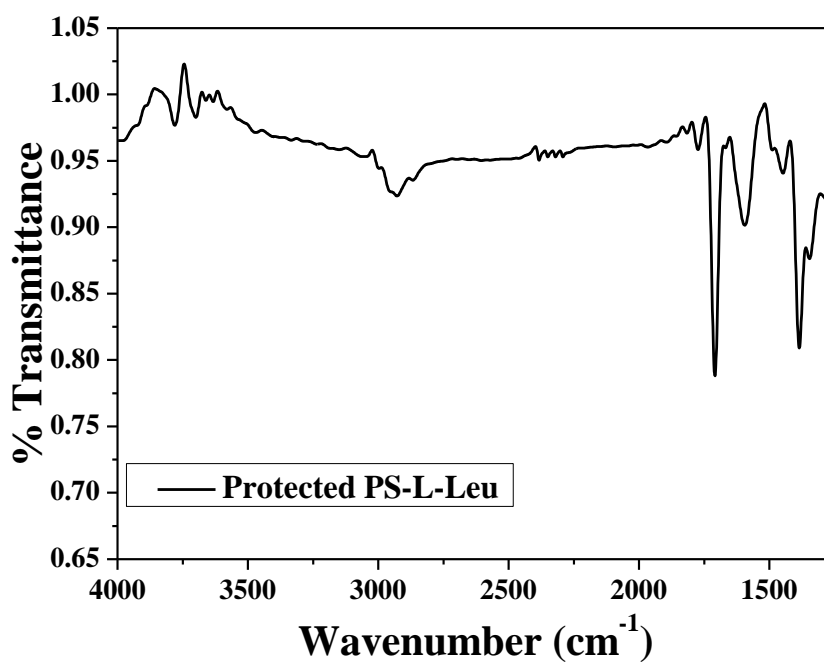**Figure 4.12** ^{13}C NMR spectrum of Protected PS-L-Leu (CDCl$_3$)

Figure 4.13 FT-IR spectrum of Protected PS-L-Leu

d) Synthesis of Deprotected PS-L-Leu polymer

500 mg of N-Phthaloyl L-leucine containing Polystyrene (N-Pth-L-Leu-PS) powder was dissolved in 50 ml toluene in 2 neck 100 ml round bottom flask. 10 ml of hydrazine hydrate was added to the reaction mixture. Further, the reaction mixture was refluxed at 120 °C for 24 hours. After the completion of the reaction, the mixture was cooled to room temperature. The toluene was evaporated at reduced pressure on a rotary evaporator. The reaction mixture was dissolved in DCM. The organic layer was washed with 2% aqueous KOH solution followed by washing with brine solution. The organic layer was dried over anhydrous sodium sulphate (Na_2SO_4). The deprotected polymer was dried completely by solvent evaporation on a rotary evaporator. Complete solvent evaporation resulted in an off-white coloured polymer. Yield 74%. ^{1}H NMR spectrum (400 MH$_Z$, CDCl$_3$) δ 7.03, 6.99 (b 3H), 6.47 (b 2H), δ 4.98-4.93 (b 1H), δ 2.02, (b 1H), δ 1.69 (b 1H), δ 0.89-0.84 (b 6H); ^{13}C NMR spectrum (100 MH$_Z$, CDCl$_3$) δ 167.68, δ 134.20, δ 131.75, δ 123.56, δ 123.41, δ 50.32, δ 37.08, δ 25.08, δ 23.31, δ 23.09, δ 20.97; FT-IR stretching frequency (υ) in cm^{-1}: 3035, 2961, 2868, 1771, 1713, 1628, 1466, 1388. **Note:** Hydrazine hydrate is carcinogenic in nature, highly toxic if inhaled, ingested or absorbed on skin, additionally it is irritant and corrosive in nature. The following safety precautions should be taken while using it.

1) Use protective clothes (apron), hand glows, and safety goggles while handling.
2) Avoid direct skin, or eye contact and avoid breathing dust/fume/gas by using mask.
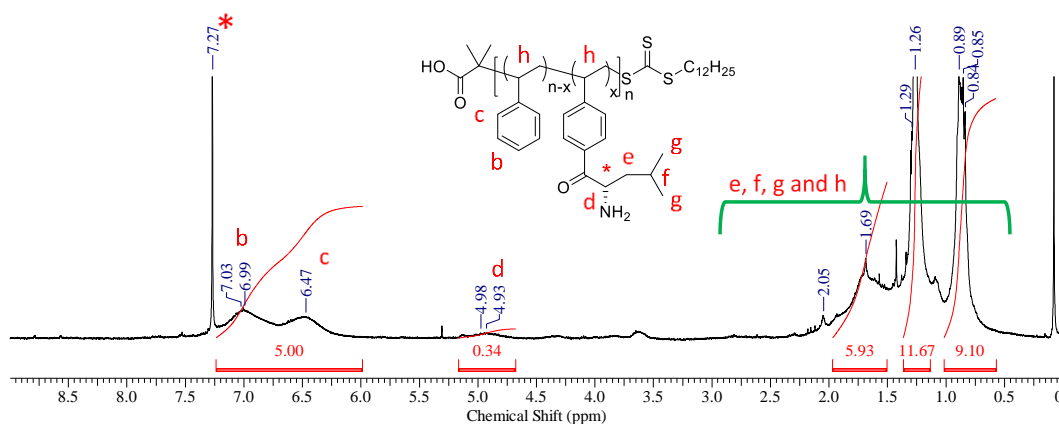3) Wash skin immediately with plenty of water if come in contact with skin as it causes severe skin burns.

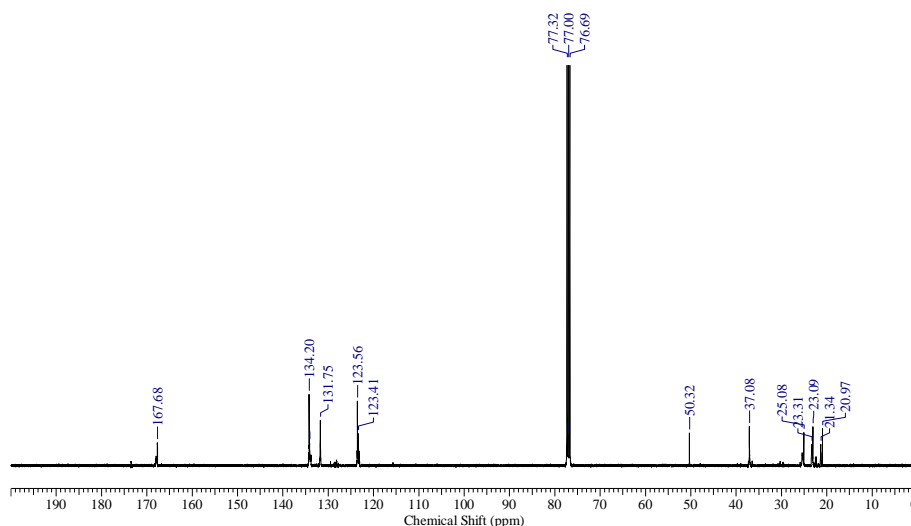**Figure 4.14** ^{1}H NMR spectrum of Deprotected PS-L-Leu (CDCl$_3$)

Figure 4.15 ^{13}C NMR spectrum of Deprotected PS-L-Leu (CDCl$_3$)
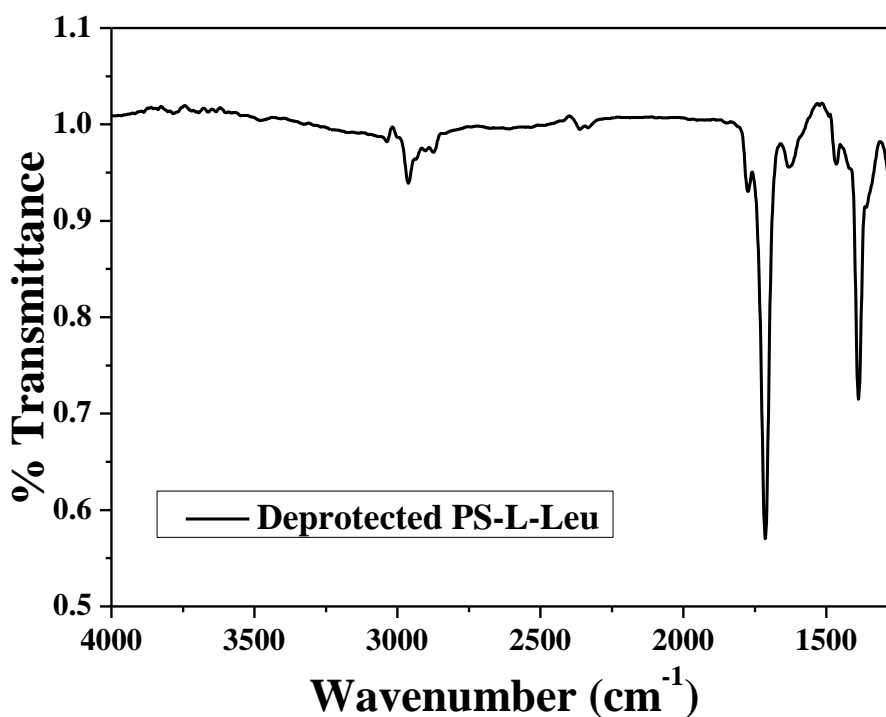
Figure 4.16 FT-IR spectrum of Deprotected PS-L-Leu

4.3 RESULT AND DISCUSSION

Scheme 4.1 outlines the overall synthetic scheme for synthesis of L-Leucine appended chiral PS. PS of pre-determined molecular weight was synthesized by RAFT polymerization (details given in synthesis and characterization section of experimental section). The proton NMR spectrum of PS indicated a number average molecular weight (*Mn*) of 20800 (Figure 4.2), which was in good agreement with the theoretical calculated molecular weight of 20500. The PS was subjected to post polymer modification following the Friedel Craft's

acylation with N-Phthaloyl-L-Leucine acid chloride to obtain chiral polystyrene (Protected PS-L-Leu). Further deprotection of N-Phthaloyl group was achieved by refluxing the protected amino acid containing PS in toluene with hydrazine hydrate to obtain the Deprotected PS-L-Leu. The detailed synthesis and characterization of small molecules (N-Phthaloyl-L-Leucine, N-Phthaloyl-L-Leucine acid chloride), post polymer modification, as well as the deprotection are given in the synthesis and characterization section of experimental section.
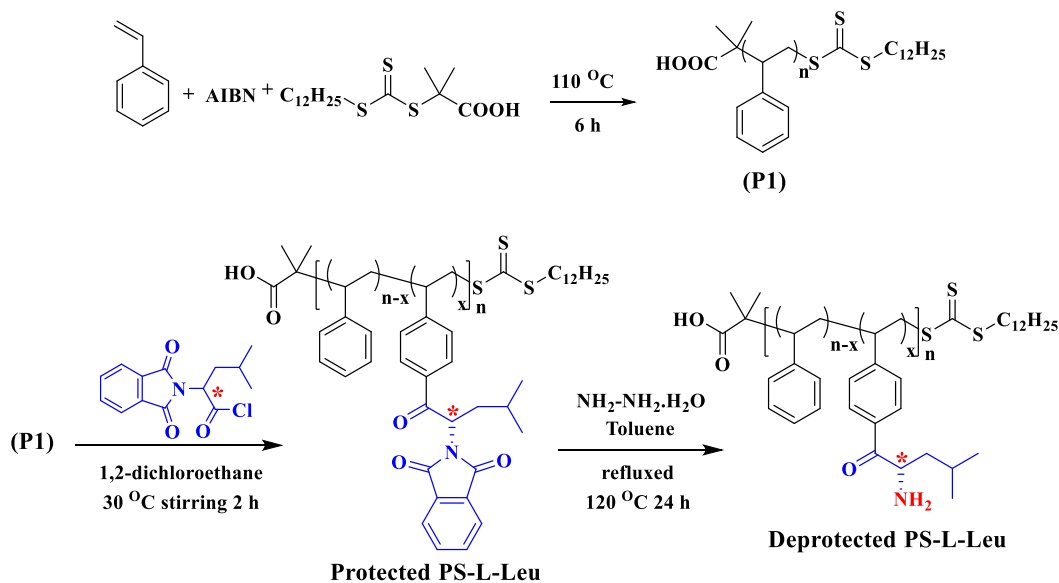
Scheme 4.1 Schematics for Synthesis of Polystyrene (P1), Protected PS-L-Leu and Deprotected PS-L-Leu

Figure 4.17 compares the expanded region in the labeled proton NMR spectra of the post polymer modified PS with pristine PS. PS (Figure 4.17a) shows two peaks in the aromatic region corresponding to the two types of aromatic protons (a and b) from the phenyl ring. The Protected PS-L-Leu (Figure 4.17b) exhibited two additional peaks, c (7.79 ppm), and d (5.74 ppm), corresponding to 4 aromatic protons of phthaloyl protection and 1 proton on chiral carbon, respectively. Figure 4.17 also compares the proton NMR spectra of the Deprotected PS-L-Leu (Figure 4.17c). The deprotection could be confirmed by the disappearance of the peaks corresponding to Phthaloyl protection i.e. peak labeled 'c' at 7.79 ppm. The peak labeled 'd' corresponding to the single proton on the chiral carbon was shifted downfield in the deprotected PS, which also confirmed complete deprotection. Quantitative estimations of the percentage modification of PS with L-Leucine was done by taking the ratio of integrations of peak 'b' from polystyrene and peak 'd' coming from the proton on the chiral carbon of deprotected polymer. The percent modification was found to be 34 %

for Deprotected PS-L-Leu. The ^{1}H NMR, ^{13}C NMR and FT-IR spectroscopic characterization details of the protected and deprotected PS samples are given in synthesis and characterization (Figure 4.2-4.16).
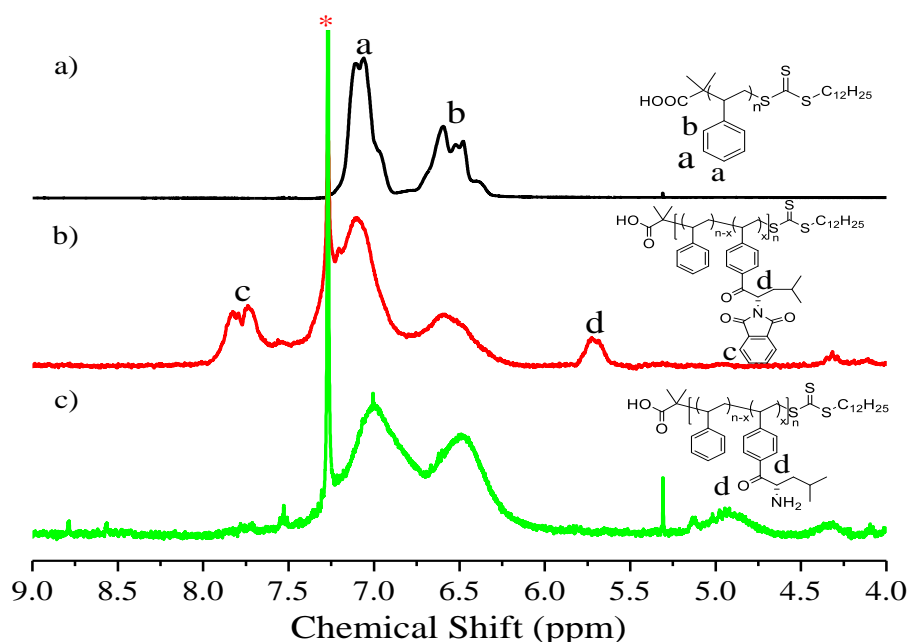
Figure 4.17 ^{1}H NMR spectra of a) polystyrene b) Protected PS-L-Leu and c) Deprotected PS-L-Leu. (CDCl$_3$)

FTIR spectra also provided clear evidence of post polymer modification with the appearance of peaks at 1709 and 1713 cm^{-1} corresponding to ketone carbonyl (C=O) for Protected PS-L-Leu and Deprotected PS-L-Leu polymers, respectively. Figure 4.18 compares the FTIR spectra (range 1800 to 1450) of the modified PS polymers (Protected PS-L-Leu and Deprotected PS-L-Leu) with that of the protected amino acids (N-Phthaloyl-L-Leu).

Figure 4.18 FT-IR spectra of polymers with protected amino acid

Compared to the pristine amino acid (protected), a shift is observed in the carbonyl stretching frequency in the modified polymers, which could be taken as additional evidence for the post polymer modification. The average molecular weights of 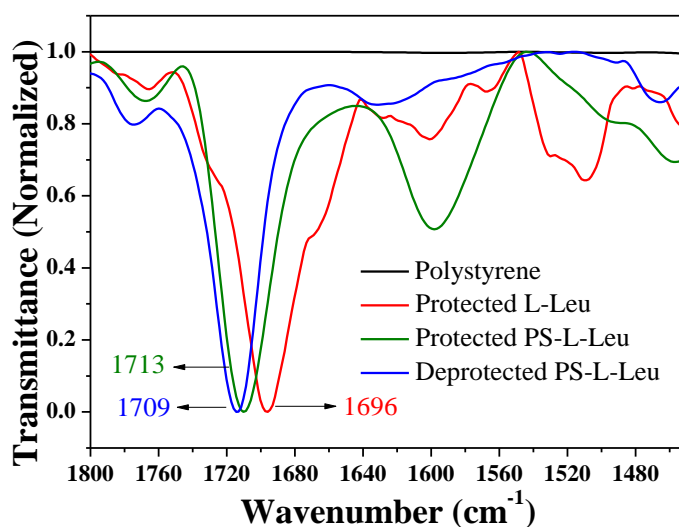the polymers were determined using gel permeation chromatography (GPC) in $CHCl_3$ (Figure 4.19). The number and weight average molecular weight (*Mn* and *Mw*) and molar mass distribution ($Đ_M$) of the polymers are given in Table 4.1. The post polymer modified PS samples exhibited reduced number average molecular weights compared to the pristine PS, which could be attributed to the different hydrodynamic volumes of the amino acid appended PS.
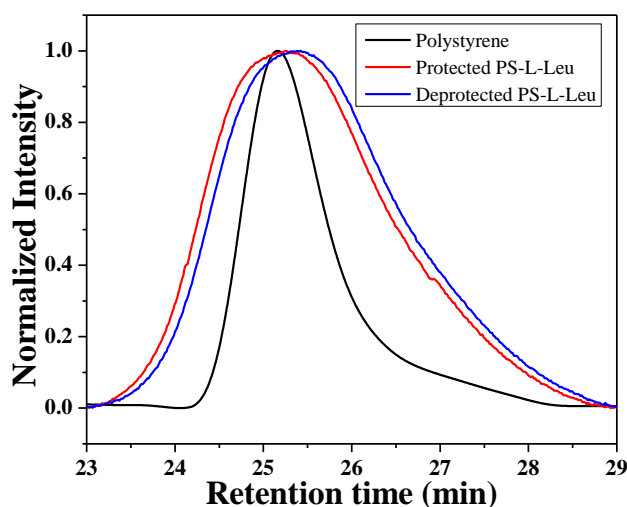
Figure 4.19 GPC chromatogram of polymers ($CHCl_3$)

Polymers	*Mn*	*Mw*	*Đ*$_M$	% Yield
Polystyrene	22800	30100	1.32	65
Protected PS-L-Leu	18500	32300	1.7	68
Deprotected PS-L-Leu	16700	29400	1.8	74

Table 4.1 Average molecular weights (*Mn* and *Mw*), polydispersity index ($Đ_M$) and % yield

The chirality of the amino acid appended PS was determined with the help of circular dichroism. Figure 4.20 compares the CD spectra for Protected PS-L-Leu and deprotected PS-L-Leu samples. The CD spectrum was also collected for pristine PS, which did not exhibit any peak as expected. The CD spectrum of Protected PS-L-Leu exhibited four peaks at 286, 307, 322, and 338 nm, while the CD spectrum of Deprotected PS-L-Leu showed peaks at 287, 300, 318, and 345 nm. From these CD spectra, it could be concluded that post polymer modification of polystyrene with protected L-amino acid induced chirality in the polymers.

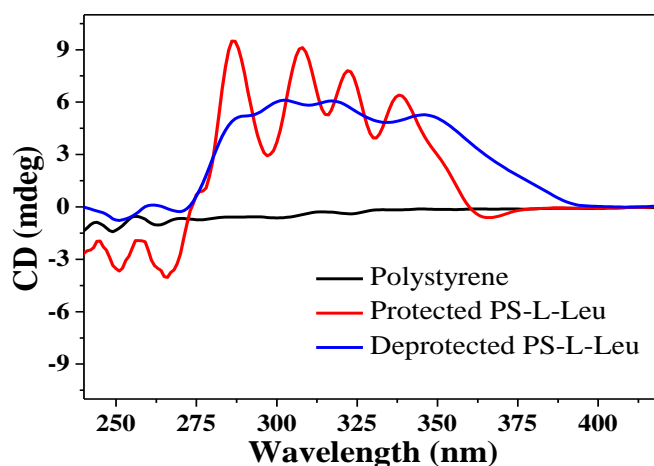**Figure 4.20** CD spectra of Protected PS-L-Leu and Deprotected PS-L-Leu plotted along with pristine polystyrene at a concentration of 0.1 mg/ml in THF.

4.3.1 Polymer Microspheres

Polymer microspheres were assembled using both protected as well as deprotected PS samples. A solution of the polymer in dichloromethane (DCM) was added to (deionized) DI water containing 4% tween 80 surfactant. The solution was homogenized, and the DCM was slowly evaporated off; the precipitated polymer microspheres was repeatedly washed with DI water and collected by centrifugation. The details of polymer microsphere preparation are given in the experimental section (methods A). The average sizes, polydispersity index (PDI), and zeta potential (ζ) of polymeric microsphere samples were determined using dynamic light scattering and zeta potential setup (the experimental section (methods B)). The average particle sizes of all microsphere samples were determined by plotting DLS histogram at 0.25 milli molar concentrations (Figure 4.21).
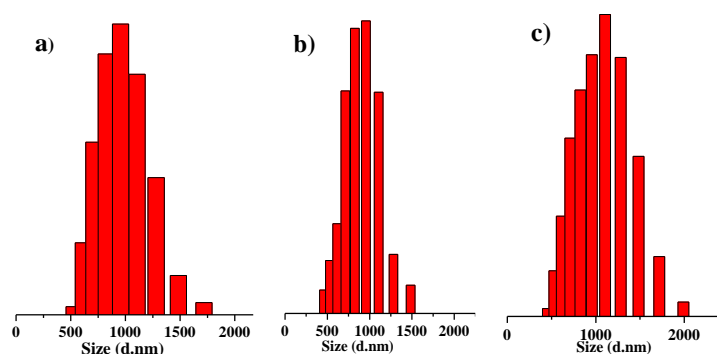

Figure 4.21 DLS histogram of a) polystyrene b) Protected PS-L-Leu C) Deprotected PS-L-Leu

Polymers	Z Average (um)[a]	PDI[a]	ζ-potential[b]	Particle diameter range (um)[c]
Polystyrene	1.38	0.814	-4.30	0.5-1.90
Protected PS-L-Leu	1.15	0.717	-15.94	0.67-1.90
Deprotected PS-L-Leu	1.04	0.636	-13.80	0.70-2.00

Values obtained from a= DLS data b = zeta potential setup c = FE-SEM micrographs.

Table 4.2 Sizes, PDI and zeta potential of polymeric microspheres samples

The average particles size for pristine polystyrene was found to be 1.38 µm. The average sizes of Protected PS-L-Leu was found to be 1.15 µm, and that for the corresponding deprotected microsphere samples was found to be 1.04 µm. The average sizes and PDI of all these polymers are tabulated in the supporting information table (Table 4.2).
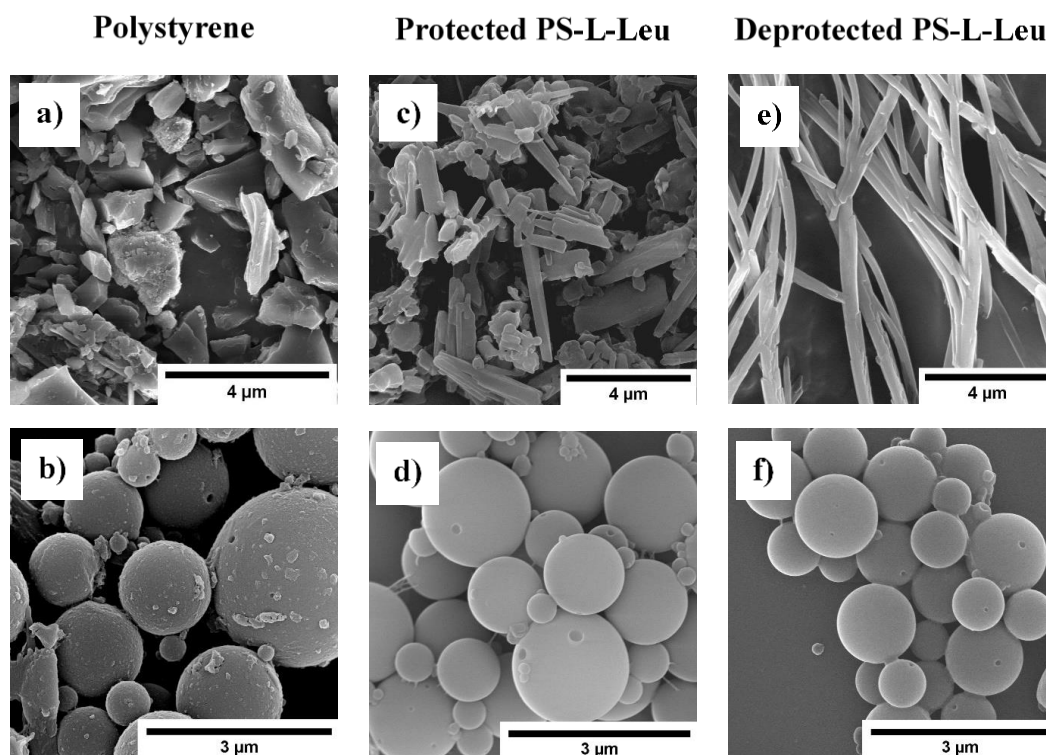
Figure 4.22 FE-SEM micrographs of a) pristine polystyrene (powder) b) pristine polystyrene (microspheres) c) Protected PS-L-Leu (powder) d) Protected PS-L-Leu (microspheres) e) Deprotected PS-L-Leu (fibers) f) Deprotected PS-L-Leu (microspheres).

The shape, size, and morphology of polymeric samples (powder and microspheres) were determined with the help of micrographs recorded on field emission scanning electron microscope (FE-SEM). Figure 4.22 compares the SEM micrographs of the pristine

polystyrene, Protected PS-L-Leu, and Deprotected PS-L-Leu polymer samples. Pristine polystyrene and Protected PS-L-Leu did not exhibit any specific morphology (Figure 4.22a and c), while the deprotected polymer exhibited fibrous morphology (Figure 4.22e). This change in morphology from irregular to fibrous nature upon deprotection could be understood by measuring water contact angle of all the polymers (figure 4.23 and methods C).

Figure 4.23 Water contact angles of a) Polystyrene b) Protected PS-L-Leu c) Deprotected PS-L-Leu

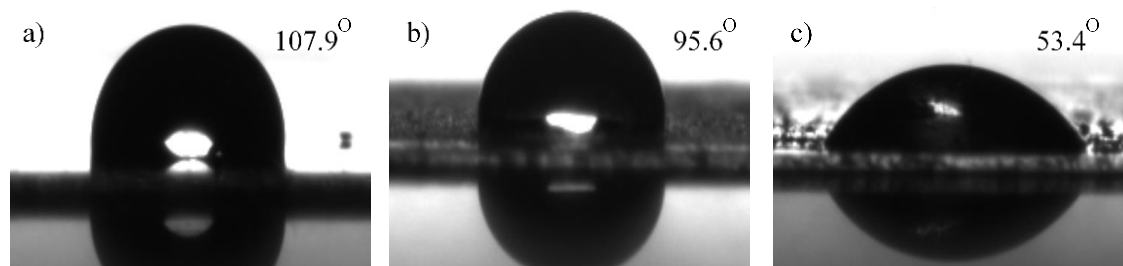The pristine PS and the protected amino acid appended PS had water contact angle > 95 ° (Figure 4.23a and b). After deprotection the contact angle reduced from 95.6 ° to 53.4 ° for deprotected PS-L-Leu (Figure 4.23c). This reduction in the water contact angle upon deprotection of the amino acid indicated enhancement in hydrophilicity.

The deprotected polymer could be anticipated to rearrange themselves so that the hydrophilic polar amine groups of the chiral amino acid are projected towards the hydrophilic environment, resulting in fibrous morphology. Figure 4.22 also compares the spherical morphology of the pristine PS and the protected and deprotected PS. The particle sizes of these polymeric spheres were computed using ImageJ freeware. The average particle size ranged from ~ 0.5-2 μm and were in reasonably good agreement with average sizes obtained from the DLS instrument.

4.3.2 Enantioselective Separation Experiments

Racemic mixtures of native amino acids like alanine, aspartic acid, glutamic acid, leucine, lysine, phenylalanine, serine, and valine were prepared by dissolving 10 mg of each D and L enantiomers in 10 ml of DI water. 5 mg of Protected PS-L-Leu powder was added to each vial and the racemic mixtures were stirred along with the polymer suspension on a magnetic stirrer for 24 hours at room temperature. After 24 h, the mixtures from the vials were filtered with the help of Whatman filter paper to remove the solid polymeric particles. The CD spectra of the filtrates were recorded for each sample. The experimental protocol is

shcematically presented in figure 4.24. It was observed that the filtrate of leucine and alanine exhibited CD signal for corresponding D-enantiomers when treated with Protected PS-L-Leu powder, while the filtrate of other amino acids did not exhibit any measurable signal. From this observation, it could be concluded that Protected PS-L-Leu powder exhibited enantioselective separation of leucine and alanine by selective adsorption of the L isomer from their racemic mixture leaving behind D-enantiomers in the filtrate.

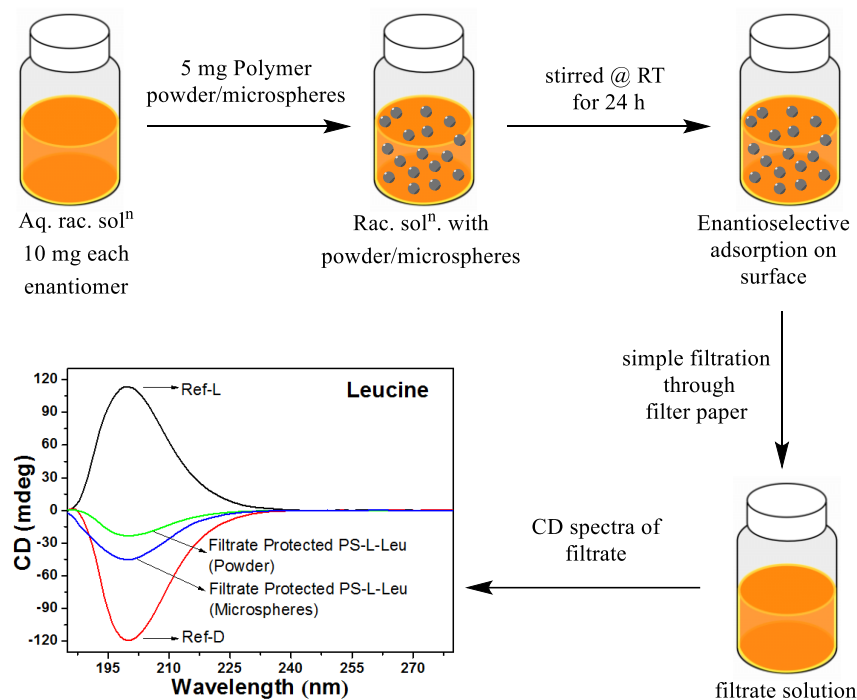**Figure 4.24** Schematic represenattion of enantioselective separation experiments with representative exampleof leucine separtion

The CD spectra of filtrate solutions were then plotted along with D and L enantiomers of corresponding amino acids (Figure 4.25).
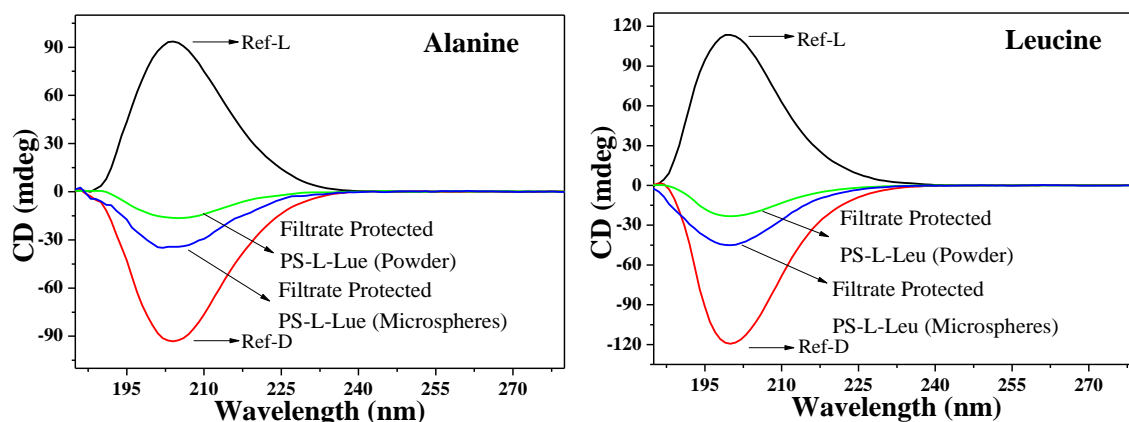

Figure 4.25 CD spectra representing the enantioselective separation of a) alanine b) leucine racemic mixtures by using Protected PS-L-Leu powder/microspheres

Figure 4.26 shows the FE-SEM micrographs of deprotected PS-L-Leu microsphere which was used for enantioselective separation followed by filtration showing adsorbed particles on the surface.
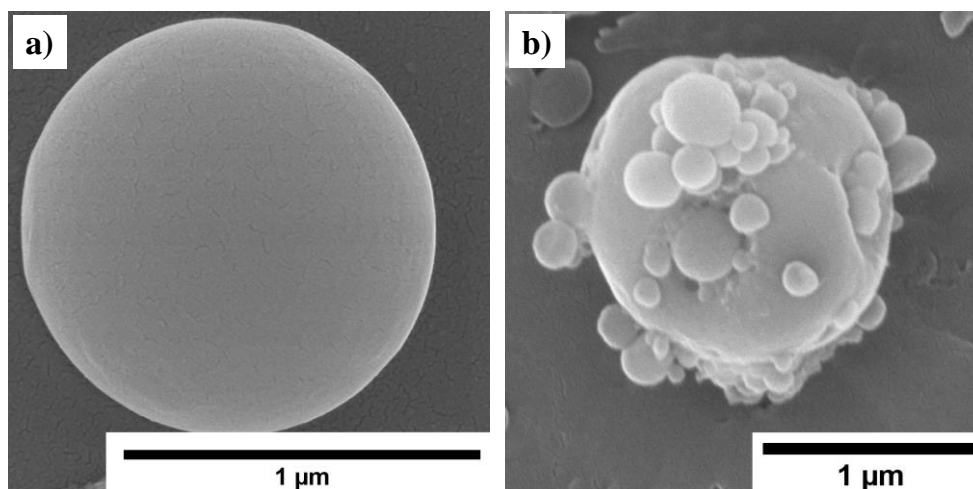
Figure 4.26 FE-SEM micrographs of chiral Deprotected PS-L-Leu microspheres a) before and b) after enantioselective separation with particles adsorbed on the surface.

The percentage enantiomeric excess (% ee) for separation was calculated by taking the ratio of area under the curve for the filtrate with that of the area under curve for the reference D enantiomer solution. The % ee values are given in Table 4.3. PS-L-Leu powder exhibited 19.45 % ee towards leucine. The ee % could be almost doubled by using the microspheres instead of the as-precipitated polymer powder. Thus, the ee % enhanced from 19.45 % to 42.06 % for the separation of leucine using protected PS-L-Leu.

Racemic mixture	% Enantiomeric excess values (% ee)	
	Protected L-Leu-PS Powder/ Microspheres	Deprotected L-Leu-PS Fibers/ Microspheres
Alanine	16.52/35.24	40.56/53.75
Leucine	19.45/42.06	49.51/58.15

Table 4.3 % enantiomeric excess (% ee) values calculated using CD data for the separation of racemic mixtures

Figure 4.25 compares the CD signal of the filtrate using the as-precipitated polymer powder as well as the assembled microspheres for the enantioselective separation. Similar enantioselective separation experiments were set up with 5 mg each of the deprotected polymer fibers as well as assembled microspheres and CD spectra of the filtrate was plotted against the reference enantiomers (Figure 4.27). Table 2 also provides the % ee for the separation of the racemic mixtures of leucine and alanine using deprotected PS-L-Leu.
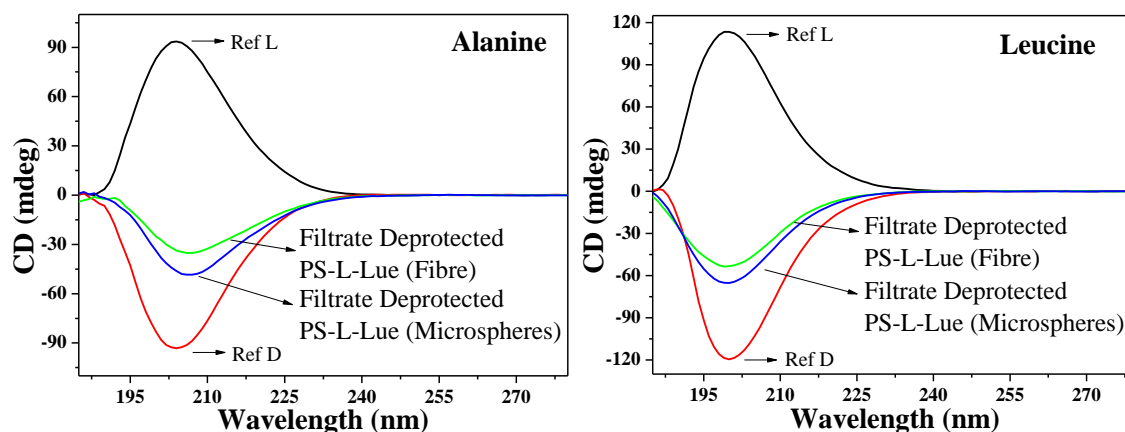
Figure 4.27 CD spectra representing enantioselective separation of a) alanine b) leucine racemic mixtures by using Deprotected PS-L-Leu fibers/microspheres

Significant improvement in % ee values was observed in case of deprotected polymer compared to the protected analogue (powder and microspheres) (Table 4.3 and Figure 4.27). Upon deprotection, the fibrous polymer sample exhibited ee % of 40.56 and 49.51 % respectively for the separation of Alanine and Leucine using PS-L-Leu compared to only 16.52 % and 19.45 % using the protected polymer powder. Upon assembling into microspheres, further enhancement in ee % was observed with a maximum separation efficiency of 53.75 % for alanine and 58.15 % for leucine using deprotected PS-L-Leu. Figure 4.28 shows representative example for enhancement in the enantioselective separation of racemic mixture of native leucine from 19.45-58.15 % ee by using 5 mg of polymer in different forms.
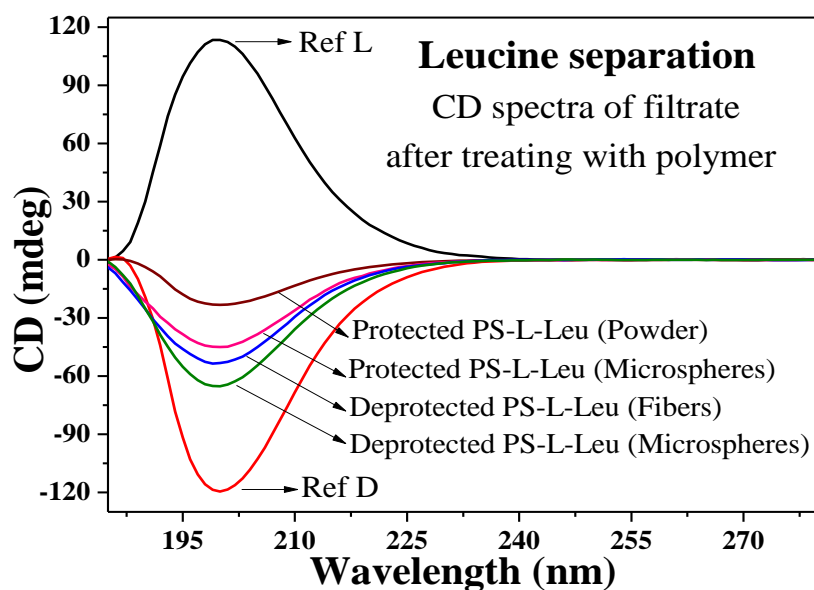
Figure 4.28 Representative example showing enhancement in enantioselective separation of racemic mixture of native leucine using Deprotected PS-L-Leu (fibers and microspheres) compared to Protected PS-L-Leu (powder and microspheres).

Increasing the amount of polymer microspheres used for the separation resulted in increased ee %. For instance, increasing the amount of deprotected PS-L-Leu microspheres from 5 mg to 9 mg for the enantioselective separation of a racemic mixture of leucine, resulted in enhancement of ee % from 58.15 to 72.84, which was further increased to 81.57 % upon using 12 mg of polymer microspheres (Figure 4.29).
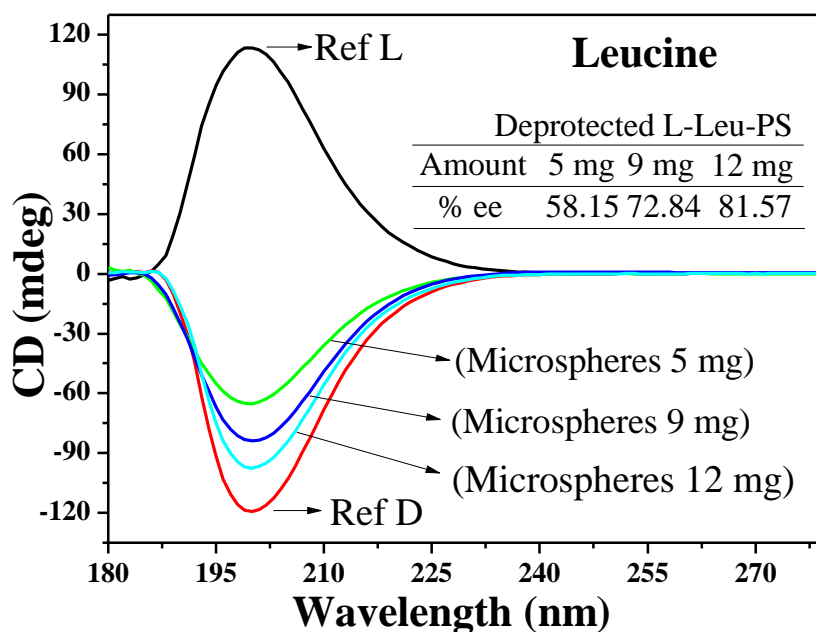
Figure 4.29 CD spectra for the separation of leucine racemic mixture using 5, 9 and 12 mg of Deprotected PS-L-Leu microspheres.

An approximate amount of 0.76 mg of L-Leucine per mg of chiral deprotected PS microspheres was estimated to be adsorbed on the surface using calculations based on the area under the CD curve. This is a reasonably good achievement given the fact that separation could be achieved using commodity polymer without any necessity for its application on any template or membrane like AAO membranes making the process commercially viable. The % ee value is anticipated to be further improved by achieving higher % chiral modification of PS or by polymerizing chiral styrene monomers.

The enhanced performance of the deprotected polymer could be attributed to the increased hydrophilicity of the polymers due to free amine groups, which significantly improved the surface wettability. Additionally, it is anticipated that the hydrophilic amine groups improved the enantioselective separation ability by self-assembling with the chiral amino acids exposed to the polymer surface. Chiral groups on the microspheres can form secondary transition state complexes of different energy with enantiomers by a "three-point interaction model.[41] Due to the difference in the stability of transition state complexes, separation is achieved. By assembling into microspheres, the overall surface area is enhanced compared to the fibrous morphology. The improvement in the surface chirality reduces the non-enantioselective adsorptions on the surface, resulting in % ee improvement.

4.4 CONCLUSIONS

In summary, chiral polystyrene was designed and synthesized by a post polymer modification approach. The modification of polystyrene with protected L-Leucine induced chirality to PS. The protected and deprotected chiral polystyrenes in the powder form as well as assembled into microspheres were used to carry out enantioselective separation of the native amino acid racemic mixture by a simple filtration-based enantioselective separation method. Protected and deprotected PS-L-Leu exhibited enantioselective separation efficiency for leucine and alanine from their racemic mixture. Better separation efficiency was achieved with microspheres compared to as-precipitated polymers in both protected and deprotected polystyrene. Among the tested amino acids, the highest separation was achieved using microspheres of deprotected polymers. The highest % ee of 81.57 was achieved for separation of leucine racemic mixture using 12 mg of deprotected PS-L-Leu microspheres. The enhanced % ee value in the deprotected polymer microsphere is attributed to rearrangement of polymer structure, improved hydrophilicity and increased surface area.

4.5 REFERENCES

(1) Calcaterra, A.; D'Acquarica, I. The Market of Chiral Drugs: Chiral Switches versus de Novo Enantiomerically Pure Compounds. *Journal of Pharmaceutical and Biomedical Analysis*. Elsevier B.V. January 5, 2018, pp 323–340.

(2) Jeschke, P. Current Status of Chirality in Agrochemicals. *Pest Management Science*. John Wiley and Sons Ltd November 1, 2018, pp 2389–2404.

(3) Sekhon, B. S. Chiral Pesticides. *Journal of Pesticide Science*. 2009, pp 1–12.

(4) Mannschreck, A.; Kiesswetter, R.; von Angerer, E. Unequal Activities of Enantiomers via Biological Receptors: Examples of Chiral Drug, Pesticide, and Fragrance Molecules. *J. Chem. Educ.* **2007**, *84* (12), 2012–2017.

(5) Engel, K. H. Chirality: An Important Phenomenon Regarding Biosynthesis, Perception, and Authenticity of Flavor Compounds. *Journal of Agricultural and Food Chemistry*. American Chemical Society September 23, 2020, pp 10265–10274.

(6) Schäfer, U.; Kiefl, J.; Zhu, W.; Kempf, M.; Eggers, M.; Backes, M.; Geissler, T.; Wittlake, R.; Reichelt, K. V.; Ley, J. P.; Krammer, G. Authenticity Control of Food Flavorings - Merits and Limitations of Chiral Analysis. *ACS Symp. Ser.* **2015**, *1212*, 3–12.

(7) Zawirska-wojtasiak, R. Chirality And The Nature Of Food Authenticity Of Aroma. *Acta Sci. Pol. Technol. Aliment.* **2006**, *5* (1), 21–36.

(8) Schmid, T.; Daiss, J. O.; Ilg, R.; Surburg, H.; Tacke, R. Enantiopure Chiral Derivatives of the Fragrance Materials Majantol and Sila-Majantol: A Bioisosteric Carbon/silicon Switch with Drastic Effects on the Sensory Characteristics. *Organometallics* **2003**, *22* (21), 4343–4346.

(9) Abate, A.; Brenna, E.; Fuganti, C.; Gatti, F. G.; Giovenzana, T.; Malpezzi, L.; Serra, S. Chirality and Fragrance Chemistry: Stereoisomers of the Commercial Chiral Odorants Muguesia and Pamplefleur. *J. Org. Chem.* **2005**, *70* (4), 1281–1290.

(10) Zhou, Y.; Wu, S.; Zhou, H.; Huang, H.; Zhao, J.; Deng, Y.; Wang, H.; Yang, Y.; Yang, J.; Luo, L. Chiral Pharmaceuticals: Environment Sources, Potential Human Health Impacts, Remediation Technologies and Future Perspective. *Environment International*. Elsevier Ltd December 1, 2018, pp 523–537.

(11) O'Brien, P. Sharpless Asymmetric Aminohydroxylation: Scope, Limitations, and Use in Synthesis. *Angew. Chemie - Int. Ed.* **1999**, *38* (3), 326–329.

(12) Verendel, J. J.; Pàmies, O.; Diéguez, M.; Andersson, P. G. Asymmetric

Hydrogenation of Olefins Using Chiral Crabtree-Type Catalysts: Scope and Limitations. *Chem. Rev.* **2014**, *114* (4), 2130–2169.

(13) Ward, T. J.; Ward, K. D. Chiral Separations: Fundamental Review 2010. *Anal. Chem.* **2010**, *82* (12), 4712–4722.

(14) McDonald, M. A.; Salami, H.; Harris, P. R.; Lagerman, C. E.; Yang, X.; Bommarius, A. S.; Grover, M. A.; Rousseau, R. W. Reactive Crystallization: A Review. *Reaction Chemistry and Engineering*. Royal Society of Chemistry March 1, 2021, pp 364–400.

(15) Yao, Q.; Xie, J. Pasteur-like Separation of Silver Nanocluster Racemates by Conglomerate Crystallization. *ACS Cent. Sci.* **2020**, *6* (11), 1862–1865.

(16) Qiu, J.; Stevens, J. M. High-Throughput Classical Chiral Resolution Screening of Synthetic Intermediates: Effects of Resolving Agents, Crystallization Solvents, and Other Factors. *Org. Process Res. Dev.* **2020**, *24* (9), 1725–1734.

(17) Ward, T. J.; Ward, K. D. Chiral Separations: A Review of Current Topics and Trends. *Anal. Chem.* **2012**, *84* (2), 626–635.

(18) Tarafder, A.; Miller, L. Chiral Chromatography Method Screening Strategies: Past, Present and Future. *J. Chromatogr. A* **2021**, *1638*.

(19) Yu, R. B.; Quirino, J. P. Chiral Selectors in Capillary Electrophoresis: Trends During 2017–2018. *Molecules* **2019**, *24* (6), 1135.

(20) Berkecz, R.; Németi, G.; Péter, A.; Ilisz, I. Liquid Chromatographic Enantioseparations Utilizing Chiral Stationary Phases Based on Crown Ethers and Cyclofructans. *Molecules* **2021**, *26* (15).

(21) Adhikari, S.; Lee, W. Chiral Separation Using Chiral Crown Ethers as Chiral Selectors in Chirotechnology. *Journal of Pharmaceutical Investigation*. Springer Netherlands May 1, 2018, pp 225–231.

(22) Suraj Koorpet, R.; Akshay, N.; Nishanth, G.; Chandan, R. S.; Tengli, A. K. A Review on Chiral Columns/stationary Phases for HPLC. *International Journal of Research in Pharmaceutical Sciences*. J. K. Welfare and Pharmascope Foundation April 11, 2020, pp 2466–2480.

(23) Zhang, Q.; Xue, S.; Li, A.; Ren, S. Functional Materials in Chiral Capillary Electrophoresis. *Coordination Chemistry Reviews*. Elsevier B.V. October 15, 2021.

(24) Shen, J.; Okamoto, Y. Efficient Separation of Enantiomers Using Stereoregular Chiral Polymers. *Chemical Reviews*. American Chemical Society February 10, 2016, pp 1094–1138.

(25) Zhou, C.; Ren, Y.; Han, J.; Xu, Q.; Guo, R. Chiral Polyaniline Hollow Nanotwists

toward Efficient Enantioselective Separation of Amino Acids. *ACS Nano* **2019**, *13* (3), 3534–3544.

(26) Senthilkumar, T.; Asha, S. K. An Easy "Filter-and-Separate" Method for Enantioselective Separation and Chiral Sensing of Substrates Using a Biomimetic Homochiral Polymer. *Chem. Commun.* **2015**, *51* (43), 8931–8934.

(27) Nikam, S. B.; Sk, A. Enantioselective Separation Using Chiral Amino Acid Functionalized Polyfluorene Coated on Mesoporous Anodic Aluminum Oxide Membranes. *Anal. Chem.* **2020**, *92* (10), 6850–6857.

(28) Abuaf, M.; Mastai, Y. Synthesis of Multi Amino Acid Chiral Polymeric Microparticles for Enantioselective Chemistry. *Macromol. Chem. Phys.* **2020**, *221* (24).

(29) Yu, Y.; Xu, N.; Zhang, J.; Wang, B.; Xie, S.; Yuan, L. Chiral Metal-Organic Framework D -His-ZIF-8@SiO2 Core-Shell Microspheres Used for HPLC Enantioseparations. *ACS Appl. Mater. Interfaces* **2020**, *12* (14), 16903–16911.

(30) Prosuntsova, D. S.; Plodukhin, A. Y.; Ananieva, I. A.; Beloglazkina, E. K.; Nesterenko, P. N. New Composite Stationary Phase for Chiral High-Performance Liquid Chromatography. *J. Porous Mater.* **2021**, *28* (2), 407–414.

(31) Mutalikdesai, A.; Pagidi, S.; Hassner, A.; Gedanken, A. Microspheres of Biomolecules/macromolecules for Enantioseparation Applications. *European Polymer Journal*. Elsevier Ltd January 5, 2021.

(32) Wang, P. X.; Hamad, W. Y.; MacLachlan, M. J. Polymer and Mesoporous Silica Microspheres with Chiral Nematic Order from Cellulose Nanocrystals. *Angew. Chemie - Int. Ed.* **2016**, *55* (40), 12460–12464.

(33) Paik, P.; Gedanken, A.; Mastai, Y. Enantioselective Separation Using Chiral Mesoporous Spherical Silica Prepared by Templating of Chiral Block Copolymers. *ACS Appl. Mater. Interfaces* **2009**, *1* (8), 1834–1842.

(34) Medina, D. D.; Goldshtein, J.; Margel, S.; Mastai, Y. Enantioselective Crystallization on Chiral Polymeric Microspheres. *Adv. Funct. Mater.* **2007**, *17* (6), 944–950.

(35) Zhang, Z.; Zhang, M.; Liu, Y.; Yang, X.; Luo, L.; Yao, S. Preparation of L-Phenylalanine Imprinted Polymer Based on Monodisperse Hybrid Silica Microsphere and Its Application on Chiral Separation of Phenylalanine Racemates as HPLC Stationary Phase. *Sep. Purif. Technol.* **2012**, *87*, 142–148.

(36) Chen, B.; Song, C.; Luo, X.; Deng, J.; Yang, W. Microspheres Consisting of Optically Active Helical Substituted Polyacetylenes: Preparation via Suspension

Polymerization and Their Chiral Recognition/release Properties. *Macromol. Rapid Commun.* **2011**, *32* (24), 1986–1992.

(37) Wu, J.; Su, P.; Guo, D.; Huang, J.; Yang, Y. Cationic β-Cyclodextrin-Modified Hybrid Magnetic Microspheres as Chiral Selectors for Selective Chiral Absorption of Dansyl Amino Acids. *New J. Chem.* **2014**, *38* (8), 3630–3636.

(38) Yang, Y.; Wu, J.; Su, P.; Yang, Y.; Huang, J.; Wang, Y. Immobilization of HSA on Polyamidoamine-Dendronized Magnetic Microspheres for Application in Direct Chiral Separation of Racemates. *J. Mater. Chem. B* **2014**, *2* (7), 775–782.

(39) Cong, H.; Xing, J.; Ding, X.; Zhang, S.; Shen, Y.; Yu, B. Preparation of Porous Sulfonated Poly(styrene-Divinylbenzene) Microspheres and Its Application in Hydrophilic and Chiral Separation. *Talanta* **2020**, *210*.

(40) Roy, M.; Rajamohanan, P. R.; Ravindranathan, S.; Asha, S. K. Self-Assembly of Bispentadecylphenol Substituted Perylenediimide with PS- B-P4VP for Structure-Property Insight into the Core of Core-Shell Micelles. *ACS Appl. Polym. Mater.* **2020**, *2* (2), 805–816.

(41) Gogoi, A.; Mazumder, N.; Konwer, S.; Ranawat, H.; Chen, N. T.; Zhuo, G. Y. Enantiomeric Recognition and Separation by Chiral Nanoparticles. *Molecules* **2019**, *24* (6), 1–31.

CHAPTER 5

Synthesis of Chiral ∏-Conjugated Polymers by DHAP Route

5.1 INTRODUCTION

The π-conjugated polymers attracted much attention from academia and industries after the discovery of highly conductive polyacetylene by Hideki Shirakawa, Alan G. MacDiarmid, and Alan J. Heeger in 1977.[1] This discovery changed the perspective about the polymers as the perfect example of insulators. ∏-conjugated polymers possesses mixed properties of metal and inorganic semiconductors (electrical conductivity and optical properties) and synthetic polymers (flexibility, lightweight, easy solution processability, and low production cost), which increases their demand and makes them the material of choice for modern-day technology.[2–6] The tailor-made conjugated polymers are designed to perform desired functions by functionalizing aromatic backbone with electron-donating or withdrawing moieties containing various heteroatoms, which helps fine-tune the optical and physical properties.[7–10] The solvent processability and the additional properties like water solubility, selectivity and sensitivity can be improved by modifying the non-conjugated side chains.[11–16] Today π-conjugated polymers are used as a semiconductor for the fabrication of thin, flexible and lightweight and wearable devices like organic field-effect transistors (OFET),[17–21] organic solar cells,[22] organic photovoltaics (OPV),[23,24] organic light-emitting diodes (OLED),[25,26] flexible and curved displays.[27] The ∏-conjugated polymers even find their wide applications in medicine bio-imaging,[28] targeted drug delivery,[29,30] gene delivery,[31] photoacoustic imaging,[32] chemical and biological sensing, as they have intrinsic fluorescence properties with high or moderately high quantum yields.[33,34] The growing demands of these conjugated homo and copolymers is fulfilled by synthesizing these polymers by conventional, reliable and robust C-C bond-forming cross-coupling reactions like Suzuki, Stille, Sonogarshira, Kumada, Negishi polymerizations.[35–37] These conventional cross-couplings are palladium or nickel catalyzed reactions between aryl halides (-Cl, -Br, and -I) and aromatic organometallic compounds (mainly organoboron, organotin, and organozinc). Though these conventional polymerization methods are highly used in academia and commercial productions of conjugated polymers, they are associated with some drawbacks like the pre-functionalization of monomers to get active aromatic organometallic monomers. This additional step subsequently increases final product cost. These coupling reactions generate a stoichiometric amount of environmentally hazardous organometallic by products.[38] Removal of these stoichiometric amount of hazardous organometallic by-products is a tedious and time-consuming process that requires multiple washings with different solvents. The presence of these organometallic compounds, even in

trace amount, hamper the desired performance of the polymers.[38,39] In biological applications, polymers without hazardous metallic impurities are highly recommended to improve their biocompatibility.

Toshio Itahara *et al.* developed a synthetic method for C-C bond forming reactions using sp^2 hybridized C-H bond with an aryl halide.[40,41] This method is further used for the synthesis of π-conjugated polymers and is called direct heteroarylation polymerization (DHAP).[42–44] DHAP method provide a promising strategy for the synthesis of π-conjugated polymers, where no pre-functionalization of monomer is needed. Thus, it requires fewer synthetic steps.[45–47] The by-products generated in DHAP are like HCl, HBr, and HI, compared to organotin, organoboron or organozinc in conventional methods that improve the atom economy of reactions.

Additionally, these generated by-products are benign which do not have an environmental impact.[48–50] Removal of by-products is easy compared to conventional methods as it does not require multiple washings. These advantages of DHAP makes it a cost-effective, greener, sustainable and attractive process with minimum environmental impact.[51]

Chapters 2 and 3 of this thesis described the synthesis of π-conjugated polyfluorenes having different chiral pendants by conventional Suzuki polymerization method, which were used for enantioselective separation of amino acid racemic mixtures. Suzuki polymerization needs per-functionalization of monomers with organoboron. This additional step adds to the final product cost. Additionally, the atom economy of reaction is low as it generates a stoichiometric amount of organoboron compounds as by-products. The current chapter focuses on synthesizing chiral π-conjugated polymers like regioregular polythiophene and fluorene-thiophene copolymers by the DHAP route. The structure-property relationships of synthesized polymers were studied using ^{1}H NMR spectroscopy and photophysical characterizations. According to our knowledge, this is the first report where amino acid appended chiral fluorene-thiophene copolymers were synthesized using the DHAP route. The effect of steric hindrance, pendant length, and time of polymerization on molecular weights of synthesized polymers was studied. This chapter is an approach toward synthesizing chiral π-conjugated polymers by cost-effective and atom economic synthetic route like the DHAP, which can be used for different applications like enantioselective sensing and separation.

5.2 EXPERIMENTAL SECTION

5.2.1 Materials

3-Thiophenemethanol, 2,7-dibromofluorene and 1-bromooctane, were purchased from TCI Chemicals India. Tetrahydrofuran (THF), toluene, dichloromethane (DCM), and methanol were purchased from Merck Chemicals. HPLC grade THF, chloroform (CHCl$_3$), and toluene were purchased from Merck Chemicals. Sodium hydroxide (NaOH), tetrabutylammonium bromide (TBAB), Dicyclohexylcarbodiimide (DCC), 4-(Dimethylamino)pyridine (DMAP), and *N*-Bromosuccinimide (NBS), were purchased from Spectrochem Pvt. Ltd India. Deuterated chloroform (CDCl$_3$), palladium acetate Pd(OAc)$_2$, caesium carbonate (Cs$_2$CO$_3$) and pivalic acid were purchased from Sigma-Aldrich. N-Boc-L-glutamic acid-1-tert-butyl ester was purchased from Alfa Aesar Chemical Ltd. 3-bromopropan-1-ol, and 6-bromohexan-1-ol were purchased from TCI Chemicals India. Petroleum ether and ethyl acetate were purchased locally and used after standard purification methods.

5.2.2 Measurements

Structural characterization of small molecules, monomers and polymers were done by recording their ^{1}H and ^{13}C NMR spectra at 25 °C temperature on Bruker-AVENS 200, 400 or 500 MHz NMR instruments. Deuterated chloroform (CDCl$_3$) was used as a solvent with a trace amount of TMS as an internal reference. Chemical shifts of the NMR peaks were reported in ppm at 25 °C. The number average (*Mn*) and weight average (*Mw*) molecular weights of the polymer were determined at 25 °C temperature with the help of size exclusion chromatography (SEC) equipped with a ViscotekVE 1122 solvent delivery system, a column packed with crosslinked polystyrene beads and ViscotekVE 3580 RI detector. HPLC grade tetrahydrofuran (THF) was used as an eluant at a constant 1ml/min flow rate. The column was calibrated with narrow polydispersity polystyrene standards from Easi-Vials PS-M from Varian Polymer Laboratories at 1ml/min flow rate, and the same flow rate was maintained during polymeric sample analysis. Solution state UV-Visible absorbance spectra of polymeric samples were recorded using double beam Perkin Elmer lambda-35 UV/Vis spectrometer with deuterium and tungsten lamps the source by dissolving in HPCL grade THF solvent (2×10^{-4} molar concentration). The Steady-state fluorescence of polymeric samples solutions with the same concentration (2×10^{-4} molar concentration) was recoded using Horiba Jobin Yvon Fluorolog 3 spectrophotometer with a 450 W xenon lamp. The

emission and excitation slit width was maintained at 1 nm throughout the experiments, and the data were obtained in S1 mode.

5.2.3 Synthesis and characterizations

1) Synthesis of thiophene monomers
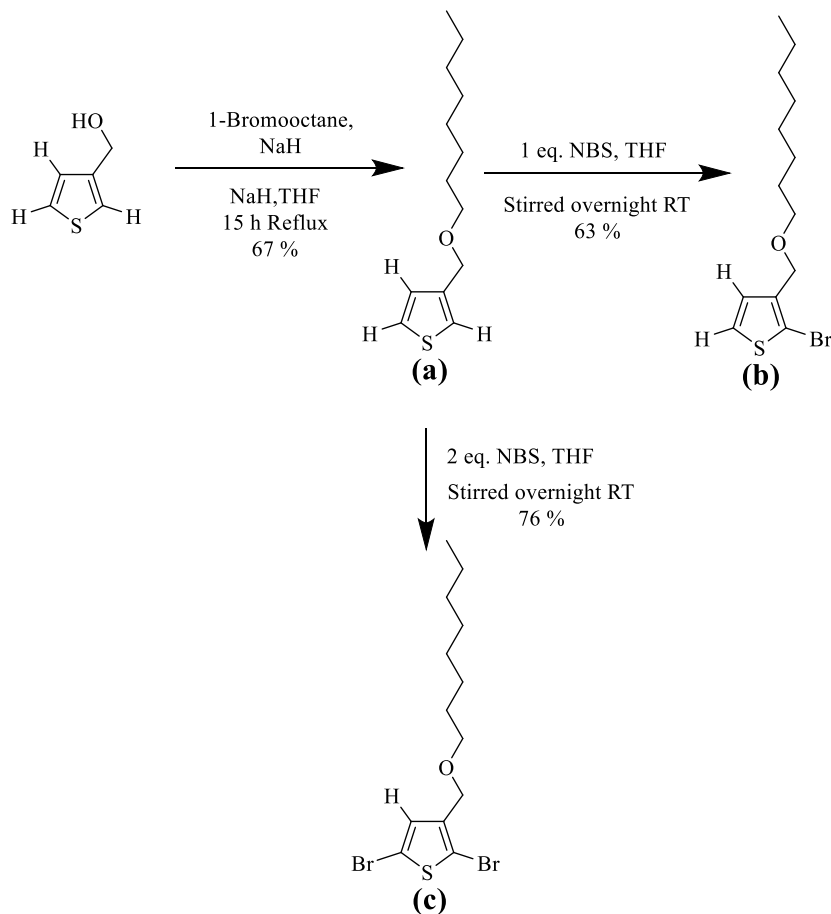
Scheme 5.1 Schematic representation of synthesis of thiophene monomers

1.a) Synthesis of 3-((octyloxy)methyl)thiophene (a)

In a 250 ml two necked round bottom flask fitted with a reflux condenser, a solution of sodium hydride (3.2 gm, 131.38 mmols) in dry THF (50 ml) was prepared and allowed to stir for 5 min in an inert atmosphere. The other neck of the flask was sealed with the help of a rubber septum. An inert atmosphere was maintained in the RB with the help of a nitrogen balloon. 3-thiophenemethanol (2.5 ml, 26.276 mmols) was added slowly to the reaction mixture using a syringe with continuous stirring. The content of the reaction mixture was allowed to reflux for 15 h. The reaction mixture was allowed to cool down slowly to room temperature. 50 ml of methanol was added to the reaction mixture to quench the sodium

hydride. The solvent was evaporated in reduced pressure on a rotary evaporator. The crude product was extracted with the DCM by solvent extraction with water and brine. The obtained product was purified using a 10 % Pet ether, ethyl acetate mixture by column chromatography. Yield 67%. ^{1}H NMR spectrum (400 MH$_Z$, CDCl$_3$) δ 7.31-7.28, (m 1H), δ 7.20, (m 1H) δ 7.20, (dd 1H), δ 4.50 (s 2H), 3.48- 3.42 (t 2H), δ 1.62-1.57 (m 2H) δ 1.27 (m 12H) δ 0.91-0.85 (t 3H) ^{13}C NMR spectrum (100 MH$_Z$, CDCl$_3$) δ 139.83, δ 127.25, δ 125.76, δ 122.41, δ 70.41, δ 68.06, δ 31.79, δ 29.71, δ 29.23, δ 26.16, δ 22.62, and δ 14.05.
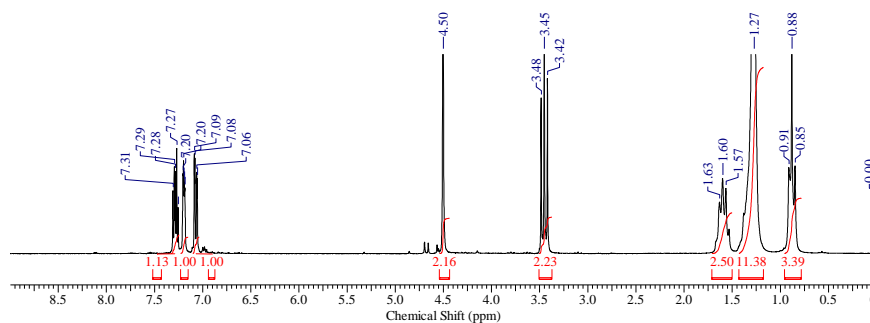

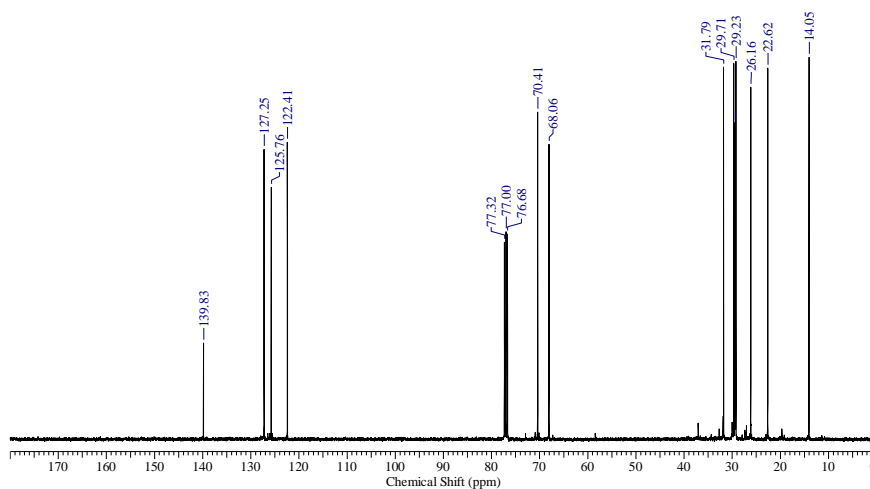**Figure 5.1:** ^{1}H NMR spectrum of 3-((octyloxy)methyl)thiophene (CDCl$_3$)

Figure 5.2 ^{13}C NMR spectrum of 3-((octyloxy)methyl)thiophene (CDCl$_3$)

1.b) Synthesis of 2-bromo-3-((octyloxy)methyl)thiophene (b)

3-((octyloxy)methyl)thiophene (1 gm, 4.417 mmols) was taken in a round bottom flask and dissolved in 30 ml of dry THF. The solution was purged with nitrogen gas. Recrystallized N-Bromosuccinimide (786 mg, 4.417 mmols) was added to the solution. The reaction mixture was allowed to stir for 12 h at room temperature in an inert atmosphere. The crude product was filtered, and the solvent was evaporated in the reduced pressure on a rotary evaporator. The crude product was purified using a 10 % pet ether, ethyl acetate mixture by

column chromatography. Yield 63 % ¹H NMR spectrum (400 MH$_Z$, CDCl$_3$) δ 7.26, 7.23 (d 1H), δ 7.01, 6.98 (d 1H), δ 4.45 (s 2H), δ 3.49-3.42 (t 2H), δ 1.60-1.57 (m 2H) δ 1.28 (s 12H) δ 0.92-0.85 (m 3H) ¹³C NMR spectrum (100 MH$_Z$, CDCl$_3$) δ 138.51, δ 128.12, δ 125.27, δ 110.77, δ 70.46, δ 66.68, δ 31.78, δ 29.21, δ 26.10, δ 22.61, δ 14.06,
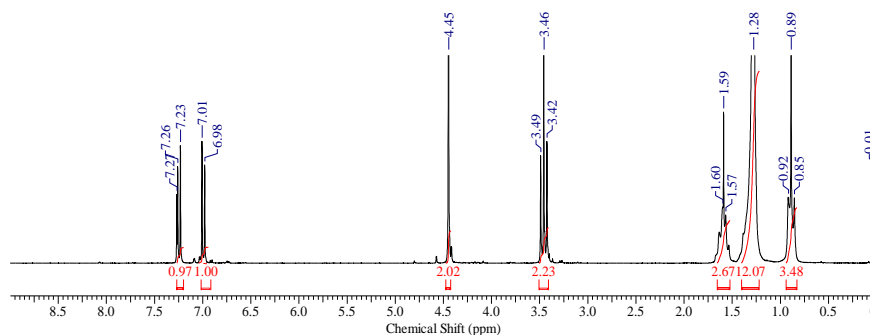

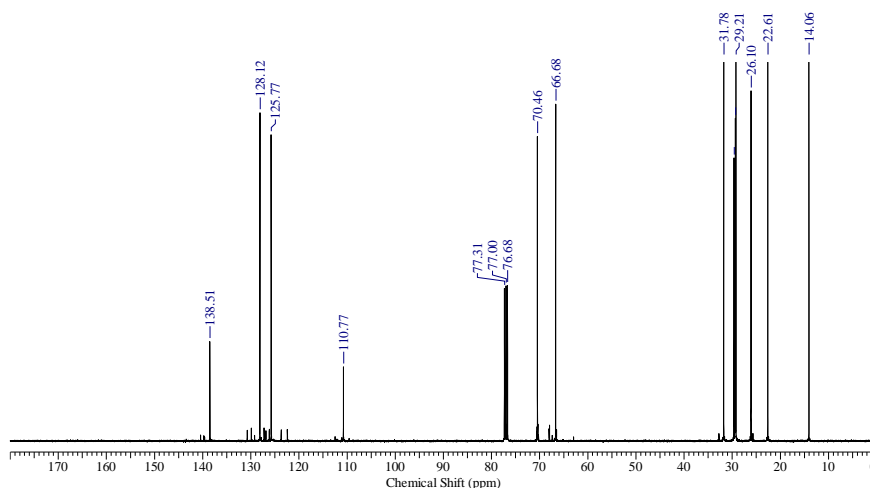**Figure 5.3** ¹H NMR spectrum of 2-bromo-3-((octyloxy)methyl)thiophene (CDCl$_3$)

Figure 5.4 ¹³C NMR spectrum of 2-bromo-3-((octyloxy)methyl)thiophene (CDCl$_3$)

1.c) Synthesis of 2, 5-dibromo-3-((octyloxy)methyl)thiophene (c)

3-((octyloxy)methyl)thiophene (1.5 gm, 6.626 mmols) was taken in a round bottom flask and dissolved in 50 ml of dry THF. The solution was purged with nitrogen gas. Recrystallized N-Bromosuccinimide (2.4 gm, 13.252 mmols) was added to the solution. The reaction mixture was allowed to stir for 12 h at room temperature in an inert atmosphere. The crude product was filtered, and the solvent was evaporated in the reduced pressure on a rotary evaporator. The crude product was purified using a 5 % pet ether, ethyl acetate mixture by column chromatography. Yield 76 %   ¹H NMR spectrum (400 MH$_Z$, CDCl$_3$) δ 6.98 (s 1H), δ 4.37 (s 2H), δ 3.48-3.41 (t 2H), δ 1.63-1.57 (m 2H) δ 1.28, 1.27 (m 12H) δ

0.92-0.83 (m 3H) ^{13}C NMR spectrum (100 MHz, CDCl$_3$) δ 139.57, δ 130.76, δ 111.14, δ 109.64, δ 70.64, δ 66.51, δ 31.79, δ 29.36, δ 26.07, δ 22.63, δ 14.08.
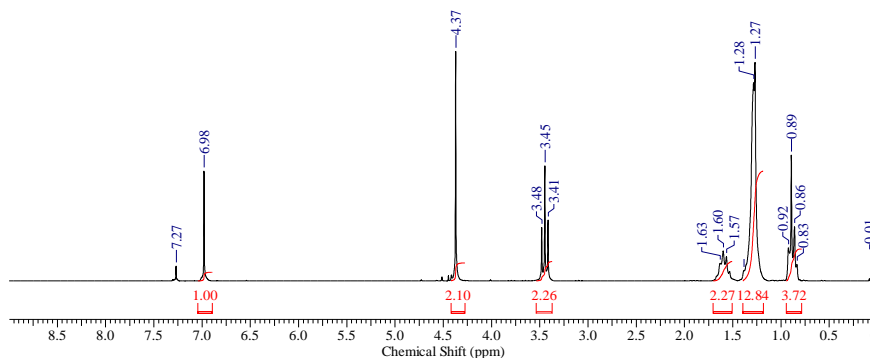

Figure 5.5 ^{1}H NMR spectrum of 2, 5-dibromo-3-((octyloxy)methyl)thiophene (CDCl$_3$)
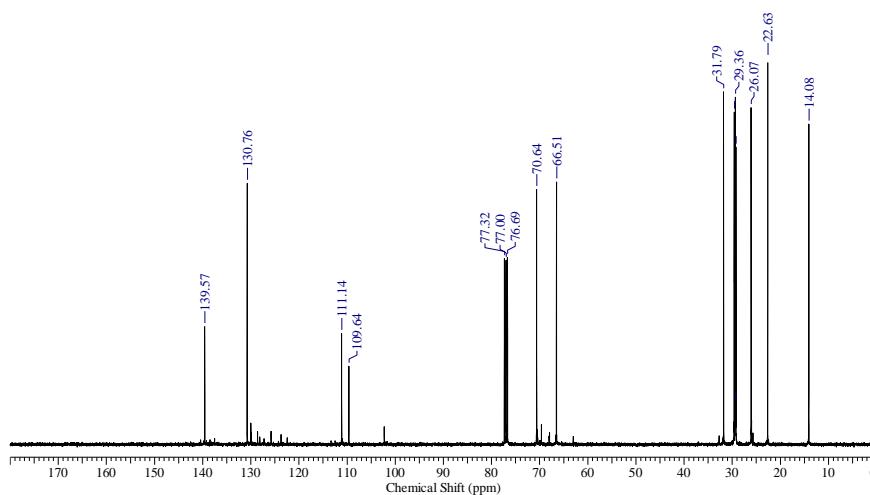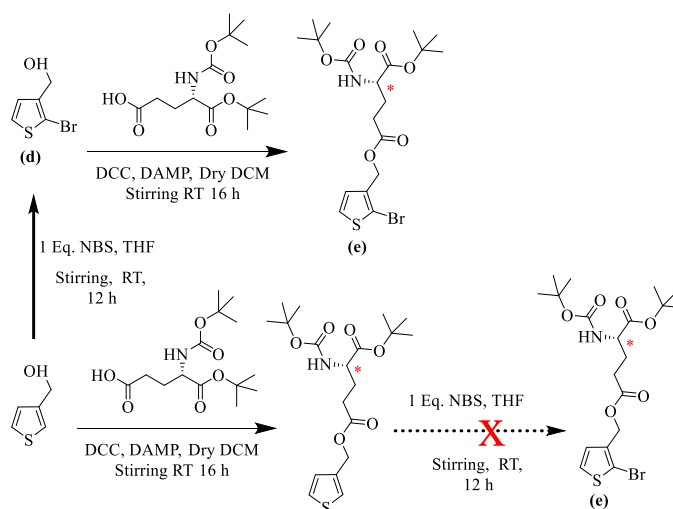

Figure 5.6 ^{13}C NMR spectrum of 2, 5-dibromo-3-((octyloxy)methyl)thiophene (CDCl$_3$)

Scheme 5.2 Schematic representation of chiral thiophene monomer synthesis

1.d) Synthesis of (2-bromothiophen-3-yl)methanol (d)

The solution of 3-thiophenemethanol (4 gm, 35.035 mmols) in dry THF 100 ml was prepared in a 250 ml round bottom flask. The solution was purged with nitrogen gas for 15 minutes with continuous stirring. After continuous stirring for 5 min, recrystallized N-bromosuccinimide (6.5 gm, 35.035 mmols) was added to the solution. The inert atmosphere was maintained throughout the reaction, and the reaction was allowed to stir at room temperature for 12 hours. The crude product was filtered through filter paper, and the solvent was evaporated in reduced pressure on a rotary evaporator. The crude product was purified using a 30 % pet ether ethyl acetate mixture by column chromatography. Yield 75% ^{1}H NMR spectrum (400 MH$_Z$, CDCl$_3$) δ 7.27, 7.24 (d 1H), δ 7.07, 6.99 (d 1H), δ 4.60 (s 2H), δ 2.21 (broad 1H).
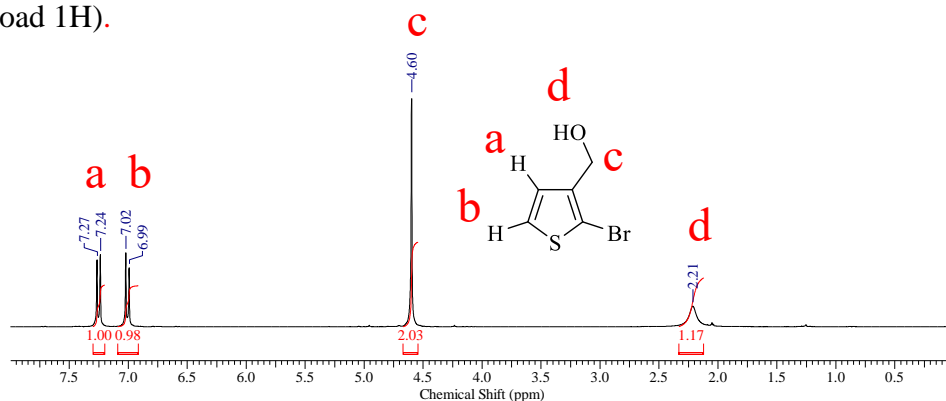

Figure 5.7 ^{1}H NMR spectrum of (2-bromothiophen-3-yl)methanol (CDCl$_3$)

1.e) Synthesis of 5-((2-bromothiophen-3-yl)methyl) 1-(*tert*-butyl) (*tert*-butoxycabonyl)-*L*-glutamate (e)

4-(N, N-Dimethylamino)pyridine (DMAP) (1.4 gm, 11.379 mmols) and N-Boc-L-glutamic acid 1-tert-butyl ester (3.2 gm, 10.504 mmols) were taken in 2-neck 250 ml round bottom flask under nitrogen atmosphere. Dry DCM (60 ml) was added to the reaction mixture with the help of a syringe. N,N'-Dicyclohexylcarbodiimide (DCC) (1.66 gm, 10.504 mmols) and (2-bromothiophen-3-yl)methanol (1.7 gm, 8.753 mmols) were added to the reaction by following conditions and time interval mentioned in the procedure for the synthesis of 1-(*tert*-butyl) 5-(thiophene-3-ylmethyl) (*tert*-butoxycarbonyl)-*L*-glutamate. The reaction was allowed to proceed for 16 hours. The crude product was extracted in an organic layer by washing with 0.2 molar NaOH solution, then with saturated NaHCO$_3$ solution, followed by washing with brine solution. The solvent was evaporated under reduced pressure on a rotary evaporator. The crude product was purified using a 20 % pet ether, ethyl acetate mixture by column chromatography. Yield 66 % ^{1}H NMR spectrum (400 MH$_Z$, CDCl$_3$) δ 7.26, 7.25 (d

1H), δ 6.98-6.97 (d 1H), δ 5.07 (m 3H), δ 4.21 (m 1H), δ 2.50-2.37 (m 2H), δ 2.17 (m 1H), δ 1.95-1.93 (m 1H), δ 1.46-1.44 (m 22H). ^{13}C NMR spectrum (100 MHz, CDCl$_3$) δ 172.53, δ 171.26, δ 155.35 δ 135.69, δ 128.34, δ 126.17, δ 112.77, δ 82.20, δ 79.78, δ 60.33, δ 53.30, δ 30.15, δ 28.27, δ 27.95, δ 18.39.
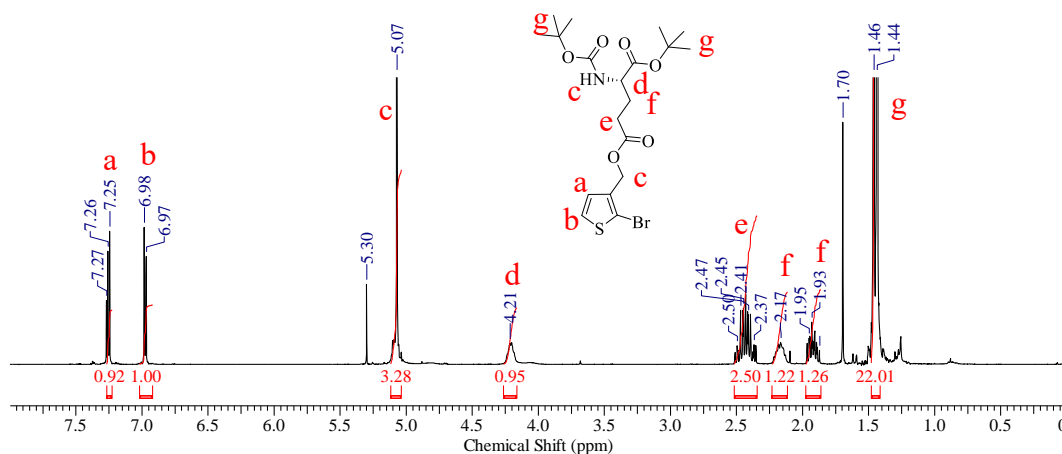

Figure 5.8 ^{1}H NMR spectrum of 5-((2-bromothiophen-3-yl)methyl) 1-(*tert*-butyl) (*tert*-butoxycabonyl)-*L*-glutamate (CDCl$_3$)
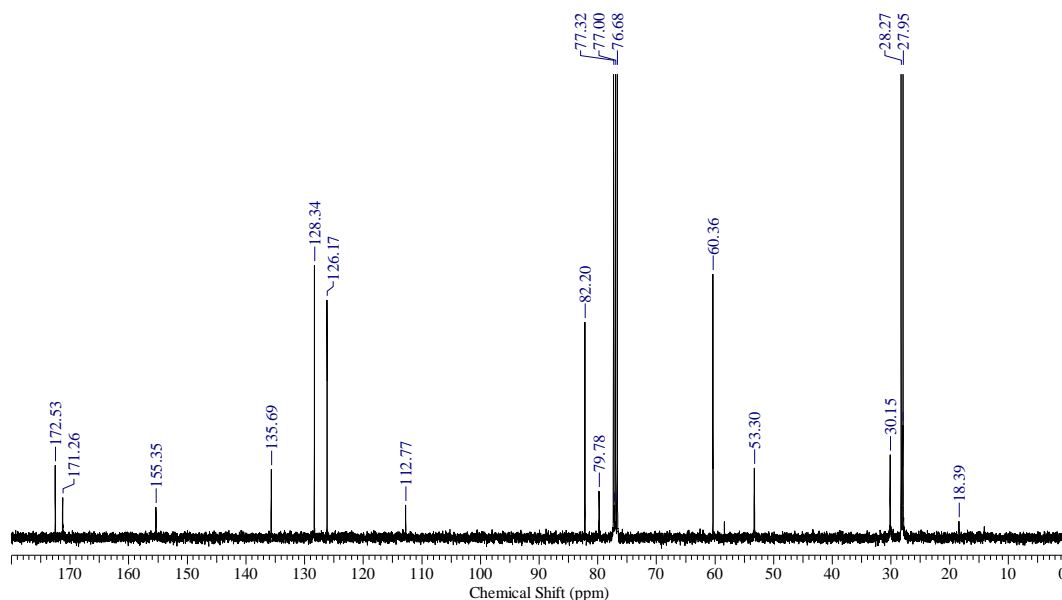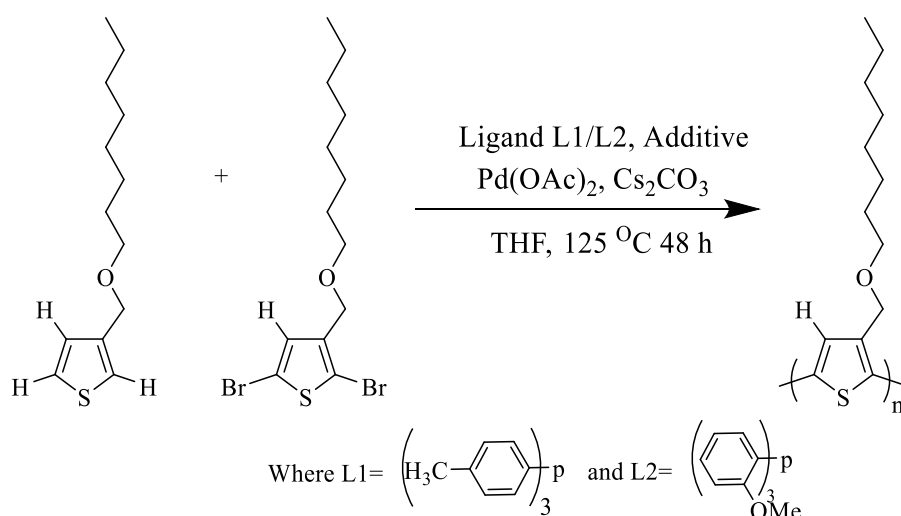

Figure 5.9 ^{13}C NMR spectrum of 5-((2-bromothiophen-3-yl)methyl) 1-(*tert*-butyl) (*tert*-butoxycabonyl)-*L*-glutamate (CDCl$_3$)

2) Polythiophene synthesis

2.a) Synthesis of poly-3-((octyloxy)methyl)thiophene (P1)

The monomers 3-((octyloxy)methyl)thiophene (a) (100 mg, 0.4417mmols) and 2, 5-dibromo-3-((octyloxy)methyl)thiophene) (b) (170 mg, 0.4417mmols) were taken in high pressure tube. The caesium carbonate (175 mg, 0.538 mmols), tris(o-methoxyphenyl)phosphine (L$_2$) (7.6 mg, 21.55×10^{-3} mmols) and Palladium(II) acetate (2.5 mg, 10.77×10^{-3} mmols) were added to the tube. The tube was closed with the help of a rubber septum. Repetitive evacuation and nitrogen flushing created the inert atmosphere in the tube. The dry THF was added to the tube with the help of a syringe. Further, the dissolved gasses from the reaction mixture were completely removed by multiple (3-4) freeze-pump-thaw cycles. The rubber septum was removed under the nitrogen environment and the tube tightly closed with the help of a Teflon screw cap. The polymerization was allowed at the elevated temperature of 125 °C for 48 hours. After completion of the reaction, the tube was cooled to room temperature. A similar polymerization reaction was set up using Tri(p-tolyl)phosphine (L$_1$). The polymerization reaction generated red coloured sticky oligomers that could not be precipitated in methanol. ^{1}H NMR spectrum (400 MH$_Z$, CDCl$_3$) δ 7.31-2.27 (m), δ 7.21 (m), δ 7.21 (m), δ 7.10, 7.09 (d), δ 6.988, (s) (aromatic region of the NMR spectrum show peaks corresponding to the monomers) δ 4.57-4.37 (m 2H), δ 3.50-3.42 (m 1H), δ 1.61, 1.57 (m 2H), δ 1.27 (m 10H), δ 0.89, 0.86 (m 3H).
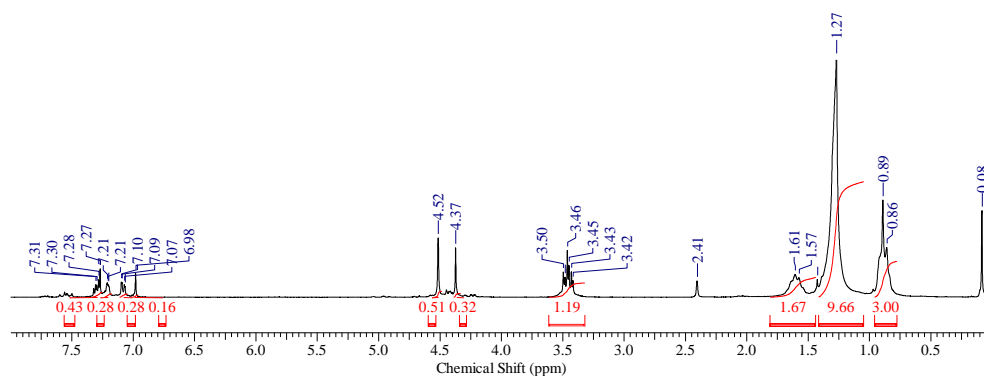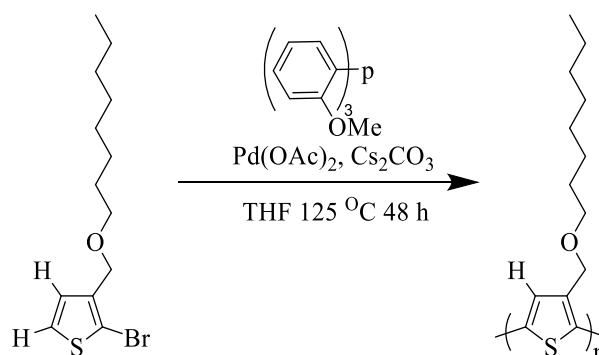
Figure 5.10 ^{1}H NMR spectrum of the oligomer (L₂ ligands) (CDCl₃)

2.b) Synthesis of poly-3-((octyloxy)methyl)thiophene (P1)

2-bromo-3-((octyloxy)methyl)thiophene (520 mg, 1.703 mmols) was taken in the high-pressure polymerization tube. Caesium carbonate (555 mg, 0.982 mmols), tris (o-methoxyphenyl)phosphine (L2) (24 mg, 68.136×10^{-3} mmols) and Palladium(II) acetate (7.6 mg, 34.04×10^{-3} mmols) were added to the tube. The tube was closed with a rubber septum and evacuated, followed by nitrogen flushing to maintain the inert atmosphere. The dry THF (1.5 ml) was added to the reaction mixture. The dissolved gasses from the tube were removed by multiple freeze-pump-thaw cycles (3 times). The rubber septum was removed under the nitrogen environment, and the tube was tightly closed with the help of a screw cap Teflon stopper. The reaction temperature was raised to 125 °C. The reaction was allowed to proceed at the same temperature for 48 hours with continuous stirring. The reaction mixture was then allowed to cool down slowly to room temperature. The polymer was precipitated in methanol followed by acetone and pet ether. Yield 71 %. ^{1}H NMR spectrum (400 MHz, CDCl₃) δ 7.25 (s 1H), δ 4.59 (s 2H), δ 3.57 (t 2H), δ 1.68 (m 2H), δ 1.44 (m 2H), δ 1.30, 1.28 (m 10H) δ 0.89-0.85 (m 3H). ^{13}C NMR spectrum (100 MHz, CDCl₃) δ 136.34, δ 134.25, δ 133.19, δ 129.39, δ 70.81, δ 66.67, δ 31.86, δ 29.52, δ 26.26, δ 22.66, δ 14.09.
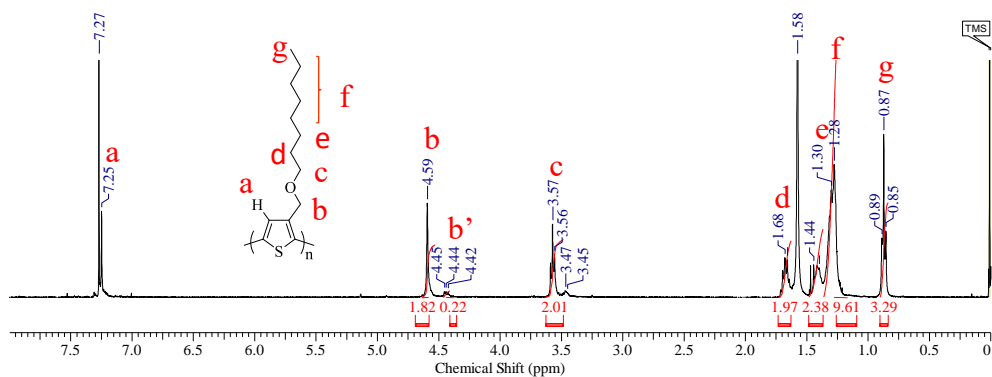
Figure 5.11 ^{1}H NMR of poly-3-((octyloxy)methyl)thiophene (regioregular polythiophene) (CDCl$_3$)
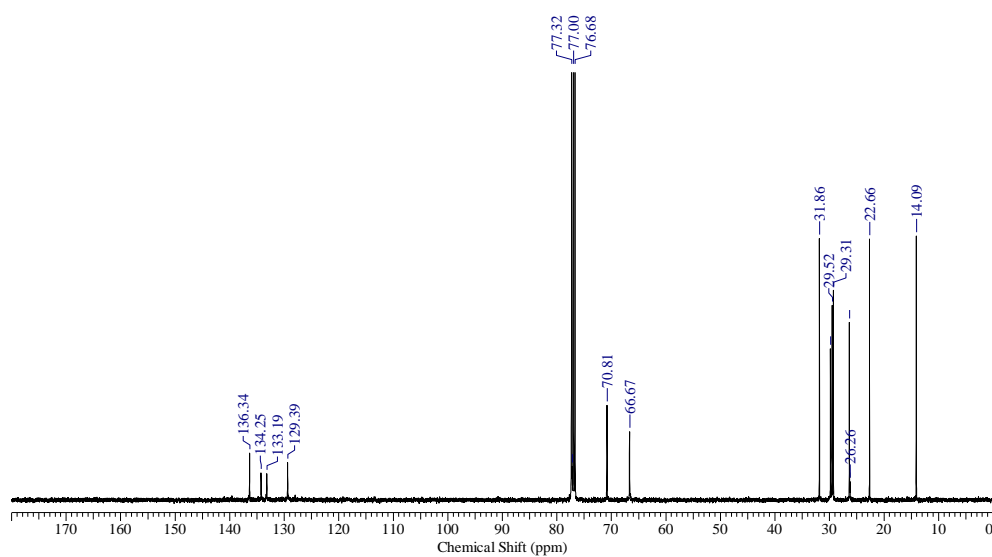

Figure 5.12 ^{13}C NMR of poly-3-((octyloxy)methyl)thiophene (regioregular polythiophene) (CDCl$_3$)

2.c) Synthesis of poly 1-(*tert*-butyl) 5-(thiophene-3-ylmethyl) (*tert*-butylcarbonyl)-*L*-glutamate (P2)
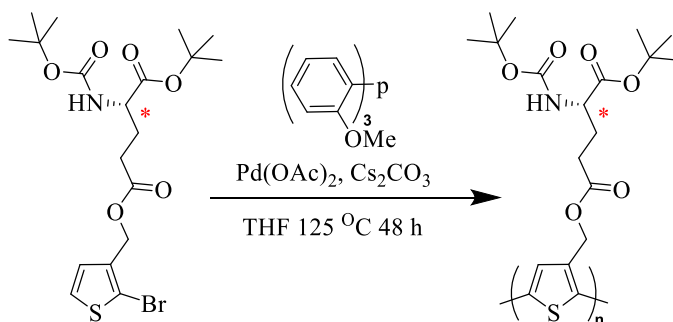
The 5-((2-bromothiophen-3-yl)methyl) 1-(*tert*-butyl) (*tert*-butoxycabonyl)-*L*-glutamate (200 mg, 0.434 mmols), caesium carbonate (142 mg, 1.302 mmols), followed by addition of tris (o-methoxyphenyl)phosphine (6.2 mg, 17.37×10^{-3} mmols) and Palladium(II) acetate (2 mg, 8.68×10^{-3} mmols) to the high pressure tube. Same reaction procedure were used as followed for the synthesis of poly-3-((octyloxy)methyl)thiophene. After completion of reaction, the reaction mixture was allowed to cool down to room temperature. No precipitate was obtained in methanol. The solvent was evaporated which gave dark red coloured sticky compound. ^{1}H NMR spectrum 400 MH$_Z$, CDCl$_3$) multiple peaks in the aromatic region δ 7.60-6.89 (m), δ 6.20 (s), δ 5.99 (s), δ 5.19-5.07 (m), δ 4.69 (s), δ 4.13-4.83 (broad peak), δ 3.57 (s), δ 2.44-2.35 (m), δ 2.21, 2.19 (m) δ 1.94, 1.82 (m) δ 1.51-1.26 (m) δ 0.89 (m)

Figure 5.13 ^{1}H NMR spectrum of the oligomers (CDCl$_3$)

3) Fluorene monomers synthesis

3.a) Synthesis of 2, 7-dibromo-9, 9-dioctyl-9H-fluorene (f)
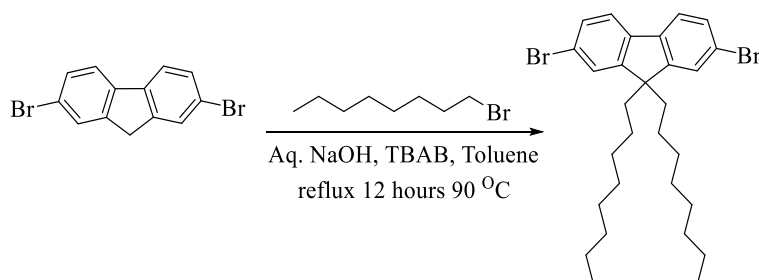
2, 7-dibromofluorene (2 gm, 6.174 mmols) and tetrabutylammonium bromide (TBAB) were dissolved in 50 ml toluene in a 250 ml round bottom flask. 25 ml of aqueous NaOH (50 %

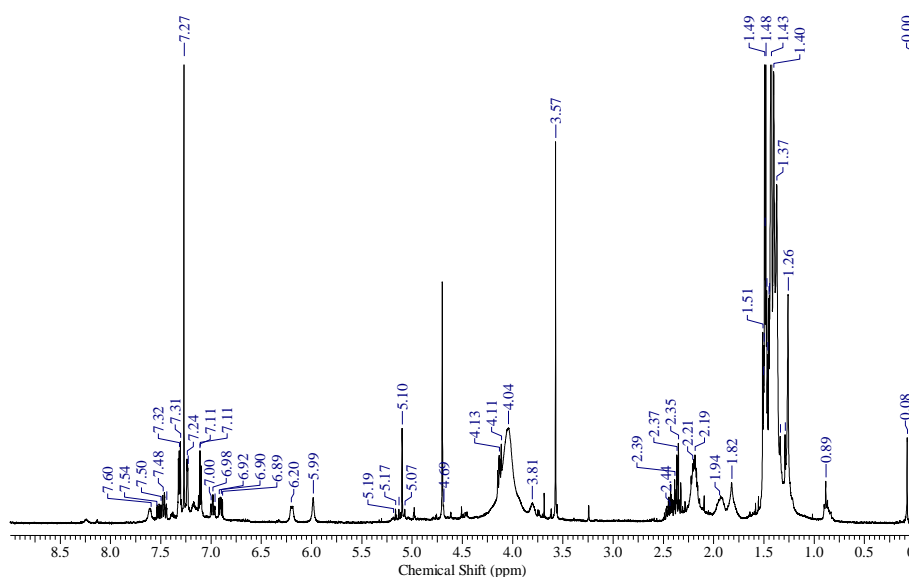w/w) was added to the reaction mixture. The reaction mixture was allowed to stir at room temperature for 5 minutes, followed by the addition of 1-bromooctane (3 ml, 15.437 mmols). The reaction temperature was raised to 60 °C. The reaction mixture was allowed to stir for 4 hours at the same temperature. The progress of the reaction was measured with the help of TLC. After completing the reaction, the reaction mixture was allowed to cool down slowly. The reaction mixture was diluted by adding 200 ml of ethyl acetate. The organic layer was washed with water, followed by brine solution. The organic layer was dried over anhydrous sodium sulphate (Na_2SO_4). The crude product was purified by column chromatography using pet ether. Yield 72%. ^1H NMR spectrum (400 MHz, $CDCl_3$) δ 7.55-7.44 (m 6H), δ 1.96-1.88 (m 4H), δ 1.21-1.06 (m 20H) δ 0.78-0.80 (m 6H) δ 0.59 (m 4H) ^{13}C NMR spectrum (100 MHz, $CDCl_3$) δ 152.53, δ 139.04. δ 126.14, δ 121.44, δ 121.10, δ 55.66, δ 40.13, δ 31.74, δ 29.14, δ 23.59, δ 22.58, δ 14.06,
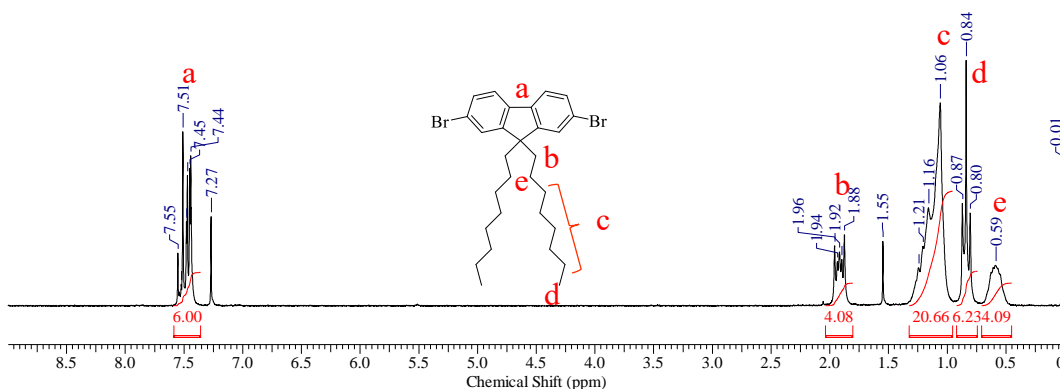
Figure 5.14 ^1H NMR spectrum of 2, 7-dibromo-9, 9-dioctyl-9H-fluorene ($CDCl_3$)
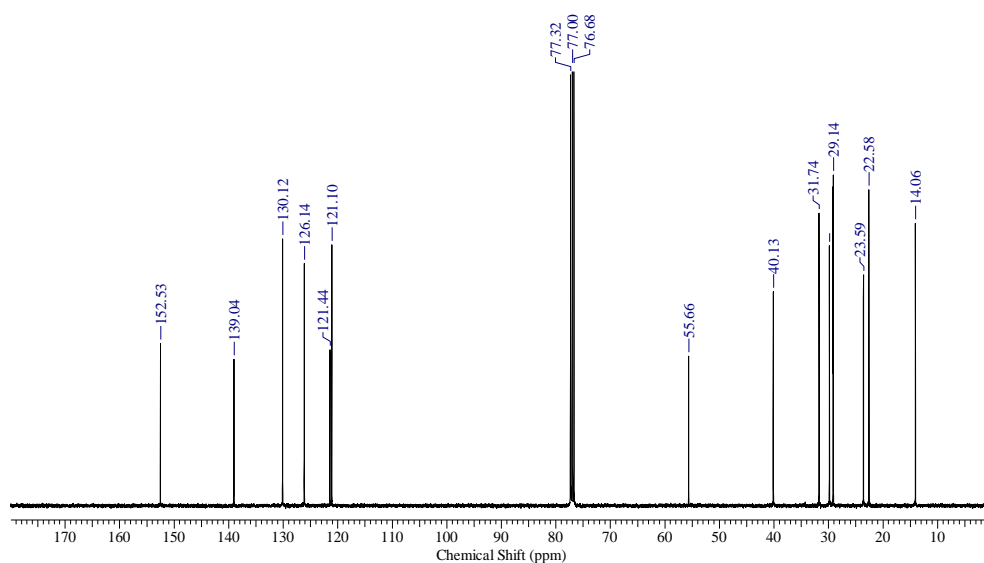
Figure 5.15 ^{13}C NMR spectrum of 2, 7-dibromo-9, 9-dioctyl-9H-fluorene ($CDCl_3$)

3.b) Synthesis of 3, 3-(2, 7-dibromo-9H-fluorene-9, 9-diyl)bis(propan-1-ol) (g)
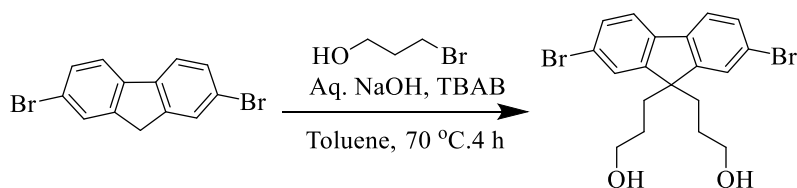
In a 250 ml two neck round bottom flask equipped with a magnetic stirring bar and reflux condenser, 2, 7-dibromofluorene (5 g, 15.46 mmol), and tetrabutylammonium bromide (2.5 g, 7.72 mmol) was dissolved in toluene (100 ml). To this reaction mixture, 50 g of 50 weight % of aqueous NaOH solution was added, followed by the addition of 3-bromopropan-1-ol (5.6 ml, 61.94 mmol). The reaction mixture was refluxed at 120 °C in an inert atmosphere for 4 hours. The reaction mixture was then allowed to cool to room temperature. The reaction mixture was transferred to water (150 ml), and the aqueous layer was extracted with ethyl acetate. The organic layer was extracted multiple times with water until the colour of the solution turned yellow. The ethyl acetate layer was dried by passing through anhydrous sodium sulphate. Ethyl acetate was evaporated under reduced pressure. The crude product obtained was purified by column chromatography with pet ether: ethyl acetate (50: 50). Yield 64 %. ^{1}H NMR spectrum (400 MHz, CDCl$_3$) δ 7.56-7.46 (m, 6H), δ 3.44-3.37 (t, 4H), δ 2.10-2.02 (m, 4H), 0.92-0.83 (m, 4H).
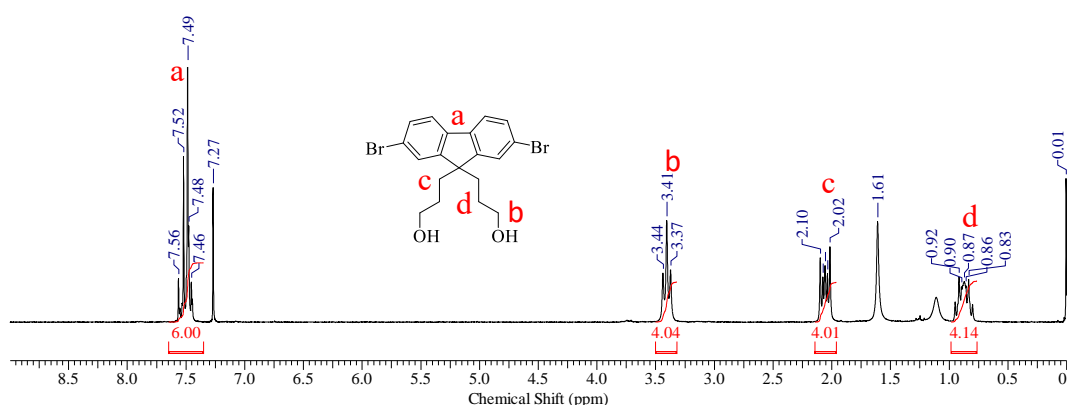
Figure 5.16 ^{1}H NMR spectrum of 3, 3-(2, 7-dibromo-9H-fluorene-9, 9-diyl)bis(propan-1-ol) (CDCl$_3$)

3.c) Synthesis of 1-(tert-butyl) 5-(3-(2, 7-dibromo-9-(5-((S)-3-oxopropoxy)-5-oxopentyl)-9H-fluorene-9-yl)propyl) (tert-butoxycarbonyl)-L-glutamate (h)
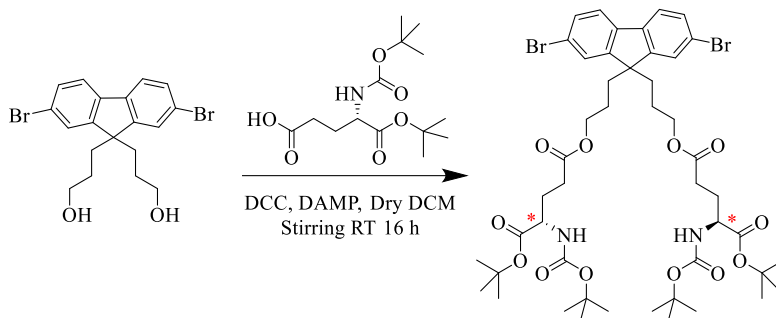
To a 250 ml 2-necked round bottom flask maintained under nitrogen atmosphere, 4-(N, N-Dimethylamino)pyridine (DMAP) (1.27 gm, 10.338 mmols) and N-Boc-L-glutamic acid 1-tert-butyl ester (3 gm, 9.889 mmols) were taken. Dry DCM (50 ml) was added to the reaction mixture with the help of a syringe. The reaction mixture was cooled to 0 °C, and stirred at the same temperature. N, N'-Dicyclohexylcarbodiimide (DCC) (1.54 gm, 9.889 mmols) was added to the reaction mixture after 5 minutes. The reaction was further stirred for 1 hour and 3, 3-(2, 7-dibromo-9H-fluorene-9, 9-diyl)bis(propan-1-ol) (1.98 gm, 4.495 mmols) was added dropwise. The reaction temperature was raised to room temperature by removing the ice bath, and the reaction was allowed to proceed for 16 hours. After completion, the reaction mixture was diluted with DCM and further stirred for 1 hour. The organic layer was extracted with 0.2 molar NaOH solution, then with saturated $NaHCO_3$ solution followed by washing with brine solution. The solvent was evaporated under reduced pressure on a rotary evaporator. The crude product was purified with the help of column chromatography using 30 % pet ether ethyl acetate. Yield 48 %. ^1H NMR spectrum (400 MHz, CDCl3) δ 7.56-7.47 (m 6H), δ δ 5.08, 5.06 (d 2H), δ 4.19-4.17 (m 2H), δ 3.83-3.78 (m 4H), δ 2.34-2.29 (m 4H), δ 2.06, 2.04 (m 6H), δ 2.02 (m 2H), δ 1.46-1.43 (m 36H) δ 0.94-0.88 (m 4H) ^{13}C NMR spectrum (100 MHz, CDCl3) δ 172.68, δ 171.34, δ 155.36 δ 139.08, δ 130.83, δ 126.06, δ 121.87, δ 121.45, δ 82.18, δ 79.75, δ 64.24, δ 54.74, δ 53.30, δ 36.21, δ 28.31, δ 27.97, δ 23.04, δ 17.08.

Figure 5.17 ^{1}H NMR spectrum of 1-(tert-butyl) 5-(3-(2, 7-dibromo-9-(5-((S)-3-oxopropoxy)-5-oxopentyl)-9H-fluorene-9-yl)propyl) (tert-butoxycarbonyl)-L-glutamate (CDCl$_3$)
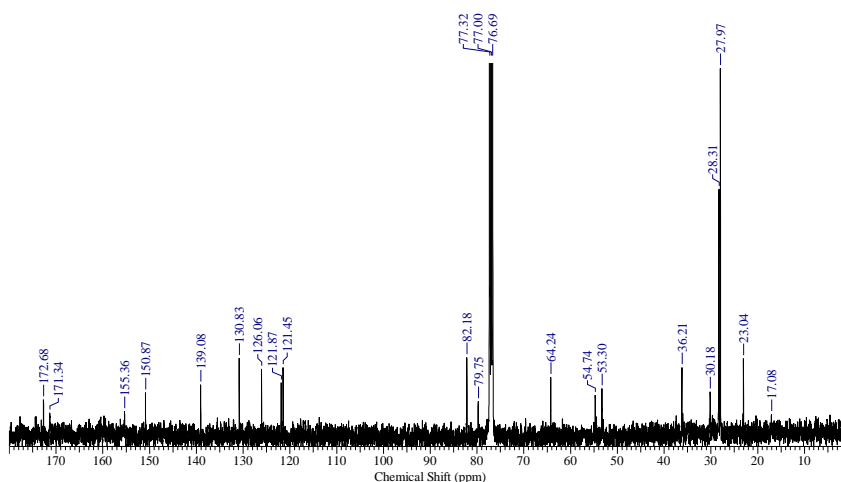
Figure 5.18 ^{13}C NMR spectrum of 1-(tert-butyl) 5-(3-(2, 7-dibromo-9-(5-((S)-3-oxopropoxy)-5-oxopentyl)-9H-fluorene-9-yl)propyl) (tert-butoxycarbonyl)-L-glutamate (CDCl$_3$)
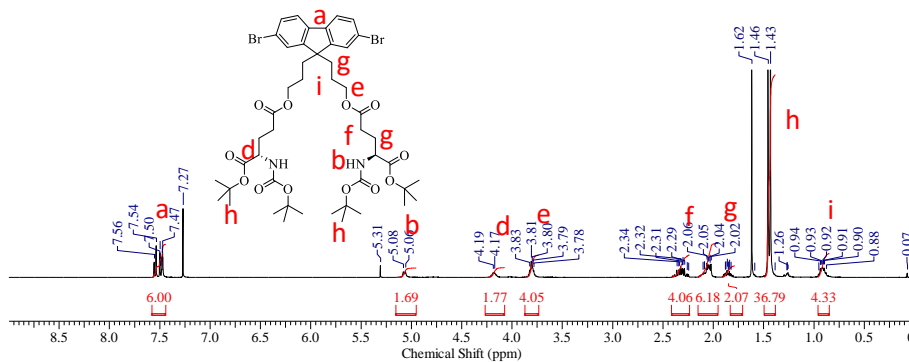
3.d) Synthesis of 1, 1'-di-tert-butyl O^5, O'^{5}-((2, 7-dibromo-9H-fluorene-9, 9-diyl)bis(hexane-6, 1-diyl)) (2S, 2'S)-butoxycarbonyl)amino)pentanediote) (i)
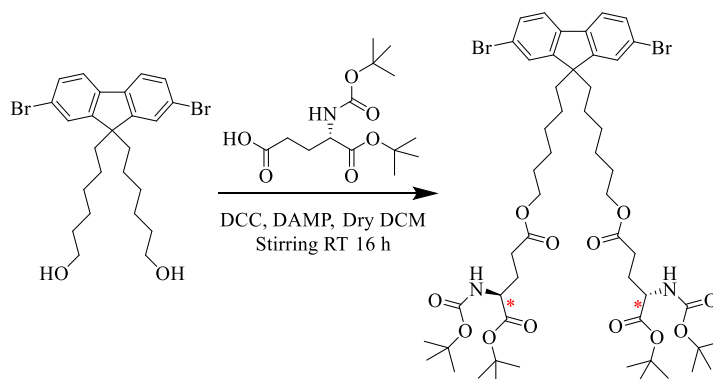
This monomer was synthesized by following the same procedure as that for the synthesis of 1-(tert-butyl) 5-(3-(2, 7-dibromo-9-(5-((S)-3-oxopropoxy)-5-oxopentyl)-9H-fluorene-9-yl)propyl) (tert-butoxycarbonyl)-L-glutamate. 4-(N,N-Dimethylamino)pyridine (DMAP) (1.1 gm, 8.773 mmols) and N-Boc-L-glutamic acid 1-tert-butyl ester (2.7 gm, 8.773 mmols) were taken in a 250 ml 2-neck round bottom flask. Dry DCM (50 ml) was added to the reaction mixture with the help of syringe. Addition of N,N'-Dicyclohexylcarbodiimide (DCC) (1.5 gm, 9.533 mmols) and 6, 6-(2, 7-dibromo-9H-fluorene-9, 9-diyl)bis(hexan-1-ol) (2 gm, 3.814 mmols) by following the same condition and after selected time interval as mentioned in the earlier procedure. The reaction temperature was raised to room temperature by removing the ice bath and reaction was allowed to proceed for 16 hours. The crude product was obtained by following same workup procedure. The crude product was purified with the help of column chromatography using 35 % pet ether ethyl acetate. Yield 60 % ^{1}H NMR spectrum (400 MH$_Z$, CDCl$_3$) δ 7.50-7.42 (m 6H), δ 5.10, 5.06 (d 2H), δ 4.17-4.15 (m 2H), δ 3.97-3.91 (m 4H), δ 2.34-2.31 (m 4H), δ 1.88 (m 6H), δ 1.41, 1.41 (m 42H), δ 1.08 (m 8H) δ 0.55 (m 4H) ^{13}C NMR spectrum (100 MH$_Z$, CDCl$_3$) δ 170.97, δ 169.94, δ 155.36, δ 152.13, δ 139.01, δ 130.25, δ 130.18, δ 126.00, δ 121.50, δ 121.18, δ 82.14, δ 79.73, δ 64.82, δ 55.51, δ 50.43, δ 40.43, δ 36.93, δ 29.44, δ 28.38, δ 28.26, δ 27.81, δ 25.50, δ 23.48.

Figure 5.19 ^{1}H NMR spectrum of 11, 1'-di-tert-butyl O^5, O'^{5}-((2, 7-dibromo-9H-fluorene-9, 9-diyl)bis(hexane-6, 1-diyl)) (2S, 2'S)-butoxycarbonyl)amino)pentanediote) (CDCl$_3$)
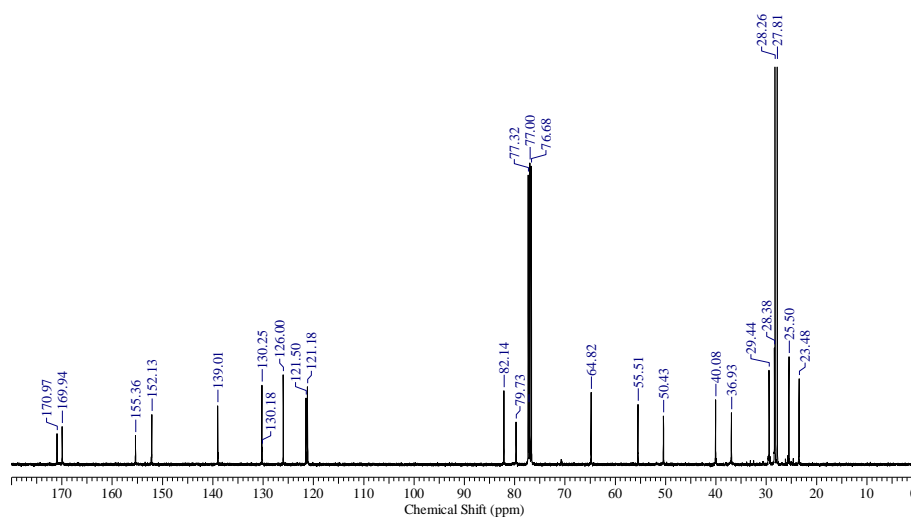
Figure 5.20 ^{13}C NMR spectrum of 11, 1'-di-tert-butyl O^5, O'^{5}-((2, 7-dibromo-9H fluorene -9, 9-diyl)bis(hexane-6, 1-diyl)) (2S, 2'S)-butoxycarbonyl)amino)pentanediote) (CDCl$_3$)

4) Synthesis of fluorene-thiophene copolymers

4.a) Synthesis of poly-9, 9-dioctyl-9H-fluorene-alt-3-((octyloxy)methyl)thiophene (P3)
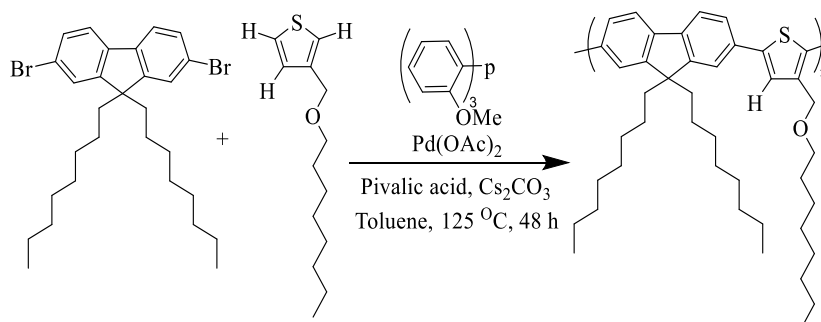
The two monomers 2, 7-dibromo-9, 9-dioctyl-9H-fluorene (344 mg, 0.627 mmols) and 3-((octyloxy)methyl)thiophene (142 mg, 0.627 mmols) were taken in a high pressure tube. Caesium carbonate (664 mg, 1.881 mmols), tris-o-methoxyphenyl phosphine (18 mg, 50.018 x 10^{-3} mmols), Palladium(II) acetate (5.6 mg, 25.09x10^{-3} mmols) and pivalic acid (64 mg, 0.627 mmols) were added to the tube. The tube was closed with a rubber septum and charged with a nitrogen environment. 1.5 ml dry toluene was added to the reaction mixture with the help of a syringe. The reaction mixture was then degassed with the help of three freeze-pump-thaw cycles. The rubber septum was removed from under the nitrogen environment, and the tube was tightly closed with the help of a Teflon screw cap. The reaction mixture was then heated to 125 °C with continuous stirring. The polymerization was then allowed to continue for 24 hours. The reaction mixture was cooled to room

temperature, and the polymer was precipitated in methanol, followed by acetone and pet ether. In another batch, polymerization was set up by following the same procedure and polymerization was allowed to continue for 48 hours. ^{1}H NMR spectrum of P3-24h polymer (400 MH$_Z$, CDCl$_3$) δ 7.78-7.60 (m 7H), δ 4.53 (m 2H), δ 3.60 (m 2H), δ 2.06 (m 4H), δ 1.76-1.72 (m 4H), δ 1.48 (m 2H), δ 1.34-1.32 (m 10H), δ 1.21-1.11 (m 22H) δ 0.82-0.74 (m 16H). ^{1}H NMR spectrum of P3-48h polymer also exhibited a similar spectrum with similar integration values.
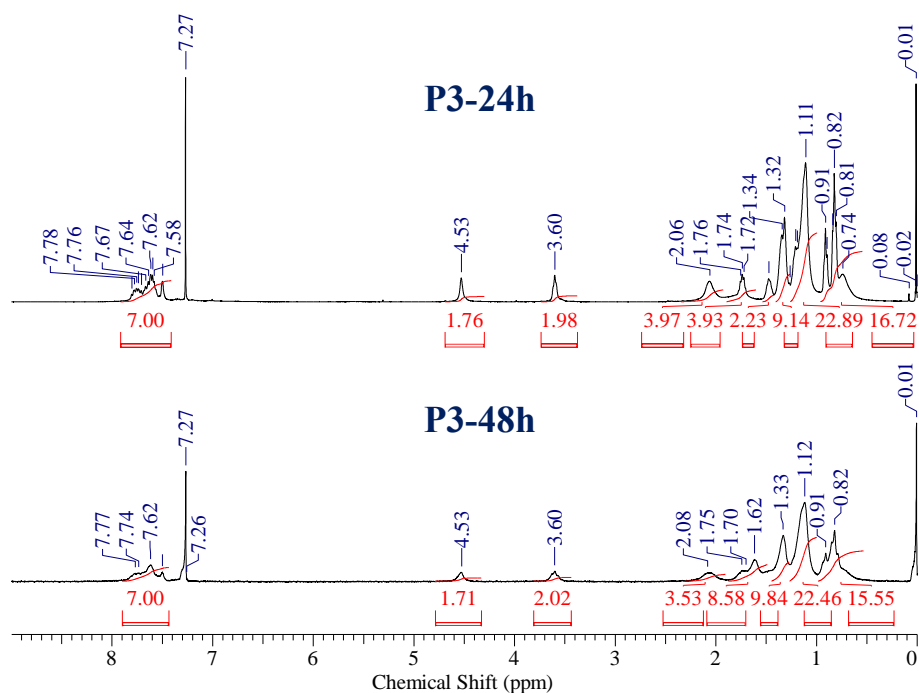
Figure 5.21 ^{1}H NMR spectrum of poly-9, 9-dioctyl-9H-fluorene-alt-3-((octyloxy)methyl)thiophene (P3-24h and P3-48h stack plotted together) (CDCl$_3$)

4.b) Synthesis of chiral fluorene-alt-thiophene copolymer (P4)
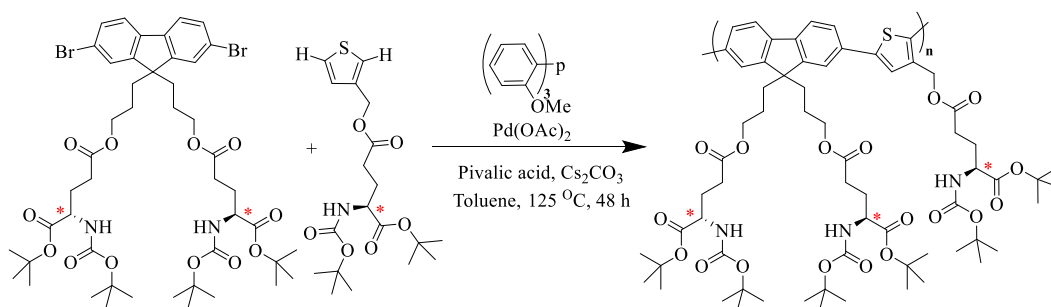
1-(tert-butyl) 5-(3-(2, 7-dibromo-9-(5-((s)-3-(tert-butoxy)-2-(tert-butoxycarbonylamino)-3-oxopropoxy)-5-oxopentyl)-9H-fluoren-9-yl) (propyl) (tert-butoxycarbonyl)-L-glutamate

(136 mg, 0.1345 mmols), 1-(tert-butyl) 5-(thiophene-3-3ylmethyl) (*tert*-butoxycarbonyl)-*L*-glutamate (54 mg, 0.1345 mmols), caesium carbonate (132 mg, 0.4036 mmols), tris-o-methoxyphenyl phosphine (4 mg, 10.07x10^{-3} mmols), Palladium(II) acetate (2 mg, 5.38x10^{-3} mmols) and pivalic acid (14 mg, 0.324 mmols) were added to the high pressure tube. The remaining reaction procedure was same as followed for the synthesis of poly-9, 9-dioctyl-9H-fluorene-alt-3-((octyloxy)methyl)thiophene. The reaction was allowed to proceed for 48 hours. At the end of the reaction, no precipitate was formed when the reaction mixture was precipitated in methanol. On solvent evaporation a dark colour sticky mass was observed. No molecular weight build-up occurred for the polymer during polymerization. Yield 43 %

^{1}H NMR spectrum (400 MH$_{Z}$, CDCl$_{3}$) multiple peaks in the aromatic region δ 7.75-7.10 (m 7H), δ 5.12 (s 1H), δ 4.71 (s 1H), δ 3.80, 3.78 (m 1H), δ 3.40, 3.37 (m 2H), δ 2.76 (m 2H), δ 2.12-2.05 (m 4H), δ 1.51-1.28 (m 2H), δ 1.23-1.15 (m 12H), δ 0.89-0.8 (m 4H).
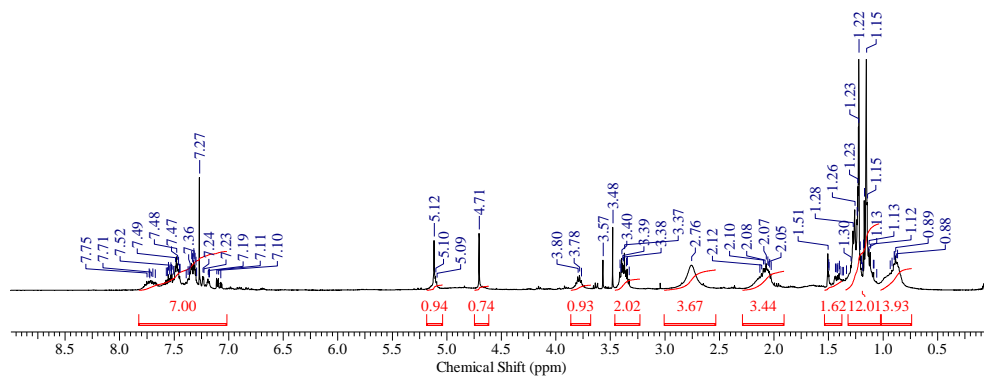
Figure 5.22 ^{1}H NMR spectrum of chiral fluorene-alt-thiophene copolymer (P4) (CDCl$_{3}$)

4.c) Synthesis of poly-*9H*-fluorene-9, 9-diyl bis-(propane-1, 3-diyl-n-boc-1-*tert*-butyl-L-glutamate-alt-3-((octyloxy)methyl)thiophene (P5)
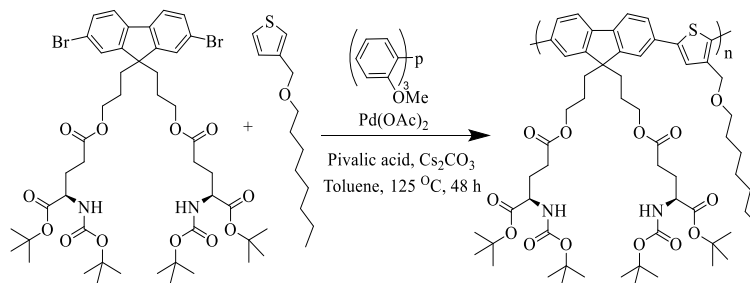
1-(tert-butyl) 5-(3-(2, 7-dibromo-9-(3-(((R)-5-(tert-butoxy)-4-((tert-butoxycarbonyl)amino)-5-oxopentanoyl)oxy)propyl)-9H-fluorene-9-yl)propyl) (tert-butoxyvarbonyl)-L-glutamate, (317 mg, 0.3135 mmols), 3-((octyloxy)methyl)thiophene (71 mg, 0.3135 mmols) were taken in high pressure tube. Caesium carbonate (307 mg, 0.9405

mmols), tris-o-methoxyphenyl phosphine (9 mg, 23.74×10^{-3} mmols), Palladium(II) acetate (3 mg, 11.87×10^{-3} mmols) and pivalic acid (32 mg, 0.2967 mmols) were added to the same tube. The tube was charged with nitrogen environment by multiple evacuation followed by nitrogen flushing. 1.5 ml of dry toluene was added to the tube with the help of syringe followed by degassing by three consecutive freeze- pump- thaw cycles. The tube was opened under the nitrogen environment and tightly packed with teflon screw cap. The reaction mixture was continuously stirred at elevated temperature of 125 °C for 48 h. For workup, the reaction mixture was cooled to room temperature and polymer was precipitated in methanol followed by acetone. Yield 88% ^{1}H NMR spectrum (400 MH$_Z$, CDCl$_3$) multiple peaks in the aromatic region δ 7.73-7.18 (m 7H), δ 5.09 (s 1H), δ 4.52, 4,49 (s 1H), δ 4.14 (1H), δ 3.83, 3.78 (b 2H), δ 3.59-3.52 (b 4H), δ 3.41, 3.40 (b 4H), δ 2.17-2.05 (b 10H), δ 1.82-1.65 (b 10H), δ 1.42-1.27 (b 40H), δ 1.01-0.89 (b 10H).
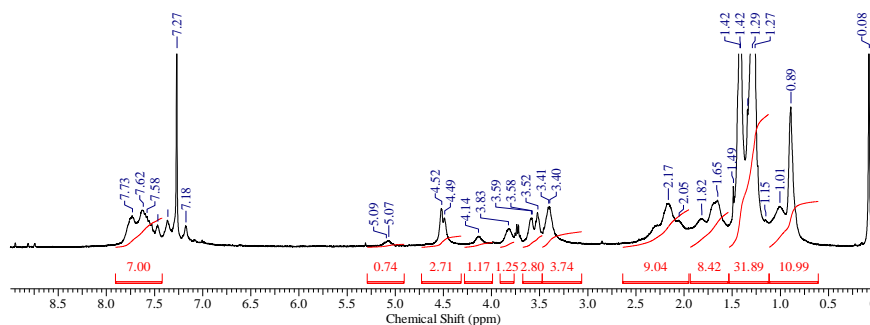
Figure 5.23 ^{1}H NMR of poly-*9H*-fluorene-9, 9-diyl bis-(propane-1, 3-diyl-n-boc-1-*tert*-butyl-L-glutamate-alt-3-((octyloxy)methyl)thiophene (CDCl$_3$)

4.d) Synthesis of poly-*9H*-fluorene-9, 9-diyl bis-(hexane-1, 6-diyl-n-boc-1-*tert*-butyl-L-glutamate-alt-3-((octyloxy)methyl)thiophene (P6)
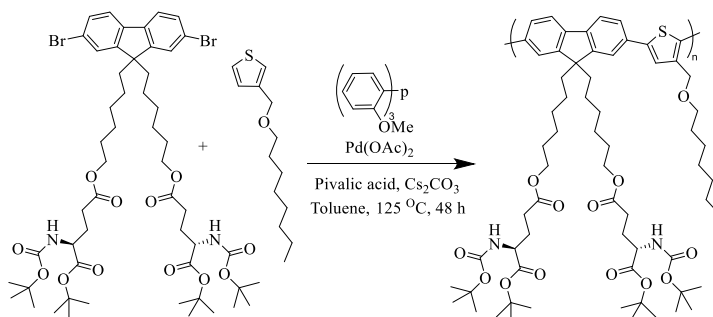
2,7-dibromo-*9H*-fluorene-9, 9-diyl bis-(hexane-1, 6-diyl-n-boc-1-*tert*-butyl-L-glutamate (335 mg, 0.3059 mmols), 3-((octyloxy)methyl)thiophene (70 mg, 0.3059mmols) caesium carbonate (299 mg, 0.9178 mmols), tris-o-methoxyphenyl phosphine (8.7 mg, 24.4757x10$^-$

³ mmols), Palladium(II) acetate (2.8 mg, 12.2378x10⁻³ mmols) and pivalic acid (32 mg, 0.3059 mmols) were added to the high pressure tube. The tube was charged with a nitrogen environment by repetitive evacuation followed by nitrogen flushing. 1.5 ml of the dry toluene was added to the tube with the help of a syringe. The solution was degassed by three freeze- pump- thaw cycles. The tube was opened in a nitrogen environment and tightly packed with a teflon screw cap. The tube was heated at an elevated temperature of 125 ^{O}C for 48 hours with continuous stirring. The reaction mixture was cooled to room temperature, and the polymer was precipitated in methanol followed by acetone. Yield 84 %. ^{1}H NMR spectrum (400 MHᴢ instrument, CDCl₃) δ 7.76-7.60 (b 7H), δ 5.43 (s 2H), δ 4.50, 4,40 (d 4H), δ 3.97, 3.95 (b 4H), δ 3.61-3.52 (b 2H), δ 2.90, 2.67 (two broad peaks 4H), δ 2.06 (b 10H), δ 1.73-1.31 (b 50H), δ 1.13 (b 8H), δ 0.90-0.89 (b 4H), δ 0.72 (b 4H).
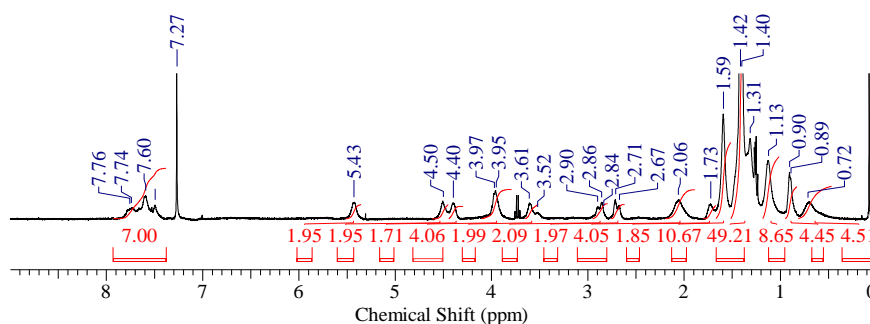
Figure 5.24 ^{1}H NMR of poly-*9H*-fluorene-9, 9-diyl bis-(hexane-1, 6-diyl-n-boc-1-*tert*-butyl-L-glutamate-alt-3-((octyloxy)methyl)thiophene (CDCl₃)

4.e) Synthesis of poly-9, 9-dioctyl-9H-fluorene-alt-1-(*tert*-butyl) 5-(thiophene-3ylmethyl) (*tert*-butoxycarbonyl)-*L*-glutamate (P7)
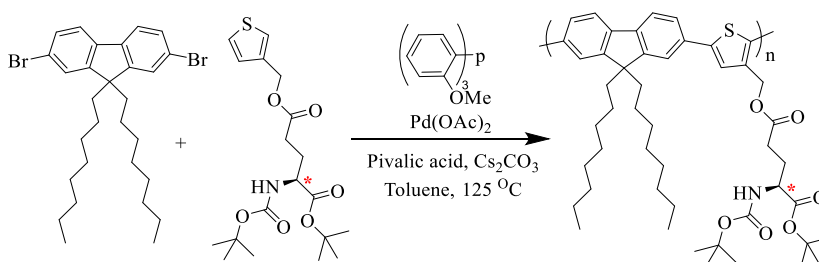
2, 7-dibromo-9, 9-dioctyl-*9H*-fluorene (206 mg, 0.375 mmols) and 1-(*tert*-butyl) 5-(thiophene-3ylmethyl) (*tert*-butoxycarbonyl)-*L*-glutamate (150 mg, 0.375), were taken in high pressure tube. To the same tube caesium carbonate (367 mg, 1.126 mmols), tris-o-methoxyphenyl phosphine (10.6 mg, 30.037x10⁻³ mmols), Palladium(II) acetate (3.5 mg, 15.018x10⁻³ mmols) and pivalic acid (39 mg, 0.375 mmols) were added. The tube was closed

with a rubber septum and charged with a nitrogen environment by evacuating and flushing nitrogen repeatedly. Dry toluene was added to the reaction mixture, and the reaction mixture was further degassed by three freeze- pump- thaw cycles. The tube was opened under a nitrogen environment and tightly packed with a teflon screw cap. The reaction mixture was heated at 125 °C with continuous stirring for 12 hours. Similar reactions were set up and stopped at different times like 24, 48 and 72 hours. After completion of the reaction, the reaction mixture was cooled to room temperature. The polymer was precipitated in methanol followed by acetone. ^{1}H NMR spectrum of 12 h polymer (400 MHz, CDCl$_3$) δ 7.77-7.53 (m 7H), δ 5.21 (s 1H), δ 4.81 (s 1H), δ 2.07 (m 4H), δ 1.56-1.47 (m 12H), δ 1.25-1.11 (m 26H), δ 0.87-0.74 (m 14H)
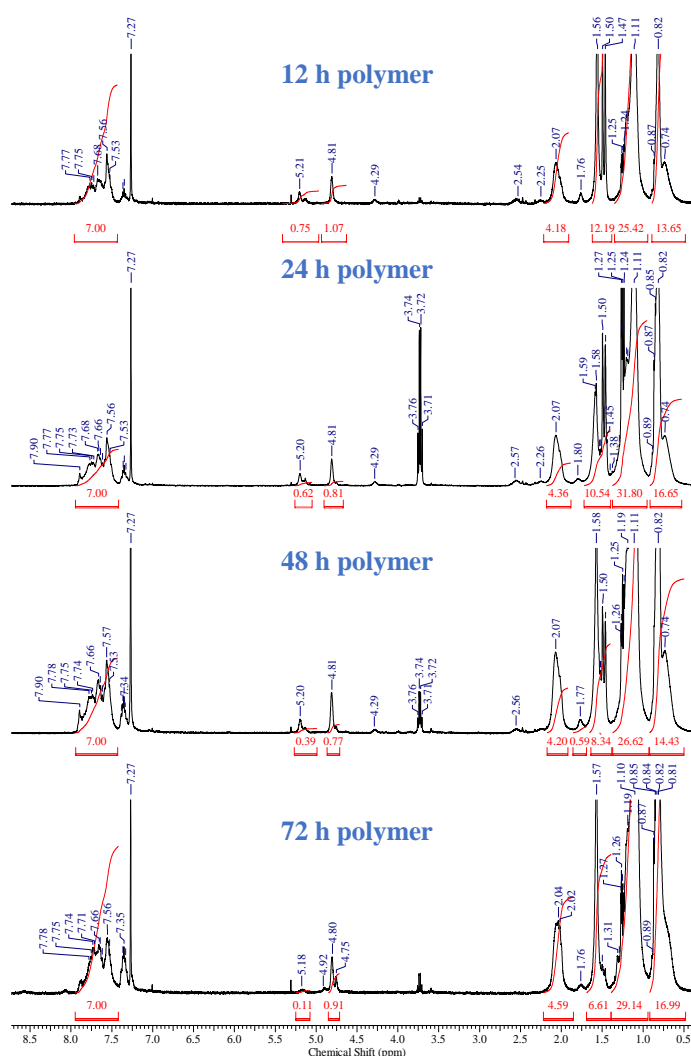
Figure 5.25 ^{1}H NMR spectra of poly-9, 9-dioctyl-9H-fluorene-alt-1-(*tert*-butyl) 5-(thiophene-3ylmethyl) (*tert*-butoxycarbonyl)-*L*-glutamate a) 12 b) 24 c) 48 and d)72 polymers. (CDCl$_3$)

5.3 RESULT AND DISCUSSION

5.3.1 Synthesis and characterizations

Achiral thiophene monomers a, b and c with octyl chain as pendants were synthesized following Scheme 1. Detailed synthetic procedures for these thiophene monomers are given in (experimental section 1.a-1.c). 3-thiophenemethanol was first modified with octyl pendent group to give 3-((octyloxy)methyl)thiophene (a). This thiophene monomer was further mono and di brominated using 1 and 2 equivalents of recrystallized NBS to give 2-bromo-3-((octyloxy)methyl)thiophene (b) and 2, 5-dibromo-3((octyloxy)methyl)thiophene (c) monomers. Figures 5.26.1 and 2 compares the labeled ^{1}H and ^{13}C NMR spectra (zoomed aromatic region) of these monomers, which provide confirmation of their structures. ^{1}H NMR spectra (Figure 5.26.1) confirmed the formation of monomers with the disappearance of aromatic protons.
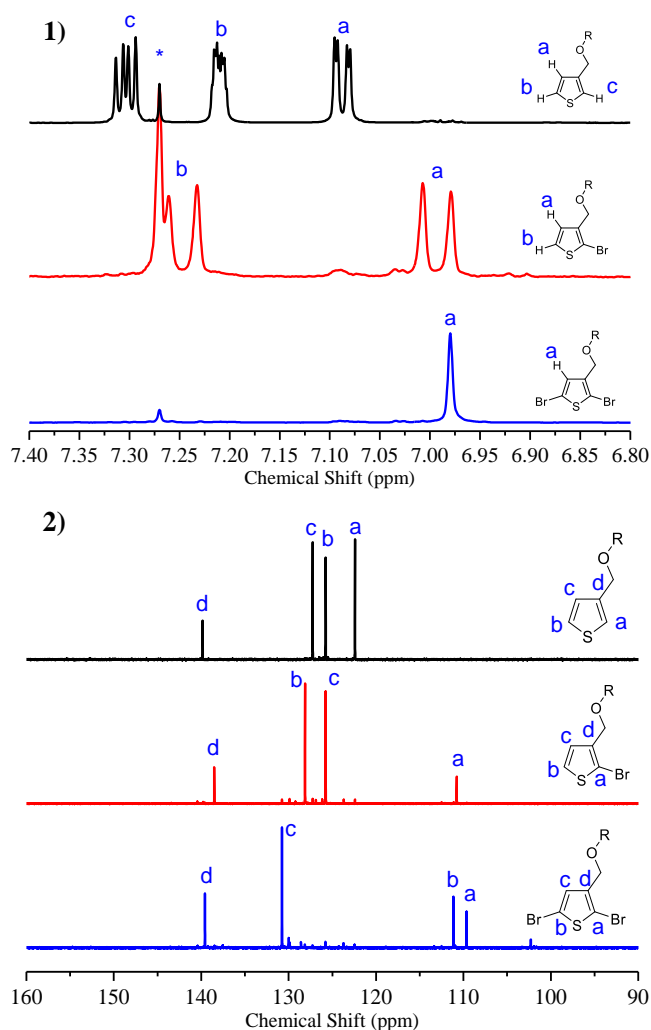
Figure 5.26 Stack plotted 1)^{1}H NMR and 2) ^{13}C NMR spectra of "a" (black), **"b"** (red) and "c" (blue) thiophene monomer (CDCl$_3$)

The 3-((octyloxy)methyl)thiophene (monomer a) showed three peaks in the aromatic region corresponding to the three aromatic protons (black), which upon monobromination showed two peaks (red) corresponding to two aromatic protons in 2-bromo-3-((octyloxy)methyl)thiophene (monomer b) while in case of dibrominated monomer "2, 5-dibromo-3-((octyloxy)methyl)thiophene" (monomer c) only one peak (blue) was observed corresponding to one aromatic proton. ^{13}C NMR spectra (Figure 5.26.2) showed four peaks corresponding to four aromatic carbons "a", "b", "c", and "d", upon mono bromination peak corresponding to "a" carbon shifted to the shielded region (red), while in case of dibrominated monomer two peaks corresponding to "a" and "b" carbons shifted to shielded region. These achiral thiophene monomers were polymerized in two ways. The bifunctional monomers (a) and (c) were polymerized by using L1 and L2 ligands in dry THF for 48 hours (Experimental section 2.a). The reaction resulted in the generation of dark red sticky oligomers. On the other hand, regioregular chiral polythiophene with considerable molecular weight was formed by homo-polymerization of monomer (b) (experimental section 2.b). The polymer formation was confirmed by recording the ^{1}H and ^{13}C NMR spectrum (Figure 5.11 and 5.12).
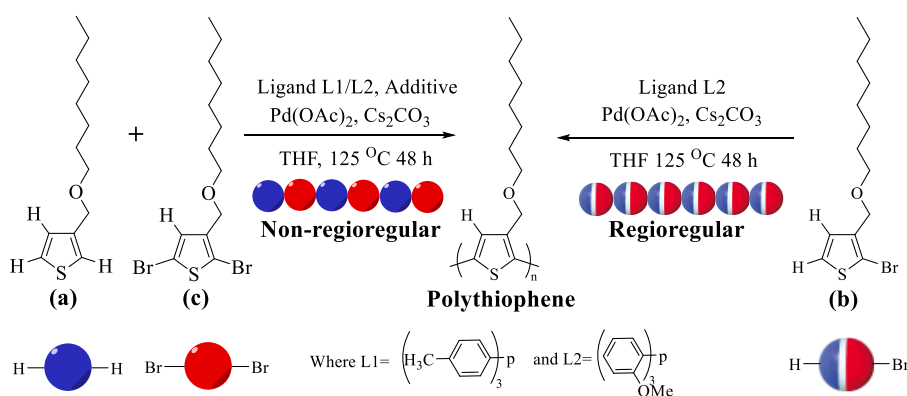
Scheme 5.3 Schematic representation for the synthesis of polythiophene by polymerizing (a and c) monomers or b monomer

General synthesis protocol and reaction conditions for formation of dark red coloured sticky oligomers and reasonably high molecular weight regioregular polythiophene is represented in Scheme 5.3. Formed dark red coloured sticky oligomers show multiple peaks in the aromatic region (7.31-6.98 ppm) corresponds to the monomers and oligomers (Figure 5.27 a), while the regioregular polythiophene show single peaks in aromatic region (5.25 ppm) which corresponds to single aromatic proton form polymeric structure (Figure 5.27)
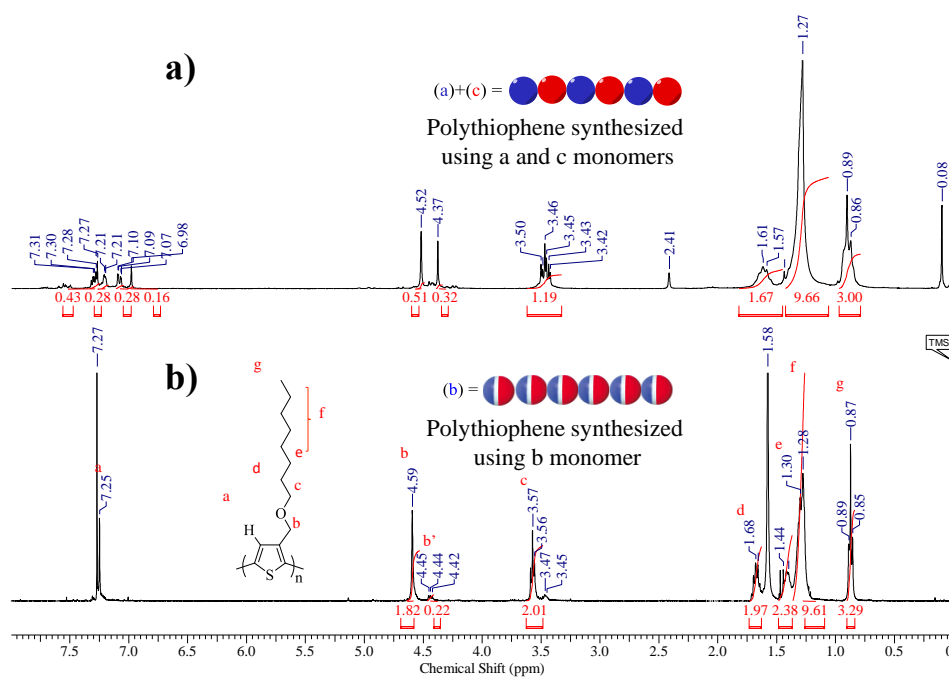
Figure 5.27 Comparison of 1H NMR spectra of polythiophene synthesized by polymerizing a) a and c monomers and b) c monomers (CDCl₃)

Figure 5.28 confirmed the polymer formation where thiophene monomer (b) (red spectrum) showed two peaks in the aromatic region corresponding to two aromatic protons a and b, upon polymerization, peak b corresponding to α-proton disappeared, and only a single peak was observed corresponding to β-proton "b" with a shift in deshielded region (black spectrum).
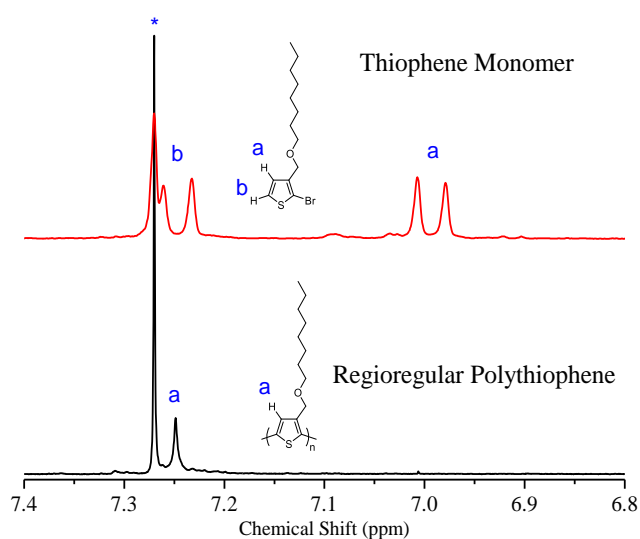
Figure 5.28 ¹H NMR spectra of thiophene monomer b and regioregular polythiophene stack plotted together (enlarged aromatic region) (CDCl₃)

The molecular weights and polydispersity index of oligomers and polymers were determined by recording GPC chromatogram using HPLC grade THF as eluent (Figure 5.29). Molecular weight details (*Mn*), polydispersity index (PDI), degree of polymerization (*Xn*) and yield of the formed oligomers and polymers is given in Table 5.1.
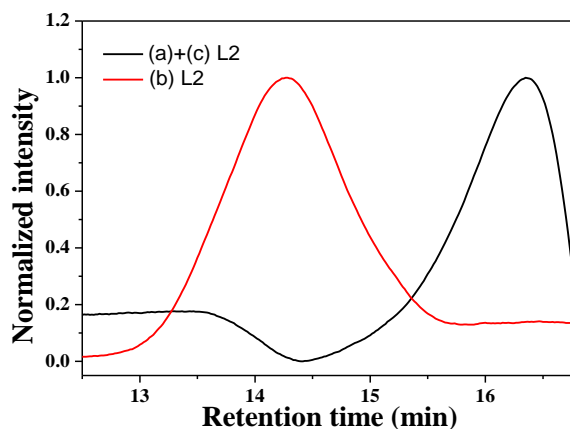
Figure 5.29 GPC chromatogram of the achiral polythiophene (THF)

Sr. no.	Monomers	Ligand	*Mn*	PDI	*Xn*	% Yield
1	(a)+(c)	L1	--	--	--	37 %
2	(a)+(c)	L2	1800	1.4	8	41 (sticky)
3	(b)	L2	23700	1.6	77	71

Table 5.1 molecular weight details and % yield of the oligomers and polymers

The synthesized polymer shows high Regioregularity by the sequential head to tail arrangement of monomers in the polymer backbone.

a) Calculating the Regioregularity of the poly-3-((octyloxy)methyl)thiophene

The Regioregularity of the polymers is an important parameter that needs to be understood correctly. Regioregular polymers show enhancement in the electron mobility through the lattice structure of the polymer formed by the ∏-stacking, which improves the optoelectronic properties. In contrast, regiorandom polymers show a non-planar structure due to the steric hindrance of alkyl chains. The non-planarity of the regiorandom polymers hamper its charge mobility resulting in poor optoelectronic properties. The % regioregularity in the polymer can be calculated with the help of ^{1}H NMR spectroscopy. The peak position

of the α-methyl proton of the alkyl chain in ^{1}H NMR spectrum determines the H-T or H-H arrangement of the repeating unit in the polymer structure. The ^{1}H NMR spectra of the polymers show a peak with chemical shift in the range of 4.59 and 4.45 ppm corresponding to the H-T and H-H arrangement of repeating units, respectively (Figure 5.30). The percentage of the polymer's H-T and H-H arrangement of the repeating unit can be calculated by taking the relative ratio of integration values for these peaks. The % regioregularity for the polymer was obtained as 90 %. In simple words, 90 % of the repeating units were arranged with the H-T arrangement.
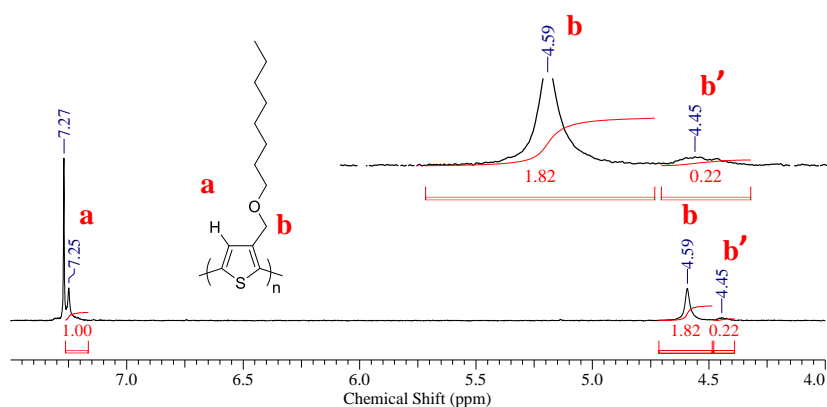
$$\% \, regioregularity = \frac{integration \, (c)}{integration \, (c + c')} \times 100$$

$$\% \, regioregularity = \frac{integration \, (1.82)}{integration \, (1.82 + 0,22)} \times 100$$

$$\% \, regioregularity = 90 \, \%$$

Figure 5.30 ^{1}H NMR spectra highlighting the integration of the peaks for H-T and H-H arrangement and the details of the calculation.

Chiral thiophene monomer containing N-Boc-L-glutamic acid-1-tert-butyl ester as pendent (e) was synthesized by following reaction sequence given in Scheme 2. Where mono bromination of 3-Thiophenemethanol followed by DCC, DMAP coupling with N-Boc-L-glutamic acid-1-tert-butyl ester (as shown in scheme 2) was performed to give particular thiophene monomer (e) (experimental section 2.d and 2.e). The monomers were characterized by recording ^{1}H and ^{13}C NMR spectra (Figure 5.7-5.9). The chiral thiophene monomer was then polymerized following similar conditions that were optimized to synthesize regioregular polythiophene. Unfortunately, chiral thiophene monomer failed to polymerize under these standardized conditions, as the reaction centre experiences high

steric hindrance due to bulky amino acid pendent groups. The ^{1}H NMR spectrum of the reaction residue showed multiple peaks in the aromatic region corresponding to the monomers and oligomers (Figure 5.13).

Synthesis of the fluorene-alt-thiophene copolymer was envisaged as an alternative approach to introduce chirality in the π-conjugated polymers. The details of the synthesis of the achiral and chiral fluorene monomers are provided in experimental section 3.a-d. The achiral fluorene monomer contains octyl pendants (monomer f), whereas chiral fluorene monomers contain N-Boc-L-glutamic acid-1-tert-butyl ester attached through (short and long spacer) 3 or 6 carbon alkyl chain pendants. The synthesized fluorene monomers were characterized by recording their ^{1}H and ^{13}C NMR spectrum (Figure 5.14-5.20). These fluorene monomers were then polymerized separately with achiral or chiral thiophene monomers. Polymerization conditions were standardized by polymerizing achiral thiophene monomer (a) with achiral fluorene monomers (f) (experimental section 4.a). Polymerization reactions were set up for 24 and 48 hours, resulting in polymers P3-24 h and P3-48 h, respectively. The polymers showed almost the same peak pattern in ^{1}H NMR spectra (figure 5.31).
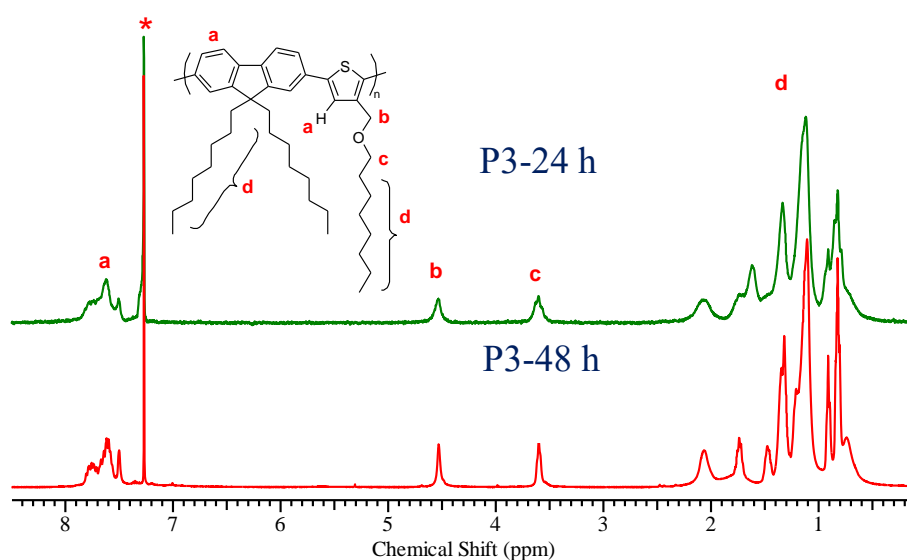
Figure 5.31 Stack plotted ^{1}H NMR spectra of the P3-24 h (green) and P3-48 h (red) polymers (CDCl$_3$)

Synthesized polymer shows almost similar molecular weights (*Mn* and *Mw*), polydispersity index (PDI) with yields ranging from 90-96 % (Figure 5.32 and Table 5.2)
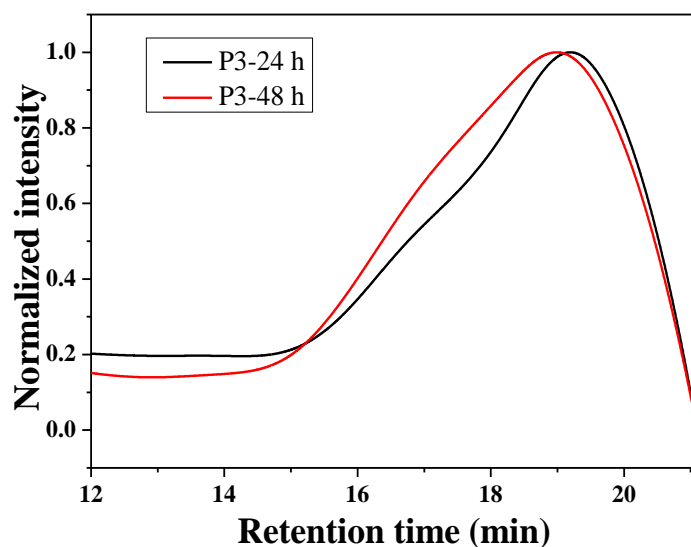
Figure 5.32 GPC chromatogram of P3-24 h and P3-48 h polymers (THF)

Sr. no.	Polymers	Time (h)	*Mn*	PDI	*Xn*	% Yield
1	P3-24 h	24	15300	2.9	49	90
2	P3-48 h	48	17100	3.2	55	96

Table 5.2 Molecular weight details of the polymers determined by GPC (THF)

Similar polymerization conditions were used to polymerize fluorene and thiophene chiral monomers containing N-Boc-L-glutamic acid-1-tert-butyl ester as pendants (experimental section 4.b). When chiral thiophene monomer (e) was polymerized with chiral fluorene monomer (h) with a shorter chiral handle (3 carbon), it did not undergo any polymerization due to the steric hindrance created by bulky groups (N-Boc-L-glutamic acid-1-tert-butyl ester) on thiophene as well as on fluorene monomer that were attached through only 3-carbon chain alkyl pendants. The reaction centre experiences a high level of steric hindrance due to a bulky chiral group close to the reaction centre. The dark red colour, sticky residue collected after solvent evaporation was used to record ^{1}H NMR spectrum and stacked plotted against corresponding monomers where polymerization residue showed multiple peaks in the aromatic region corresponding to monomers and oligomers (Figure 5.33)
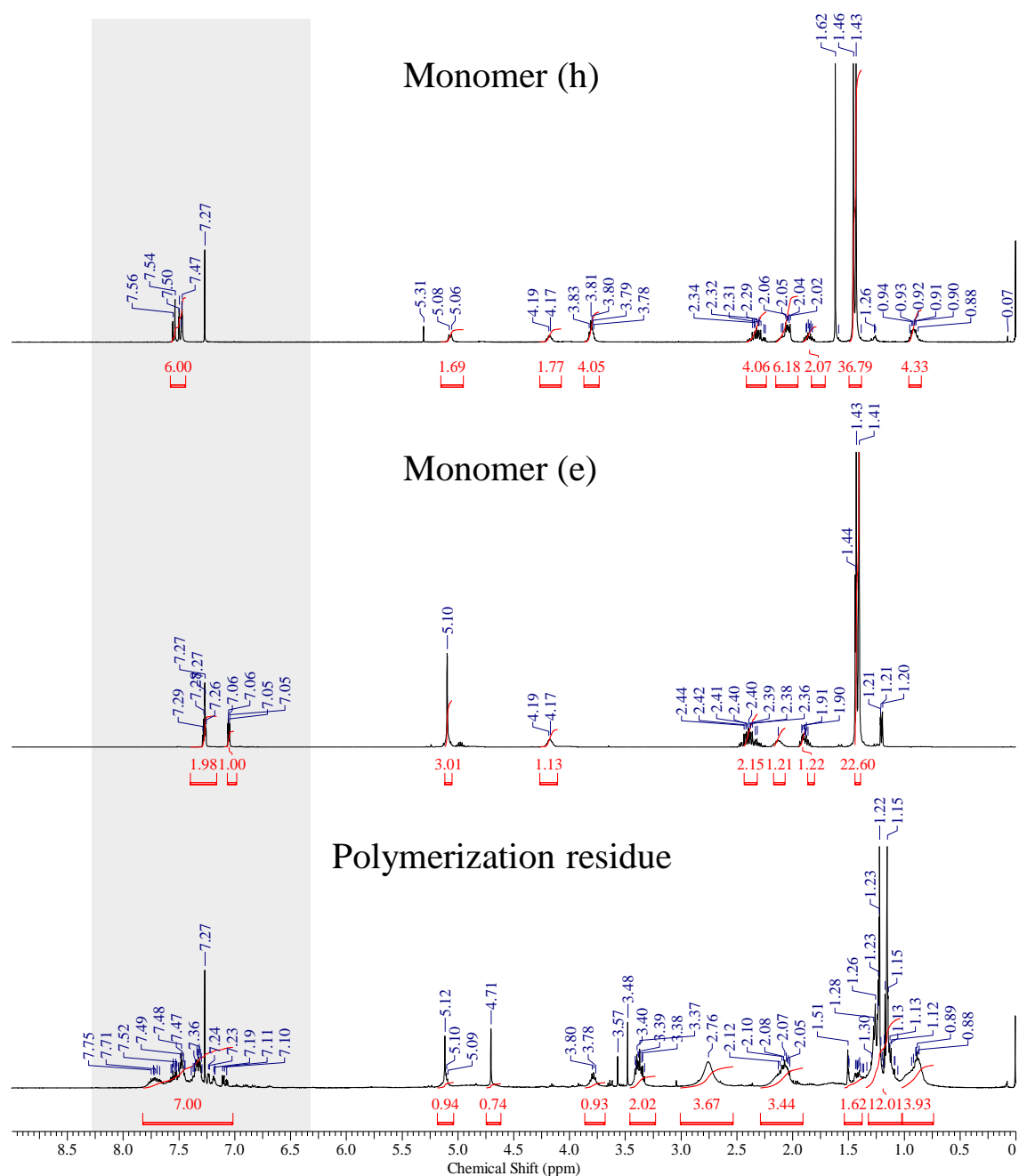
Figure 5.33 stack plotted ^{1}H NMR spectra of fluorene monomer (h) thiophene monomer (e) and polymerization residue (CDCl$_3$)

Steric hindrance arising from the bulky chiral groups was avoided by replacing chiral thiophene monomer (e) with less bulky achiral thiophene monomer (a) containing octyl pendant group. The thiophene monomer (a) was polymerized with chiral fluorene monomer (h) with N-Boc-L-glutamic acid-1-tert-butyl ester (experimental section 4.c). This polymerization could not generate high molecular weight polymers and formed only dimer or trimer (P5). The reaction generated a dark red, sticky compound where less bulky thiophene monomer underwent dehydrogenative homocoupling.[52] Peaks a and b arising

from the dehydrogenative homocoupling can be seen in Figure 5.34 (black spectrum).[53] These peaks are absent in Figure 5.34 (red spectrum) where chiral fluorene monomer (i) with long handle (6 carbon) was polymerized with achiral thiophene monomer (experimental section 4.c), to generate solid polymer (P6).
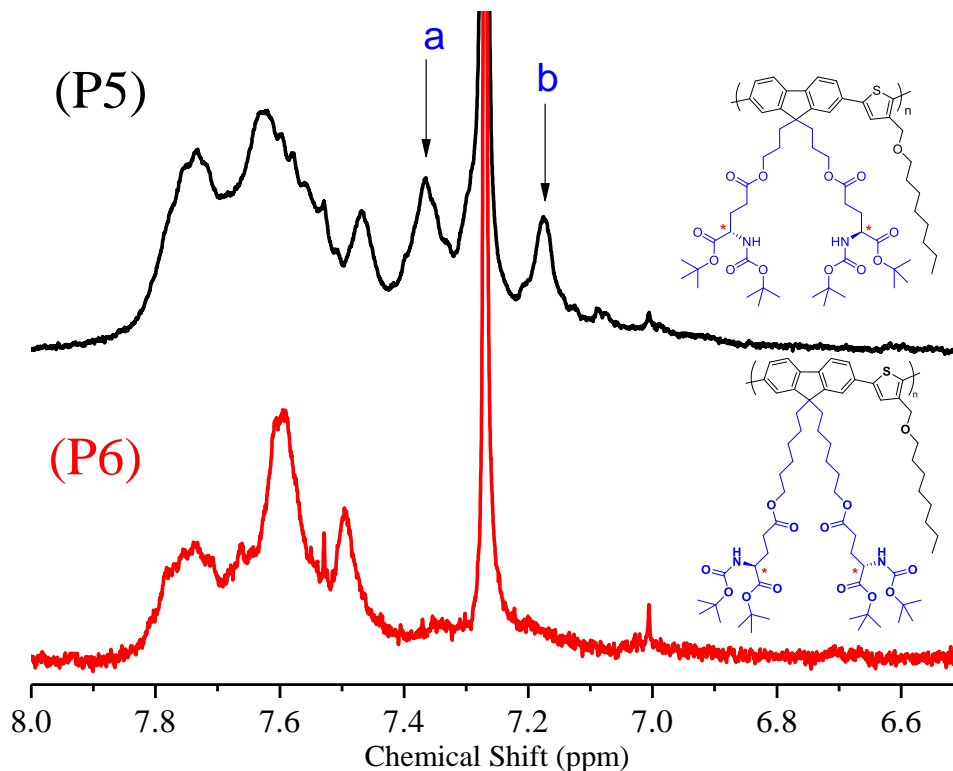
Figure 5.34 ^{1}H NMR spectra of short chiral handle oligomer P5 (black) and long handle polymer P6 (red) (enlarged aromatic region) (CDCl₃)

The excessive homocoupling in initial reaction time during P5 polymer synthesis created the stoichiometric imbalance between monomers that hampered the build-up of high molecular weight polymer.[54] On the other hand, the long handle containing chiral fluorene monomer (i) with bulky chiral pendants placed away from reaction centre experience lesser steric hindrance. The monomer underwent polymerization without dehydrogenative homocoupling between thiophene monomer. Solid polymer with reasonable molecular weight formed in this case compared to the short chiral handle fluorene monomer (Figure 5.35). The number average molecular weight (*Mn*), polydispersity index (PDI) and degree of polymerization (Xn) for polymers are given in Table 5.3.
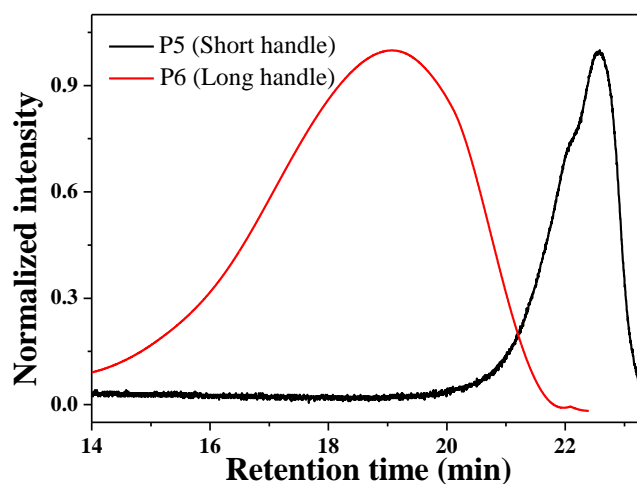
Figure 5.35 GPC chromatogram of short chiral handle P5 (black) and long handle P6 (red) chiral fluorene containing polymers (THF)

Sr. No	Polymers	*Mn*	PDI	*Xn*
1	P5 (Short handle)	1000	2.9	2
2	P6 (Long handle)	12300	1.9	21

Table 5.3 Number average molecular weight (*Mn*) Polydispersity index (PDI) and degree of polymerization (*Xn*) of P5 and P6 polymers (obtained from THF GPC)

Another way to introduce chirality in a polymer is by polymerizing chiral thiophene monomer (e) with achiral fluorene monomer (h), as shown in polymer P7 (experimental section 4.e). Polymerization reactions were set up for different time intervals like 12, 24, 48 and 72 hours to study the defect formation during the reaction. ^{1}H NMR spectra of polymers obtained from different polymerization reaction times are stack plotted in Figure 5.36. Change in the intensity of peaks a, b, and c was observed with an increase in reaction time. Peak intensity for peak "a" increased with an increase in reaction time. The origin of the peak is believed to arise from the defect that became more prominent with increasing time. The most probable defect that can form is β-defect, where a fluorene monomer with a less bulky alkyl chain can be coupled to the β positions on thiophene. The low energy difference (4.3 kcal mol^{-1}) between α and β positions on thiophene makes the β position susceptible to coupling generating defects in the polymer, which increases with an increase in reaction time.[55] The amine proton showed two peaks, b and b', depending upon the connectivity of thiophene with fluorene monomer. The connectivity defines the surrounding chemical and

magnetic environment. The peak intensity of these peaks decreases with an increase in reaction time due to the β defect where less bulky achiral fluorene monomer binds at β position, and overall thiophene content in the polymer structure decreases. Similarly, the α methyl proton on the thiophene monomer shows a single peak c in 12 hours reaction. With increasing reaction time, reaction at β position increase (β defect), which changes the chemical environment of α methyl proton and give rise to peak c' whose intensity increases with increase in time. 12- and 24-hours polymers were entirely soluble in organic solvents like THF, chloroform and toluene, while 48- and 72-hours polymers were only partially soluble. This insolubility in longer polymerization time polymers comes from complex structures due to side reactions.
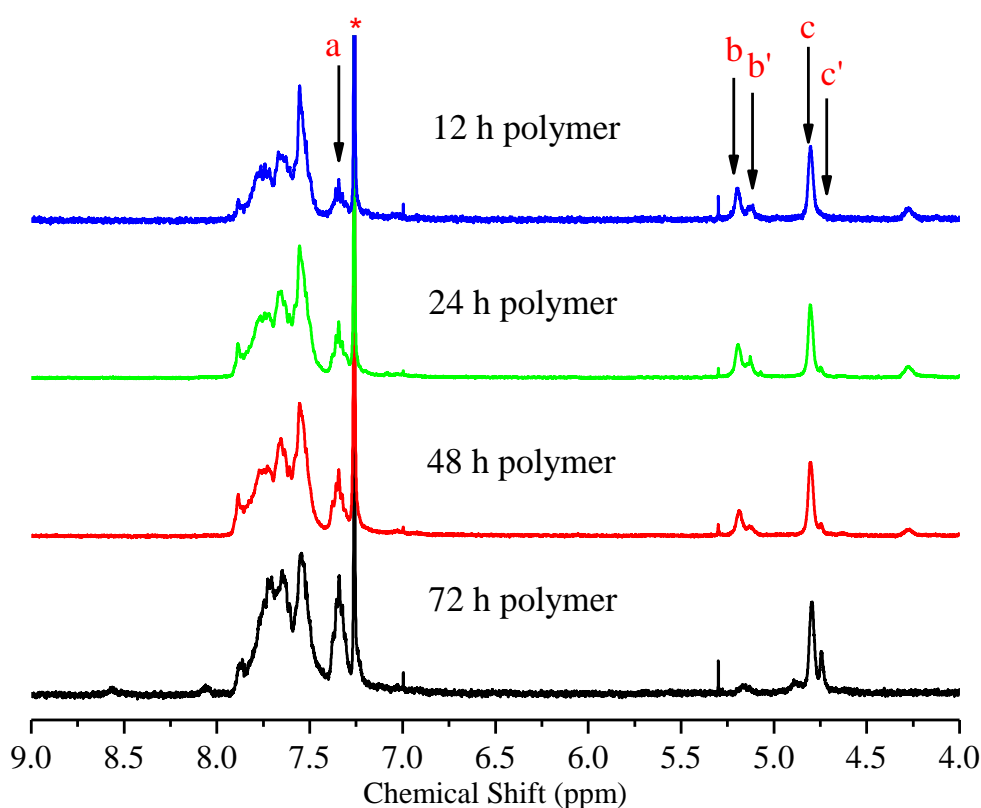
Figure 5.36 ^{1}H NMR spectra of 12, 24, 48 and 72 h polymers stack plotted together (enlarged aromatic region) (CDCl$_3$)

Molecular weights of soluble fractions of polymers were determined by recording the GPC chromatogram using THF as eluent (Figure 5.37). The number average molecular weight (*Mn*), PDI, the yield of reactions are given in Table 5.4, which revealed that 12- and 24-hours polymers showed almost similar molecular weights, while 48- and 72-hours polymers started forming partially soluble polymers. The soluble fraction, when checked, showed a reduction in the molecular weight. Chromatogram of 48 and 72 h polymers showed the

appearance of a new shoulder peak in the high retention time region. This bimodal distribution in the lower molecular weight region arises from the property of defect polymer that undergoes gelation or aggregation.[54,56]
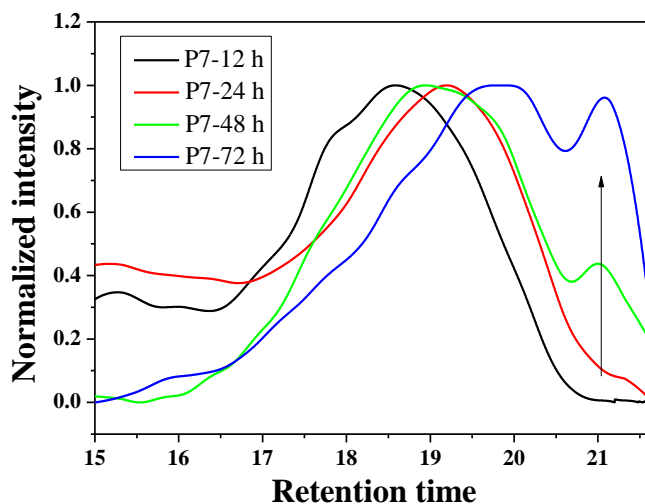
Figure 5.37 GPC plots of polymers THF as eluent. Column calibrated with narrow polydispersity (PDI) polystyrene standards

Sr. No.	Time	*Mn*	PDI	Yield
1	12 h	11200	2.2	61 %
2	24 h	10800	1.6	58 %
3	48 h	8400[a]	2.3	59 %
4	72 h	6400[a]	2	53 %

a = soluble portion

Table 5.4 Polymerization time, average molecular weights of polymers, polydispersity and % yields of polymers

5.3.2 Photophysics of polymers

Conjugated unsaturation in polymeric structures enables polymers to absorb electromagnetic radiation. The polymer's molar extinction coefficient depends on the molecular weight, planarity, and defects in the polymeric structure. Additionally, conjugated polymer shows the property of luminescence, where the quantum yield of polymers is highly dependent upon conformation, conjugation and rigidity.[57]

This chapter, described the synthesized of four polymers P1, P3, P6 and P7, with reasonable molecular weights. Among the synthesized polymer, two (P1 and P3) were achiral, whereas (P6 and P7) contained chiral pendants group (N-Boc-L-glutamic acid-1-tert-butyl ester) in one of the monomers.

The achiral polymer P1 showed absorption maxima (λmax) at 440 nm (Figure 5.38.a) and upon excitation at this wavelength gave intense orange colour emission in the 560 nm region (Figure 5.38.b). The excitation spectra for polymer recorded by exciting at 560 nm showed maxima around 420 nm, conveying that the chemical species absorbing at 420 nm electromagnetic radiation were the actual emitting species (Figure 5.38.b dotted line).
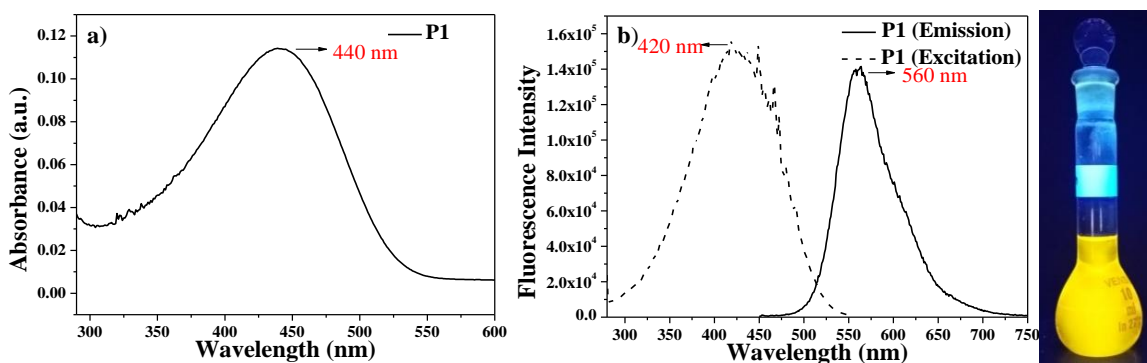
Figure 5.38 a) Absorption b) emission (solid line) and excitation (dotted line) spectra and image of intense (yellow) colour emission of P1 polymer

The P3 (fluorene-alt-thiophene copolymer) showed absorption maxima (λmax) at 405 nm (Figure 5.39.a). Upon excitation at 405 nm, cyan coloured emission with maximum at 457 nm (Figure 5.39.b) was observed. The excitation spectra of P3 polymer was recorded by exciting at emission maxima (457 nm) which gave excitation maxima at 395 nm. Both 24- and 48-hours polymers showed almost similar molar absorptivity coefficient and emission intensity as both had similar molecular weights. Absorption spectra did not show any shoulder peak at low energy wavelength, which additionally confirmed that the formed polymer was with low or no defect.[52]
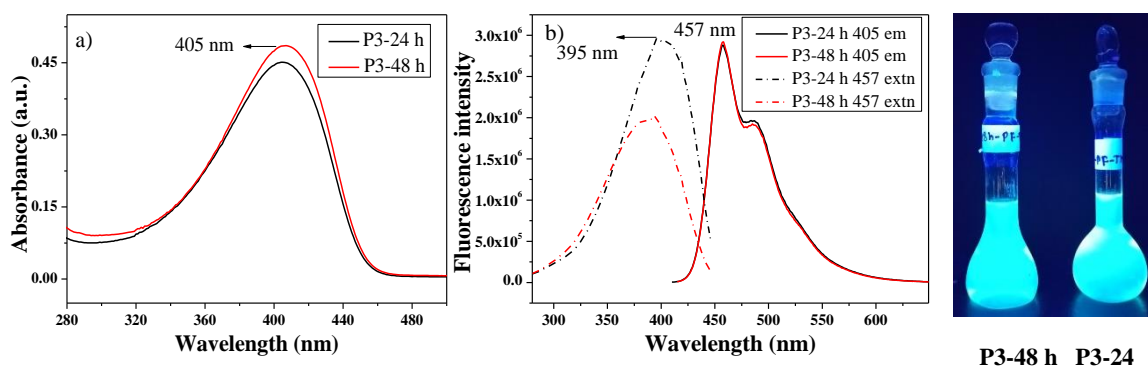
Figure 5.39 a) Absorption b) emission (solid line) and excitation (dotted line) spectra and image of intense cyan colour emission of P3 polymer

Chiral fluorene-alt-thiophene copolymers (P5 and P6) containing chiral fluorene and achiral thiophene were analysed for their photophysical properties. P5 with short handle, which generated only oligomers, showed absorption maxima (λmax) at 392 nm, whereas P6 with long (6 carbon) chiral handle showed absorption maxima (λmax) at 405 nm due to extended conjugation in higher molecular weight polymer.[58] Additionally, the molar absorptivity coefficient of P5 was low compared to P6 (Figure 5.37.a). Both (P5 oligomers and P6) polymers showed emission maxima at 457 nm with cyan coloured emission (Figure 5.37.b). P5 emission intensity was lesser than P6 due to lower molecular weight oligomer formation in P5. Excitation spectra of polymers were recorded by exciting at 457 nm wavelength, which showed maxima around 391 nm. (Figure 5.40.b).
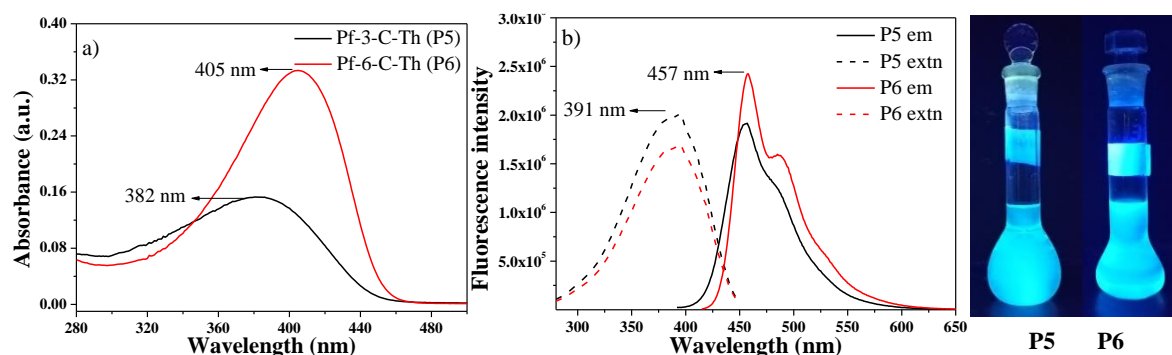
Figure 5.40 a) Absorption b) emission (full) and excitation (dotted) spectra and image of intense cyan colour emission of P1 polymer

P7 (achiral fluorene-alt-chiral thiophene) polymers were synthesized by polymerising for different periods like 12, 24, 48 and 72 hours. Polymers showed defect formation with increased reaction time, affecting their photophysical properties. The 12, 24 and 48 h polymer showed absorption maxima (λmax) at 400 nm, whereas 72 hours polymer exhibited absorption maximum at a lower wavelength of 392 nm due to higher defects in polymeric structure (Figure 5.41.a). All P7 polymers showed emission maxima at 492 nm with intense cyan colour emission. Additionally, the shoulder peak at 460 nm started appearing, whose intensity increased with an increase in reaction time (Figure 5.41.b). Shoulder peaks at lower wavelength may arise from the β-defect from the coupling of fluorene at β position on thiophene. Polymers were excited at 492 nm to record their excitation spectra, which showed excitation maxima around 395 nm. It was observed from Figure 5.41.c that the emission

intensity of polymers decreased with an increase in reaction time due to the increasing defects.
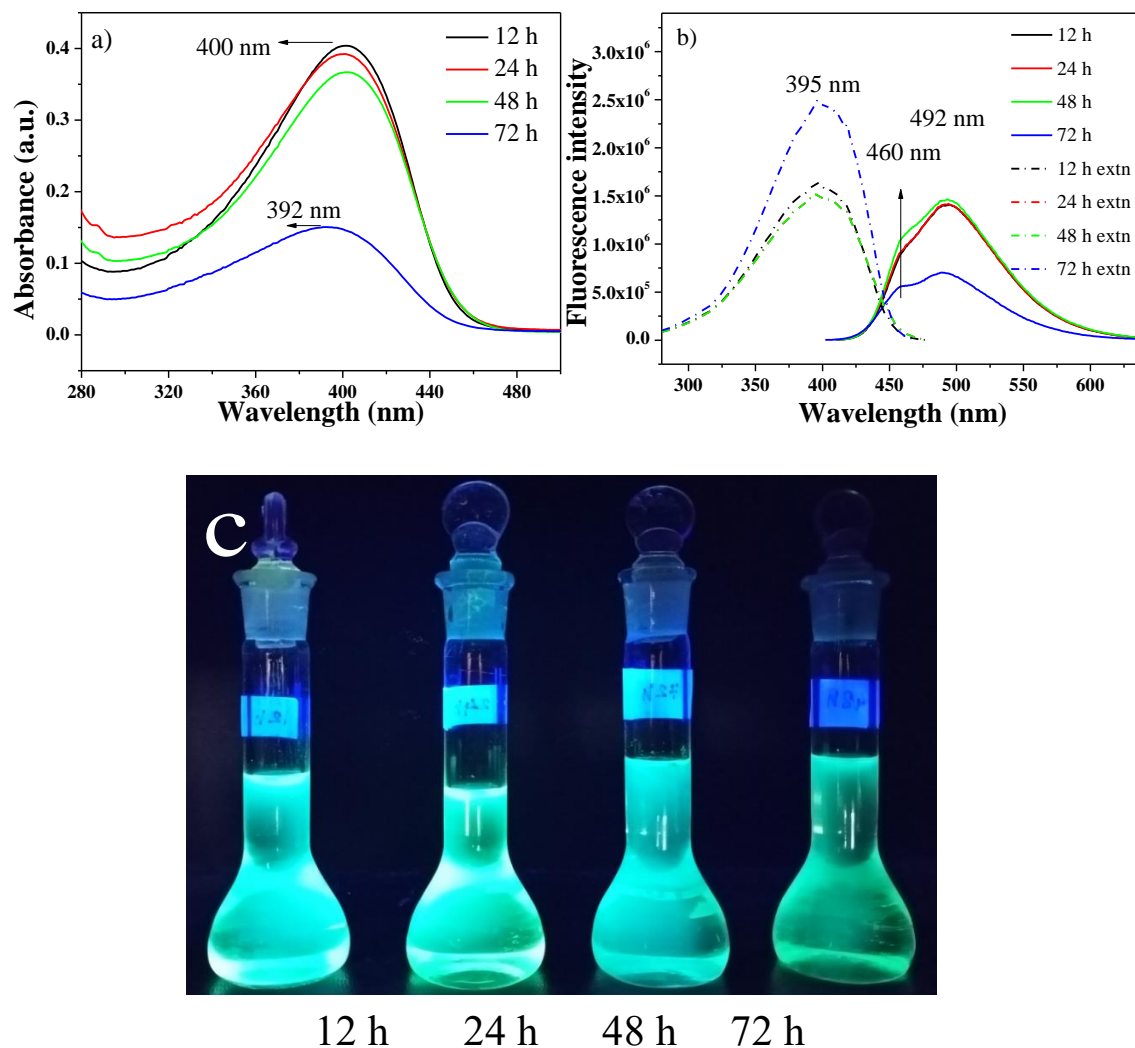
Figure 5.41 a) Absorption b) emission (solid line) and excitation (dotted line) spectra and image of intense cyan colour emission of P7 polymer

5.4 CONCLUSION

The achiral and chiral π-conjugated polymers (P1, P3, P6 and P7) were successfully synthesized by the green approach of DHAP. Polymers with reasonable molecular weights were synthesized in all four cases. In P6 and P7 polymers, chiral pendant (N-Boc-L-glutamic acid-1-tert-butyl ester) was successfully incorporated, either through fluorene (long chiral handle P6) or thiophene (P7). ^{1}H NMR spectra of polymers was analysed to understand the defect formation during polymerization. It was observed that the bulkiness of the chiral pendants had a significant impact on polymerization. The monomer with no bulky pendant or bulky group placed away from the reaction centre generated polymer with reasonable

molecular weights. The defect formed during polymerization significantly impacted the polymers' optoelectronic properties. UV-visible absorbance and emission spectra of polymers were recorded to understand the defects. It can be safely concluded that the DHAP approach can be used as a promising method for the synthesis of π-conjugated polymers if steric impact due to bulky group is managed.

5.5 REFERENCES

(1)   Shirakawa, H.; Louis, E. J.; MacDiarmid, A. G.; Chiang, C. K.; Heeger, A. J. Synthesis of Electrically Conducting Organic Polymers: Halogen Derivatives of Polyacetylene, (CH). *J. Chem. Soc. Chem. Commun.* **1977**, No. 16, 578–580.

(2)   Lu, H.; Li, X.; Lei, Q. Conjugated Conductive Polymer Materials and Its Applications: A Mini-Review. *Front. Chem.* **2021**, *9* (September), 6–11.

(3)   Wang, Y. J.; Yu, G. Conjugated Polymers: From Synthesis, Transport Properties, to Device Applications. *J. Polym. Sci. Part B Polym. Phys.* **2019**, *57* (23), 1557–1558.

(4)   Taylor, D.; Dalgarno, S. J.; Xu, Z.; Vilela, F. Conjugated Porous Polymers: Incredibly Versatile Materials with Far-Reaching Applications. *Chem. Soc. Rev.* **2020**, *49* (12), 3981–4042.

(5)   Morin, P. O.; Bura, T.; Leclerc, M. Realizing the Full Potential of Conjugated Polymers: Innovation in Polymer Synthesis. *Mater. Horizons* **2016**, *3* (1), 11–20.

(6)   Kertesz, M.; Choi, C. H.; Yang, S. Conjugated Polymers and Aromaticity. *Chem. Rev.* **2005**, *105* (10), 3448–3481.

(7)   Rochat, S.; Swager, T. M. Conjugated Amplifying Polymers for Optical Sensing Applications. *ACS Appl. Mater. Interfaces* **2013**, *5* (11), 4488–4502.

(8)   Klingstedt, T.; Nilsson, K. P. R. Conjugated Polymers for Enhanced Bioimaging. *Biochim. Biophys. Acta - Gen. Subj.* **2011**, *1810* (3), 286–296.

(9)   Van Den Eede, M. P.; Van Gestel, L.; Koeckelberghs, G. Expression of Chirality in Tailor-Made Conjugated Polymers. *Macromolecules* **2018**, *51* (17), 6602–6608.

(10)   Pecher, J.; Huber, J.; Winterhalder, M.; Zumbusch, A.; Mecking, S. Tailor-Made Conjugated Polymer Nanoparticles for Multicolor and Multiphoton Cell Imaging. *Biomacromolecules* **2010**, *11* (10), 2776–2780.

(11)   Mei, J.; Bao, Z. Side Chain Engineering in Solution-Processable Conjugated Polymers. *Chem. Mater.* **2014**, *26* (1), 604–615.

(12)   Liu, B.; Bazan, G. C. Homogeneous Fluorescence-Based DNA Detection with Water-Soluble Conjugated Polymers. *Chem. Mater.* **2004**, *16* (23), 4467–4476.

(13)   Zhu, C.; Liu, L.; Yang, Q.; Lv, F.; Wang, S. Water-Soluble Conjugated Polymers for Imaging, Diagnosis, and Therapy. *Chem. Rev.* **2012**, *112* (8), 4687–4735.

(14)   Wang, K. L.; Leung, M. K.; Hsieh, L. G.; Chang, C. C.; Lee, K. R.; Wu, C. L.; Jiang, J. C.; Tseng, C. Y.; Wang, H. T. Conjugated Polymers Containing Electron-Deficient Main Chains and Electron-Rich Pendant Groups: Synthesis and Application to Electroluminescence. *Org. Electron.* **2011**, *12* (6), 1048–1062.

(15)   Drewniak, A.; Tomczyk, M. D.; Knop, K.; Walczak, K. Z.; Ledwon, P. Multiple Redox States and Multielectrochromism of Donor-Acceptor Conjugated Polymers with Aromatic Diimide Pendant Groups. *Macromolecules* **2019**, *52* (21), 8453–8465.

(16)   Higgins, S. J. Conjugated Polymers Incorporating Pendant Functional Groups—

synthesis and Characterisation. *Chem. Soc. Rev.* **1997**, *26* (4), 247–257.

(17) Pandey, M.; Kumari, N.; Nagamatsu, S.; Pandey, S. S. Recent Advances in the Orientation of Conjugated Polymers for Organic Field-Effect Transistors. *J. Mater. Chem. C* **2019**, *7* (43), 13323–13351.

(18) Kimpel, J.; Michinobu, T. Conjugated Polymers for Functional Applications: Lifetime and Performance of Polymeric Organic Semiconductors in Organic Field-Effect Transistors. *Polym. Int.* **2021**, *70* (4), 367–373.

(19) Lei, T.; Cao, Y.; Fan, Y.; Liu, C.; Yuan, S.; Pei, J. High-Performance Air-Stable Organic Field-Effect Transistors: Isoindigo-Based Conjugated Polymers. **2011**, 6099–6101.

(20) Yang, J.; Zhao, Z.; Wang, S.; Guo, Y.; Liu, Y. Insight into High-Performance Conjugated Polymers for Organic Field-Effect Transistors. *Chem* **2018**, *4* (12), 2748–2785.

(21) Zhu, Y.; Babel, A.; Jenekhe, S. A. Phenoxazine-Based Conjugated Polymers: A New Class of Organic Semiconductors for Field-Effect Transistors. *Macromolecules* **2005**, *38* (19), 7983–7991.

(22) Gu, S.; Neugebauer, H.; Sariciftci, N. S. Conjugated Polymer-Based Organic Solar Cells. **2007**, 1324–1338.

(23) Xue, J. Perspectives on Organic Photovoltaics. *Polym. Rev.* **2010**, *50* (4), 411–419.

(24) Leclerc, N.; Chávez, P.; Ibraikulov, O. A.; Heiser, T.; Lévêque, P. Impact of Backbone Fluorination on π-Conjugated Polymers in Organic Photovoltaic Devices: A Review. *Polymers (Basel).* **2016**, *8* (1).

(25) Yang, Y.; Wang, S.; Zhu, Y.; Wang, Y.; Zhan, H.; Cheng, Y. Thermally Activated Delayed Fluorescence Conjugated Polymers with Backbone-Donor/Pendant-Acceptor Architecture for Nondoped OLEDs with High External Quantum Efficiency and Low Roll-Off. *Adv. Funct. Mater.* **2018**, *28* (10), 1–6.

(26) Lu, W.; Kuwabara, J.; Iijima, T.; Higashimura, H.; Hayashi, H.; Kanbara, T. Synthesis of π-Conjugated Polymers Containing Fluorinated Arylene Units via Direct Arylation: Efficient Synthetic Method of Materials for Oleds. *Macromolecules* **2012**, *45* (10), 4128–4133.

(27) Zhang, D.; Huang, T.; Duan, L. Emerging Self-Emissive Technologies for Flexible Displays. *Adv. Mater.* **2020**, *32* (15), 1–42.

(28) Senthilkumar, T.; Parekh, N.; Nikam, S. B.; Asha, S. K. Orientation Effect Induced Selective Chelation of Fe2+ to a Glutamic Acid Appended Conjugated Polymer for Sensing and Live Cell Imaging. *J. Mater. Chem. B* **2015**, *4* (2), 299–308.

(29) Zhang, Z.; Lu, Z.; Yuan, Q.; Zhang, C.; Tang, Y. ROS-Responsive and Active Targeted Drug Delivery Based on Conjugated Polymer Nanoparticles for Synergistic Chemo-/photodynamic Therapy. *J. Mater. Chem. B* **2021**, *9* (9), 2240–2248.

(30) Feng, X.; Lv, F.; Liu, L.; Tang, H.; Xing, C.; Yang, Q.; Wang, S. Conjugated Polymer Nanoparticles for Drug Delivery and Imaging. *ACS Appl. Mater. Interfaces* **2010**, *2*

(8), 2429–2435.

(31) Feng, X.; Lv, F.; Liu, L.; Yang, Q.; Wang, S.; Bazan, G. C. A Highly Emissive Conjugated Polyelectrolyte Vector for Gene Delivery and Transfection. *Adv. Mater.* **2012**, *24* (40), 5428–5432.

(32) Abelha, T. F.; Dreiss, C. A.; Green, M. A.; Dailey, L. A.; Abelha, T. F. Conjugated Polymers as Nanoparticle Probes for Fluorescence and Photoacoustic Imaging. *J. Mater. Chem. B* **2020**, *8* (4), 592–606.

(33) Mcquade, D. T.; Pullen, A. E.; Swager, T. M. Conjugated Polymer-Based Chemical Sensors. **2000**.

(34) Wang, T.; Zhang, N.; Bai, W.; Bao, Y. Fluorescent Chemosensors Based on Conjugated Polymers with N-Heterocyclic Moieties: Two Decades of Progress. *Polym. Chem.* **2020**, *11* (18), 3095–3114.

(35) Cheng, Y. J.; Yang, S. H.; Hsu, C. S. Synthesis of Conjugated Polymers for Organic Solar Cell Applications. *Chem. Rev.* **2009**, *109* (11), 5868–5923.

(36) Okamoto, K.; Luscombe, C. K. Controlled Polymerizations for the Synthesis of Semiconducting Conjugated Polymers. *Polym. Chem.* **2011**, *2* (11), 2424–2434.

(37) Advincula, R. C. Review of Conjugated Polymer Synthesis: Methods and Reactions. *J. Am. Chem. Soc.* **2011**, *133* (14), 5622.

(38) Usluer, Ö.; Abbas, M.; Wantz, G.; Vignau, L.; Hirsch, L.; Grana, E.; Brochon, C.; Cloutet, E.; Hadziioannou, G. Metal Residues in Semiconducting Polymers: Impact on the Performance of Organic Electronic Devices. *ACS Macro Lett.* **2014**, *3* (11), 1134–1138.

(39) Bannock, J. H.; Treat, N. D.; Chabinyc, M.; Stingelin, N.; Heeney, M.; De Mello, J. C. The Influence of Polymer Purification on the Efficiency of poly(3-Hexylthiophene):fullerene Organic Solar Cells. *Sci. Rep.* **2016**, *6* (February), 1–8.

(40) Itahara, T. Arylation of N-Acyl-Pyrroles and -Indoles with Arenes and Palladium Acetate. *J. Chem. Soc. Chem. Commun.* **1981**, No. 5, 254–255.

(41) Itahara, T. Arylation of Aromatic Heterocycles with Arenes and palladium(II) Acetate. *J. Org. Chem.* **1985**, *50* (25), 5272–5275.

(42) Se´vignon, M.; Papillon, J.; Schulz, E.; Lemaire, M. New Synthetic Method for the Polymerization of Alkylthiophenes. *Tetrahedron Lett.* **1999**, *40* (32), 5873–5876.

(43) Wang, Q.; Takita, R.; Kikuzaki, Y.; Ozawa, F. Palladium-Catalyzed Dehydrohalogenative Polycondensation of 2-Bromo-3-Hexylthiophene: An Efficient Approach to Head-to-Tail Poly(3-Hexylthiophene). *J. Am. Chem. Soc.* **2010**, *132* (33), 11420–11421.

(44) Giraud, L.; Grelier, S.; Grau, E.; Hadziioannou, G.; Brochon, C.; Cramail, H.; Cloutet, E. Upgrading the Chemistry of π-Conjugated Polymers toward More Sustainable Materials. *J. Mater. Chem. C* **2020**, *8* (29), 9792–9810.

(45) Gobalasingham, N. S.; Thompson, B. C. Direct Arylation Polymerization: A Guide

to Optimal Conditions for Effective Conjugated Polymers. *Prog. Polym. Sci.* **2018**, *83*, 135–201.

(46)   Pouliot, J. R.; Grenier, F.; Blaskovits, J. T.; Beaupré, S.; Leclerc, M. Direct (Hetero)arylation Polymerization: Simplicity for Conjugated Polymer Synthesis. *Chem. Rev.* **2016**, *116* (22), 14225–14274.

(47)   Ran, Y.; Guo, Y.; Liu, Y. Organostannane-Free Polycondensation and Eco-Friendly Processing Strategy for the Design of Semiconducting Polymers in Transistors. *Mater. Horizons* **2020**, *7* (8), 1955–1970.

(48)   Mercier, L. G.; Leclerc, M. Direct (Hetero)arylation: A New Tool for Polymer Chemists. *Acc. Chem. Res.* **2013**, *46* (7), 1597–1605.

(49)   Burke, D. J.; Lipomi, D. J. Green Chemistry for Organic Solar Cells. *Energy Environ. Sci.* **2013**, *6* (7), 2053–2066.

(50)   Mainville, M.; Leclerc, M. Direct (Hetero)arylation: A Tool for Low-Cost and Eco-Friendly Organic Photovoltaics. *ACS Appl. Polym. Mater.* **2021**, *3* (1), 2–13.

(51)   Mooney, M.; Nyayachavadi, A.; Rondeau-Gagné, S. Eco-Friendly Semiconducting Polymers: From Greener Synthesis to Greener Processability. *J. Mater. Chem. C* **2020**, *8* (42), 14645–14664.

(52)   Hendriks, K. H.; Li, W.; Heintges, G. H. L.; Van Pruissen, G. W. P.; Wienk, M. M.; Janssen, R. A. J. Homocoupling Defects in Diketopyrrolopyrrole-Based Copolymers and Their Effect on Photovoltaic Performance. *J. Am. Chem. Soc.* **2014**, *136* (31), 11128–11133.

(53)   Lombeck, F.; Komber, H.; Gorelsky, S. I.; Sommer, M. Identifying Homocouplings as Critical Side Reactions in Direct Arylation Polycondensation. *ACS Macro Lett.* **2014**, *3* (8), 819–823.

(54)   Hendsbee, A. D.; Li, Y. Performance Comparisons of Polymer Semiconductors Synthesized by Direct (Hetero)Arylation Polymerization (DHAP) and Conventional Methods for Organic Thin Film Transistors and Organic Photovoltaics. *Molecules* **2018**, *23* (6).

(55)   Gobalasingham, N. S.; Thompson, B. C. Direct Arylation Polymerization: A Guide to Optimal Conditions for Effective Conjugated Polymers. *Prog. Polym. Sci.* **2018**, *83*, 135–201.

(56)   Bijleveld, J. C.; Gevaerts, V. S.; Di Nuzzo, D.; Turbiez, M.; Mathijssen, S. C. J.; De Leeuw, D. M.; Wienk, M. M.; Janssen, R. A. J. Efficient Solar Cells Based on an Easily Accessible Diketopyrrolopyrrole Polymer. *Adv. Mater.* **2010**, *22* (35), 242–246.

(57)   Lakowicz, J. R. *General Features of Protein Fluorescence*; 2006.

(58)   Hayashi, S.; Yamamoto, S. I.; Koizumi, T. Effects of Molecular Weight on the Optical and Electrochemical Properties of EDOT-Based π-Conjugated Polymers. *Sci. Rep.* **2017**, *7* (1), 1–8.

CHAPTER 6

Conclusion and Future Perspectives

Chapter 6: *Conclusion and Future Perspectives*

CONCLUSION AND FUTURE PERSPECTIVES

6.1 Conclusion

The thesis entitled "**Synthesis of Various Classes of Chiral Polymers and their Application in Enantioselective Separation**" highlighted the design and synthesis of different chiral polymers and their utility in enantioselective separation. The chirality induction in polymeric structure was achieved by using chiral pendant groups or post polymer modification of a chiral polymer with chiral moiety. Protected amino acids such as D/L-aspartic acid, L-glutamic acid, and L-tryptophan were used as chiral pendants in polyfluorene, while phthaloyl protected L-leucine acid chloride was used for post polymer modification of achiral polystyrene. Polyfluorenes with chiral pendent groups achieved better separation compared to modified chiral polystyrene, as all repeating units in polyfluorene possessed two chiral centers in their pendant, whereas only ~34% post polymer chiral modification could be achieved in the case of polystyrene. Different strategies such as the coating on mesoporous AAO membranes or making polymeric microspheres induced porosity and increased available surface area. These polymer-coated porous AAO membranes and chiral polymeric microspheres were employed to achieve enantioselective separation of an aqueous racemic mixture of different native amino acids by simple enantioselective filtration assay. The developed assay achieved separation without using any costly, high-end chromatographic instrument.

In the first working chapter, we have designed and synthesized protected D/L-aspartic acid-containing polyfluorenes. These chiral polymers were coated on mesoporous AAO membranes (200 nm pore size). The chiral polymer-coated AAO membranes show an ability to distinguish between enantiomers of amino acids. The enantiomers with the same chirality selectively get adsorbed inside chiral pores leaving behind others in solution, resulting in the enantioselective separation by simply removing the membranes from the solution. The quantification of enantioselective separation was determined by recording the CD spectra of the remaining solution after performing an enantioselective assay. % ee values for enantioselective separation were determined by taking the ratio of area under the curve of the remaining solution and reference solution. Among tested amino acid racemic mixtures highest separation was achieved for glutamic acid (~95 % ee) in 24 h. Other amino acids like alanine, leucine, lysine, and aspartic acid are separated with ee % > 80. The highest separation value of ~98 % ee was achieved in 48 h using four membranes. By varying the

pore size of the AAO membrane, the ee % can be modulated as the pore size controls the degree of confinement of the chiral polyfluorene.

In the second working chapter, we studied the effect of a different chiral handle on the separation efficiency. Polyfluorenes containing different chiral handles like Protected L-glutamic acid and protected L-tryptophan (PF-LTrp and PF-LGlu) were synthesized and coated on 200 nm pore sized AAO membranes to induce porosity in polymeric microstructures. A simple enantioselective filtration assay developed in the first working chapter was utilized to separate different amino acid racemic mixtures. PF-LTrp@AAO membranes with chiral aromatic pendants achieved the highest separation for aromatic amino acids like tryptophan (91.3 % ee) and phenylalanine (87.6 % ee), while PF-LGlu@AAO membranes with aliphatic pendants achieved the highest separation for glutamic acid racemic mixture (~92 % ee). These differences in the selectivity shown by these polymeric chiral selectors depend upon the type and extent of interactions. Aromatic pendant containing PF-LTrp@AAO membranes separate aromatic amino acids like tryptophan and phenylalanine with the highest % ee due to π-π interactions in addition to H-bonding interactions. The protected glutamic acid-containing polyfluorenes membranes (PF-LGlu@AAO) separate glutamic acid and other aliphatic amino acids with the highest % ee due to hydrogen bonding interactions. The tailor-made chiral selectors can achieve enantioselective separation of desired racemic mixtures if interaction and structures are studied carefully.

The first two working chapters demonstrated the fabrication and application of chiral π-conjugated polyfluorene coated AAO membranes for simple filtration based enantioselective separation. In the third working chapter, we mainly focus on the synthesis of chiral polystyrene (commodity polymer), a cost-effective alternative. Polystyrene with desired molecular weight and controlled polydispersity synthesized using RAFT polymerization, followed by post polymer Friedel Crafts acylation with phthaloyl protected L-leucine acid chloride. Post polymer modification with leucine induced chirality in polymeric structure. The synthesized protected polymer (Protected PS-L-Leu) was deprotected to give deprotected PS-L-Leu. Deprotection enhances the polymer hydrophilicity and changes its morphology from irregular to fibrous. These protected and deprotected polymers were used as-is as well as self-assembled in the form of microspheres to carry out enantioselective separation of leucine and alanine racemic mixture by developed enantioselective assay. The highest separation was achieved using deprotected polymeric

(Deprotected PS-L-Leu) microspheres. The enhancement in the % ee in the deprotected polymeric microsphere arises from high available surface area and enhanced surface wettability due to increased hydrophilicity. The highest % ee of 81.57 was achieved for separating leucine racemic mixture using 12 mg of deprotected PS-L-Leu microspheres.

In the fourth working chapter, we synthesized chiral π-conjugated polymers by the green DHAP approach. The DHAP method does not require pre-functionalization of monomers and does not produce hazardous organometallic by-products, making it an economically viable and green method compared to conventional C-C bond-forming cross-coupling reactions. We could synthesize fluorene thiophene copolymers containing protected L-glutamic acid as a pendant group with reasonable molecular weight. Steric hindrance created by bulky chiral pendant groups restricts the molecular weight build-up. The steric hindrance issue was addressed by using chiral-achiral monomer combinations or placing the chiral center away from the reaction center. ^{1}H NMR spectra were analyzed to understand the defect formation during polymerization due to bulky chiral pendent groups. It was observed that the bulkiness of the chiral pendants had a significant impact on polymerization. The monomer with no bulky pendant or bulky group placed away from the reaction center generated polymer with reasonable molecular weights. The defect formed during polymerization significantly impacted the polymers' optoelectronic properties. UV-visible absorbance and emission spectra of polymers were recorded to understand the defects. It can be safely concluded that the DHAP approach can be used as a promising method for the synthesis of π-conjugated polymers if steric impact due to bulky group is managed.

6.2 Future Perspective

Developing an enantioselective separation strategy using a simple and cost-effective method and chiral selectors is of great commercial interest due to the growing demand for enantiopure compounds in pharmaceutical, agrochemical, and aroma or fragrance industries. The use of commodity polymers as chiral selectors can serve the purpose. Synthesis of functionalized chiral styrene monomers, followed by its polymerization using some crosslinker, will give cost-effective material. Polymerization of chiral styrene monomers ensures the maximum chiral center polymeric structure, where non-selective adsorption can be avoided while using a crosslinker will provide additional stability to the polymeric particles and help in retaining shape and morphology. Different chiral moieties can be covalently stitched to styrene monomer using simple click chemistry, DCC DMAP or

EDC/NHS coupling. The crosslinker like divinylbenzene (DVB) or glutaraldehyde can be used as crosslinker. The representative example of L-glutamic acid-containing polystyrene synthesis is shown in Scheme 1.
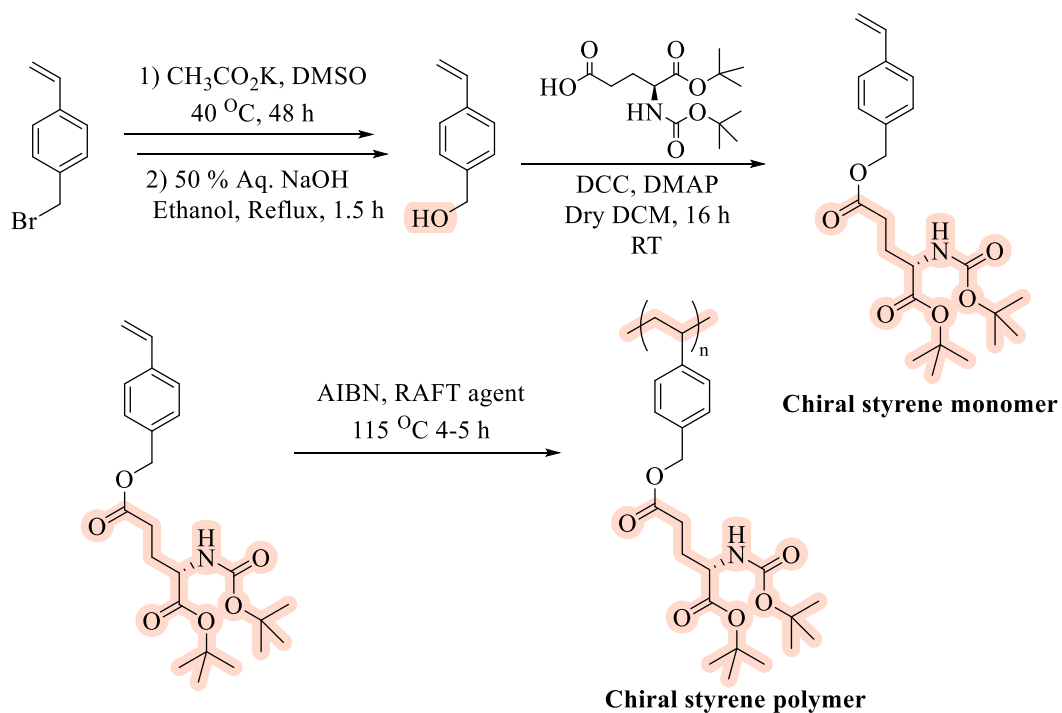
Scheme 1: General Scheme for Synthesis of Chiral Polystyrene

ABSTRACT

Name of the Student: Shrikant Babanrao Nikam	**Registration No.:** 10CC15A26027
Faculty of Study: Chemical Science	**Year of Submission:** 2021
AcSIR academic centre/CSIR Lab:	**Name of the Supervisor:** Dr. Asha S.K.
CSIR-National Chemical Laboratory, Pune	

Title of the thesis: Synthesis of Various Classes of Chiral Polymers and their Application in Enantioselective Separation

----

The production of chemical compounds in enantiopure forms is of great interest in drug, agrochemical, food, and fragrance industries. Despite having the same chemical structures, enantiomers of drugs differ significantly in their therapeutic efficacy and pharmacokinetics, resulting in diversified pharmacological actions and pharmacodynamics, which developed the scientific quest to obtain chemical compounds in enantiopure form. The approaches to obtaining enantiopure compounds are subdivided into chiral and racemic approaches. The chiral approach deals with synthesizing a single enantiomer, while the racemic approach deals with the separation of enantiomers. Different methods like enantioselective crystallization, chiral chromatographic methods, converting enantiomers into diastereomers, and membrane-based filtration are developed. All these enantioselective separation methods need chiral selectors that can distinguish between enantiomers. The different chiral selectors like cyclodextrins, polysaccharides, micelles, proteins, macrocyclic glycopeptides, crown ethers, metal-organic framework (MOF), covalent organic framework (COF), high Miller index metal surfaces, and polymers are used. This thesis aims to develop chiral polymeric chiral selectors and a cost-effective enantioselective filtration method. Chapter 1 discuss and compare different enantioselective separation methods and chiral selectors in literature. Chiral polyfluorene-coated anodic aluminium oxide (AAO) membranes were used in chapter 2 to separate the native amino acid racemic mixture by a simple filtration method. The effect of different chiral handles on selectivity and separation efficiency was studied in chapter 3. Cost-effective commodity polymer (chiral polystyrene) microspheres were used to separate the native amino acids racemic mixture by a simple enantioselective filtration method. In chapter 5, chiral π-conjugated polymers were synthesized using a relatively green direct heteroarylation (DHAP) polymerization method. Overall, the thesis provides a simple, cost-effective, and efficient enantioselective filtration method using chiral polymeric membranes or microspheres as a chiral selector.

List of Publications Emanating from the Thesis Work

1. **Shrikant B Nikam,** Asha S.K. Enantioselective Separation Using Chiral Amino Acid Functionalized Polyfluorene Coated on Mesoporous Anodic Aluminium Oxide Membranes. *Anal. Chem.* **2020**, *92*, 10, 6850–6857.

2. **Shrikant B. Nikam,** Asha S. K. Enantioselective separation of amino acids using chiral polystyrene microspheres synthesized by post polymer modification approach *ACS Polymer Au*

3. **Shrikant B. Nikam,** Asha S. K. Synthesis of Chiral ∏-Conjugated Polymers by DHAP Route *(Manuscript under preparation)*

List of Publications Non-Emanating from the Thesis Work

1. T. Senthilkumar, N. Parekh, **Shrikant B Nikam**, Asha S. K. Orientation effect induced selective chelation of Fe^{2+} to a glutamic acid appended conjugated polymer for sensing and live-cell imaging. *J. Mater. Chem. B,* **2016**, *4*, 299-308.

2. B. P. Mali, S. R. Dash, **Shrikant B. Nikam**, A. Puthuvakkal, K. Vanka, K. Manoj and R. G. Gonnade. Five concomitant polymorphs of a green fluorescent protein chromophore (GFPc) analogue: understanding variations in photoluminescence with p-stacking interactions. *Acta Cryst. B* **2020**, *76*, 1-15.

Patents

1. **Shrikant B. Nikam**, Asha S. K. A Process for Enantioselective Separation of Amino Acids Using Chiral Polystyrene *(Provisional application number 202111058074)*

List of Posters Presented with Details

National Science Day 2016 Poster presentation at CSIR-National Chemical Laboratory, Pune, (India). (February **2016**)

Title: Glutamic Acid Appended Water-Soluble Conjugated Polymers for Fluorescence Sensing and Imaging of Fe^{2+} Ions in Live Cells

Abstract: Intracellular detection of labile Fe^{2+} ions and live-cell imaging using a water-soluble biocompatible probe is essential in tracking physiological processes and maintaining a healthy balance of ions. Here we have developed a water-soluble polymer-based probe for the fluorescence sensing and live-cell imaging of labile Fe^{2+} ions with high selectivity and sensitivity. A water-soluble conjugated polyfluorene probe was developed, appended with amino acid (L-glutamic acid). The polymeric probe showed excellent cell viability (90%) even at a 300 μg/ml concentration when checked using MTT assay. L-glutamic acid appended polyfluorene exhibited selective chelation to Fe^{2+} ions over other ions resulting in immediate sensing activity for Fe^{2+} ions in water and living cells with fluorescence turn-off response. The PF-Ph-GA polymer probe's detection limit was 46 (±2) nM. The polymer exhibited improved sensing activity in an intracellular pH range of 5–9, which is an advantage in differentiating endogenous changes. The probe was successfully applied for the fluorescence imaging of intracellular and supplemented labile Fe^{2+} pools in living HeLa cells.

SPSI MACRO 2017 Poster Presentation at International Conference on Polymers Science and Technology Thiruvananthapuram (India). (January **2017**)

Title: Glutamic Acid Appended Water-Soluble Conjugated Polymer for Fluorescence Sensing and Imaging of Fe2+ Ions in Live Cells

Abstract: The ferrous state of iron (Fe^{2+}) is predominantly favored inside the cell by inherent factors such as reductive environment, higher water solubility, and ferric reductase enzyme presence. Iron flexibly shuttles between Fe2+/Fe3+ oxidation states. The levels of iron and the balance in the oxidation states must be maintained as iron overloading causes a variety of disorders such as cell damage, abnormal production of reactive oxygen species, hepatitis, organ

dysfunction, Alzheimer's and Parkinson's diseases. Intracellular detection and imaging of labile iron (II) pools are crucial in tracking physiological processes, cell metabolism, and in addition, it facilitates access for understanding the mechanisms of biological reactions that demand new and rapid sensing probes. The polymer probe was based on conjugated polyfluorene, which was appended with amino acid (L-glutamic acid). Simple glutamic acid did not show selectivity towards any of the divalent ions. However, glutamic acid appended polyfluorene exhibited selective chelation to Fe2+ ions resulting in immediate sensing activity for Fe2+ ions in water and living cells with fluorescence turn-off response. The biocompatibility of the polymer was confirmed from an MTT assay which demonstrated > 90% cell viability even at 300 μg ml^{-1} loading of polymers. The PF-Ph-GA polymer probe's detection limit was 46 ($\pm$2) nM, which indicated high sensitivity for Fe2+ over other ions reported in the literature. The polymer also exhibited improved sensing activity in the range of intracellular pH (5–9), which differentiates endogenous changes. The probe was successfully applied for the fluorescence imaging of intracellular and supplemented labile iron (II) pools in living HeLa cells.

NCL-RF annual students' Conference Oral Presentation at CSIR-National Chemical Laboratory, Pune, (India). (November **2018**) **Best Oral Presentation**

Title: Chiral Amino acid Functionalized Polyfluorenes Supported on Mesoporous Anodic Aluminium Oxide (AAO) Membranes for Enantioselective Separation

Abstract: Functionalization of conjugated polymers with chiral moieties like amino acids are known to confer homochirality to the parent conjugated polymer. Homochiral materials can perform chiral sensing as well as enantioselective separation. Although asymmetric synthesis is one of the most common methods reported for obtaining chiral materials, it is limited that high enantiomeric purity can be achieved only for exceptionally enantioselective reactions. In this regard, protected L-glutamic acid appended polyfluorene was shown to achieve efficient heterogeneous enantioselective separation and chiral sensing of a wide variety of substrates from their aqueous racemic mixture.

This work presents optically active polyfluorenes bearing protected chiral amino acids (D & L Aspartic acid) as pendant groups. Mesoporous anodic aluminium oxide (AAO) membranes with 200 nm pore size were used to immobilize these chiral amino acids appended polyfluorenes. D

or L Aspartic acid appended polyfluorene dissolved in tetrahydrofuran (THF) as solvent was passed through the alumina membrane under suction to generate enantioselective chiral porous membranes. Circular dichroism (CD) spectroscopy was used to demonstrate the enantioselective separation.

SPSI MACRO 2018 Oral Presentation at International Conference on Polymers Science and Technology Pune, (India). (December **2018**)

The chiral materials are of interest for scientific and economic reasons. Achieving novel enantiomerically pure compounds is very difficult. The most common methods for obtaining chiral materials reported so far are based on asymmetric synthesis. Despite the noticeable advantages, the asymmetric synthesis has an obvious limitation, like it gives high enantiomeric purity only for exceptionally enantioselective reactions. The ability of the enantiomers to differentiate chiral environment sets a basis for the resolution of enantiomers from their racemic mixtures. The membrane-based enantioselective separation of enantiomers is an attractive method-as it does not require high-end chromatographic instruments and a skilled workforce.

Here we demonstrated the synthesis of optically active polyfluorenes bearing protected chiral amino acids (D & L Aspartic acid) as pendant groups. These optically active polymers were coated on the anodic aluminium oxide (AAO) membranes with 200 nm pore size. These chiral polymers coated porous membranes were used to carry out enantioselective separation of 9 different amino acid racemic mixtures from their aqueous racemic mixture. The results were investigated using a CD spectrophotometer. The highest 95 % ee is achieved for a glutamic acid racemic mixture.

 Humboldt Kolleg poster presentation Innovation and Entrepreneurship: sole of science and Technology, Kashid, (India). (February **2019**) **Best Poster Award**

Title: Effect of Different Pore-Sized Anodic Aluminium Oxide Membranes (AAO) on Enantioselective Separation.

Abstract: Homochiral materials possess the potential to perform chiral sensing as well as enantioselective separation. Functionalisation of conjugated polymers with chiral moieties like amino acids confer homochirality to the parent conjugated polymer. Asymmetric synthesis is

one of the most widely used methods reported for synthesizing chiral materials. The method has a limitation that high enantiomeric purity can be achieved only for exceptionally selective reactions. The second most common method is enantioselective separation. In this regard, efficient heterogeneous enantioselective separation and chiral sensing of a wide variety of analytes from their aqueous racemic mixture is achieved by the use of protected L-glutamic acid appended polyfluorene. This work presents optically active polyfluorenes bearing protected chiral amino acids (D & L Aspartic acid) as pendant groups. Mesoporous anodic aluminium oxide (AAO) membranes with different pore sizes (200, 100, 20 nm) were used to support the immobilization of these chiral amino acids appended polyfluorenes. D or L Aspartic acid appended polyfluorene dissolved in tetrahydrofuran (THF) as solvent. The polymer solution was passed through the alumina membrane under suction to generate enantioselective chiral porous membranes. Circular dichroism (CD) spectroscopy was used to demonstrate the enantioselective separation.

National Science day Poster presentation at CSIR-National Chemical Laboratory, Pune, (India). (February **2019) NCL-RF Agnimitra memorial best poster award**

Title: Effect of Different Pore-Sized Anodic Aluminium Oxide Membranes (AAO) on Enantioselective Separation.

Abstract: Homochiral materials possess the potential to perform chiral sensing as well as enantioselective separation. Functionalisation of conjugated polymers with chiral moieties like amino acids confer homochirality to the parent conjugated polymer. Asymmetric synthesis is one of the most widely used methods reported for synthesizing chiral materials. The method has a limitation that high enantiomeric purity can be achieved only for exceptionally selective reactions. The second most common method is enantioselective separation. In this regard, efficient heterogeneous enantioselective separation and chiral sensing of a wide variety of analytes from their aqueous racemic mixture are achieved by the use of protected L-glutamic acid appended polyfluorene. This work presents optically active polyfluorenes bearing protected chiral amino acids (D & L Aspartic acid) as pendant groups. Mesoporous anodic aluminium oxide (AAO) membranes with different pore sizes (200, 100, 20 nm) were used to support the immobilization of these chiral amino acids appended polyfluorenes. D or L Aspartic acid appended polyfluorene dissolved in tetrahydrofuran (THF) as solvent. The polymer

solution was passed through the alumina membrane under suction to generate enantioselective chiral porous membranes. Circular dichroism (CD) spectroscopy was used to demonstrate the enantioselective separation.

MACROMEET-2021 Oral presentation at CSIR-National Chemical Laboratory, Pune, (India). (November **2021**)

Title: Synthesis of Various Classes of Chiral Polymers and their Application in Enantioselective Separation

Abstract: Enantiopure compounds have a vast market in the pharmaceutical, food, fragrance and agricultural industries. Commercially enantioselective separation is a costly process due to the use of costly high-end chromatographic instruments or enantiopure sacrificial agents, which subsequently add up to the final product cost. We present polymer-based approaches where enantiopure compounds could be obtained using a simple filtration method without using any costly high-end chromatographic instrument. Polymers like polyfluorenes and commodity polymer like polystyrene were modified with chiral amino acids to develop a cost-effective and commercially viable, filtration based enantioselective separation without the requirement for high-end chromatographic instruments

List of Conference Attended with Details

SPSI MACRO International Conference on Polymers Science and Technology Thiruvananthapuram, (India). **2017**

FCS International Conference on Fluorescence and Raman Spectroscopy at IIT Guwahati, (India). **2017**

SPSI MACRO International Conference on Polymers Science and Technology IISER Pune, (India). **2018**

(**Humboldt Kolleg**) "Humboldt kolleg on innovation and entrepreneurship: role of science and technology" Kashid, (India). **2019**

ABOUT THE AUTHOR

Mr. Shrikant was born to Shri. Babanrao and Smt. Alka Nikam in 1990 at Arak, a small village in the Washim district of Maharashtra (India). The author started his primary schooling at Z. P school in the same village and moved to Jawahar Navodaya Vidyalaya, Washim, and completed higher secondary education in 2008. He completed his graduation from Shri. Shivaji College of Arts, Commerce, and Science, Akola (Maharashtra) (2011). The author pursued his master's degree in Chemistry from the Post Graduate Teaching Department of Chemistry, SGB Amaravati University, Amravati (Maharashtra). After qualifying CSIR-UGC National Eligibility Test (NET-JRF) examination with AIR 51, he joined the Polymer Science and Engineering (PSE) Division of CSIR-National Chemical Laboratory, Pune, India, as a Junior Research Fellow (JRF) to pursue his Ph.D. degree under the supervision of Prof. Dr. S. K. Asha (August 2015). He has received the research fellowship (JRF and SRF) from the Council of Scientific and Industrial Research (CSIR), New Delhi, India, to carry out the Ph.D. thesis work.

Correction to Enantioselective Separation Using Chiral Amino Acid Functionalized Polyfluorene Coated on Mesoporous Anodic Aluminum Oxide Membranes

Shrikant B. Nikam and Asha SK*

Cite This: *Anal. Chem.* 2021, 93, 10388−10388

Read Online

ACCESS | Metrics & More | Article Recommendations

The author information in the original manuscript should be corrected from

Asha SK − Polymer Science and Engineering Division, CSIR-National Chemical Laboratory, Pune 411008, India; Academy of Scientific and Innovative Research, New Delhi 110025, India; orcid.org/0000-0002-3999-4810; Email: sk.asha@ncl.res.in; Fax: 0091-20-25902615
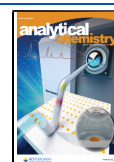
Shrikant B. Nikam − Polymer Science and Engineering Division, CSIR-National Chemical Laboratory, Pune 411008, India; Academy of Scientific and Innovative Research, New Delhi 110025, India; orcid.org/0000-0001-6718-9002

to

Asha SK − Polymer Science and Engineering Division, CSIR-National Chemical Laboratory, Pune 411008, India; Academy of Scientific and Innovative Research (AcSIR), Ghaziabad 201002, India; orcid.org/0000-0002-3999-4810; Email: sk.asha@ncl.res.in; Fax: 0091-20-25902615

Shrikant B. Nikam − Polymer Science and Engineering Division, CSIR-National Chemical Laboratory, Pune 411008, India; Academy of Scientific and Innovative Research (AcSIR), Ghaziabad 201002, India; orcid.org/0000-0001-6718-9002

Enantioselective Separation Using Chiral Amino Acid Functionalized Polyfluorene Coated on Mesoporous Anodic Aluminum Oxide Membranes

Shrikant B. Nikam and Asha SK*

Read Online

ACCESS | Metrics & More | Article Recommendations | SI Supporting Information

ABSTRACT: Homochiral mesoporous anodic aluminum oxide membranes (AAO) were prepared by coating protected chiral D/L aspartic acid appended polyfluorene in the pores. These chiral AAO membranes successfully demonstrated enantioselective recognition and separation of a range of amino acids from their aqueous racemic mixture by simple filtration. Enantioselective separation was achieved by selective adsorption of one enantiomer from the aqueous racemic mixture into the chiral pores of the AAO membrane leaving the filtrate enriched with the other enantiomer. Extraction and quantification of the adsorbed amino acid (glutamic acid) demonstrated that 1 mg of homochiral polyfluorene could effectively extract about 3.5 mg of glutamic acid with 95% enantiomeric excess in 24 h. This is one of the highest enantiomeric excesses (ee %) and yields reported so far in the literature for a racemic mixture of glutamic acid. The pore size of the AAO membrane influenced the efficiency of separation with a reduction in pore size from 200 to 20 nm leading to reduced ee % (∼95% to ∼28%). These results raise the possibility for a facile method to carry out enantioselective separation.
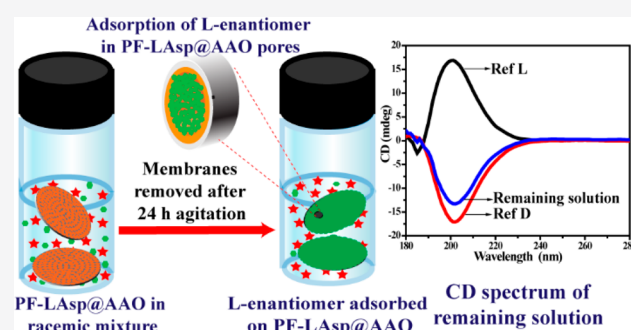
Chirality is omnipresent in nature; the handedness of biomolecules like DNA,[1] proteins,[2] enzymes, sugars,[3] and amino acids have a large influence on the life on Earth[4,5] The active sites of biomolecules bind exclusively to only one enantiomer of chiral substrates. This handedness of biomolecules often contributes to the exceptional specificity and selectivity toward metabolic processes and therapeutic efficacy.[6] In this context, it is important to realize that more than 50% of the drugs currently in pharmaceutical use have at least one chiral center in their structure.[7] The enantiomers of many chiral drugs differ significantly in their pharmacokinetic parameters resulting in diversified pharmacological actions and pharmacodynamics despite having the same chemical structure.[8−10] The requirement for the safe and effective therapeutic use of the drug has resulted in a scientific quest for the development of robust, scalable, and efficient strategies for the synthesis of drugs in their enantiopure form.[11] This quest has given a tremendous boost in the progress of asymmetric synthesis, which is the most common approach for the synthesis of a single enantiomer.[12−15] Although this is the currently favored approach for accessing enantiopure molecules, it has several disadvantages including its requirement for expensive and environmentally hazardous transition metal catalyst with homochiral ligands and highly enantiopure starting material.[16−21] The regioselectivity observed with some of these asymmetric reactions are such that small

changes in the nature of the ligand, solvent, or even that of the protecting groups can severely skew the isolated yields of the enantiomerically pure compound.[16] Resolution of a racemic mixture in enantiomerically pure form is another approach that has attracted great attention in the recent decades. Generally this is achieved with the help of various chromatographic techniques which usually need a skilled operator for handling the high end instrumentation.[22,23] These resolution techniques need homochiral selectors, which should discriminate between pairs of enantiomers. The most commonly used chiral selectors are polysaccharides, cyclodextrins, proteins, crown ethers, micelles, and macrocyclic glycopeptides.[24,25] Apart from these, homochiral polymers is a distinct class of material which is used as a chiral selector for carrying out enantioselective separation of racemic mixtures.[26−31] In most of the published reports, homochiral polymers are coated on solid mesoporous materials which makes the surface homochiral in nature.[32−35] Mesoporous material not only acts as a solid support but also gives additional stability to the
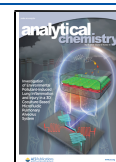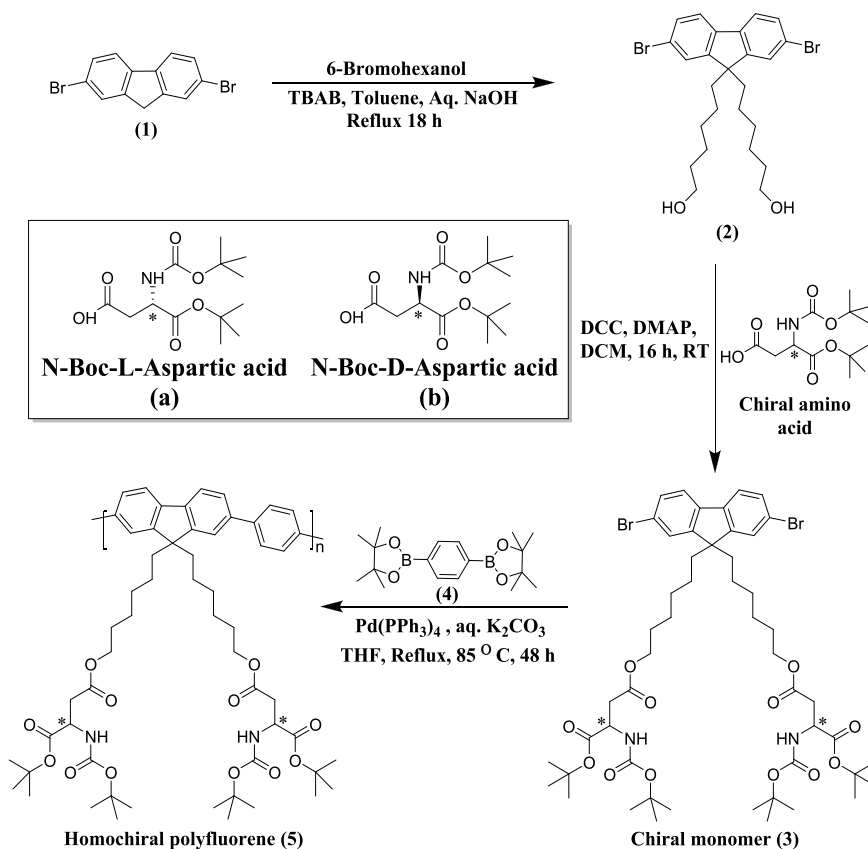
Scheme 1. Schematics for the Synthesis of Homochiral Polyfluorenes PF-LAsp (5a) and PF-DAsp (5b) Having N-Boc-L-Aspartic Acid (a) and N-Boc-D-Aspartic Acid (b) as Pendent Groups, Respectively

homochiral polymers and provides high surface area for enantioselective separation.[36,37] Among homochiral polymers, polyfluorenes were synthesized and studied extensively by Meskers et al. in terms of its chiroptical properties, supramolecular chirality, liquid crystalline, and biomimetic properties.[38−42] Very few reports are available where chiral polyfluorene was used for carrying out an enantioselective separation of the racemic mixture.[43,44] In our group, L-glutamic acid (protected) appended homochiral polyfluorene was synthesized and applied for the heterogeneous enantioselective separation of a wide range of racemic mixtures of amino acids, sugars, amino alcohol, hydroxy acid, ascorbic acid, etc. from their aqueous solution.[45] A helical porous morphology enabled the enantioselective uptake of the L-form of the enantiomer from their racemic mixture in water leaving the water enriched with the D-enantiomer.

In the current research article, we focus on the enantioselective separation of racemic mixtures using mesoporous anodic aluminum oxide (AAO) membranes coated with homochiral polyfluorene. Two optically active homochiral polyfluorenes, PF-LAsp and PF-DAsp, bearing protected L- and D-aspartic acid as pendant groups, respectively, were synthesized and coated on AAO membranes. The 2D (dimensional) confinement of the homochiral polymer within the cylindrical channels of the AAO membrane was expected to increase the available chiral surface area, resulting in enhanced enantioselective chiral separation.[46−48] An unprecedented ee of ~95% could be achieved for the separation of glutamic acid from its aqueous racemic mixture. This is the first article where polyfluorene-coated homochiral AAO mem-

branes are reported for enantioselective separation of an aqueous racemic mixture of amino acid in their native form. The current work also explores the enantioselective uptake, kinetics of separation, and effect of pore size of AAO membrane on separation efficiency.

■ EXPERIMENTAL SECTION

Materials. 2,7-Dibromofluorene and 6-bromo-1-hexanol were purchased from TCI Chemicals. 4-Dimethylaminopyridine (DMAP), dicyclohexylcarbodiimide (DCC), and tetrabutylammonium bromide (TBAB) were purchased from Spectrochem Pvt. Ltd. (India). Pd(PPh₃)₄, benzene-1,4-diboronic acid, IR grade potassium bromide (KBr), and CDCl₃ were purchased from Sigma-Aldrich. N-Boc-L-aspartic acid-1-tert butyl ester, N-Boc-D-aspartic acid-1-tert butyl ester, N-Boc-L-glutamic acid-1-tert butyl ester and N-Boc-D-glutamic acid-1-tert butyl ester (Boc = tert-butoxycarbonyl) were purchased from Alfa Aesar Chemical Ltd. NaOH, Na₂SO₄, Na₂CO₃, K₂CO₃, and solvents like toluene, tetrahydrofuran (THF), methanol, and dichloromethane (DCM) were purchased from Merck Chemicals. Ethyl acetate and pet ether were purchased locally. Solvents were dried by standard drying procedures. HPLC grade THF was purchased from Merck Chemicals. Anodic aluminum oxide membrane with nominal pore diameters of 200, 100, and 20 nm respectively, diameter 13 mm, mass 10−20 mg, 50 μm nominal thickness, porosity of 0.12−0.15, pore density 5×10^8 ($\pm20\%$), 2×10^9 ($\pm20\%$), and 5.8×10^{10} ($\pm20\%$) cm^{-2}, respectively, air permeability at 20 °C in the range of 10^{-8} to 10^{-4} cm/s/Pa and water permeability at 20 °C in the range of 10^{-10} to 10^{-6}

cm/s/Pa were purchased from SPI supplies USA (the characterization details are as provided by the supplier).

Synthesis and Characterization. The synthesis of the D- and L-aspartic acid appended polyfluorene PF-DAsp and PF-LAsp was completed as shown in Scheme 1.

The detailed synthesis and characterization can be found in the Supporting Information (sections S8 and S9, Figures S2–S18). The molecular weights of polymers were determined by GPC using THF as the solvent (Figure S18). The number and weight-average molecular weight (Mn and Mw), polydispersity index ($Đ_M$), and degree of polymerization (Xn) for both the polymers PF-LAsp and PF-DAsp are shown in Table S1. PF-LAsp has an Mn of 25 000 (∼51 repeating units), while PF-DAsp has an Mn of 21 400 (∼43 repeating units). For comparative studies, the D/L glutamic acid appended polyfluorene (PF-D/LGlu previously reported by us[45]) was freshly synthesized (section S10) and characterized, the details of which are provided in Figures S19–S25 and Table S2.

■ RESULTS AND DISCUSSION

Figure 1 shows the FE-SEM micrographs of the bare (a) and polymer coated (b) homochiral AAO membranes.
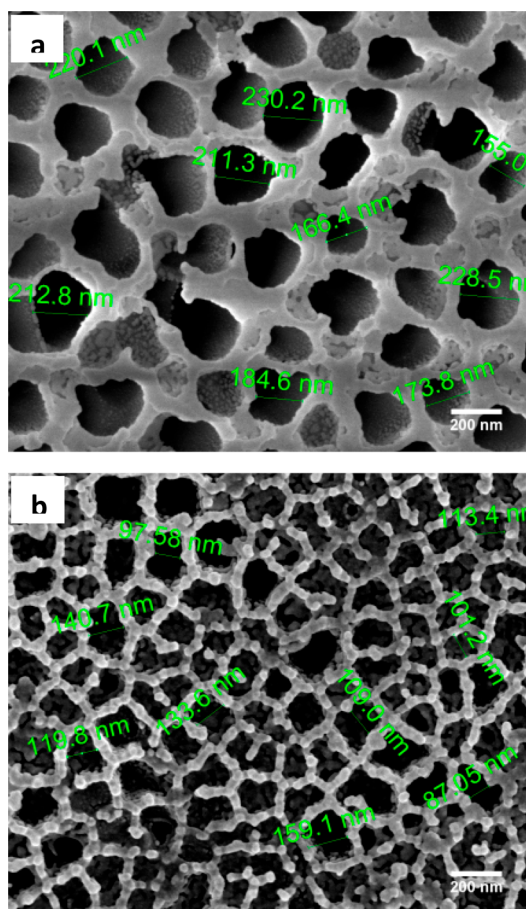

Figure 1. FE-SEM micrographs of (a) bare AAO (200 nm) membrane and (b) polymer-coated homochiral AAO membrane.

The pore size dimensions computed using ImageJ software shows a reduction of average pore size from ∼200 nm for the bare AAO membrane to 100−160 nm for the polymer-coated membrane. Although the SEM images provide clear visual evidence for a decrease in pore diameter, it is only qualitative
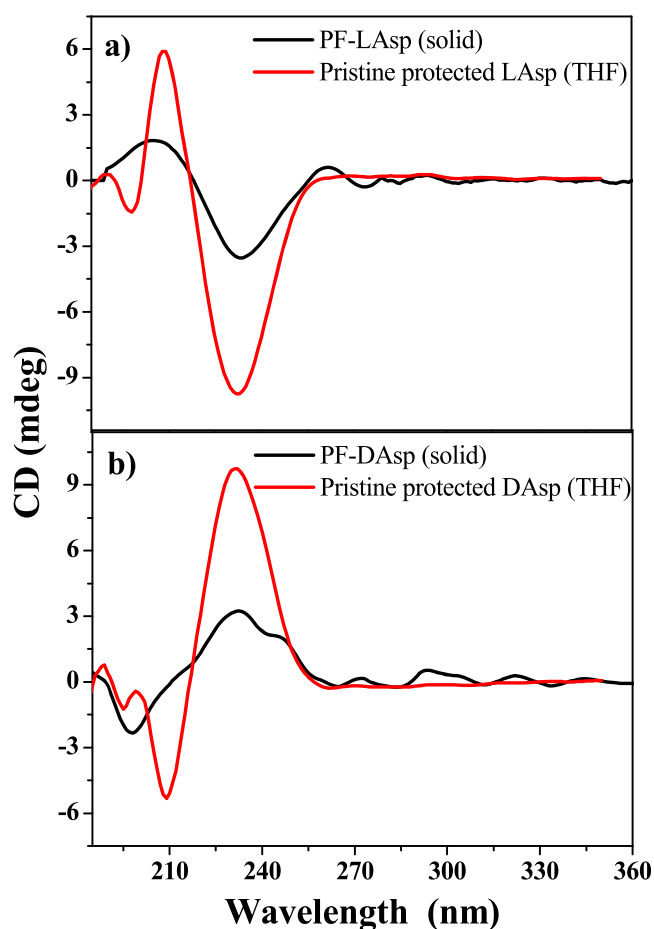

Figure 2. CD spectra of (a) PF-LAsp extracted from the AAO membrane in solid state (KBr) along with protected L-aspartic acid (THF) (b) PF-DAsp extracted from AAO membrane in solid state (KBr) along with protected D-aspartic acid (THF).

information. Solute diffusion studies through the membrane were carried out to obtain a more quantitative estimate of the reduction in pore dimensions upon polymer modification of the AAO membrane.[49−51] Using Fick' law of diffusion, the relative average pore diameter was obtained as 131 nm (details of calculation are given in Supporting Information section S6 and Figure S26). This value is in concurrence with the observed pore size reduction upon polymer modification in the SEM image. The FE-SEM micrographs also show the polymer organized around the walls of the pores (Figure 1b).

The chiral nature of the coated polymer was analyzed by extracting the polymer from the AAO membrane and subjected to CD analysis. The finely crushed and powdered AAO membrane was extracted with HPLC grade THF multiple times until the polymer was completely removed. Complete extraction of the polymer was confirmed by the disappearance of the polymer fluorescence from the washing solvent under a hand-held UV lamp. Figure 2 compares the CD spectra of the polymer recorded in the solid state with that of the respective pristine protected D/L aspartic acid. Pristine protected L-aspartic acid shows a peak maxima at 208 nm and a minima at 232 nm, while a mirror image CD spectra is observed in the case of pristine protected D-aspartic acid with a minima at 208 nm and maxima at 232 nm. The CD spectra of both homochiral polymers resemble that of the corresponding protected aspartic acid enantiomer indicating the ability of the
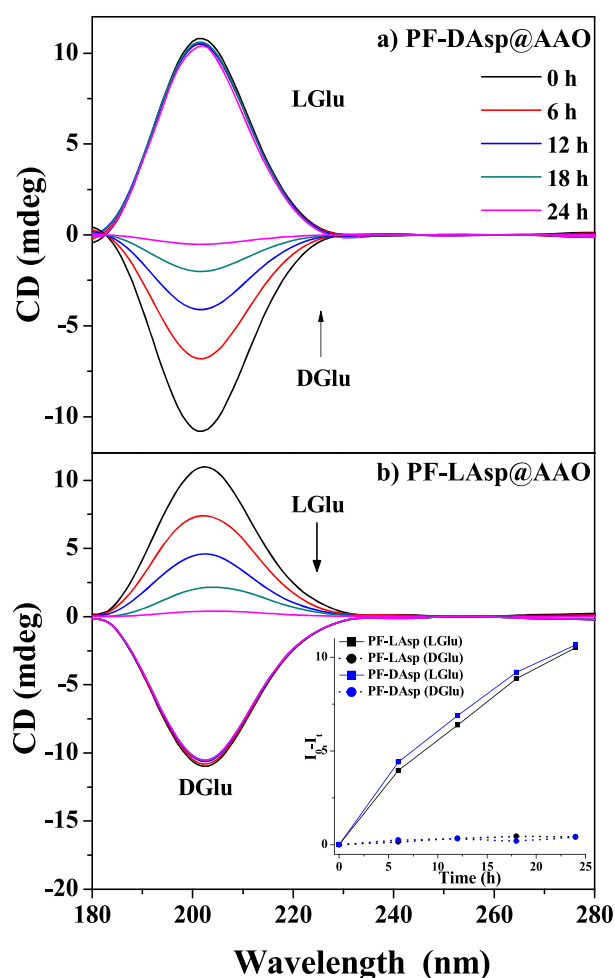
Figure 3. (a) CD spectra to show enantioselective recognition of D-glutamic acid by PF-DAsp coated AAO membranes (PF-DAsp@AAO) and (b) CD spectra to show enantioselective recognition of L-glutamic acid by PF-LAsp coated AAO membranes (PF-LAsp@AAO). (Inset) Combined plot showing enantioselective sensing of D and L-glutamic acid by PF-DAsp and PF-LAsp coated homochiral AAO membranes, respectively.

Figure 4. CD spectra for enantioselective separation of racemic mixture of glutamic acid using PF-DAsp@AAO and PF-LAsp@AAO membranes. (Inset) Kinetics of enantioselective separation of racemic mixture.

Table 1. % Enantiomeric Excess (ee) Values Obtained from CD Data

racemic mixture (native amino acids)	% enantiomeric excess (ee)[a]	
	PF-LAsp@AAO	PF-DAsp@AAO
glutamic acid	95.2	94.7
alanine	88.3	91.3
leucine	80.6	82.9
lysine	80.8	83.3
aspartic acid	80.2	79.0
phenylalanine	72.0	71.5
proline	66.1	66.9
serine	63.0	60.7
valine	46.4	47.7

[a]% Enantiomeric excess (ee) obtained by taking ratio of area under the CD curve.

appendage to induce chirality in the polymers. A quantitative estimation of the amount of polymer coated on the AAO membrane was carried out using the absorption coefficient value (54.95×10^3 L mol^{-1} cm^{-1} in THF) of the polymer calculated using the Beer−Lambert equation (Figure S27). The polymer was extracted completely from two homochiral AAO membranes, dissolved in HPLC grade THF, and used as the unknown sample for the estimation. An average amount of 0.14 mg of polymer is found to be coated on a single AAO membrane.

Enantioselective Recognition, Separation, and Kinetics. Evidence for the chiral nature of the pore channels was sought from enantioselective recognition experiments conducted to study the ability of the AAO membranes to discriminate between pairs of enantiomers. Figure 3a bottom shows the reduction in intensity of the CD spectra over time for a solution of native D-glutamic acid into which two PF-DAsp coated AAO membranes (PF-DAsp@AAO) were suspended, indicating its adsorption into the pore channel of the AAO membrane. The top plot in Figure 3a corresponds to a similar experiment conducted in a solution of native L-
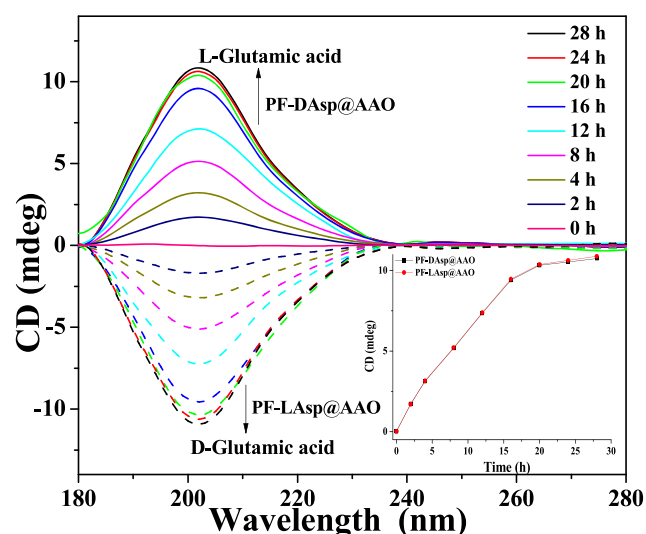
glutamic acid, which remains intact without any reduction in intensity despite the prolonged exposure time. The same is true for PF-LAsp@AAO, which selectively adsorbs L-glutamic acid from the solution resulting in reduction in intensity of the CD spectra only when immersed in solution of L-glutamic acid (Figure 3b, top plot). Inset is a combined plot of the difference in peak intensity ($I_0 - I_t$) at λ_{max} 202 nm as a function of time, where I_t and I_0 are peak intensity of CD signal at time t and at time $t = 0$ h, respectively. The combined plot summarizes the observations from these experiments confirming that polymer coated homochiral AAO membranes have the ability to discriminate between pairs of enantiomers. PF-LAsp@AAO adsorbs only L-glutamic acid whereas PF-DAsp@AAO membrane adsorbs only D-glutamic acid; the adsorption of enantiomers with opposite chirality is negligible.

After establishing the selective recognition ability of the AAO membranes toward the different enantiomers, the ability to bring about enantioselective separation of racemic mixtures was tested. For this, the polymer coated AAO membranes were suspended in a solution of an equimolar racemic mixture of 1 mg each of D and L native amino acid (D and L-glutamic acid as a representative analyte) dissolved in 3 mL of Milli-Q water as
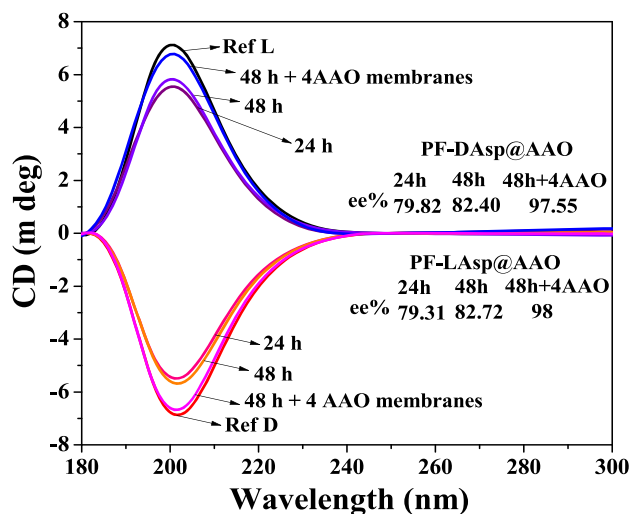
Figure 5. CD spectra for enantioselective separation of racemic mixture of native aspartic acid using PF-D/LAsp@AAO membranes incubated for 24 h, 48 h, and 48 h with the addition of two fresh polymer coated membranes at the end of 24 h. Inset: Table showing % ee for the different time periods.
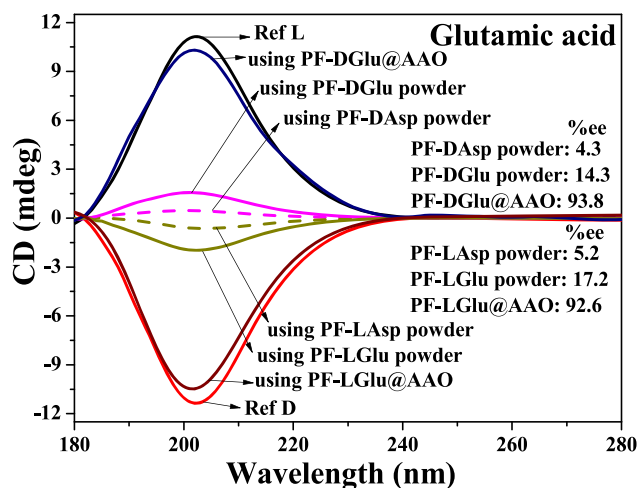

Figure 6. CD spectra for enantioselective separation of racemic mixture of glutamic acid using PF-D/LAsp, PF-D/LGlu polymer powder, and PF-D/LGlu@AAO membranes, which was stirred for 48 h. Inset: Table showing % ee for the different polymer powders and AAO membranes.

shown schematically in Figure S28.The racemic mixture treated with PF-LAsp@AAO started showing peak for D-glutamic acid (Figure 4, bottom plot (dotted lines)) while the racemic mixture treated with PF-DAsp@AAO started showing peak for L-glutamic acid (top plot). The peak intensity increases with the increase in time. It is also seen that both the polymer coated homochiral AAO membranes exhibits almost similar kinetics for separation of racemic mixture and most of the enantioselective separation is accomplished within the first 20 h (Figure 4 inset plot); thereafter, the change in the CD spectrum is marginal. This demonstrates that 24 h is sufficient for enantioselective separation to occur.

Similar enantioselective separations were carried out for racemic mixtures of various other native amino acids like alanine, aspartic acid, leucine, lysine, serine, phenylalanine, proline, and valine in Mili-Q water for 24 h. The chemical structures of native D and L amino acids screened in the present study are given in (Figure S29) and the CD spectra plotted are given in (Figure S30). The % ee was calculated from the ratio of areas under the curve of CD spectra for the solution remaining after 24 h to that of the pure enantiomer. Table 1 summarizes the % ee separation obtained from CD data for the various native amino acids used as analytes. Both the D and L aspartic acid appended polymer coated AAO membranes exhibits similar separation capabilities. From the table it is seen that the maximum ee of ∼95% is observed when glutamic acid is the analyte.

The % ee can be improved by adding two fresh polymer coated AAO membranes to the racemic mixture at the end of 24 h. Figure 5 shows that although prolonging the time of incubation of two polymer coated AAO membranes with the racemic mixture of aspartic acid does not bring about noticeable improvement in % ee, almost complete enantiomeric separation of racemic mixture is achieved with a total of four PF-D/LAsp polymer coated AAO membranes.

An experiment was conducted to recover the adsorbed native amino acid from the AAO membrane and to quantify it. For this, two homochiral AAO membranes were crushed and sonicated in small amount of milli-Q water repeatedly. The polymer and residues of the membrane remain insoluble in the water, which is separated by simple filtration. The water is removed completely by freeze-drying, and the recovered amino acid is solubilized again in 3 mL of fresh milli-Q water. The solution state CD spectra was recorded (Figure S31), and its quantification was done by taking the ratio of areas under the curve against that of pure enantiomer (1 mg of pure enantiomer in 3 mL of Milli-Q water). Analyte recovery was carried out for a few representative examples of glutamic acid, aspartic acid, serine, and valine. The value obtained from the CD data is comparable with ee % values obtained from the CD signal of the remaining solution (Table S3). As discussed earlier, the PF-D/LAsp coated on the AAO membrane was quantified using the Beer−Lambert equation to be on an average about 0.14 mg/membrane. The amino acid adsorbed on the AAO membranes was also quantified after extracting them from the crushed membranes. Using simple arithmetic, it can be seen that about 3.5 mg of D/L glutamic acid can be separated and recovered using 1 mg of homochiral AAO membrane in 24 h.

Previously we had reported the application of glutamic acid appended polyfluorene (PF-LGlu) for the enantiomeric separation of aqueous racemic mixtures by directly dispersing the polymer without the support of the AAO templates.[45] A similar experiment was carried out with PF-D/LAsp by dispersing the polymer (0.4 mg) directly into aqueous racemic mixture of 1 mg each of D- and L-glutamic acid in water (3 mL), stirring the contents for 48 h followed by filtering off the polymer and recording the CD spectrum of the remaining solution. A similar amount of the inherently porous PF-D/LGlu polymer was also dispersed in water (3 mL) containing 1 mg each of D- and L-glutamic acid. Figure 6 compares the CD spectra of the remaining solution after the polymer was filtered and removed.

Compared to the inherently porous PF-D/LGlu, the enantiomeric separation efficiency of PF-D/LAsp is poor (as seen from the % ee values given in the inset table in Figure 6). On the other hand, the ee % efficiency is enhanced by several fold by coating the same polymers on AAO membranes and using the polymer coated AAO membranes for the
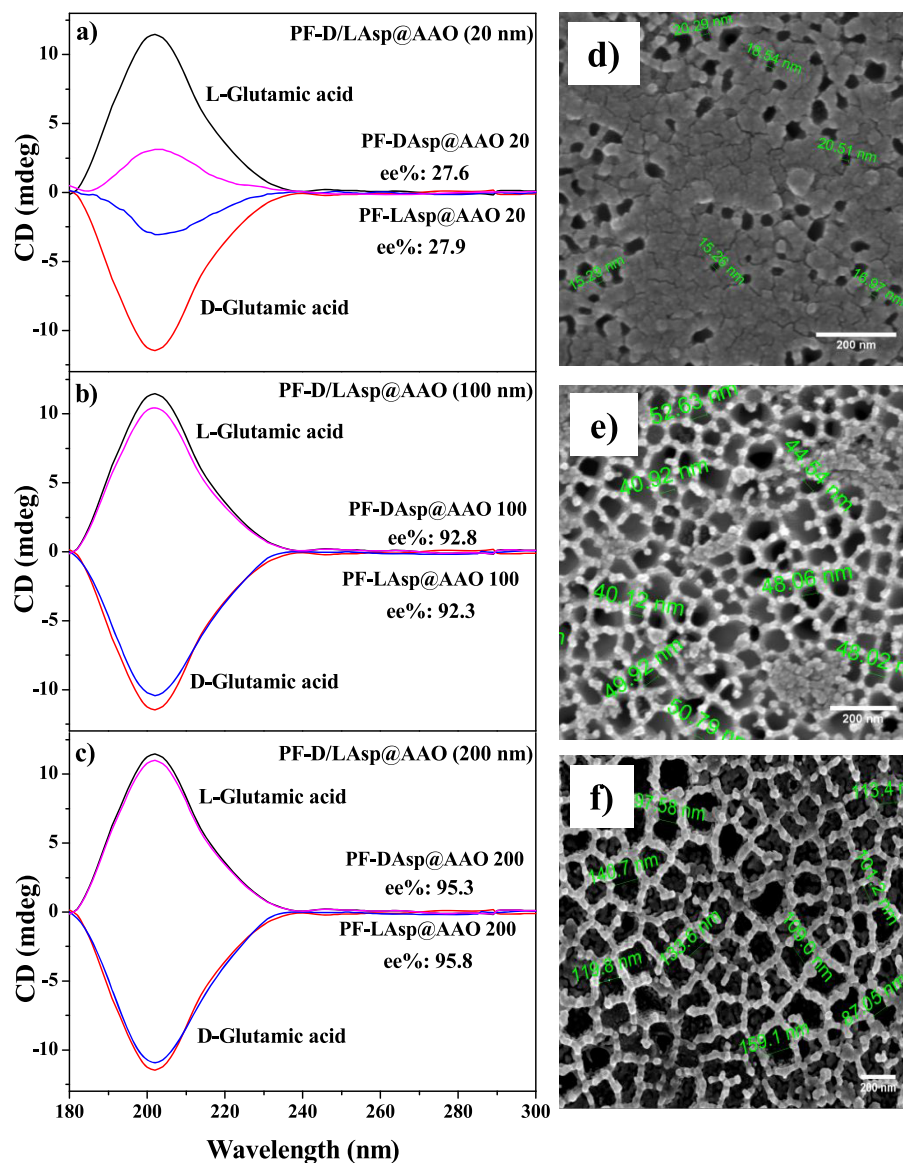
Figure 7. (a−c) CD spectra of enantioselective separation of glutamic acid racemic mixture with 20, 100, and 200 nm pore size homochiral AAO membranes, respectively. Inset: Table showing % ee. (d−f) FE-SEM micrographs of polymer coated homochiral AAO membranes with different sizes 20 nm, 100 nm, and 200 nm.

enantioselective separation. The ee % increased from a mere 14.3% (17.2%) for the PF-DGlu (PF-LGlu) powder to 93.8% (92.6%) for the PF-DGlu@AAO (PF-LGlu@AAO). The template approach adopted in this work not only provides increased surface area for separation, but it also eliminates the requirement of inherent porous fibrous morphology as a prerequisite for the chiral amino acid appended polyfluorene to achieve enantioselective separation of racemic mixtures. The direct dispersion of the chiral polyfluorene in water for 48 h results in a change in pattern of the CD signal (our previous report) whereas no change in CD signal pattern is observed when the PF-D/LAsp polymers are coated on the AAO membrane (Figure S32).

Effect of Pore Size on Enantioselective Separation. The size of the nanoporous channel could be expected to have an influence on the % ee separation. In order to understand the role of pore size on the efficiency of enantioselective separation

and also to analyze whether the separation occurs inside homochiral pore or on the membrane surface as well, AAO membranes with different pore sizes (200, 100, and 20 nm) were chosen to coat the D- and L-aspartic acid appended polyfluorene. These different pore sized homochiral AAO membranes were used to carry out the enantioselective separation of the native glutamic acid racemic mixture as a representative analyte. The CD spectra of the remaining solution after 24 h interaction with the AAO membrane was recorded and plotted against the pure enantiomers (Figure 7). From the figure, it is seen that the 100 nm pore size polymer coated membranes also achieves similar enantiomeric excess (∼93%) as that of the 200 nm pore size membranes (∼95%), but the separation efficiency is drastically decreased in the case of the 20 nm AAO membranes (∼28%). The values of enantiomeric excess are tabulated in the inset in Figure 7. The reason for the drastic decrease of separation efficiency in the

case of 20 nm pore sized membrane can be elaborated with the help of FE-SEM micrographs of the polymer coated membranes (Figure 7d−f). In the case of the 100 and 200 nm pore sized polymer coated membrane; the average pore size reduces to 49−72 nm and 100−160 nm, respectively, with a clear opening of the pores (as observed from the pore size dimensions determined using ImageJ software). However, in the case of the 20 nm AAO membrane, the pores are severely clogged with polymer and the average pore size drastically reduces to 15−17 nm. This experiment clearly conveyed that the separation is severely hampered when the pores are clogged. Thus, one can safely conclude that the process of enantiomer separation occurs inside the chiral pores and not on the surface of the membranes.

DISCUSSION

An important step in the chiral recognition and enantiomeric separation involving chiral polymeric selectors is the formation of labile diastereoisomeric complexes between the enantiomers and the chiral selector. The ability to discriminate between the enantiomers arises from the different points of interaction of the two enantiomers with the selector.[52] One of the commonly accepted mechanisms for the formation of the labile diastereoisomeric complex is by a 3-way interaction, where only one enantiomer can match exactly the three sites of interaction on the chiral carbon of the selector, while for the other enantiomer, only two sites of interaction would be possible after all possible rotations.[53] These points of interaction, which should be between three different substituents of the chiral analyte and selector, could be either hydrogen bonding, $\pi-\pi$, or even repulsive interactions. With amino acid selectors, hydrogen bonding is expected to be at the forefront of interactions. Indeed, FTIR experiments indicated the existence of differential interaction of the D and L-protected amino acid appended selector polymer toward D-glutamic acid in its native form as a typical analyte. Details of the FTIR experiments are provided in the Supporting Information Figure S33 and Table S4. The existence of such differential interaction supports the matched and mismatched orientation mechanism for enabling chiral recognition and enantiomeric separation.

CONCLUSIONS

In summary, we have demonstrated a simple filtration method for the enantioselective separation of native amino acids using homochiral D/L aspartic acid appended polyfluorene coated AAO membranes. Although porous AAO membranes have been widely reported for fabrication of polymer nanostructures by the templating approach, this is the first report as far as we are aware, where it has been used for enantioselective separation. The polymer coated homochiral AAO membranes have the ability to discriminate between pairs of enantiomers from an aqueous racemic mixture and to bring about their separation by selectively adsorbing one enantiomer within the chiral pores leaving the filtrate enriched with the other enantiomer. The adsorbed amino acid can be recovered from the AAO membrane by repeated extraction with milli-Q water. A maximum enantiomeric excess of 95% is achieved when glutamic acid is the analyte, while other amino acids like alanine, leucine, lysine, and aspartic acid are separated with ee % > 80. The ee % can be enhanced for these amino acids also by increasing the number of polymer coated AAO membranes

used for the separation process. By varying the pore size of the AAO membrane, the ee % can be modulated as the pore size controls the degree of confinement of the chiral polyfluorene.

ASSOCIATED CONTENT

ⓈI Supporting Information

The Supporting Information is available free of charge at https://pubs.acs.org/doi/10.1021/acs.analchem.9b04699.

Materials, measurements, preparation of homochiral membranes, pore dimension analysis by diffusion studies, sample preparation for CD spectra, synthesis and structural characterization of all the compounds including monomers and polymers using NMR, UV−vis, FTIR, MALDI-TOF, FE-SEM, GPC, table showing the structure of analytes, CD spectra, as well as tables summarizing the % ee (PDF)

AUTHOR INFORMATION

Corresponding Author

Asha SK − *Polymer Science and Engineering Division, CSIR-National Chemical Laboratory, Pune 411008, India; Academy of Scientific and Innovative Research, New Delhi 110025, India;* ⓞ orcid.org/0000-0002-3999-4810; Email: sk.asha@ncl.res.in; Fax: 0091-20-25902615

Author

Shrikant B. Nikam − *Polymer Science and Engineering Division, CSIR-National Chemical Laboratory, Pune 411008, India; Academy of Scientific and Innovative Research, New Delhi 110025, India;* ⓞ orcid.org/0000-0001-6718-9002

Complete contact information is available at:
https://pubs.acs.org/10.1021/acs.analchem.9b04699

Notes

The authors declare no competing financial interest.

REFERENCES

(1) Watson, J. D.; Crick, F. H. C. *Nature* **1953**, *171*, 737−738.
(2) Giuliano, M. W.; Maynard, S. J.; Almeida, A. M.; Guo, L.; Guzei, I. A.; Spencer, L. C.; Gellman, S. H. *J. Am. Chem. Soc.* **2014**, *136*, 15046−15053.
(3) Shallenberger, R. S.; Wienen, W. J. *J. Chem. Educ.* **1989**, *66*, 67−73.
(4) Wang, Z.; Xu, W.; Liu, L.; Zhu, T. F. *Nat. Chem.* **2016**, *8*, 698−704.
(5) Mason, S. F. *Nature* **1984**, *311*, 19−23.
(6) Müller, T. A.; Kohler, H. P. E. *Appl. Microbiol. Biotechnol.* **2004**, *64*, 300−316.
(7) Mane, S. *Anal. Methods* **2016**, *8*, 7567−7586.
(8) Hutt, A. J.; O'Grady, J. J. *Antimicrob. Chemother.* **1996**, *37*, 7−32.

(9) Landoni, M. F.; Soraci, A. L.; Delatour, P.; Lees, P. *J. Vet. Pharmacol. Ther.* **1997**, *20*, 1−16.

(10) Davies, N. M.; Teng, X. W. *Adv. Pharm.* **2003**, *1*, 242−252.

(11) Diéguez, M.; Pàmies, O.; Claver, C. *Chem. Rev.* **2004**, *104*, 3189−3215.

(12) Farina, V.; Reeves, J. T.; Senanayake, C. H.; Song, J. J. *Chem. Rev.* **2006**, *106*, 2734−2793.

(13) Bhadra, S.; Yamamoto, H. *Chem. Rev.* **2018**, *118*, 3391−3446.

(14) Enders, D.; Hüttl, M. R. M.; Raabe, G.; Bats, J. W. *Adv. Synth. Catal.* **2008**, *350*, 267−279.

(15) Wang, X.; Ma, Z.; Lu, J.; Tan, X.; Chen, C. *J. Am. Chem. Soc.* **2011**, *133*, 15350−15353.

(16) O'Brien, P. *Angew. Chem., Int. Ed.* **1999**, *38*, 326−329.

(17) Verendel, J. J.; Pàmies, O.; Diéguez, M.; Andersson, P. G. *Chem. Rev.* **2014**, *114*, 2130−2169.

(18) Steinreiber, J.; Schürmann, M.; Wolberg, M.; Van Assema, F.; Reisinger, C.; Fesko, K.; Mink, D.; Griengl, H. *Angew. Chem., Int. Ed.* **2007**, *46*, 1624−1626.

(19) Seebach, D.; Sting, A. R.; Hoffmann, M. *Angew. Chem., Int. Ed. Engl.* **1996**, *35*, 2708−2748.

(20) Huang, K.; Breitbach, Z. S.; Armstrong, D. W. *Tetrahedron: Asymmetry* **2006**, *17*, 2821−2832.

(21) Zhang, L.; Fu, N.; Luo, S. *Acc. Chem. Res.* **2015**, *48*, 986−997.

(22) Gübitz, G.; Schmid, M. G. *Biopharm. Drug Dispos.* **2001**, *22*, 291−336.

(23) Ward, T. J.; Ward, K. D. *Anal. Chem.* **2010**, *82*, 4712−4722.

(24) Scriba, G. K. E. *J. Chromatogr. A* **2016**, *1467*, 56−78.

(25) Scriba, G. K. E. *TrAC, Trends Anal. Chem.* **2019**, *119*, 115628.

(26) Prasad, B. B.; Tiwari, M. P.; Madhuri, R.; Sharma, P. S. *J. Chromatogr. B: Anal. Technol. Biomed. Life Sci.* **2011**, *879*, 364−370.

(27) Xiao, Y.; Wang, H. Q.; Zhang, H.; Jiang, Z. Q.; Wang, Y. Q.; Li, H.; Yin, J.; Zhu, Y. Y.; Wu, Z. Q. *J. Polym. Sci., Part A: Polym. Chem.* **2017**, *55*, 2092−2103.

(28) Zhu, F.; Du, Y.; Chen, J.; Chen, B.; Zhu, Y.; Zhai, X.; Xu, S.; Zhou, W. *Chromatographia* **2009**, *69*, 1315−1320.

(29) Okamoto, Y. *Prog. Polym. Sci.* **2000**, *25*, 159−162.

(30) Zhu, B.; Yao, Y.; Deng, M.; Jiang, Z.; Li, Q. *Electrophoresis* **2018**, *39*, 2398−2405.

(31) Zhou, C.; Ren, Y.; Han, J.; Xu, Q.; Guo, R. *ACS Nano* **2019**, *13*, 3534−3544.

(32) Paik, P.; Gedanken, A.; Mastai, Y. *ACS Appl. Mater. Interfaces* **2009**, *1*, 1834−1842.

(33) Armstrong, D. W.; Jin, H. L. *Anal. Chem.* **1987**, *59*, 2237−2241.

(34) Xie, R.; Chu, L.-Y.; Deng, J.-G. *Chem. Soc. Rev.* **2008**, *37*, 1243−1263.

(35) Kong, J.; Mu, Y.; Xiong, Y.; Zheng, M.; Wang, Y. *J. Electron. Mater.* **2019**, *48*, 964−971.

(36) Ha, J. J.; Hyun, M. H. *Bull. Korean Chem. Soc.* **2016**, *37*, 1385−1388.

(37) Ghosh, S.; Fang, T. H.; Uddin, M. S.; Hidajat, K. *Colloids Surf., B* **2013**, *105*, 267−277.

(38) Lakhwani, G.; Meskers, S. C. J.; Janssen, R. A. J. *J. Phys. Chem. B* **2007**, *111*, 5124−5131.

(39) Lakhwani, G.; Meskers, S. C. J. *J. Phys. Chem. A* **2012**, *116*, 1121−1128.

(40) Savoini, M.; Wu, X.; Celebrano, M.; Ziegler, J.; Biagioni, P.; Meskers, S. C. J.; Duò, L.; Hecht, B.; Finazzi, M. *J. Am. Chem. Soc.* **2012**, *134*, 5832−5835.

(41) Lakhwani, G.; Janssen, R. A. J.; Meskers, S. C. J. *J. Phys. Chem. B* **2009**, *113*, 14165−14171.

(42) Savoini, M.; Biagioni, P.; Meskers, S. C. J.; Duò, L.; Hecht, B.; Finazzi, M. *J. Phys. Chem. Lett.* **2011**, *2*, 1359−1362.

(43) Ozawa, H.; Fujigaya, T.; Niidome, Y.; Hotta, N.; Fujiki, M.; Nakashima, N. *J. Am. Chem. Soc.* **2011**, *133*, 2651−2657.

(44) Akazaki, K.; Toshimitsu, F.; Ozawa, H.; Fujigaya, T.; Nakashima, N. *J. Am. Chem. Soc.* **2012**, *134*, 12700−12707.

(45) Senthilkumar, T.; Asha, S. K. *Chem. Commun.* **2015**, *51*, 8931−8934.

(46) Chi, M. H.; Su, C. H.; Cheng, M. H.; Chung, P. Y.; Peng, C. H.; Chen, J. T. *Macromol. Rapid Commun.* **2016**, *37*, 2037−2044.

(47) Cepak, V. M.; Martin, C. R. *Chem. Mater.* **1999**, *11*, 1363−1367.

(48) Xue, J.; Xu, Y.; Jin, Z. *Langmuir* **2016**, *32*, 2259−2266.

(49) Das, C.; Krishnamoorthy, K. *Chem. Commun.* **2014**, *50*, 5905−5908.

(50) Das, C.; Jain, B.; Krishnamoorthy, K. *Chem. Commun.* **2015**, *51*, 11662−11664.

(51) Clark Wooten, M. K.; Koganti, V. R.; Zhou, S.; Rankin, S. E.; Knutson, B. L. *ACS Appl. Mater. Interfaces* **2016**, *8*, 21806−21815.

(52) Berthod, A. *Chiral Recognition in Separation Methods: Mechanisms and Applications*; Springer: Berlin Heidelberg, Germany, 2010.

(53) Easson, L. H.; Stedman, E. *Biochem. J.* **1933**, *27*, 1257−1266.

Erratum

Detailed structural characterization of 1, 4-benzenediboronic acid bis(pinacol)ester (Chapter 2) like ^{13}C NMR spectrum and FT-IR spectrum are given here as suggested by reviewer.
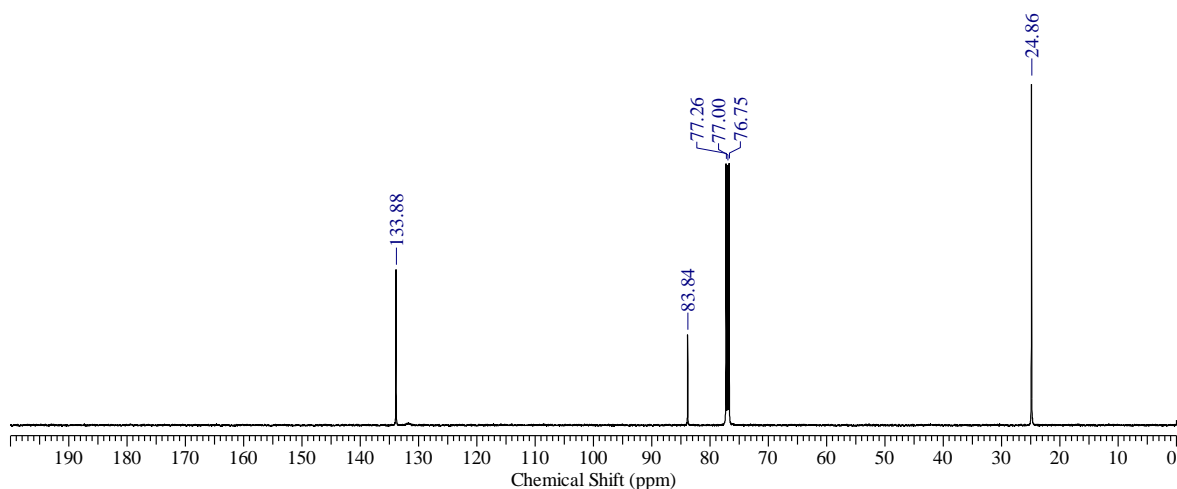

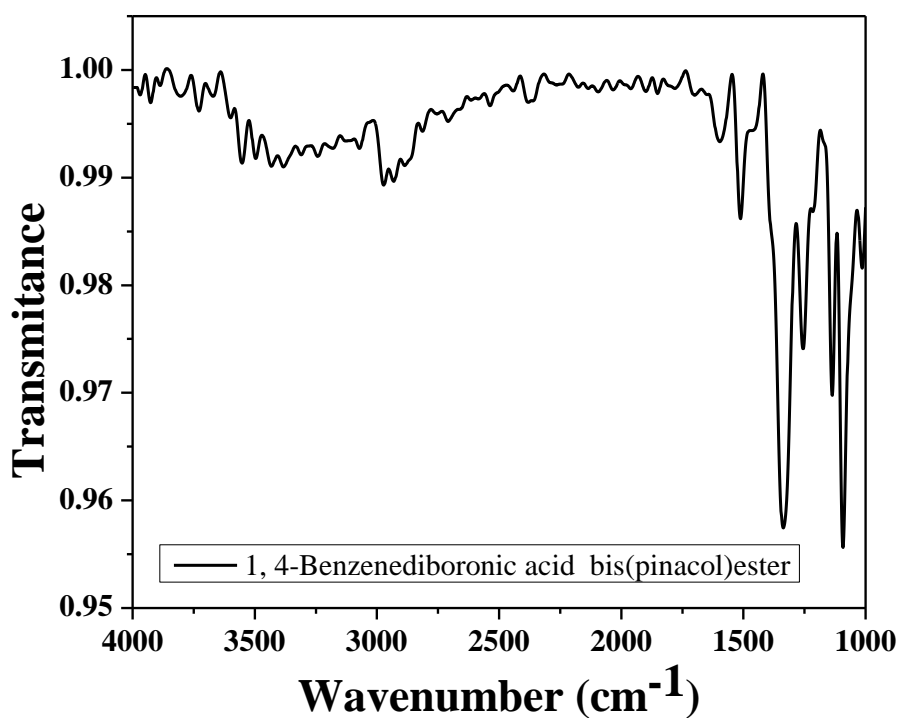**Figure 1.** ^{13}C NMR spectrum of 1, 4-benzenediboronic acid bis(pinacol)ester (CDCl3)

Figure 2. FT-IR spectrum of 1, 4-benzenediboronic acid bis(pinacol)ester